Univerza *v Ljubljani*
Fakulteta *za elektrotehniko*

Robert Baždarić

PRISTOPI VODENJA PREKLOPNIH HIBRIDNIH SISTEMOV NA PODLAGI MEHKIH MODELOV

DOKTORSKA DISERTACIJA

Raziskovalni mentor: prof. dr. Igor Škrjanc, univ. dipl. inž. el.
Raziskovalni somentor: prof. dr. Drago Matko, univ. dipl. inž. el.

Ljubljana, 2017

Zahvala

Ta študija, ki zajema številne discipline, ne bi postala disertacija brez nasvetov, usmerjanja in teoretične podpore, ki jo je podal moj mentor. Zato se zahvaljujem prof. dr. Igorju Škrjancu. Zahvaljujem se tudi svojemu somentorju prof. dr. Dragu Matku za konstruktivne predloge skozi celoten študij in razumevanje mojega pristopa k raziskovanju.

Posebna zahvala gre mojemu mentorju pri prejšnjih študijah, prof. dr. Danjelu Vončini in njegovi celotni podpori, potrpežljivosti pri dolgih razpravah in podpori pri eksperimentalnem delu te študije. Zahvala gre tudi Laboratoriju za regulacijsko tehniko in močnostno elektroniko, še posebej dr. Alešu Lebanu za njegovo predano delo pri postavitvi testnega okolja in razumevanju vseh podrobnosti, povezanih z algoritmi vodenja.

Zahvaliti se moram tudi Laboratoriju za avtonomne mobilne sisteme in še posebej prof. dr. Gašperju Mušiču za njegove prijazne nasvete.

Nenazadnje, hvala moji soprogi Snježani za njeno nesebično podporo, ki je bila ključnega pomena za nadaljevanje študija. Prav tako hvala mojima otrokoma Ivani in Luki, mojim staršem Milici in Borisu ter mojemu bratu Marinu za prijazno poslušanje, razumevanje in podporo mojega študija.

Povzetek

V zadnjih dvajsetih letih je vodenje hibridnih sistemov vzpodbudilo velik znanstveni interes. Glavni razlogi se skrivajo predvsem v uporabnosti hibridnih sistemov za širok spekter fizičnih sistemov, še posebej tistih, ki so nastali v sklopu sodobnega tehnološkega razvoja. Cilj naše študije je razvoj pragmatičnega izogibanja nelinearnim fenomenom pri vodenju hibridnih sistemov, s fokusom na podmnožici preklopnih hibridnih sistemov. Razviti zakoni vodenja predstavljajo avtorjevo splošno idejo o vodenju nelinearnih dinamičnih sistemov. Ti zakoni se bodo uporabljali za namen *vodenja na podlagi hevrističnega principa*. Glavni poudarek bo na vodenju na osnovi *identifikacije mehkih modelov*, kot univerzalnem aproksimacijskem pristopu k modeliranju in izboljšanju več strukturnih in globalnih modelov. Prva faza se nanaša na identifikacijo ustaljenega stanja hibridnih sistemov. Druga faza se nanaša na identifikacijo dinamičnega modela hibridnega sistema (sprejemljive natančnosti), ki z analitičnega stališča predstavlja kvalitativne in kvantitativne lastnosti sistema.

Pri razvoju algoritmov bo poudarek na *prediktivnih metodah vodenja hibridnih sistemov na osnovi mehkih modelov*, ki bodo v večji meri odpravile glavno negativno značilnost takšnih metod in sicer tj. kompleksnost obdelave v realnem času. Prilagojena različica algoritma, ki predvideva *sub-optimalno* vodenje, pa je širše uporabna in sicer tudi za sisteme, ki imajo vgrajen šibkejši mikroprocesor. Tradicionalno poenostavljanje modelov hibridnih sistemov je (v skladu s teorijo elektronskih vezij) običajno izvedeno s tako imenovanim *postopkom povprečja*, pri katerem se izogibamo modernim pristopom kombiniranja diskretnih in zveznih sistemov. V nasprotju s tem bodo v naši študiji (poleg tradicionalnih) harmonično integrirani tudi moderni pristopi k obravnavi hibridnih sistemov. Takšno homogeniziranje dveh nasprotnih pristopov bo afirmiralo modeliranje nelinearnih sistemov na podlagi identifikacije. Slednja predstavlja vodilno strategijo na poti k izdelavi modela za širšo uporabo. Osnovna ideja je še vedno zgraditi model kompleksnega sistema (sestavljenega iz diskretnih in zveznih elementov) v obliki nadomestnega zveznega modela, pri čemer se moramo zavedati kompleksnosti prehodov iz enega načina delovanja v drugi način. Ti prehodi hkrati vplivajo na končno in edinstveno obliko modela. Obravnavani sistemi imajo merljive spremenljivke stanj, kot tudi parametre procesa. Ta predpostavka spodbuja glavno idejo in odpira možnost zajema podatkov z opazovanjem kompleksnih prehodov stanj (pri katerih gre za sočasno spremembo zveznih trajektorij in diskretnih stanj). Ta informacija se kasneje še vedno ohranja v končni transformaciji iz prostora stanj v psevdo-normiran prostor. Te ideje ustvarjajo čvrste temelje za končno formiranje nove metode vodenja ter prispevajo k parcialnim in ciljnim dosežkom.

Primer sistema, ki omogoča uporabo predstavljene metodologije, je DC-DC pretvornik navzgor. Ta ni samo dober primer preklopnega sistema, ampak je hkrati tudi primer vsesplošno uporabnega vira napetosti, ki je prisoten predvsem pri alternativnih energetskih virih. Njegova pomembnost se kaže tudi v obliki številnih študij, ki so nastale od začetka uporabe polprevodnikov. Izogibanje nelinearnim fenomenom [1,7-10,56,57] je ena od glavnih motivacij in ciljev pri izdelavi algoritma vodenja, ki je inteligenten, robusten in ekonomičen v smislu porabe časa procesiranja.

V nasprotju s prvimi ugotovitvami avtorjev Ćuk, Ericson in Middlebrook [23,24] je natančnost matematičnega modeliranja v veliki meri odvisna od prehodnih pojavov med stanji sistema in nezveznosti njihovih funkcij pri istem času. Ti problemi so bili odkriti že v sredini prejšnjega stoletja, šele proti koncu prejšnjega stoletja pa so se pojavili v obravnavi »chattering« efektov, »Zeno« obnašanja in nelinearnih fenomenov tudi pri dobro poznanih metodologijah HS.

S stališča linearne teorije vodenja sistemov vodenje na osnovi majhnih signalov (kot so to imenovali omenjeni avtorji) dobro deluje v okolici delovne točke sistema. Torej, z linearizacijo v izbrani delovni točki in analitičnim pristopom je model (omenjeni avtorji navajajo, da gre za »povprečni model«) mogoče uporabiti na širšem območju delovanja. Kot je že bilo omenjeno, z namenom, da bi dosegli robustno delovanje algoritma vodenja, je potrebno pri širjenju področja delovanja DC-DC pretvornika in preklopnih hibridnih sistemov upoštevati teorijo vodenja nelinearnih dinamičnih sistemov.

Z obravnavanjem hibridne strukture [2,3], robustne rešitve [3,4], naravne limite [3], redukcije kompleksnosti [5,6] in vseprisotnega problema izogibanja nelinearnim pojavom [7-10] se pojavijo zelo zanimivi izzivi, ki jih je potrebno rešiti za uspešno vodenje DC-DC pretvornikov. Najuspešnejše sodobne rešitve [3] temeljijo na linearni matrični neenakosti in optimizaciji HS [3,5,6], na algoritmih za zmanjšanje kompleksnosti [11], na formalizmu komplementarnosti (za namen zmanjšanja nedoločenosti modela) [12,13], na metodi drsnega načina vodenja [14,15], na metodi hevrističnega vodenja, na nevronskih mrežah in na metodi mehkega vodenja [10,16, 138]. Slednja metoda [16,138] je obravnavana in podrobno predstavljena v tej disertaciji, tako da formira enotno in izboljšano metodologijo vodenja na področju preklopnih hibridnih sistemov, kamor sodi tudi obravnavani DC-DC pretvornik navzgor.

Ključne besede: hibridni sistemi, preklopni hibridni sistemi, nelinearno vzbujeni pojavi, DC-DC pretvornik, modeliranje DC-DC pretvornika na vzgor, identifikacija nelinearnih sistemov, mehki modeli, identifikacija na osnovi mehkih modelov, prediktivno vodenje, prediktivno vodenje na osnovi mehkih modelov, prediktivno vodenje na osnovi mehkih modelov in dinamične matrike , generalno prediktivno vodenje na osnovi mehkih modelov, prediktivno funkcijsko vodenje na osnovi mehkih modelov

1. Uvod

1.1 Pregled vsebine doktorske disertacije

Razlogi za to študijo, ki so že bili izpostavljeni v povzetku, zahtevajo vpeljavo izbranega pristopa za izpolnitev vseh ciljev. Izbrani fizični sistem je hibriden in ga lahko opišemo z zveznimi in diskretnimi stanji. Kljub znanim hibridnim metodam vodenja in hibridnemu modeliranju, ta študija podaja alternativno metodo, ki vključuje identifikacijo nelinearnega dinamičnega sistema. Razlog za to se skriva v teoriji HS, ki se razvija v smeri oblikovanja splošnega modelirnega formalizma za sisteme z zveznimi in diskretnimi signalnimi pojavi, ki nastopajo v poljubnih kombinacijah [2,62-64] . V poglavju II bodo predstavljene temeljne definicije HS, ki pojasnjujejo splošni deterministični pristop k modeliranju teh sistemov in s tem osnovno idejo te disertacije. Slednja bo izvedena z razdelitvijo problema, ki pa se nato interpretira kot trojna strategija v poglavjih III in IV.

Prvič, pozornost bo posvečena simulaciji na splošno, z namenom razvoja simulacijskega modela, ki bo po obnašanju kar se da podoben fizičnemu sistemu, ob upoštevanju, da nas lahko uporaba vnaprej določenih simulacijskih objektov zlahka zavede pri nadaljnjem razvoju vodenja. Prednosti sodobne simulacijske platforme in numeričnih integracijskih metod bodo uporabljene za natančno konstrukcijo in sinhrono simulacijo diskretnih in zveznih funkcij fizičnega sistema. Poznavanje obravnavanega modela bo pomagalo pri naslednjih korakih razvoja.

Drugič, sledeča študija se izvaja na drugačen način kot poznana študija o pretvornikih PECs, predvsem z namenom, da bi našli natančno metodo modeliranja, ki ohranja robustno in splošno znanje o sistemu. Ta mora zagotavljati matematično obliko, ki je nadalje uporabna znotraj dobro razvitih metod vodenja. Metoda, ki temelji na sistemu z merljivimi stanji, bo prenesla glavno breme obravnave nelinearnega dinamičnega sistema izključno na »offline« problem, vključno z vso njegovo kompleksnostjo. V nasprotju s tem, kar je že znano, se bo nadaljnja študija izognila uporabi lokalnih linearnih modelov za izbrani način delovanja sistema. Metoda bo identificirala lokalni linearni model za privzeto kombinacijo vseh načinov delovanja sistemov v eni preklopni periodi sistema. Za uresničitev ideje in formalizacijo primerne oblike modela, ki jo določa algoritem vodenja, se bosta uporabili dve različni metodi identifikacije. Oba modela bosta določena z uporabo mehke identifikacije [34-36,65] na vhodno-izhodnih podatkih (poglavje III).

Tretjič, analiza sistema z uporabo mehke identifikacije in modeliranja bo predstavljala osnovo za razvoj naprednih algoritmov vodenja. Ker so bile metode in cilji identifikacije različni, bo razvoj algoritmov vodenja prikazan v sklopu dveh novih metod vodenja. Na podlagi modela ustaljenega stanja pretvornika in uporabe metodologije dveh prostostnih stopenj [44], bo izpeljan nov algoritem vodenja. Po drugi strani pa bo na osnovi obravnavanega dinamičnega mehkega modela načrtan nov mehki modelno-prediktivni algoritem vodenja [18,20,38] (poglavje IV).

V sklepni fazi razvoja bosta identifikacija in vodenje preizkušena na fizičnem procesu in nato ustrezno ovrednotena (poglavje IV). Končni sklep je podan v poglavju V.

1.1.1 Uveljavljene metodologije za iskanje naprednega algoritma vodenja v sistemu SAS

Metodologija, ki bo uporabljena za dosego zgoraj omenjenih ciljev ter kasneje za formiranje doktorske disertacije, bo pri razvoju nove metode vodenja hibridnih sistemov upoštevala sodobne in napredne mehke metode za identifikacijo in modeliranje. Kljub obstoju že razvitih naprednih metod hibridnega vodenja, in sicer MPC, ki temelji na modelih MLD, LC vodenje in vodenje na osnovi simboličnega modela [6,12,13,17,26,63] (poglavje II), bo naša metodologija dopolnila uveljavljene MPC pristope.

V disertaciji bomo izpostavili glavne pomanjkljivosti uveljavljenih metodologij, ki bodo vodile naše delo v drugo smer.

Izbrali smo MPC metodologijo, ki zahteva popolno predanost modeliranju takšnih sistemov. Če se preprosto osredotočimo na razvoj sodobnih metod, ki obravnavajo DC-DC pretvorbo, potem lahko zaključimo naslednje.

Hibridno modeliranje in vodenje predstavljata najsodobnejši pristop k raziskovanju in načrtovanju pulzno energijskih pretvornikov (Pulse Energy Converters – PECs) [3], za katere avtorji podajajo kratek pregled in primerjavo hibridnih pristopov (ki v večini primerov temeljijo na linearni matrični neenakosti - LMI) ter analizo optimizacije s konveksnim programiranjem ali optimizacije stabilnosti s funkcijo Ljapunova. Sistematični pristopi k vodenju temeljijo na lineariziranem podatkovno-vzorčenem modelu ter na implementaciji LQ optimizacije [42] ali H_∞ vodenju [4] z namenom, da bi zagotovili določeno robustnost za sisteme ki imajo deloma poznane matematične modele. V nasprotju s tem, dinamično programiranje, ki omogoča iskanje rešitve pri časovno limitirajoči konvergenci, naredi optimizacijo bolj kompleksno in odpre znani problem izbire funkcije Ljapunova [11]. Prav tako je pomembna obravnava splošno uporabnih pristopov, ki temeljijo na trenutnem vodenju, znanem tudi kot drsni režim vodenja (ang. sliding mode control) [14,15].

V disertaciji se osredotočamo na vodenje izhodne napetosti, ki je povezano z večino omenjenih pristopov hibridnega modeliranja, hkrati pa je v skladu s cilji razvoja vodenja PEC pretvornika. Čeprav MPC [5,17] odpira vprašanje o modeliranju delovnega cikla (ang. duty-cycle) in o aproksimaciji z ν-ločljivostjo (resolucijo), se v tem delu izogibamo striktni ločljivosti, ki je relativna in v veliki meri odvisna od izbire pripadnostnih funkcij mehkega modela. Mehčanje omejitev območja HS z mehko logiko se izvaja na grafičnem modelu, ki pa ni polieder z ostrimi robovi. Zato se uporablja kompleksna foliacija (ang. foliation), pri kateri ni potrebno upoštevati robov in mehčati prehodov. Ugotovimo lahko, da je uporaba mehke identifikacije povezana z dinamičnim programiranjem [11] in relaksacijsko metodo, ki pa vrača enake rezultate glede na stabilnost optimizacijskih algoritmov, napoved konvergenčnega časa in problem zaustavitve. To krepi naše izkušnje in potrjuje stališče, da je na tem mestu, kljub upoštevanju zmogljivosti sodobnih procesorjev, še vedno potrebna »offline« optimizacija.

Z namenom, da bi lahko uporabili napreden in uveljavljen MPC, ki je primeren tudi za sisteme, ki so relativno trivialni in hitri, smo spremenili pristop k modeliranju sistema, kar je opisano v tej disertaciji. To disertacijo smo pripravili, ker se način modeliranja sistema ne more določiti (z reševanjem matematičnega problema) samo na podlagi končnega aplikacijskega cilja in vodenja, temveč mora biti pridobljen na osnovi fizikalnega ozadja. Poglavje II vključuje obsežen pregled ter

obravnava več zadev povezanih z modeliranjem SAS sistema, pri čemer je poudarek na DC-DC pretvorniku navzgor. Skratka, pri analizi problema DC-DC pretvornika navzgor lahko izpostavimo nekatere zelo značilne povezave z že predstavljenimi in objavljenimi rešitvami. V poglavju III si prizadevamo najti nek alternativen in identificiran matematični model, ki bi združeval prednosti in slabosti poznanih preteklih študij.

V eni preklopni periodi T_S dobimo več menjav položajev polprevodnikov in obvezno tudi topologijo vezja. Večina predhodnih modeliranj [1,7,8] temelji na zaporednem dodajanju odsekoma afinih modelov ali formiranju povprečno-preklopnega modela, kot sta to predstavila Middlebrook in Ćuk [43]. Rešitev modeliranja temelji na perturbacijski metodi, ki je veljavna za »majhno« signalno vrednosti. Poleg tega isti avtorji, skupaj z Ericksonom [24], predlagajo natančnejše modeliranje, imenovano »veliko« signalno modeliranje (ang. large signal modelling), ki se uporablja tudi za robustne aplikacije. V sodobnih rešitvah vodenja je večji poudarek na eliminiranju nelinearnih pojavov [1,7-10], kar pa neizogibno vodi do matematične razprave o dobri pogojenosti in obstoju rešitve pri modeliranju hibridnih sistemov [27]. Iz stališča sodobnih matematičnih aspektov, modeliranje DC-DC pretvornikov vodi do komplementarnega formalizma [13,27], ki ga je potrebno ustrezno obravnavati. Ta namreč omogoča boljši vpogled v problem preklapljanja ter kvalitativno in kvantitativno strukturo trajektorije sistemskih stanj [13]. Komplementarno ogrodje se uporablja pri rešitvah za drsni režim vodenja [12], v praksi pa se ni izkazal za zelo uporabnega [13]. Problem modeliranja zagotovo postane še bolj zapleten pri obravnavi pravih vezij, kjer so idealni preklopi izključeni, pojavlja pa se nepredvidena ocenjena zaporedna upornost (ang. estimated serial resistance -ESR) skupaj z različnimi spremembami parametrov sistema.

V disertaciji bodo sodobne in omenjene metodologije ostale enake, le kombinacija znanih orodij bo zgrajena z multidisciplinarnim pristopom. To bo izključilo robni pogled iz tehnologije vodenja, matematične in računalniške znanosti ali lastnosti fizičnega sistema. Kljub temu vsi ti pristopi vplivajo na metodologijo, ki je uporabljena pri končnih algoritmih vodenja. S sklicevanjem na že objavljene študije, bi lahko poudarili nekaj sovpadajočih točk.

V nasprotju z nekaterimi znanimi rešitvami mehkega vodenja PEC pretvornikov [10], ki uporabljajo preprost mehanizem mehkega sklepanja in ad hoc uglaševanje, ali napredne in zapletene mehke rešitve v [9], ta študija izpostavlja hevristični pristop k mehkemu Takagi-Sugeno [21] modeliranju. Pri slednjem zmanjšuje število pravil in omogoča deterministično formulacijo posledičnih funkcij, ki se nadalje uporabljajo znotraj MPC vodenja. Nekatere novejše izdaje [22] so se izkazale za uspešne pri uporabi zmogljive mehke metodologije, to delo pa povečuje paradigmo pri modeliranju hibridnih sistemov, z namenom, da bi zmanjšali sprotno (on-line) kompleksnost in povečali uporabnost.

Eksplicitno modelno prediktivno vodenje (EMPC) zmanjšuje celotno kompleksnost MPC-ja [6] in doprinaša novosti pri reševanju problema »offline« optimizacije. Enaka ideja velja tudi za »offline« mehko identifikacijo, ki (že v fazi modeliranja) omeji kompleksnost, ki jo v večji meri doprinese napredni hibridni sistem. Pri ohranitvi podobne natančnosti bodo identificirani modeli predstavljeni kot globalni modeli. Zato lahko to disertacijo uvrstimo med študije, ki obravnavajo globalne sistemske lastnosti, ne pa tudi lastnosti specifične rešitve [61].

V poglavju IV bo pristop k modelnemu prediktivnemu vodenju, ki je del metode z dvema prostostnima stopnjama, predstavljen kot metodologija in ne kot posamezna tehnika [19], čeprav vključuje večino značilnosti, integriranih v MPC. Obravnavanje modela dinamičnega sistema nas je spodbudilo k uporabi MPC-ja na osnovi mehkega modela (FMPC) pri sistemu SAS [31-33,39-41]. Na področju mehkega vodenja [65] je uporaba mehke logike, kot polivalentne logične rešitve, pri odsotnosti čiste tavtologije (poglavje III), integrirane v MPC okolje, zelo malo verjetna.

Matematični okvir ne bo eksakten ter predstavljen kot problem diferencialne inkluzije in komplementarnega formalizma, temveč bo podan z rešitvami v psevdonormalnem vektorskem prostoru (poglavje III). Teoretično je dobro opisan v delu [28], sicer pa je elementarno povezan z aproksimacijo in operacijo glajenja disjunktnih množic znotraj Lebesgue-ovega prostora.

Večji del študije bo izveden v okolju MATLAB/SIMULINK [29] z uporabo lastnih (sprogramiranih) in vgrajenih podprogramov. Veliko pozornosti je bilo posvečeno izbiri trivialnih Matlab-ovih blokov in funkcij (ki se razlikujejo od običajnega objektno orientiranega programiranja), z namenom, da bi razkrili vse možne dogodke, ki so včasih prikriti z naprednim programiranjem.

1.1.2 Preverjanje sistema SAS glede na njegovo globalno lastnost

Na osnovi standardnih in uveljavljenih metodologij, ki smo jih že navedli, so v poglavju III predstavljene identifikacijske metode in teorija o tem, kako zmanjšati zapletenost pri vodenju, z iskanjem natančnejšega modela. Poenostavitev gre v smeri primarne dekompozicije kompaktne MPC metode na razlikovalne elemente, ki metodo naredijo kot zmogljivo orodje vodenja. Na to vsekakor vpliva dejstvo, da je obravnavani predstavnik sistema SAS (tj. DC-DC pretvornik navzgor) v odprti zanki stabilen sistem. Težava se pojavlja pri mehanizmu zaprtozančnega vodenja, ki lahko pride v neskladje s kompaktno rešitvijo vodenja. V disertaciji se osredotočamo na globalno lastnost sistema, pri čemer ima velik vpliv kvalitativna matematična teorija. To lastnost je potrebno preučiti s kvalitativnimi in kvantitativnimi značilnostmi sistema. Poznavanje sistemskega globalnega prostora stabilnih točk (kvantitativna značilnost) bo zagotovo poenostavilo končno rešitev vodenja. Kvalitativna lastnost dinamičnega sistema ali njegovega dinamičnega in globalnega modela bo omogočila celovito rešitev vodenja, ki bo vključevala vse cilje.

Zaradi želje po ustaljenem stanju robustnega modela DC-DC pretvornika navzgor, bo uporabljena metoda c-tih povprečij rojenja [36], ki bo omogočila izgradnjo globalnega in robustnega modela. S tem bo informacija o stabilnem delovnem ciklu enakovredno upoštevana za katerikoli izbor parametrov fizičnega sistema pri v vnaprej določenih univerzumih diskurzov, ki so bili naravno omejeni. Izbor univerzumov diskurzov ne vpliva na splošnost razvite metode, ampak le povečuje njeno končno uporabnost, kar je eden izmed glavnih ciljev.

S standardnim analitičnim modeliranjem pri aproksimaciji delovnega cikla (za določeno ustaljeno stanje) v omejenem območju [0,1] ne dobimo enakomerno porazdeljene napake. Z ozirom na to, se naše delo izogiba striktnim delitvam regij, ki so relativne in močno odvisne od izbire pripadnosti mehkega modela. Kot je bilo omenjeno, grafični model ni polieder odsekoma afinih sistemov z ostrimi robovi,

temveč kompleksna foliacija, ki jo dobimo z izogibanjem robovom in mehčanjem nedoločenih prehodov.

Naša tako zasnovana metoda temelji na trojnem pristopu. Prvi pristop vključuje prenos kompleksnosti izračuna v »offline« način. Pri drugem pristopu je glavni del raziskave posvečen ravnotežnim stanjem, v globalnem in robustnem smislu. Tretji pristop vključuje spremenljivke stanj, kot spremenjene povprečne vrednosti, saj privzema, da imamo popolnoma merljiv sistem.

Pri »offline« mehki identifikaciji, ki je predstavljena v tej disertaciji, gre za globalno rekonstrukcijo delovnega cikla ali MISO model. Slednji je predstavljen kot zbirka stacionarnih preslikav, lahko pa je tudi grafično povezan z različnimi procesnimi parametri. Katerikoli izbor izmerjenih vhodnih spremenljivk na vhodnih univerzumih diskurza je v celoti povezan z mehko strukturo z enoličnim stacionarnim delovnim ciklom. Identificirani model je globalni in eksplicitni model, ki predstavlja osnovo za prediktivno vodenje. Ta pristop se razlikuje od klasičnega prediktivnega horizonta MPC-ja, saj vrača časovno nespremenljivo rešitev, ki je bolj podobna neskončnemu horizontu, in ne zahteva izračuna inverza funkcije. V literaturi [9,10] avtorji obravnavajo hevristični pristop k mehkemu vodenju (ta se razlikuje od klasičnega mehkega vodenja), ki vključuje mehko identifikacijo. Nasproti poznanih rešitev na osnovi mehkih modelov [9,10], v našem pristopu se izogibamo striktno analitični strukturi, ki temelji na odsekoma linearni funkciji. Fragmentacija MPC metode nam pomaga pri izgradnji algoritma vodenja z dvema prostostnima stopnjama (poglavje IV), kjer linija krmiljenja z upoštevano motnjo določa stacionarni delovni cikel, ki temelji na eksplicitnem mehkem MPC-ju (EFMPC). Delovni cikel je nadalje popravljen z optimiziranim (za majhne signale) PI regulatorjem.

Ta študija pri obravnavi vseh zgoraj omenjenih ciljev predlaga in izpostavlja hevristični pristop, še posebej pri reševanju dvoumnosti modeliranja, kar jo v splošnem loči od drugih hevrističnih pristopov. V psevdo-Banachovem prostoru, ki je uporabljen s predpostavko, da je proces v celoti merljiv, lahko zgradimo Lebesgue-jev normirani prostor zveznih trajektorij. Z izključitvijo časa je v tem prostoru mogoče ustvariti pod-prostor stacionarnih stanj (poglavje IV). Slednji predstavlja edinstven pristop k napovedovanju dinamičnega ravnotežja, ki se kasneje uporablja pri povečevanju krmilne dinamike standardne rešitve vodenja. Kot taka je predikcija, ki temelji na ravnotežnem delovnem ciklu, bolj natančna kot analitična predikcija pri širokem spektru delovnih točk. Z namenom, da bi preučili kvantitativno/kvalitativno lastnost sistema, smo v disertaciji predstavili edinstven način modeliranja DC-DC pretvornika navzgor. To nas je vodilo tudi do razvoja nove tehnike vodenja, ki jo imenujemo prediktivno vodenje na osnovi mehkega modela (Fuzzy Model Based Predictive Control - FMPC). Ta tehnika minimizira dodatno on-line procesno zahtevnost.

1.1.3 FMPC kot sinteza naprednega algoritma vodenja in sodobnih ciljev

V tej disertaciji novo MPC metodo imenujemo FMPC, ker smo tehniko MPC uporabili v kombinaciji z mehkim identificiranim modelom.

MPC [18,19] kot kompaktna in standardizirana rešitev vodenja za časovno spremenljive sistemske matrike [20], v kombinaciji z mehkim modelom, predstavlja

napredno rešitev v smislu prilagodljivosti časovno odvisnega faktorju dušenja kriterijske funkcije. FMPC bo z izogibanjem kompleksnemu kvadratičnemu programiranju omogočal sub-optimalno vodenje.

Zato so nas standardne MPC metode, zgrajene na osnovi standardnih konceptov modeliranja (vhodno-izhodne oblike in prostor stanj), usmerile v kreiranje novega in uporabnega dinamičnega modela, ki temelji na mehki identifikaciji. Torej bomo v nasprotju s prejšnjim podpoglavjem 1.1.2 sedaj obravnavali mehki dinamični model. Glavni identifikacijski problem bo razčlenjen na večnivojsko identifikacijo, zgrajeno z mehko konjunkcijo identificiranih in lokalnih linearnih modelov. Poleg kvantitativnih lastnosti, ki so predstavljene v normiranem Banachovem prostoru, bo novi model vključeval tudi kvalitativne lastnosti sistema. Zato bo omogočal boljšo vodljivost ob prehodnih pojavih.

Čeprav je področje vodenja DC-DC pretvornikov že zelo dobro raziskano z vidika tehnik vodenja [3], modelno prediktivno vodenje (MPC) ostaja ena izmed najbolj pogosto uporabljenih in sistematičnih metod [5]. Široka paleta aplikacij za vse tipe pulzno energijskih pretvornikov (PEC) narekuje glavne značilnosti algoritmov vodenja in posledično omejuje celotne rešitve. MPC sistematično obravnava problem omejitev, hkrati pa dodatno obremenjuje procesor (povečuje čas izvajanja), kar zagotovo pojasnjuje glavno pomanjkljivost metode, ki se nanaša na zahtevnost računanja. Kompleksni algoritmi zagotovo doprinesejo nov scenarij nelinearnih pojavov v prehodnem času vodenja in v stacionarnem stanju sistema, kar škoduje stabilnosti sistema. Večina problemov, povezanih z vodenjem DC-DC pretvornikov, ki so bili obravnavani v preteklih delih, je bila v smislu negotovosti pri matematičnem modeliranju PEC pretvornikov.

To vodi k novi metodologiji vodenja, imenovani prediktivno vodenje na osnovi mehkega modela (Fuzzy Model Based Predictive Control - FMPC), ki minimizira on-line zahtevnost obdelave. Ta regulator, v nasprotju z že pojasnjenim TDOF regulatorjem, omogoča boljšo vodljivost ob prehodnih pojavih ter popolnoma izključuje referenčne prevzpone. Namreč, regulator predvideva asimptotično približevanje ustaljenemu stanju, običajno v skladu z odzivom sistema prvega reda.

Glavna inovacija regulatorja se kaže v kombinaciji Takagi-Sugeno (TS) mehke identifikacije in modelno prediktivega vodenja. V nasprotju z drugimi znanimi MPC pristopi k vodenju DC-DC pretvornikov (predvsem najbolj razvito eksplicitno modelno prediktivno vodenje (EMPC) [6]), ki uvajajo inovativnost pri reševanju optimizacijskega problema striktno »offline«, je v tej študiji bila razvita aproksimacija hibridnega dinamičnega sistema z zveznim modelom. Ta aproksimacija temelji na »offline« identifikaciji. Prednost nove metodologije je dvojna. Prvič, zmanjšuje kompleksnost s tem, da ohranja red sistema povprečno-preklopnih modelov (red sistema se običajno dvigne z večpomenskimi spremenljivkami [3,4,17]) in hkrati zmanjšuje število regij v robustnem smislu. Drugič, metodologija doseže boljšo natančnost modela za robustne in še posebej za fizične primere, pri čemer je preklopna perioda enaka času vzorčenja. Ta metoda usklajuje stopnjo natančnosti s kompleksnostjo ali uporabnostjo. Zato je ta rezultat spodbudil identifikacijo sistema, ki sicer že ima analitično pridobljen model za robustne rešitve. Zvezna aproksimacija sistema je nato predstavljena v diskretni obliki, ki je osnova standardnega modelsko prediktivnega regulatorja s prediktivnim horizontom. Matrike v prostoru stanj za model DC-DC pretvornika navzgor niso pridobljene analitično, ampak kot časovno odvisni izhodi mehkega mehanizma, ki

hevristično povezuje predhodno identificirane regije. Kot primer denimo, da imamo v obliki treh matrik (27x5, 3x3 in 3x3), ki so shranjene v pomnilniku procesorja, podane, eksperimentalno pridobljene informacije o sistemu. S preprosto »online« aritmetiko je mogoče pridobiti te informacije, ki so zapisane v polju realnih števil. Vse konveksne optimizacije se izvajajo »offline«, »online« računska zahtevnost pa je povezana s tipičnimi problemi MPC-ja oz. v našem primeru tudi z matrikami z zmanjšanim rangom, ki pripadajo poenostavljenemu linearnemu modelu. Metoda je uporabna tudi za bolj zapletene sisteme (MIMO); v disertaciji je predstavljen model NARX MISO. Ugotovljeno je bilo, da je bil poskus z identificiranim MIMO modelom v našem primeru nepotreben, v smislu primerjave natančnosti modelov, kar je bil eden izmed pristop pri izbiri regresijskih vektorjev.

Zgoraj omenjene trditve so bile potrjene z eksperimentalnim vrednotenjem metodologije.

1.2 Pričakovani in originalni prispevki k znanosti

- Poglobljena analiza problematike modeliranja DC-DC pretvornikov iz vidika nelinearnosti, nezveznosti in pričakovane stopnje natančnosti matematičnega opisa.
- Razvoj novih identifikacijskih pristopov za mehko modeliranje DC-DC pretvornikov, ki so primerni za izvedbo vodenja.
- Predlog novega pristopa vodenja preklopnih afinih sistemov z uporabo hevristike in dvoprostosnega vodenja, kjer je predkrmiljenje izvedeno s statičnim inverznim mehkim modelom in vodenje z regulatorjem PI.
- Vpeljava prediktivnega vodenja na osnovi mehkih dinamičnih modelov z majhno računsko zahtevnostjo in delovanjem v relanem času.

University *of Ljubljana*
Faculty *of Electrical Engineering*

Robert Baždarić

APPROACHES TO THE FUZZY-MODEL-BASED CONTROL OF SWITCHED AFFINE SYSTEMS

DOCTORAL DISSERTATION

Supervisor: Prof. Dr. Igor Škrjanc
Co-supervisor: Prof. Dr. Drago Matko

Ljubljana, 2017

Acknowledgements

This study, covering a wide range of disciplines, would not have become this dissertation without the guidance, advices, and the theoretical support given by my supervisor. Thus, many thanks to Prof. Dr. Igor Škrjanc. Not less important is thanking my co-supervisor Prof. Dr. Drago Matko for his understanding of my approach to the research, corrective thinking, and constructive suggestions throughout the study.

Many thanks to my supervisor in previous studies, Prof. Dr. Danjel Vončina and his overall support, patience in long discussions and finally support in the experimental part of this study. Thanks to the Laboratory of Control Engineering and Power Electronics, especially to Dr. Aleš Leban, for his devoted work to the setup on the testing bench and understanding of most detailed subjects related to the control algorithms.

I must thank in general the Laboratory of Autonomous Mobile Systems, and exceptionally to Prof. Dr. Gašper Mušič and his always-friendly advice.

Last but not least, thanks to my family in general, to my loving wife Snježana, for her unselfish sharing of good spirit that has been crucial to the continuation of my studies. Also, thanks to my loving children, Ivana and Luka, my parents Milica and Boris, and my brother, Marin, for their kindness in listening, understanding and supporting my studies.

Abstract

Hybrid systems control has been of great scientific interest over the past two decades. This is mostly because of its applicability to a broad range of physical systems, especially those resulting from technological advances. The aim of this study is developing a pragmatic avoidance of nonlinear phenomena in the control of hybrid systems (HSs), focusing on the subgroup of switched affine systems (SASs). The developed control laws will propagate the heuristic approach and present the author's general idea for the control of nonlinear dynamical systems. The main emphasis will be given to Fuzzy Identification as the universal approximation in the modelling and evolving of multi-structural and global models in two directions. First, we identify the steady and stable states of a HS and model it into the global knowledge of a nonlinear dynamical system. Second, we identify the dynamical model of the HS with arbitrary accuracy, which presents the system's qualitative and quantitative characteristics in an analytical way.

The control methods derived accordingly should emphasize the Fuzzy Model Predictive Control (FMPC) of the HS by reducing the main drawback in the complexity of online computing. Furthermore, the combination with suboptimal control gives a wider applicable control algorithm, even in systems consisting of less-powerful microprocessors. Traditionally, the simplification of a HS, i.e. the *averaging* method in the modelling of electronic circuits, in which the system is presented with an avoidance of the mixed discrete and continuous states by a simple continuous model, as well as the modern theory of hybrid system modelling, will be harmoniously integrated in this study. The conciliation of those two modelling extremes affirms nonlinear identification-based modelling as the leading strategy towards a wider applicable solution. The main idea is still to model a complex discrete/continuous system with a continuous counterpart, but by being aware of its complexity caused by the mode transitions influencing their final and unique model. The systems explored are full state measurable. This condition supports the main idea and opens the possibility to gather the system's information by the measurement of the complex states' transitions (continuous trajectories and discrete states of the system simultaneously). Later, the information remains preserved by the final state-space transformation into the pseudo-normed space. These ideas form a firm basis for the novel control methods and the achievement of the defined objectives.

Selected as an example of such a system for performing the expressed methodology, a DC-DC Boost converter is not only a good SAS representative, but a contemporary one of the widely used power supplies, applicable in most alternative-energy sources. Its importance has occupied various types of researchers since the first developed semiconductors. The exclusion of the nonlinear phenomena [1,7-10,56,57] is one of the main motivations and the objective in seeking a control algorithm that is more intelligent, robust and economical in the use of processing space.

The accuracy of the mathematical modelling, in contrast to the first known modelling of the aforementioned system in the works of Ćuk, Ericskon, Middlebrook

[23,24], places the emphasis on the transition moment of the states and the function's discontinuity at that time. Although these problems were well recognized in the middle of the 20th century, but no less importantly they are emerging again in definitions of the *chattering* effects, the *Zeno behaviour* and the nonlinear phenomena, even in the established HS methodologies.

A small signal control derived from linear theory gives satisfactory results in the neighbourhood of the operating point, and a linearized model (Averaged-Switch Model) opens up the possibility of a complete analytical examination. However, as mentioned previously, to achieve robustness of the control algorithm, the theory of nonlinear dynamical systems must have the main role in improvements to the operating range of the DC-DC converters and SAS in general.

The hybrid structure [2,3], robust solution [3,4], natural constraints [3], complexity reduction [5,6] and emerging problem of nonlinearities exclusion [7-10], can all be recognized as appealing tasks for the control of a DC-DC boost converter. State-of-the-art control solutions [3] are mostly based on Linear Matrix Inequalities (LMIs) optimizations in hybrid systems [3,5,6], relaxation algorithms in the sense of complexity reduction [11], complementarity formalism in reducing the modelling ambiguity [12,13], sliding mode control [14,15] and heuristic approaches, neural networks and fuzzy controls [10,16,138]. The latest [16, 138] work is synthesized, in detail presented in this thesis and forms a unique and advanced control methodology in field of SAS control as a result of excessive research done on the DC-DC boost converter.

Keywords: hybrid system, switched affine system, nonlinear phenomena, DC-DC converter, modelling of a DC-DC boost converter, identification of nonlinear systems, fuzzy models, fuzzy model based identification, predictive control, fuzzy model predictive control, fuzzy dynamic matrix control, fuzzy generalized predictive control, fuzzy predictive functional control.

Acronyms

AC	Alternated Current
ARX	AutoRegressive eXogenous
CCM	Continuous Conduction Mode
DC	Direct Current
DCM	Discontinuous Conduction Mode
DHA	Discrete Hybrid Automata
DMC	Dynamic Matrix Control
EFMPC	Explicit Fuzzy Model Predictive Control
EG	Event Generator
ELC	Extended Linear Complementarity
EMI	Electro Magnetic Interferences
EMPC	Explicit Model Predictive Control
ESR	Estimated Series Resistance
FDMC	Fuzzy Dynamic Matrix Control
FEM	Fuzzy Explicit Model
FGPC	Fuzzy Generalized Predictive Control
FIRM	Finite Impulse Response Model
FL	Fuzzy Logic
FLC	Fuzzy Logic Controller
FMPC	Fuzzy Model Predictive Control
FNARX	Fuzzy Nonlinear AutoRegressive eXogenous
FPFC	Fuzzy Predictive Functional Control
FSM	Finite State Machine
FSRM	Finite Step Response Model
GPC	Generalized Predictive Control
HDS	Hybrid Dynamical System
HS	Hybrid System

HYSDEL	HYbrid System DEscription Language
IC	Integrated Circuit
IDB	IDentification Based
IO	Input Output
IP	Integer Programming
ITAE	Integral Time Absolute Error
LC	Linear complementarity
LCP	Linear Complementarity Problem
LMI	Linear Matrix Inequality
LP	Linear Programming
MF	Membership Function
MIMO	Multiple Input Multiple Output
MIP	Mixed Integer Programming
MISO	Multiple Input Single Output
MLD	Mixed Logical Dynamical
MLP	Multiparametric Linear Programming
MMPS	Max-Min-Plus-Scaling
MPC	Model Predictive Control
MQP	Multiparametric Quadratic Programming
MS	Mode Selector
MSE	Mean Squared Error
NARMAX	Nonlinear AutoRegressive Moving Average eXogenous
NARX	Nonlinear AutoRegressive eXogenous
NBJ	Nonlinear Box-Jenkins
NFIR	Nonlinear Finite Impulse Response
NMPC	Nonlinear Model Predictive Control
NOE	Nonlinear Output Error
ODE	Ordinary Differential Equation

OP	Operating Point
PEC	Pulse Energy Converter
PFC	Predictive Functional Control
PI	Proportional Integral
PLC	Programmable Logic Controller
PWA	Piecewise Affine
PWARX	Piecewise AutoRegressive Exogenous
PWL	Piecewise Linear
PWM	Pulse Width Modulation
RMS	Root-Mean-Square
SARX	Switched Affine AutoRegressive Exogenous
SAS	Switched Affine System
SISO	Single Input Single Output
SSE	Sum of Squared Errors
T-S	Takagi-Sugeno
TDOF	Two Degrees Of Freedom

Table of Contents

Chapter I

Introduction

1.1 Overview of the content of the doctoral thesis

The motivations of the study already underlined in the abstract, must introduce the approach to fulfil all our objectives. The selected physical system is a hybrid, and can be described by continuous and discrete states. Despite the already-known hybrid control methods, and the hybrid modelling, as mentioned previously, this study gives an alternative method involving the identification of a nonlinear dynamical system. The reason for this lies deep in the theory of HS, which is progressing towards the creation of a general modelling formalism for systems with the co-existence of the continuous and discrete signal phenomena appearing in arbitrary combinations [2,62-64]. The Chapter II of this thesis will provide the fundamental definitions of HS that explains an overall deterministic approach in modelling of those systems and based on that the main idea of this thesis. The idea will be carried out through the thesis by problem partitioning, which is then rendered as a threefold strategy in Chapters III and IV.

First, close attention will be given to the simulation in general, meaning to develop the simulation model as close as possible to the physical system's behaviour, bearing in mind that the use of predefined simulation objects can easily mislead us in our further development of the controls. In contrast, the advantage of the modern simulation platform and the numerical integration methods will be used to construct and synchronously simulate discrete and continuous functions of the physical system so accurately. A knowledge of the examined model will help in the following steps of development.

Second, the following study is carried out differently from that known in PECs to find an accurate modelling, which also preserves a robust and general knowledge of the system. It must provide the mathematical form that is subsequently applicable for the well-developed control methods. The method based on a state measurable system will transfer the main burden of a nonlinear dynamical system examination strictly to the offline problem, with all its complexity. In contrast to what is already known, further study will avoid the use of local linear models for a particular mode of the system operation. It will identify the local linear model for the natural combination of all the modes of the systems' operation in one system's switching period. To realize the idea and to formalize the applicable form of the model, dictated by the final control algorithm, two different methods of identification will be applied. Both models will be derived by the Fuzzy Identification [34-36,65] of the input/output data (Chapter III).

Third, the system's examination via fuzzy identification and modelling will be a base for a development of the advanced control algorithms. As the identification methods and goals were different, equally the development of the control algorithms

will evolve in the two novel control methods. Based on the model of the converter's steady state and using the two degrees of freedom methodology [44], the new control algorithm will be derived. Oppositely and based on the rendered dynamical fuzzy model, a new fuzzy model predictive control algorithm will be designed [18,20,38] (Chapter IV).

Finally, both sides of development, the identification and control, will be tested on the physical process and accordingly evaluated (Chapter IV). Chapter V concludes with a short retrospective of the thesis in general and its achievements.

1.1.1 Established methodologies in seeking for an advanced control algorithm in SAS

The methodology to be used in achieving the aforementioned objectives, later forming the doctoral thesis, will be integrating modern and advanced fuzzy methods in the identification and modelling, developing a novel method of hybrid systems control. Even in the presence of already-developed advanced hybrid control methods, namely MPC based on MLD models, LC-based control and Symbolic Model-Based Control [6,12,13,17,26,63] (Chapter II), our methodology will refresh the standard MPC approaches.

In this thesis, we will point out the main misfortunes of the established methodologies that will direct our work differently.

Mainly, we have selected a MPC methodology demanding a comprehensive devotion to the modelling of such systems. If we simply concentrate to a development of the modern methods strictly focusing the DC-DC conversion, then we can conclude the following.

Hybrid modelling and control represent the state of the art in the exploration and design of Pulse Energy Converters (PECs)[3], for which the authors give a short overview and a comparison of the profiled hybrid approaches, mostly based on *LMI*, and optimization by convex programming or a *Lyapunov-function-motivated* stability optimization. Systematic control approaches implement *LQ* optimization [42] or H_∞control [4] in a sense to provide a certain robustness to the plant's uncertainty and are all based on a linearized sampled data model. In contrast, relaxing the dynamic programming introduces a complexity to the optimization and opens up the well-known Lyapunov-function selection problem [11], with a solution in time-limiting convergence. Of no less importance is to consider the overall applicable approaches based on current control and known as *sliding mode control* [14,15].

This thesis focuses strictly on output-voltage control that has a correlation with most of the mentioned hybrid modelling approaches, but mostly it is in agreement with the objectives in the present, PEC control development. Generally, while the MPC [5,17] is opening the discussion of duty-cycle modelling and an approximation with ν-resolution, in this work we avoid the strict resolution that is relative and very much depends on the *Fuzzy Model Membership* construction. The softening of HS region constraints by the *Fuzzy Logic* evolves in the graphical model that is not a polyhedron with sharp edges, but rather by avoiding the edges and softening transits, it is a complex foliation. We can see that the usage of the Fuzzy Identification has a correlation with dynamical programming [11] and the relaxation method that produces the same findings in relation to the stability of the optimization algorithms, the prediction of the convergence time and the stopping

problem. This reinforces our experiences and supports the opinion that there is still a necessity for offline optimization, even considering of modern processors' capabilities.

To employ the advanced and established MPC, but still applicable for the systems that are relatively trivial and fast, this thesis is changing an approach in the phase of the system's modelling. We bring a thesis that the system's modelling cannot be just extruded from the final application goal and control as a mathematical task, but it has to be a genuine part of that goal as the final physical exploitation. Chapter II of this thesis provides a comprehensive survey, and gives several concerns in the established modelling of SAS focusing the DC-DC boost converter. In short, and strictly connected to the problem of a boost DC-DC converter we can pose some the most characteristic relations to already exemplified and published. In Chapter III we seek an alternative and identified mathematical model that is mediating the benefits and misfortunes of the previous and known studies.

In one switching period T_s we receive multiple changes to the semiconductors' positions and, necessarily, the circuit's topology. Most of the previous modelling [1,7,8] are based on the successive adding of the piecewise affine models or forming an average-switched model well presented in the publication of Middlebrook and Ćuk [43]. The modelling solution is based on the perturbation method, and it is valid for small signal values. Furthermore, the same authors, together with Erickson [24], provide more precise modelling, called *large signal* modelling, which is also applicable for robust applications. In today's control solutions, more interest is put on nonlinear phenomena exclusion [1,7-10], which necessarily leads the mathematical discussion to well-posedness and solution existence in the modelling of hybrid systems [27]. From modern mathematical aspects, the modelling of DC-DC converters leads to complementarity formalism [13,27] and has to be treated accordingly. It gives a better insight into the switching problem and a qualitative and quantitative system-state trajectories' pattern [13]. A complementarity framework is used in sliding-mode control solutions [12], but with no wider control applicability [13]. The modelling problem certainly becomes more complicated by assuming real circuits, where the ideal switches are excluded and an unpredicted estimated serial resistance (ESR) is encountered, combined with a different system's parameter changes.

In the subsequent thesis the modern and mentioned methodologies will remain the same, but the combination of known tools will be constructed by the multidisciplinary view. That will exclude the corner view from the control technology, mathematical and computer science or the physical system properties enforced in the final application. Nevertheless, all these approaches have influenced the methodology presented in the final control algorithms. By constructing the cross-reference with similar published studies, we could underline some coinciding points.

In contrast to some of the known fuzzy control solutions in PEC [10], using a simple fuzzy inference mechanism and ad-hoc tuning, or advanced and complex fuzzy solutions in [9], this study underlies the heuristic approach in the fuzzy modelling of Takagi-Sugeno [21] by reducing the number of rules in the rule base and allowing a deterministic formulation of the consequent functions further used in MPC. Some newer releases [22] are successful in employing a powerful fuzzy methodology, but this work is augmenting the paradigm in the modelling of the system's hybrid nature in order to minimize the online complexity and increase the applicability.

Explicit Model Predictive Control (EMPC) brings novelty in tackling the optimization problem strictly offline, reducing the overall MPC complexity [6]. Following the same idea, already in the phase of modelling, in this study, offline fuzzy identification overcomes the complexity mostly caused by involving the advanced hybrid system to raise the model's degree of accuracy. By preserving a similar accuracy, the identified models will be *Global Models*, whereby the following thesis is considered to be a global system properties' examination, rather than the unusual properties of a specific solution [61].

It will be presented in Chapter IV that the model based predictive control approach in the two degrees of freedom method of this thesis is emphasized as more of a methodology than a single technique [19], but has most of the MPC-integrated features in the compact control technique. In contrast, a rendering of the dynamical system model will promote the Fuzzy-Model-Based MPC or simply FMPC in SAS [31-33,39-41]. In the field of the fuzzy controls [65] using the Fuzzy Logic just as the polyvalent logic solution in the absence of the pure tautology (Chapter III), integrated into the MPC framework is very unlikely.

The mathematical framework will not be exact and exemplified as a problem of *differential inclusion* and *complementarity formalism*, but rather solutions in the pseudo norm vector space (Chapter III). Theoretically, it is strongly supported in [28], and elementarily connected to the approximation and smoothing operation of disjoint sets in the Lebesgue space.

The major part of the study will be done on the MATLAB/SIMULINK platform [29] using the author's programmed and embedded subroutines. A great deal of care is given to the selection of the trivial *Matlab* blocks and functions (again different than the usual object-based programming) in order to magnify and possibly reveal all the natural events, sometimes masked by the advanced programming.

1.1.2 Examination of the SAS by its global property

On the bases of standard and established methodologies expressed earlier, the Chapter III of this thesis is presenting the identification methods and theory that overcome the complexity in controls by seeking for a more accurate model. The simplification goes in a direction to primary decomposing of the compact MPC method on distinctive substances that make the method a powerful control tool. That is certainly influenced by the fact that the examined representative of the SAS, a DC-DC boost converter, is an open-loop stable system. The problem appears with a feedback control mechanism that can be entangled deeply with the compact control solution. Being influenced by a qualitative mathematical theory, this thesis is focusing the global property of the system. That property has to be examined by the system's qualitative and quantitative characteristics. Having the knowledge of the system's global space (quantitative characteristic) of the stable points will certainly simplify a final control solution. However, the qualitative property of the dynamical system, or its dynamical and global model in general will give the comprehensive control solution that integrates all objectives.

The interest in the steady-state robust pattern of a DC-DC Boost Converter will employ the c-means clustering method [36] to build up the global and robust model.

This is to equally contain the stable duty cycle information for any selection of the physical system's parameters in the predefined universes of discourses that were naturally constrained. The selection of the universes of discourses does not influence the generality of the developed method, but only increases its final applicability, which is one of the main objectives.
Standard analytical modelling does not give a uniformly spread error for the duty-cycle (for the specific steady state) approximation in the constrained range **[***0,1***]**. With respect to this, our work avoids strict region separations that is relative and strongly depends on the *Fuzzy Model Membership* construction. With this approach and, as mentioned, a graphical model is not a polyhedron of the piece-wise affine systems with sharp edges, but rather by avoiding edges and softening uncertain transits, it is a complex foliation.
Our thus-based method is built on the basis of a three-fold approach. First, transfer the complexity of the computation to the offline regime. Second, concentrate the major part of the examination on the equilibriums in a global and robust sense. Third, by assuming a fully measurable system, involve the state variables as transformed average values.
The Offline Fuzzy Identification presented here is a global duty-cycle reconstruction, or MISO model as an atlas of the steady-state mappings or graphically a folium related to different process parameters. Any selection of the measured input variables on the input universes of discourse is associated throughout the fuzzy engine with a single and unique steady-state duty cycle. The identified model is the *Global and Explicit Model*, which then constructs the bases for a predictive control. This approach differs from the classic preceding horizon MPC as it gives a time-invariable solution that is more similar to the infinity horizon solution, hence being explicitly driven without the necessity for an inverse function calculation. Also different than a classic fuzzy control [9,10], this paper supports the heuristic approach that implements the fuzzy identification, and after a modelling, moves from the strict analytical framework built on the piecewise linearity. The fragmentation of the MPC method leads us to the construction of the Two Degrees of Freedom Control (Chapter IV), in which the feed-forward line selects the explicit fuzzy MPC's (EFMPC) based steady duty cycle, further corrected by the small signal PI optimized controller.
This study, in considering all of the objectives mentioned above, is suggesting and underlining the heuristic approach, but only in tackling the modelling ambiguity, which makes it different than other heuristic approaches, in general. In the pseudo-Banach space, developed with the assumption that the process is fully measurable, the Lebesgue 2 normed space of continuous trajectories can be constructed. With the time exclusion, this space gives an ability to form the steady-state's subspace (Chapter IV). It presents a unique approach to the prediction of control equilibrium, later used in the boosting of the control dynamics of a simple and standard control solution. As such, the steady-state duty cycle-based prediction is more accurate than the analytically driven one for a wide range of operating points. Subsequently, to evolve the examination of the quantitative system's property to the quantitative/qualitative property, this thesis presents a unique modelling principle of a DC-DC Boost Converter. This leads to a new control technique called Fuzzy Model Based Predictive Control (FMPC), but with minimized extra online processing complexity.

1.1.3 FMPC as a synthesis of an advanced control algorithm and the modern objectives

In this thesis, the new MPC method is called a FMPC because of the MPC technique applied on the fuzzy identified model.
The MPC [18,19] as a compact and standardized control solution for time-variable system matrices [20], integrating the fuzzy model and, therefore, is advanced in the adaptive time-dependent cost function's suppression factor and will represent the sub-optimal control with the avoidance of complex quadratic programming.

Hence, the standard MPC methods built up on the standard modelling principles (the input/output forms and the state space) are taking us in the direction of forming a novel and applicable dynamical model that is also based on fuzzy identification. Now, in contrast to the previous (Subsection 1.1.2), it will be a fuzzy dynamical model. The main identification problem will be decomposed in the multilevel identification, built in the fuzzy conjunction of the identified and local linear models. In addition to the quantitative properties, similarly rendered in the normed Banach space, a newly derived model will also comprehensively consist of the system's qualitative properties. Subsequently, it will pursue better controllability in the transient times.
Even though the control of DC-DC converters has been very well examined from different aspects with respect to control techniques [3], model predictive control (MPC) remains one of the most systematic and frequently used methods [5]. The wide range of applications for all type of pulsed-energy converters (PECs) dictate the main features of control algorithms and as a result place constraints on the overall solutions. MPC systematically handles the problem of constraints, but at the same time puts an extra burden on the processor's time of execution and certainly explains the method's main drawback, which relates to the complexity of computation. The complex algorithms then necessarily affirm a new nonlinear phenomena scenario in the transition time of the control and the system's steady state, thus harming the stability of the system. Most of the problems addressed in previous work on the control of DC-DC converters were in terms of the uncertainties in the mathematical modelling of PECs.
This leads to a new control methodology called Fuzzy Model-Based Predictive Control (FMPC), but with minimized extra online processing complexity. Differently than in the previously explained TDOF controller, the following has better controllability in transients and completely excludes the set-point overshoots; it asymptotically approaches to the steady state, typically for the first-order system response.
The main controller's innovation is found in the combination of the Takagi-Sugeno (TS) Fuzzy Identification and the Model Predictive Control. In contrast to any other known MPC approaches in the control of DC-DC boost converters, especially the most developed Explicit Model Predictive Control (EMPC) [6], that bring innovation in tackling the optimization problem strictly offline, this study builds a continuous model approximation of a hybrid dynamical system based on offline identification. Here, the advantage of the new methodology is twofold. First, it reduces the complexity by preserving the system order of the averaged-switch models, usually lifted by ambiguity variables [3,4,17], and at the same time reduces the number of regions in a robust sense. Second, it achieves better model accuracy for robust and

especially physical cases where the switching period is equal to the sampling time. Finally, this method conciliates the grade of the accuracy, with either complexity or applicability. This is why that result encouraged the approach of identifying the system that has an already known, analytically driven and arbitrary accurate model for the robust solutions. The continuous system's approximation is afterwards presented in its discrete form as the base for the standard model predictive control problem with the preceding horizon principle. The state-space matrices are not analytically driven for the DC-DC Boost converter, but these are time-dependent outputs of the fuzzy engine that heuristically correlates the previously identified regions. As the example, the experimentally rendered system's knowledge is presented by three arrays (27×5, 3×3 and 3×3) stored in the processor's memory. The simple online arithmetic extracts the knowledge written in the arrays of real numbers. All the convex optimization is made offline, and the online calculation's complexity is related to the typical MPC problems, but now with the matrices of a reduced rank of a simpler linear model. The method is applicable for more complex systems (MIMO); even in this thesis, the presented model is NARX MISO. The experiment with the MIMO identified model, for our example, was found to be unnecessary, as a consequence of the models' accuracy comparison, which was either the approach in the selection of the regression vectors.

As a conclusion, the experimental evaluation of the methodology confirms the aforementioned statements.

1.2 Expected and original scientific contributions of the doctoral thesis

- This study presents a paradigm in the mathematical modelling of a DC-DC Boost Converter developed from the aspects of nonlinearity, the system's discontinuity, and the degree of its mathematical model accuracy.
- It develops novel fuzzy model identification principles for a DC-DC Boost Converter that are applicable to the construction of the control methods.
- It suggests a new approach in controls of Switched Affine Systems based on the heuristics and Two-Degrees-of-Freedom control that defines the feedforward line based on the inverse fuzzy model and PI controller.
- It applies the fuzzy model predictive control methodology that minimizes the processing complexity and the processor's real time of execution.

Chapter II

Hybrid systems, the modelling paradigm of SAS

2.1 Hybrid Systems

Hybrid dynamical systems occupy broad range of scientific interest. One of the reasons could be found in the fact that the modern technology growth remains based on digital processing, and pushing towards the infinitely short time of executions. Indeed, that is a progress to provide as small as possible electronic components with the less energy consumption. Allegedly it widely opens the door for different development directions in a wider range of disciplines. As a product of that process, it is almost impossible not to find examples of that system in our urban surroundings, starting from a simple water heating system (boiler) to the complex aircraft control. Mainly it is a result of human needs in the controlling of natural processes and producing the special mechanisms or devices.
We can simply say that those systems are dated from the first appearance of the relay. Even though they were present earlier, the main renaissances of the theory of the hybrid dynamical systems emerged roughly 25 years ago.
The Hybrid Dynamical System (HDS) is considered to be a system built up from combinations of naturally continuous and discrete parts.
The modelling paradigm of HDS starts with a thoughtful transformation of that system into the completely continuous or oppositely discrete model. According to the literature [66], and mostly because of some authors' specific distinctions in the approaches, we can assign groups; e.g. of those participating in the aggregation, continuation, automata or system methods. All of the approaches just give an arbitrarily accurate solution, simultaneously containing both advantages and disadvantages, which is why this problem still inspires or motivates scientific solutions. Scientists are pursuing their analysis via fully deterministic forms or slightly relaxed with no determinism. It is demanding to give a general survey throughout the massive literature available from the HDS realm and such a work can be found in [2,66].
As the HDS attract multidisciplinary interest, the research contributions can be generally recognized in typical categories: the modelling, the analysis, the control and a design of HDS.
This thesis will contribute to the modelling, control and analysis. It is common for modern control solutions focus on the modelling of nonlinear dynamical system. Thus, HDS modelling is appealing by its discrete part of the system that is tangled together with the system's continuous or analog parts. The discrete phenomena in HDS appear as:

1. autonomous switching
2. autonomous jumps
3. controlled switching
4. controlled jumps.

Most of the previous authors found the appropriate modelling approach driven by different systems discrete paradigms [66]. Referring to their work, some of their methods are named after them, e.g. Witsenhausen's model, Tavernini's model, the Back-Guckenheimer-Mayers model, the Nerode-Kohn model, the Antsaklis-Stiver-Lemmon Model, the Brockett's model, etc. In the mathematical analysis of these models, similarities and differences can be found [65], but commonly the main characteristic of those methods was not the idea of forming the general framework or methodology in the modelling of all HDS. In contrast, those attempts are rather specifically oriented methods driven by the final goal in the system's application.
Modern methodologies are driven by the generalization in the theory of HDS; accordingly, this thesis is supporting that approach. Of course, that generalization will have its topological varieties applicable in the wider range of HDS.

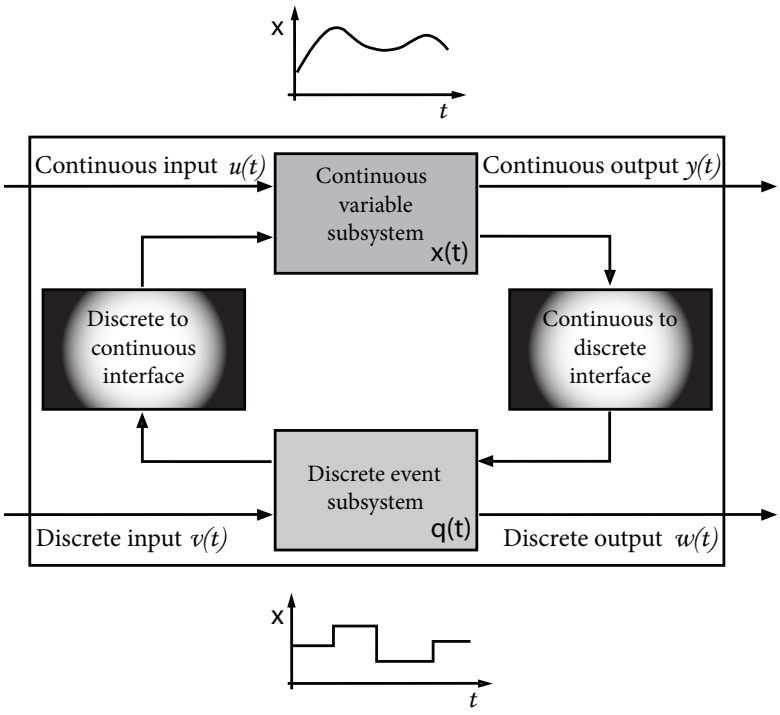

Fig. 2.1 Structure of hybrid system

Our approach in modelling emphasizes that idea, but at the same time amplifies the importance of switching phenomena in the modelling, very much in common with the old methodologies. As the HDS is a broader realm, it is even today very controversial with regards to group specific modelling approaches, and is rarely comprehensive. We are going to point out a few the most distinctive approaches [2]:
- hybrid automata
- timed automata and timed or hybrid Petri nets
- PWL and PWA
- switched systems
- differential automata
- mixed logical dynamical models
- real-time temporal logics and time communicating sequential processes

• complementarity systems
• hybrid inclusions.

Fig. 2.1 is very common for the explanation of the hybrid system's nature; it can help us in presenting the main approaches in HDS model classes. Modelling differences are mostly related to the correlation between the continuous variable subsystem and discrete event subsystem. The interaction leads are presented by "discrete-to-continuous interface" and "continuous-to-discrete interface". The first is defined by the discrete system's state change, also called an injector. In contrast, the second is an event generator usually referring to the continuous trajectories hitting the switching surface.

2.1.1 Hybrid automata

The most comprehensive modelling approach of hybrid systems is the Hybrid Automata. Branicky [62,66] in his survey of modelling of hybrid systems found it as a distinctive way of pursuing the hybrid systems' modelling by automata. The theory of hybrid automata is a continuation of studies of the finite state machines and evolves by integrating the continuous and discrete dynamics together into the infinite state machine.
A milestone in the definition of the hybrid automata was in Henzinger's "Theory of the Hybrid automata" [62], and consisting of: *variables*, *control graph*, *initial, invariant, flow condition, jumps and events.*
We are more in favour of a definition that is more broadly applicable, in the form presented by Definition 2.1 [2,62,63].

****Definition 2.1**[2] (**Hybrid Automaton**) A hybrid automaton **H** is a 10-tuple*
$\boldsymbol{H} = (Q, X, f, Init, Inv, \Theta, \mathcal{G}, \mathcal{R}, \Sigma, \lambda)$,

where

* $Q = (q_1,...,q_k)$ *is a finite set of discrete states* (*control locations*);
* $X = (x_1,...,x_n)$ *is a finite set of continuous variables*;
* $f : Q \times \mathbb{R}^n \to \mathbb{R}^n$ *is an activity function over* X;
* $Init \subset Q \times \mathbb{R}^n$ *is the set of initial states*;
* $Inv : Q \to \mathbb{R}^n$ *describes the invariants of locations*;
* $\Theta \subseteq Q \times Q$ *is the transition relation;*
* $\mathcal{G} : \Theta \to 2^{\mathbb{R}^n}$ *is the guard condition*;
* $\mathcal{R} : \Theta \to 2^{\mathbb{R}^n} \times 2^{\mathbb{R}^n}$ *is the reset map*;
* Σ *is a finite set of sinchronization lables*;
* $\lambda : \Theta \to \Sigma$ *is the labling function*.

The automaton **H** *describes a set of hybrid states* $(q, \boldsymbol{x}) \in \mathcal{H} = Q \times \mathbb{R}^n$.

This form is generalized for the hybrid system with more advanced topology built on the multiple hybrid automata. Further on in those constructions the weight is given to the synchronization and time in general. The theory of hybrid automata evolves in the approximated symbolic models for control. Mathematically based on the theory

of sets, it can be proven that those approximations are having arbitrarily accurate similarity to the real systems. In a literature, the definition of hybrid automata appears in different forms motivated by authors' scientific discipline. For example, from the aspects of the systems' control, and following observations of the fundamental hybrid systems (not composed of more than one HS), it is formulated and can be found in [63].
Theoretically, with hybrid automata we can define all hybrid dynamical systems bearing in mind that most of them are a combination of the characteristics of the finite-state and the infinite-state systems. Certainly, it is a nontrivial task to define the tangled guards, invariants and reset maps for such a system.
Therefore, this troublesome task can be simplified by partitioning of such a system into a multiple finite-state system of the reduced complexity. Besides mentioning the most fundamental the *linear hybrid automata* or the *rectangular hybrid automata* as a unified hybrid constructive element of a more complex hybrid system, we can also point out in the literature [63] some other simpler modelling cases: Transition Hybrid System and the Timed Automata. Those systems are used in providing of feasibility to cumbersome methods of verification and synthesis (Transition Hybrid Systems) or in giving the profundity in systems containing the clock variables (Timed Automata).

2.1.2 Piecewise affine (PWA) system

It should be highlighted that the fragmentation of the complex nonlinear systems unconditionally brings into focus PWA systems as the one of the basic hybrid modelling approaches. The system could be naturally PWA, but frequently is also a product of a problem partitioning. As mentioned earlier, different strategies in the modelling and classifications of a hybrid dynamical system can be divided in two main directions. The first is generally modelling of the hybrid dynamical system from the hybrid natural aspects of tangled evolution of continuous and discrete states, posed by the theory of hybrid automata. The second, motivated by the applicability of the theory of hybrid dynamical systems, is based on distinctive system constraints and particularities. Hence, the latter is a direction that certainly simplifies the analysis and control of such a system. From that perspective, we are presenting distinct hybrid model types starting with PWA systems. The state space expression in (2.1) presents the PWA modelling form.

$$\begin{aligned} x(k+1) &= A_i x(k) + B_i u(k) + v_i \\ y(k) &= C_i x(k) + D_i u(k) + w_i \\ for \begin{bmatrix} x(k) \\ u(k) \end{bmatrix} &\in \Omega_i \quad \Omega_i - convex\ polyhedra \end{aligned} \tag{2.1}$$

The subscripts in expressions denote the hybrid regions $i \in \{1,\ldots,m\}$, where the finite number m does not necessarily coincide with the system order.
To clarify the expression, we have to subsequently introduce the basic definitions of PWA systems already known in literature [67]. *A, B, C,* and *D* matrixes are the state space matrixes of an appropriate dimension, while the *x*, *y* and *u* denotes the states, the output and the control or input variable respectively. All variables in general are

vectors of the arbitrary dimensions. Further on v_i and w_i are functions that present a non-modelled dynamics, mostly connected to the system noise.

****Definition 2.2**[67] (**PWA, PWL**) Consider the function f over the polyhedral set Ω.*
$f : \Omega \to \mathbb{R}^n$ with $n \in \mathbb{N}$ is piecewise affine (PWA), if a partition $\{\Omega\}_{i=1}^m$ of set Ω exists, such that $f(x) = A_i x + a_i$ if $x \in \Omega_i$. Further, if $a_i = 0$ the function is called piecewise linear (PWL).

****Definition 2.3**[67] (**Polyhedron, Half Space and Vertex Representation**) the polyhedron is a set of the form*

$$\mathcal{Q} = \{x \in \mathbb{R}^n \mid a_i x \geq b_i,\ i = 1,\ldots,m\} \tag{2.2}$$

or, equivalently;

$$\mathcal{Q} = \{x = V\zeta + \mathcal{R}\eta \mid \sum_i \zeta_i = 1,\ \zeta \geq 0,\ \eta \geq 0\} \tag{2.3}$$

where $\zeta = [\zeta_1\ \zeta_2\ \ldots \zeta_m]^T$ and $\eta = [\eta_1\ \eta_2\ \ldots \eta_j]^T$. The equations (2.2) and (2.3) are presenting the polyhedron in two different ways, i.e. as the intersections of finite number of halfspaces, and as the set addition (Minkowski sum) of the convex hull of the columns of the matrix V, and the conic hull of the columns of the matrix $\mathcal{R}$, respectively. The columns of matrix V are called vertices of the polyhedron, and the columns of the matrix $\mathcal{R}$ extreme rays.
A polytope is bonded polyhedron and it can be represented by

$$\mathcal{Q} = \{x = V\zeta \mid \sum_i \zeta_i = 1,\ \zeta \geq 0\}\ . \tag{2.4}$$

Analogically the representation of the polyhedron in the form (2.2) is called the halfspace and in the form (2.3) the vertex.

****Definition 2.4**[67] (**Polytopic/Polyhedral Partition**) A collection of polytopic/polyhedral sets $\{\mathcal{Q}_i\}_{i=1}^m = \{\mathcal{Q}_1, \mathcal{Q}_2, \ldots, \mathcal{Q}_m\}$ is a polytopic/polyhedral partition of polytopic/polyhedral set $\boldsymbol{\Omega} \subseteq \mathbb{R}^n$ if*
i) $\bigcup_{i=1}^n \mathcal{Q}_i \subseteq \boldsymbol{\Omega}$
ii) $(\mathcal{Q}_p \setminus \hat{\mathcal{Q}}_p) \bigcap (\mathcal{Q}_q \setminus \hat{\mathcal{Q}}_q) = \varnothing,\ \forall p \neq q / p,q = 1,2,\ldots,m,\ \hat{\mathcal{Q}}$ *– denotes boundary of* $\mathcal{Q}$
iii) if $\mathcal{Q}_p \bigcap \mathcal{Q}_q \neq \varnothing$, where $p \neq q$, then $\mathcal{Q}_p \bigcap \mathcal{Q}_q$ is a common face of $\mathcal{Q}_p$ and $\mathcal{Q}_q$.

Thus, the equation (2.1) is a *lifted* model of the PWA system from Definition 2.2, taking into consideration the extension for a vector space of inputs that are in the same convex polyhedral $\bigcup_{i=1}^n \boldsymbol{\Omega}_i \subseteq \boldsymbol{\Omega}$ for $n \geq m$.

2.1.3 Switched Affine System (SAS)

For the above-presented PWA system, it is a hard assumption to expect that for all arbitrary initial conditions $x_0 \in \Omega_i$ our trajectory $f(x)$ will stay bounded in the one polyhedral partition Ω_i. More likely in the natural cases, for a certain initial condition, the trajectory will violate two or more borders of regions defined by Ω_i for $i = 1,\ldots,m$. In the subsequent theory, we will constrain our interest in the finite set $\Omega = \bigcup_i \Omega_i$. The switching of regions causally brings the paramount theory of that effect. Allegedly, this effect, brings fundaments for further distinction in the modelling of hybrid dynamical system. Even though it could be said that some of these switchings do not characterize the hybrid system, we cannot separate it from its hybrid nature. Rather pragmatically, the switching is an event for the more distinctive theory of HS, starting with this question: is it for an autonomous switching and jumps or for a controlled switching and jumps?
Figure 2.2 is a concise graphical representation showing the autonomous and controlled switching.

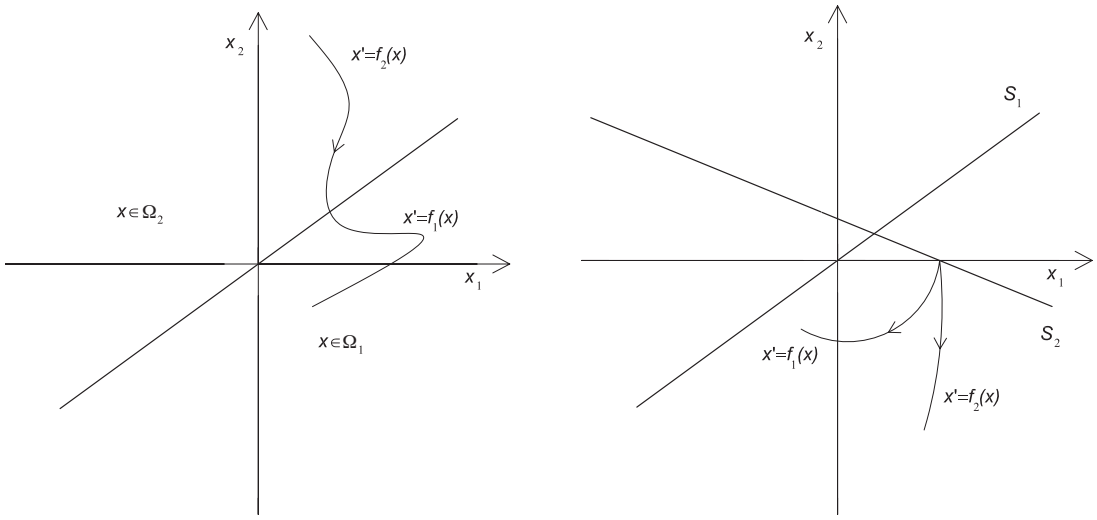

a) **b)**

Fig. 2.2 Autonomous (a) and controlled switching phenomena (b), graphical representation

Therein the control of switching is assigned with the switching surfaces S_i, and in contrast to that the natural switching surface or border between the two vector fields $f_i(x)$, bounded in the sets of states Ω_i, is an unassigned line. Further on, the terminology connected to the autonomous switching system is frequently characterized by *switching affine systems*, but opposite to that the systems with the controlled switching are assigned to be Switched Affine Systems (SAS). The SAS do not exclusively consider controlled switching, which means that those systems include the natural and autonomous switching happening with uncontrolled manner while intending to control the system. This kind of effect, and SAS in general, motivates the subsequent thesis.
In the state space, the SAS systems are defined by the most general expression and hence

$$\begin{aligned} x(k+1) &= f(x(k),u(k),q(k)) \\ y(k) &= g(x(k),u(k),q(k)) \quad for\ x(0) = x_0 \end{aligned}. \tag{2.5}$$

We see that the expression (2.5) is an augmented version of the general discrete state-space by the function of states $q(k)$ modelling the hybrid nature. Subsequently, we will mostly rely on the discrete system representation and equally treat the control systems as a discrete time control. As mentioned earlier the function $q(k)$ denotes the switching logic caused naturally or done by controls. The equation (2.5) evolves into a more distinctive form

$$\begin{aligned} x_c(k+1) &= A_{i(k)}x_c(k) + B_{i(k)}u_c(k) + v_{i(k)} \\ y_c(k) &= C_{i(k)}x_c(k) + D_{i(k)}u_c(k) + w_{i(k)} \quad for\ k \in \mathbb{Z}^+ \end{aligned}, \tag{2.6}$$

where index *c* means that the equation is the discrete counterpart of the continuous system representation. Further on, $x_c \in X \subseteq \mathbb{R}^{n_c}$, $y_c \in Y \subseteq \mathbb{R}^{p_c}$, $i(k) \in Q = \{1,\ldots,m\}$ and denotes the region or the mode of a system's operation that is in the closed and finite set of the integer numbers, including the set of the state-space matrixes $\{A_i, B_i, C_i, D_i\}$ and functions v_i, w_i that denote the undefined dynamics.
The final and relaxed hybrid structure of the SAS is presented by

$$\boldsymbol{z}(k+1) = \begin{cases} \boldsymbol{A}_1\boldsymbol{x}_c(k) + \boldsymbol{B}_1 u_c(k) + v_1 & if\ i(k) = 1 \\ \quad + & \\ \quad \vdots & \\ \quad + & \\ \boldsymbol{A}_m\boldsymbol{x}_c(k) + \boldsymbol{B}_m u_c(k) + v_m & if\ i(k) = m \end{cases}. \tag{2.7}$$

We must underline a distinction in variables of the continuous states $\boldsymbol{x}_c$ and the final variable of the hybrid model trajectory evolution $\boldsymbol{z}$, which is more closely defined in Chapter IV.
The term "relaxed" is used because of the presentation of time, which is not the hybrid time, but rather discrete time. It can easily be concluded that the hybrid time evolution (from the set of real numbers) could be transformed to the discrete time (the set of natural and positive numbers) by the assumption that the sampling time is infinitesimally small.

Although the time category is diminished above, this thesis is magnifying the recognition of the time of hybrid trajectories' progressing. The time role is differing our hybrid systems in a group of synchronous discrete state progressing or asynchronous discrete state progressing hybrid systems. The latter is characteristically related to the definition of the hybrid automata, while the synchronous modelling is more common in the control technology. Furthermore, it is ubiquitously observed and exemplified in different disciplines. The assumptions taken in the analysis and synthesis of this type of SAS resolve the problem of Live-lock* and Zeno* effects that are common for HS. Theoretically, this statement is proven in the literature [68], but in a natural system it is rather unlikely. The

* Live lock is an effect of infinite switches in zero time. Zeno is an effect of infinite switches in finite time.

problem appears in the instant discrete changes, which is just a theoretical reconstruction of infinitesimal time, but in the natural events still a real value. In the nonlinear phenomena scenarios, it presents a too coarse assumption, beyond determinism, and only the convention makes the infinitesimal time instants negligible.

Nevertheless, the system theory based on the abovementioned assumption is rendered by the theory of *Discrete Hybrid Automata* (DHA). The theory tackles a missing part of the equation (2.7) referring to the logics of the discrete variable $i(k)$. Hence, three additional mathematical objects define the logic: Event Generator (EG), Finite State Machine (FSM) and Mode Selector (MS). Figure 2.3 presents a DHA by the block diagram.

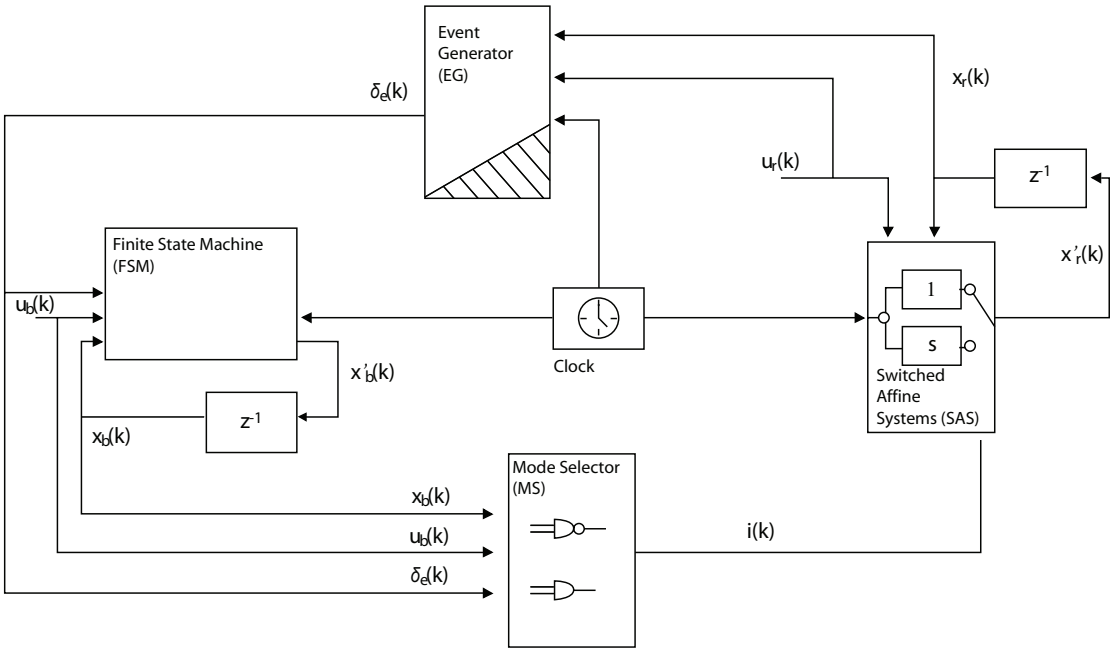

Fig. 2.3 Block diagram of a DHA system [2]

A decision on linear affine constraints (true/false) in the form $a^T x_c(k) + b^T u_c(k) \le c$ is given by the logic signal

$$\delta_e(k) = f_H(x_c(k), u_c(k), k) \tag{2.8}$$

as a function of a linear hyperplane $f_H : X_c \times U_c \times \mathbb{Z}^+ \to D \subseteq \{0,1\}^{n_e}$, resulting in the vector of Boolean variables of a length n_e. Posed by the mathematical logic, the equation (2.8) is a combination of two statements:

$$\begin{aligned} &[\delta_e{}^i(k) = 1] \leftrightarrow [a_i{}^T x_c(k) + b_i{}^T u_c(k) \le c_i] \\ &[\delta_e{}^i(k) = 1] \leftrightarrow [kT_S \ge t_0]\,. \end{aligned} \tag{2.9}$$

The first is referring to the *threshold event* and the second to the *time event* or synchronization. In equation (2.9) i denotes the ith component of the vector $\delta_e(k)$, T_S is a discrete system sampling time and t_0 a starting time. A mathematical object producing this vector is called an *Event Generator*.

The *Finite State Automaton or Machine* is a discrete dynamical process changing its states by an endogenous logic function

$$x'_b(k) = f_B(x_b(k), u_b(k), \delta_e(k)) \tag{2.10}$$

where $x_b(k) \in X_b \subseteq \{0,1\}^{n_b}$, exogenous $u_b(k) \in U_b \subseteq \{0,1\}^{m_b}$ and the $\delta_e(k)$ is the endogenous input coming from the EG. This logic automaton has an associated Boolean output

$$y_b(k) = g_B(x_b(k), u_b(k), \delta_e(k)) \quad y_b(k) \in Y_b \subseteq \{0,1\}^{p_b} \quad . \tag{2.11}$$

The final confirmation and action taken, resulting in the switching of SAS, is done by the *Mode Selector* function

$$i(k) = f_M(x_b(k), u_b(k), \delta_e(k)) \quad f_M : X_b \times U_b \times D \to Q \, . \tag{2.12}$$

This tool certainly forms the framework for a further investigation of the SAS based on the current computational resources, meaning hardware abilities related to the microprocessors, computers or industrial PLCs. A DHA approach will be used in this study to construct the simulation model as the closest approximation to the physical process by taking the sampling time t_{SAMPLE} as short as possible and limited by the maximal resolution of the simulation tool. It will be taken into consideration that DHA simulation time $t_{SAMPLE} << T_S$, where T_S is a sampling time of the physical system in general (practically difficult to achieve for the processes with a high natural frequency, and that is a fact in the example of this thesis). Authors defining the above theory of DHA are also the most involved in developing of the programming language HYSDEL [29] that is the tool in the modelling of the applicable class of hybrid systems, also known as Mixed Logical Dynamical (MLD) systems.

2.1.4 Mixed Logical Dynamical (MLD) systems

A theory of SAS and modelling of the nonlinear dynamical systems with that methodology has deep roots in the modern mathematics and computer science. Feasibility in simulating and solving our modelling demands is directly related to current computational capabilities and also unconditionally constrained by discrete processing. Basically, human reasoning and building of the likewise inference engine relies on the mathematical logic. The most fundamental mathematical logic is Boolean algebra or more generally called the Propositional *Logic or Calculus*. Wider and richer logic, also consisting of propositional logic is *Predicate Calculus* or in some literature called *First Order Logic* [69,70]. These two mathematical tools compose the logics' framework for a further development of *mathematical algorithms* used to resolve our modelling paradigm. Thus, in the system classes, where modelled by MLD systems, we use the conventional propositional calculus to model the logical parts of processes as on/off switches, discrete mechanisms, combinational and sequential networks. Our physically operating events that include dynamics and logic have to be modelled in statements: that is, to agree with

the toolbox that we have available. Consonant to the SAS, especially if we consider the switched affine linear systems, our modelling bases on the *mixed-integer linear inequalities*. Thus, the presented strategy evolves in the computational algorithms known as *Linear and Integer Programming*.
Although, Linear Programming is naturally connected to the optimization algorithms, it is an unavoidable tool in current control theories, e.g. minimization of the performance index in the Model Predictive Control. To clarify, the basic tool in transforming the physical problems in the mathematical or (precisely) the formal semantics will be presented here.
The problem of the maximizing or minimizing of a linear expression, subject to a number of linear constraints that take the form of linear expressions $a_i x_i \sim c_i$, where the conjunctive condition $\sim \in \{\leq, \geq, =\}$ is a *Linear Programming (LP)*. Subsequently the *Integer Programming (IP)* is restricted LP by the employment of integer variables. On occasions when the integer variables are used partially, the programming is called *Mixed Integer Programming (MIP)*.
Most practical modelling approaches restrict the integer variables on 0 and 1, so the MLD is one of the good examples. That restriction cannot be considered hard, as we know that any integer can be binary coded. Once the integer variables 0 and 1 are used, one can easily represent the propositional logic statements and decision based on YES/NO. A typical integer variable δ_i is introduced that has to lie in the range from 0 to 1 and restricts it to two values $\delta_i \in \{0,1\}$. Table 2.1 is consisting the propositional calculus' connectives transferred to the integer variable constraints.

Logic connective	0/1 integer constraints
$\vee$	$\delta_1 + \delta_2 \geq 1$
$\wedge$	$\delta_1 + \delta_2 = 2$
$\neg$	$\delta_1 = 0$
$\rightarrow$	$\delta_1 \leq \delta_2$
$\leftrightarrow$	$\delta_1 = \delta_2$
$\oplus$	$\delta_1 + \delta_2 = 1$

Table 2.1 Transformation of logic connectives to the 0/1 integer constraints

Except for transformation of logic connectives to the integer constraints, it is necessary mostly in the physical systems modelling, but also for the computational feasibility, to provide the lower and upper bounds to our linear expressions

$$m_i \leq \sum_j a_{ij} x_j \leq M_i \quad . \tag{2.13}$$

If that is impossible in the some of the examples, then the condition may not be possible to express by MIP. In equation (2.13) we are omitting the strict inequalities assigned by "<" or ">" as it is important to provide the *maximum* M and *minimum* m

to the linear expression. Otherwise, in cases in which the strict inequalities are present, then our bounds become the *suprema* (least upper bound) or *infima* (greatest lower bound). Despite the non-strict inequalities, we have to provide bounds with a realistic degree of approximation denoted by the symbol ε (infinitesimally small number).

In the following example, the main idea can be easily verified.

Example 2.1
Represent the following conditions

i. $[\sum_j a_{ij}x_j \le c_i] \rightarrow [\delta_i = 1]$
ii. $[\delta_i = 1] \rightarrow [\sum_j a_{ij}x_j \le c_i]$
iii. $\sum_j a_{ij}x_j \le c_i] \leftrightarrow [\delta_i = 1]$
by the IP involving a $\delta_i \in \{0,1\}$.

For better understanding, the truth table of the logic implication has to be known. Usually it is more convenient to have the simpler expression from the left-hand side so the logic expression (i) will be negated and imposed by

$[\delta_i = 0] \rightarrow [\sum_j a_{ij}x_j > c_i]$. Furthermore, as mentioned, a strict inequality will be omitted and the more convenient condition sign "≤" used. The final logic expression is derived to $[\delta_i = 0] \rightarrow [-\sum_j a_{ij}x_j \le -c_i - \varepsilon]$. We see that the right-hand side has to be relaxed by number ε to agree with the non-strict inequality.
At this moment, we have to use the minimum $m_i \le \sum_j a_{ij}x_j$ in order to provide the certain truth on the lowest border of the linear expression. It is certain that the left-hand side of the inequality will be satisfied (if the solution is feasible) by $-m_i + c_i + \varepsilon \le 0$. Now we can construct the IP expression of (i) that is

$$-\sum_j a_{ij}x_j + (m_i - c_i - \varepsilon)\delta_i \le -c_i - \varepsilon. \qquad (2.14)$$

The condition (ii) has already been in the convenient logic form with the non-strict inequality. We start with the certainty on the top border and use the maximum $\sum_j a_{ij}x_j \le M_i$, which suffices to express $0 \le -M_i + c_i$. Hence, the IP expression of (ii) is

$$\sum_j a_{ij}x_j + (M_i - c_i)\delta_i \le M_i. \qquad (2.15)$$

The third condition (iii) has to be expressed by both IP derived expressions (2.14) and (2.15).

Moreover, very often in the modelling of dynamical systems, where the products of continuous and discrete variables are handled, it is necessary to introduce the auxiliary variables. The difference is whether we substitute the product of logical variables or mixed product of the continuous and logic variables [26]. Namely, the product of logic variables $\delta_1\delta_2$ can be substituted by $\delta_3 = \delta_1\delta_2$. Thus,
$[\delta_3 = 1] \rightarrow [\delta_1 = 1] \wedge [\delta_2 = 1]$ and further the equivalent inequality expressions are

$$(\delta_3 = \delta_1\delta_2) = \begin{cases} -\delta_1 + \delta_3 \le 0 \\ -\delta_2 + \delta_3 \le 0 \\ \delta_1 + \delta_2 - \delta_3 \le 1 \end{cases} . \tag{2.16}$$

Therefore the mixed product $\delta f(x)$, where $f : \mathbb{R}^n \rightarrow \mathbb{R}$ and $\delta \in \{0,1\}$, can be replaced by an auxiliary real variable $y = \delta f(x)$ that satisfies $[\delta = 0] \rightarrow [y = 0]$ and $[\delta = 1] \rightarrow [y = f(x)]$. If we recall now (2.13) and assumed that linear expression is replaced by the arbitrary function in the space of real variables then the following is equivalent:

$$(y = \delta f(x)) = \begin{cases} y \le M\delta \\ y \ge m\delta \\ y \le f(x) - m(1-\delta) \\ y \ge f(x) - M(1-\delta) \end{cases} . \tag{2.17}$$

The above-presented tools suffice in constructing a final mixed logical dynamical model in state space:

$$\begin{aligned} x(k+1) &= Ax(k) + B_1u(k) + B_2\delta(k) + B_3z(k) \\ y(k) &= Cx(k) + D_1u(k) + D_2\delta(k) + D_3z(k) \\ E_2\delta(k) + E_3z(k) &\le E_1u(k) + E_4x(k) + E_5 \end{aligned}$$

where (2.18)

$$x(k) = \begin{bmatrix} x_c^{\,T}(k) \\ x_b^{\,T}(k) \end{bmatrix}, \quad x_c(k) \in \mathbb{R}^{n_c}, x_b(k) \in \{0,1\}^{n_b},$$

$$u(k) = \begin{bmatrix} u_c^{\,T}(k) \\ u_b^{\,T}(k) \end{bmatrix}, \quad u_c(k) \in \mathbb{R}^{m_c}, x_b(k) \in \{0,1\}^{m_b},$$

$$y(k) = \begin{bmatrix} y_c^{\,T}(k) \\ y_b^{\,T}(k) \end{bmatrix}, \quad y_c(k) \in \mathbb{R}^{p_c}, y_b(k) \in \{0,1\}^{p_b}$$

$$z(k) \in \mathbb{R}^{r_c}, \ \delta(k) \in \{0,1\}^{r_b},$$

In model representation (2.18) the subscripts *b* and *c* are respectively presenting the logic/binary and continuous states, the $z(k)$ denotes an auxiliary real variable earlier in (2.17) assigned by *y*. All $A, B_i, C, D_i, and\ E_i$ are the state space matrices of the suitable dimensions to suit the vector lengths denoted by n, m, p and r.

2.1.5 Linear Complementarity (LC) Systems

Throughout the above presentation of the different classes of the HS we intended to progressively present the development of the modelling paradigm in the direction of its applicability on a wider range of physical systems. From the complete theoretical and conventional approach of modelling of HS by hybrid automata, characteristically formalized by mathematicians, the modelling approach more based on physics can be recognized in the theory of complementarity systems [27]. While the DHA and MLD systems are fundamentally related to the computer science and programming, we found the complementarity systems' modelling to be a more applicative and generalized approach.
As earlier presented in MLD systems, and their relation to LP and IP, the modelling paradigm of complementarity systems is related to the mathematical programming problem called Linear Complementarity Problem (LCP).
Similarly to the MLD system, this class of systems also consists of inequalities combined with the differential equations.
The LCP is defined as follows [17,72].

Given a matrix $M \in \mathbb{R}^{nxn}$ and $q \in \mathbb{R}^n$, find $u, y \in \mathbb{R}^n$ such that

$$\begin{aligned} y &= q + Mu \\ 0 \le y \perp u &\ge 0 \end{aligned}. \qquad (2.19)$$

Thus, the expressed problem is usually denoted by $\mathrm{LCP}(q, M)$. Therefore, the conditions $y \ge 0, u \ge 0,\ u^T y = 0$ are called *complementarity conditions* that are collectively presented in (2.19). The pairs (u, y) are called complementarity variables. From the linear algebra and matrix classes the existence of solutions is derived.

****Theorem 2.1**[71] If $M \in \mathbb{R}^{nxn}$ is positive definite, then the LCP (q, M) has a unique solution for all $q \in \mathbb{R}^n$.*

****Definition 2.5**[71] A matrix $M \in \mathbb{R}^{nxn}$ is said to be **P**-matrix if all its principal minors are positive. The class of such matrices is denoted **P**.*

****Theorem 2.2**[71] For a given matrix $M \in \mathbb{R}^{nxn}$, the problem $LCP(q, M)$ has a unique solution for all vectors $q \in \mathbb{R}^n$ if and only if M is a **P**-matrix.*

From the above results in the literature [71] the following modelling paradigm is formulated. The LC system is provided by the simultaneous continuous equations

$$\begin{aligned} \dot{x}(t) &= Ax(t) + B_1 u(t) \\ y(t) &= Cx(t) + Du(t) \\ 0 \le y(t) \perp u(t) &\ge 0 \end{aligned}. \qquad (2.20)$$

The functions u,x and y take values in $\mathbb{R}^n$, $\mathbb{R}^m$ and $\mathbb{R}^n$ respectively; A,B,C and D are matrices of appropriate dimensions. We see that values in u and y have the same dimensions and it has to be stated that for every component of those vectors $i=1,...,n$ either $u_i(t)=0$ or $y_i(t)=0$. The set of indices for which $y_i(t)=0$ is called *mode* or *active index set* and may change during the system's time evolution. This statement coincides with the aforementioned HS modelling formalisms as the system's operating mode.
However, the expression (2.20) and complementarity conditions of the variables (u,y) have great potential in applicability on a wider range of physical systems. We can easily recognize that the nonnegativity and orthogonality of two variables have a physical equivalence with the ideal diode (current and voltage) and ideal valve (flow and pressure). Except in the electronics and hydraulics, it is applicable in other areas of engineering. The comprehensive expertise of the linear complementarity problem pursued on mechanical system of two rigid bodies is given in [71]. For a long time, this modelling approach was closely connected to the ideal switching control schemes; in the later work of Schaft and Schumacher and after Vasca [13,27], the authors give a new insight to this formalism.
They underline that when the ideal switching scheme is considered, the well-posedness of the resulting closed-loop systems may easily fail. This is quite in contrast with the solution when the smooth control is applied. The ideal switching is naturally impossible to achieve. This statement must present an intriguing objective for systems with the fast refreshing time rates, and is also one of the basic motives for this thesis. The well-posedness is proven on *bimodal systems* [72-76], and it is known to be hardly sufficient for wider applicability.
Schaft and Schumacher, as authors with a great contribution in the field of hybrid systems, particularly in complementarity systems, augment a problem of discrete states (locations) that are actually the product space obtained by combining several switches. It is revealed that in many cases, the dynamical systems associated with different locations will not be completely independent, but will rather have many equations in common. These observations guided the authors in the direction of *product decomposition* of HS.
Generally, the *core dynamics* are

$$F(z(t),\dot{z}(t))=0 \tag{2.21}$$

that form the dynamics of each particular location, for the vector $z(t)\in\mathbb{R}^n$ containing all continuous variables of the system. There are k switches, with a finite set Λ_i of the possible positions associated with each switch $i=\{1,...,k\}$. In turn, we see that each combination of the switch positions gives rise to a different state, so the set of locations is the product $\prod_{i=1}^{k}\Lambda_i$. If we assigned each position of i^{th} switch with s, then the additional dynamics, rising for the particular location have a form

$$G_i^s(z(t),\dot{z}(t))=0 \quad . \tag{2.22}$$

The set of invariants will be formed as

$$H_i^s(z(t)) \geq 0 \tag{2.23}$$

and present all the inequalities corresponding to the switch position together. Arising rules from the above formulations;

i) All switches are binary, i.e. $\Lambda_i = \{0,1\}$ for all i.
ii) All additional dynamic equations corresponding to switch position are algebraic and scalar, i.e. they are of the form $g_i^s(z(t)) = 0$ where $g_i^s : \mathbb{R}^n \to \mathbb{R}$.
iii) Also, the invariants corresponding to switch positions are scalar, so they are of the form $h_i^s(z(t)) \geq 0$ where $h_i^s : \mathbb{R}^n \to \mathbb{R}$.
iv) The functions defining the additional dynamics and the invariants associated with each switch position change roles when the switch is turned; i.e. $g_i^0(z(t)) = h_i^1(z(t))$ and $g_i^1(z(t)) = h_i^0(z(t))$ for all i as the *complementarity condition*.

Systems that can be described according to the above rules are called *complementarity systems*.
For clarity, we assigned two substitution variables $y_i = g_i^0(z(t))$ and $u_i = h_i^0(z(t))$ to the complementarity condition functions. These substitution variables are forming the general complementarity variables. The core dynamics in this general complementarity formalism are functions over the continuous variables $z(t)$ that consist of the arbitrary combinations of states, input functions and outputs $z(t) = (x_1, x_2, ..u_1, u_2, ...y_1, y_2, ...)$.
In some of the new releases [2] the complementarity formalism receives a more compact form that evolves from the (2.20) to

$$\begin{aligned} \dot{x}(t) &= Ax(t) + B_1u(t) + Ev(t) \\ y(t) &= Cx(t) + Du(t) + Fv(t) \\ 0 &\leq y(t) \perp u(t) \geq 0 \end{aligned} \quad . \tag{2.24}$$

Equally as in (2.20) the A, B, C, D, E and F are matrixes of the suitable dimensions and $v(t)$ is the forced variable mostly used to model the additional noise in the system. Further generalization of that form enriches the expression (2.24) in order to allow the incorporation of equality and inequality together.
The complementarity relation takes the following form

$$\boldsymbol{C} \ni y(t) \perp u(t) \in \boldsymbol{C}^* \quad . \tag{2.25}$$

where $\boldsymbol{C}$ is a cone in $\mathbb{R}^n$ and $\boldsymbol{C}^*$ is the dual cone defined by

$$\boldsymbol{C}^* = \{u \mid (y,u) \geq 0 \ \textit{for all}\ y \in \boldsymbol{C}\} \quad . \tag{2.26}$$

Taking in consideration the overall generalization of the complementarity systems in equations (2.21)-(2.23), where the complementarity pairs are not necessarily the state and input variables, the LC system in discrete time is expressed by

$$\begin{aligned} x(k+1) &= Ax(k) + B_1u(k) + B_2w(k) \\ y(k) &= Cx(k) + D_1u(k) + D_2w(k) \\ v(k) &= E_1x(k) + E_2u(k) + E_3w(k) + g_4 \\ 0 \le v(k) \perp w(k) &\ge 0 \quad v^T(k)w(k) = 0 \\ v(k), w(k) &\in \mathbb{R}^s - \textit{complementarity variables} \end{aligned} \quad . \tag{2.27}$$

It is imposed that $(v(k),w(k))$ denotes the complementarity pair, while A,B_i,C,D_i and E_i are the matrixes of the suitable dimensions. The residual and non-modelled part in the expression (2.27) that gives the relations of complementarity variables is denoted by g_4.
The LC systems are also upgraded to the Extended Linear Complementarity systems (ELC)[2,25]. The main difference can be found in the ability of incorporating the system's inequalities directly instead of transferring them to the complementarity conditions by using the slack variables [25].
Further on, there are other distinctive and established modelling principles and hybrid system examples, e.g. max-min-plus-scaling (MMPS) [2,25] that can also be presented as an equivalent expression to the already mentioned [2,25]. Because of their reduced applicability to the SAS, in this thesis, they will be omitted.

2.2 Problems in modelling of HS

Inherently, the HSs are nonlinear and non-smooth, so the problem appearance must be viewed from that aspect and knowledge. Additionally, the hybrid systems have inherited some anomalies directly from the grade of accuracy of the applied modelling and control. In this section of Chapter II, we will point out both. First, we present some of anomalies that are strictly connected to the basic formalism in hybrid systems, arising from the above explained most recent methodologies in modelling of HS. Second, taking in consideration that HSs are nonlinear dynamical systems, we present some typical and general nonlinear phenomena.

2.2.1 Hybrid Time Sets, Executions and Zeno effect

Particularly the Hybrid Automata, but also in general the Hybrid Systems involve the continuous states determined by differential equations and discrete states by difference equations. From the physical point of view the continuous states can be considered as a "flow" and the discrete ones as a "jump". However, to characterize the evolution of the states one has to think of the set of times that contains both the continuous intervals and the distinguished discrete points at the time a discrete transition happens. This time set is called *hybrid time set* [78].

****Definition 2.6**[78] (**Hybrid Time Set**) A hybrid time set is a sequence of intervals* $\tau = \{I_0, I_1, \ldots, I_n\} = \{I_i\}_{i=0}^{N}$, *finite or infinite (i.e.* $N = \infty$ *is allowed) such that*

i) $I_i = [\tau_i, \tau_i^{'}]$ *for all* $i < N$;

ii) *if* $N < \infty$ *then either* $I_N = [\tau_N, \tau_N^{'}]$ *or* $I_{N+1} = [\tau_{N+1}, \tau_{N+1}^{'}]$; *and*
iii) $\tau_i < \tau_i^{'} = \tau_{i+1}$ *for all* i.

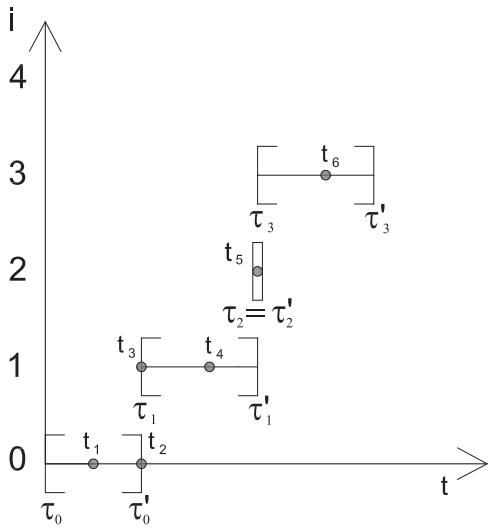

Fig. 2.4 A hybrid time set $\tau = \{\tau_i, \tau_i^{'}\}_{i=0}^{3}$ [78]

Figure 2.5 explicitly shows the hybrid time progression in the time set.
There are two main characteristics of the hybrid time set shown in Figure 2.4. The right endpoint of the interval i coincides with the left of the interval $i+1$. That fact makes it possible to have two instants (i.e. labelled t_2 and t_3) instantaneously. In other words, the discrete transition is assumed to be instantaneous. Furthermore, this convention allows the ability of multiple discrete transitions at the same instant, in which case $\tau_{i-1}^{'} = \tau_i = \tau_i^{'} = \tau_{i+1}$.
Based on the presented convention, the mixture of discrete and continuous state must be defined as the evolution of the hybrid system in the defined time set.

****Definition 2.7**[78] (**Hybrid Trajectory**) A hybrid trajectory is a triple* (τ, q, x) *consisting of a hybrid time set* $\tau = \{I_i\}_0^N$ *and two sequences of functions* $q = \{q_i(\cdot)\}_0^N$ *and* $x = \{x_i(\cdot)\}_0^N$ *with* $q_i : I_i \to Q$ *and* $x_i : I_i \to \mathbb{R}^n$.

Above Definition 2.7 must be considered by the restrictions in the sets defined in Definition 2.1 similarly as in Definition 2.8.

****Definition 2.8**[78] (**Execution**) An execution of a hybrid automaton **H** is a hybrid trajectory,* (τ, q, x)*, which satisfies the following conditions:*

i) *Initial condition*: $(q_0(0), x_0(0)) \in Init$
ii) *Discrete evolution: for all* i,
$(q_i(\tau_i^{'}), q_{i+1}(\tau_{i+1})) \in \Theta$, $x_i(\tau_i^{'}) \in \mathcal{G}(q_i(\tau_i^{'}), q_{i+1}(\tau_{i+1}))$, *and*
$x_{i+1}(\tau_{i+1}) \in \mathcal{R}(q_i(\tau_i^{'}), q_{i+1}(\tau_{i+1}), x_i(\tau_i^{'}))$.
iii) *Continuous evolution: for all* i,
1. $q_i(\cdot) : I_i \to Q$ *is constant over* $t \in I_i$, *i.e.* $q_i(t) = q_i(\tau_i)$ *for all* $t \in I_i$;

2. $x_i(\cdot): I_i \to X$ *is the solution to the differential equation* $\dot{x}_i = f(q_i(t), x_i(t))$ *over* I_i *starting at* $x_i(\tau_i)$; and
3. *for all* $t \in [\tau_i, \tau_i^{'}),\ x_i(t) \in Inv(q_i(t))$.

The restrictions (condition iii)) imposed by Definitions 2.7 and 2.8 are evolving into the definition of the classification of executions.

****Definition 2.9**[78] (**Classification of executions**) An execution* (τ, q, x) *is called:*

- ***Finite**, if* τ *is a finite sequence and the last interval* τ *is closed.*
- ***Infinite**, if* τ *is an infinite sequence, or if sum of the time intervals in* τ *is infinite, i.e.* $\sum_{i=0}^{N}(\tau_i^{'} - \tau_i) = \infty$.
- ***Zeno**, if it is infinite but* $\sum_{i=0}^{\infty}(\tau_i^{'} - \tau_i) < \infty$
- ***Maximal**, if it is not strict prefix of any other execution of* ***H**. (strict prefix means that one of two different time sets* τ *is shorter and not equal to another).*

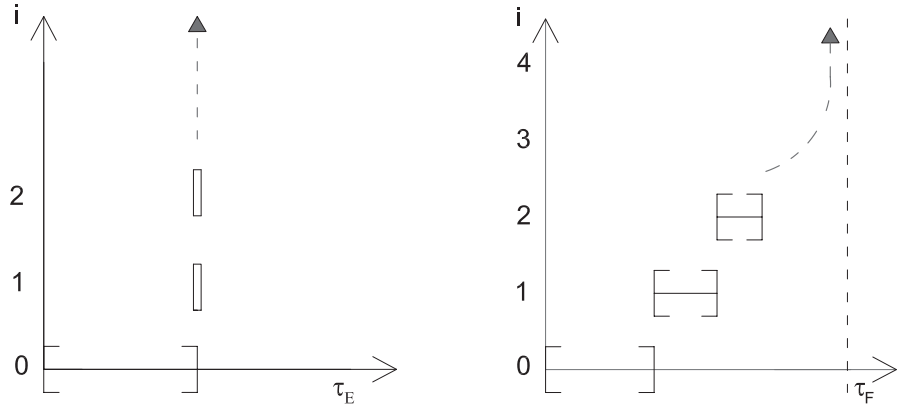

Fig. 2.5 Two examples of Zeno executions for time sets τ_E *and* τ_F [78]

Figure 2.5 graphically presents the Zeno execution, which is considered to be the unwilling or the ill hybrid system's condition. Zeno behaviour is the phenomenon that in a dynamical system an infinite number of events occur in a finite length of the time-interval. It prevents the existence of global solutions, and it is directly related to the well-posedness, as the existence of the solutions given an initial condition. The problem of Zenoness is not harming just an analysis of the hybrid systems, but also the simulations. Most of the time, this problem is already resolved in the simulation programs and it is hardly noticeable. But the existence of that anomaly in HS modelling must be considered seriously, especially because of its impact on the further analysis and synthesis into the control systems.
For a deterministic view of the presented problem, it is crucial in hybrid systems, but also in the general dynamical system to define the uniqueness and existence of the solution. Thus, in HS one has to define if from the initial state (q_0, x_0), there is the reachable state $(\hat{q}, \hat{x})$ for any of the executions.

****Definition 2.10**[78] (**Reachable state**) A state $(\hat{q},\hat{x})\in Q\times X$ of a hybrid automaton **H** is called reachable if there exists a finite execution (τ,q,x) ending in $(\hat{q},\hat{x})$, i.e. $\tau=\{[\tau_i,\tau_i^{\cdot}]\}_0^N$, $N<\infty$, and $(q_N(\tau_N^{\cdot}),x_N(\tau_N^{\cdot}))=(\hat{q},\hat{x})$.*

In the continuation, we define the reachable set that consists all reachable states: $Reach\subseteq Q\times X$ of a hybrid automaton **H**, that initially satisfies $Init\subseteq Reach$.
By recalling the restrictions from the Definition 2.8, and related to the continuous evolution, the possibility must be considered that for some of the states the continuous evolution is impossible or immediately for some of the states violate the Inv set. Those states are forming the set $Trans$ that consists of all such states called *transition states*.
The definition of $Trans$ can be expressed with the following mathematical grammar:

$$Trans=\{(\hat{q},\hat{x})\in Q\times X\,|\,\forall\varepsilon>0\;\exists t\in[0,\varepsilon)\ such\ that\ (\hat{q},x(t))\notin Inv(\hat{q})\}.$$

The exact definition of $Trans$ can be quite involved and it will be omitted here. However, the above definitions suffice to express the determinism in hybrid automata.

****Definition 2.11**[78] (**Non-Blocking and Deterministic**) A hybrid automaton **H** is called non-blocking if for all initial states $(\hat{q},\hat{x})\in Init$ there exists an infinite execution starting at $(\hat{q},\hat{x})$. It is called deterministic if for all initial states $(\hat{q},\hat{x})\in Init$ there exists at most one maximal execution starting at $(\hat{q},\hat{x})$.*

****Lemma 2.1**[78] A hybrid automaton, **H**, is non-blocking if for all $(\hat{q},\hat{x})\in Reach\cap Trans$, there exists $\hat{q}'\in Q$ such that $(\hat{q},\hat{q}')\in\Theta$ and $\hat{x}\in\mathcal{G}(\hat{q},\hat{q}')$. If **H** is deterministic, then it is non-blocking if and only if this condition holds.*

****Lemma 2.2**[78] A hybrid automaton, **H**, is deterministic if and only if for all $(\hat{q},\hat{x})\in Reach$*

i) If $\hat{x}\in\mathcal{G}(\hat{q},\hat{q}')$ for some $(\hat{q},\hat{q}')\in\Theta$, then $(\hat{q},\hat{x})\in Trans$
ii) If $(\hat{q},\hat{q}')\in\Theta$ and $(\hat{q},\hat{q}'')\in\Theta$ with $\hat{q}'\neq\hat{q}''$ then $\hat{x}\notin\mathcal{G}(\hat{q},\hat{q}')\cap\mathcal{G}(\hat{q},\hat{q}'')$; and
iii) If $(\hat{q},\hat{q}')\in\Theta$ $\hat{x}\in\mathcal{G}(\hat{q},\hat{q}')$ then $\mathcal{R}(\hat{q},\hat{q}',\hat{x})=\{\hat{x}'\}$, i.e. the set contains a single element.

The following Theorem 2.3 is constructed from the above Lemmas that have their complete proofs in [78-80].

****Theorem 2.3**[78] (**Existence and Uniqueness**) A hybrid automaton **H** accepts a unique infinite execution for each initial state if it satisfies all the conditions of Lemmas 2.1 and 2.2.*

Throughout the definitions of hybrid systems, including the hybrid time set, the hybrid trajectory and executions, and later the theorem of Existence and Uniqueness, we see numerous conventional restrictions that are difficult to comply with in the realistic or physical cases. In the general theory of HSs there is a formulation behind the non-determinism that can undertake the ambiguity in the

modelling of realistic issues. The non-deterministic hybrid systems are in a turn just opposite from the definition of the deterministic HSs. Equivalently, the verification of the determinism can be considered as defining of the reachable sets. As this programming issue cannot be solved in the real time, and for most of the cases, this way is not found to be the most conventional. Therefore, a non-deterministic HS allows the ambiguity to enter in a number of places: the choices of the continuous evolutions, the choices of a discrete transition destination, and the choices of relation in-between continuous evolution and the discrete transition. The mentioned choices unconditionally provide the impact and disturbance that add the ambiguity in the modelled and possible evolutions. In addition to the choices that violate our sets of invariants, there are many cases in which the control technology is used to steer the system evolution in the space of the infinite possibilities, still impossible to grasp by the imperfect deterministic approaches.
This is acknowledged as one of the motivations that guided the subsequent thesis.
In the work of Branicky [66], we see that nondeterminism is connected to "jump" systems, switched systems and variable structure systems. There is a ubiquitous interest in modern science for this type of systems. Different approaches to the problem lead us to think that there is still an open question; which of the approach is the most appropriate? The emerging realm of the theory of chaos and the nonlinearity exclusion is pointing out those anomalies, mostly arising from the inaccurate modelling and hard assumptions. Equally important and added to the earlier presented ambiguity in HSs modelling, the possible nonlinear phenomena in HSs will be subsequently posed in brief.

2.2.2 Nonlinear phenomena in SAS

The drawbacks of different mathematical expressions referring to the impact to the grade of accuracy of the natural physical systems, present a complex objective for an applied mathematical science. Therefore, the continuous and discrete dynamical systems, including the HS, consist of "strange" characteristics or rather "anomalies" related to their dynamics. While the former are very well described by the modern qualitative mathematical theory, the HS and their behaviour are significantly less so. More commonly, we are dividing it in the smooth and the non-smooth systems. The latter contains a piecewise smooth or the piecewise affine systems. Apart from the aforementioned theory of hybrid systems, we see that, from the aspects of the qualitative theory, those systems are called an *event driven* by a sense that smoothness is lost at instantaneous event [1]. A good example of that event is an applied switch. It is pointed out that even though the all-realistic systems are smooth, at least from sizes bigger than molecular, this statement can mislead. On the microscopic time scale, there is certainly a discontinuity in the instant of the impact.
The loss of smoothness is exactly the moment at which HS can develop the nonlinear phenomena. Those "strange" dynamics are possible for the continuous and smooth nonlinear dynamical system of the rank equal or higher than three. For the HS, and because of discrete events, it is possible even for the lower rank systems. This statement is analytically supported in the literature [1,82]. Subsequently, we provide some basic definitions and terminology for a better understanding of the main motives. As the main concern will be discontinuity, we must classify it for the

piecewise-smooth systems, but now with the slightly generalized *Definition 2.2,* and from a side of the mathematical qualitative theory.

****Definition 2.12**[1] A piecewise-smooth flow (2.32) is given by a finite set of ordinary differential equations (ODEs), and piecewise-smooth map (2.33) by finite set of smooth maps,*

$$\dot{x} = F_i(x,\mu), \ for \ \ x \in \Omega_i \tag{2.32}$$
$$x \to \mathcal{F}_i(x,\mu), \ for \ \ x \in \Omega_i \tag{2.33}$$

where $\cup_i \Omega_i = \Omega \subset \mathbb{R}^n$ *and each* Ω_i *has a non-empty interior. The intersection* $\Sigma_{ij} := \overline{\Omega}_i \cap \overline{\Omega}_j$ *is either an* $\mathbb{R}^{(n-1)}$*-dimensional manifold included in the boundaries* $\Delta\Omega_i$ *and* $\Delta\Omega_j$*, or is the empty set. In both cases, each vector field* F_i *(2.32) or function* $\mathcal{F}_i$ *(2.33) is smooth for the state* x *and parameter* μ *for any open subset* U *of* Ω_i*. The vector field* F_i*(2.32), and differently than* $\mathcal{F}_i$ *(2.33), define a smooth flow* $\phi_i(x,t)$ *which is well defined on both boundaries* $\Delta\Omega_i$ *and* $\Delta\Omega_j$*. On the other side,* $\mathcal{F}_i$ *is a map that presents points of a smooth flow in the equidistant time intervals.*

In Definition 2.12, we have intentionally confronted definitions of the pricewise-smooth flow and map. The complexity in defining the intersection for the mapping that is based on the sampling approach of the continuous and smooth system consisted in the Ω_i should be pointed out. The non-empty intersection $\Sigma_{ij} := \overline{\Omega}_i \cap \overline{\Omega}_j$ will be called also a *discontinuity set*, *discontinuity boundary* or *switching manifold*. As stated, it is $(n-1)$*-dimensional and* smooth manifold. The classification of smoothness is related to the interior point of the mentioned switching manifold.

****Definition 2.13**[1] A degree of smoothness at point* x_0 *in a switching set* Σ_{ij} *of a piecewise-smooth ODE is the highest order r such the Taylor series expressions of* $\phi_i(x_0,t)$ *and* $\phi_j(x_0,t)$ *with respect to t, evaluated at t=0, agree up to terms of* $O(t^{r-1})$*. Hence the first non-zero partial derivative with respect to* t *of the difference* $[\phi_i(x_0,t) - \phi_j(x_0,t)]_{t=0}$ *is of order r.*

As is known, the flow $\phi_i(x,t)$ is generated by $F_i(x,\mu)$, which means that $\frac{\partial(\phi_i(x,t))}{\partial t} = F_i(x)$.
Thus, in other words, if $F_i(x_0) \neq F_j(x_0)$ in a point $x_0 \in \Sigma_{ij}$, then the smoothness is of degree one. Also, the first higher degree is obtained if the Jacobian derivatives of border functions differ $\partial_x(F_i(x_0)) \neq \partial_x(F_j(x_0))$ in the same point. The latter condition gives the smoothness of the switching manifold of degree two. Furthermore, in that case, the system can be considered as a piecewise-smooth continuous system.

Our interest is devoted to the combination of flows (2.32) and maps (2.33) for the smoothness degree of less than two in the switching manifold. Combinations of the

flow and the maps lead to the hybrid dynamical system. Therefore, the formalism based on the qualitative theory reveals the special dynamical characteristics that are mostly theoretically omitted by restrictions and conventions explicitly presented in Subsection (2.2.1).
We are defining a special case of the piecewise-smooth hybrid systems that is called the impacting hybrid system.

****Definition 2.14**[1] For a piecewise-smooth hybrid system defined by the set of ODEs*

$$\dot{x} = F_i(x,\mu), \ \ for \ \ x \in \Omega_i \tag{2.34}$$

and the set of reset maps

$$x \to R_{ij}(x,\mu), \ \ for \ \ x \in \Sigma_{ij} := \overline{\Omega}_i \cap \overline{\Omega}_j \ , \tag{2.35}$$

where the following holds:

i) $\cup_i \Omega_i = \Omega \subset \mathbb{R}^n$ *and each* Ω_i *has a non-empty interior*

ii) $\forall \Sigma_{ij}$ *is either* $\mathbb{R}^{n-1}$ *dimensional manifold included in the boundaries* $\Delta\Omega_i$ *and* $\Delta\Omega_j$*, or is the empty set*

iii) $\forall F_i \wedge \forall R_{ij}$ *are smooth and well defined in open neighbourhoods around* Ω_i *and* Σ_{ij} *respectively,*

we call the ***impacting hybrid system*** *if* $R_{ij} : \Sigma_{ij} \to \Sigma_{ij}$ *and flow is constrained locally to lie on one side of the boundary* $\overline{\Omega}_i = \Omega_i \cup \Sigma_{ij}$.

Figure 2.2b presents the impacting hybrid system if we assume that $F_i = f_i$ as a case of SAS.

The qualitative theory is an emerging mathematical discipline that still does not have a well-designed toolbox and framework. Some of the physical scenarios in the higher order continuous systems and similarly for a much lower order discontinuous dynamical systems have no qualitative explanation. That is why the well-defined nonlinear dynamics for simpler physical systems give us just a rough insight into the demanding events of the more complex nonlinear dynamical systems. The following example, well examined in the literature [134,135], presents the common dynamics that are applicable in the field of the impact hybrid system with restricted complexity.

Let us consider such a restricted impact hybrid system, which has only one impact surface Σ and one constrained region of dynamics Ω^+:

$$\begin{aligned} &\dot{x} = F(x) \ \ for \ \ f(x) > 0 \\ &x \to R(x) \ for \ \ f(x) = 0 \\ &\Sigma = \{x : f(x) = 0\} \quad \Omega^+ = \{x : f(x) > 0\} \end{aligned} \ . \tag{2.36}$$

Our reset map $R(x)$ in Definition 2.14 and expression (2.36) is the impact rule. Furthermore $f(x)$ denotes an arbitrary continuous function. For a smooth and well-defined vector field $F(x)$, around the switching manifold Σ, at time t_0, the flow $\Phi(t_0)$ hits and intersects Σ. The intersection points $\{x^-,x^+\}\in\Sigma$ are related to the time events just an instant before and after an impact, respectively.
At this point we need a deep insight into the physical process to devise a reset map (besides Definition 2.14 also defined in other HS formalisms, Section 2.1) or the impact rule

$$x^+ = R(x^-) \ . \tag{2.37}$$

To achieve the knowledge of the dynamics at the moment t_0, we are interested in the velocity and acceleration of our trajectory's approach to the switching manifold. That is directly related to the smooth function $f(x)$ and yield:

$$v(x) = \frac{df}{dt} = \frac{df}{dx}\frac{dx}{dt} = d_x(f)F \tag{2.38}$$

$$a(x) = \frac{d^2f}{d^2t} = d_x(d_x(f)F) = d_x{}^2(f)FF + d_x(f)d_x(F)F \ . \tag{2.39}$$

In Figure 2.6, we have illustrated the flow events in this example.

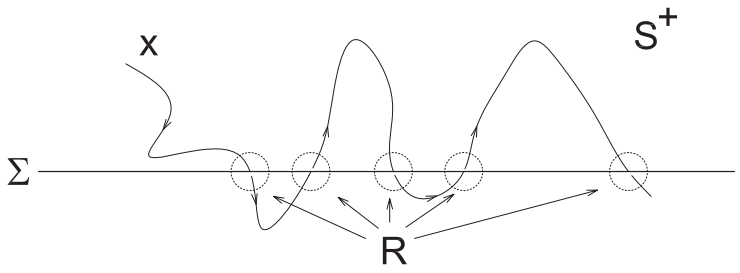

Fig. 2.6 Impacting hybrid systems trajectory, events of multiple impacts for one switching manifold

As in the example shown, both qualifying functions (velocity and acceleration) are positive if flow is moving away from the switching manifold. Further discussion is guided by a combination of different scenarios of qualifying functions. The scenarios are further differentiated as the switching manifold is divided into subsections around the intersection points (x^-,x^+).
A flow approaching the intersection point $x^-\in\Sigma^-\subset\Sigma$ where $\Sigma^- = \{x\in\Sigma : v(x) < 0\}$ is defined by $\Phi(x^-,t)$, for $t < t_0$. An impact happens at the time t_0 and triggers the reset map (2.37).
The instant switching of the dynamics to the intersection point $x^+\in\Sigma^+\subset\Sigma$ is considered in the conventional HS formalisms, Section 2.1. There $\Sigma^+ = \{x\in\Sigma : v(x) > 0\}$ and consequently the flow is defined by $\Phi(x^+,t)$. Differently, our concern is in the natural or physical systems, where the theoretical convention's violation is very possible, as is the induction of scenarios in the switching section $\Sigma^0 = \{x\in\Sigma : v(x) = 0\}$.

One of the scenarios is $v(x^-)=0$, also called a *grazing point* where the impact low is an identity map and differentiated by the relation to the acceleration. The effect of sliding appears if the flow becomes stuck in the boundary

$$\Sigma^0 = \{x \in \Sigma : f(x)=0,\ v(x)=0,\ a(x)<0\}. \tag{2.40}$$

The set (2.40) is also known as a *sticking subset*. Different physical systems develop all varieties of different scenarios and have to be devised in the relation to the sticking regions. The sticking vector fields and reset mapping enrich their mathematical models, and overcome the possibility of the hard omissions by simple assumptions. The *Zeno phenomenon,* impossible in the instant transitions and strict conventions, but present in the physical environment, gets its natural sibling known as the *chattering sequence*. Analytically examined, the impacting hybrid systems are entering the sticking regions by the chattering sequence. It is shown in Figure 2.7 [1] that the impacting hybrid system's flow impacts the switching manifold section Σ^-, resets, and enters the chattering sequence of the infinity impacts at the finite time. Afterwards, it sticks to the section Σ^0, influenced by the infinitesimally small velocity and the negative acceleration. Consequently, it exits the switching manifold influenced by $v(x), a(x) > 0$.

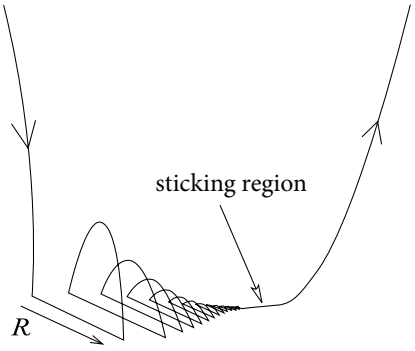

Fig. 2.7 Typical scenario of the impacting hybrid system at the time of impact [1]

Following Definitions 2.13 and 2.14 of the smoothness for the impacting hybrid systems, we can conclude that the main difference versus the general HS is in the type of jumps. While the general HS considers the state jumps, the impacting HS consists of the flow jumps. Therefore, the general HS has a zero degree of smoothness in a discontinuity boundary. In this statement, we can recognize the important knowledge that has to be considered in order to avoid misleading tracks in the modelling of the natural systems. Thus, the physical insights into the natural system should not be unknown or easily neglected, even for trivial cases.
The aforementioned scenarios of the impacting systems are given by observing from a side of the flow switching dynamics and disturbing the continuity. A discontinuity in general brings other qualitative changes that appear to be harmful nonlinear phenomena from the side of the control system technology. With no loss of generality, we will present some terminology and definitions related to the continuous nonlinear systems.

If we consider that

$$\dot{x} = F(x,\mu),\ \ for\ \ x \in X \subset \mathbb{R}^n, \mu \in \mathbb{R}^m \tag{2.41}$$

is a continuous dynamical system, where X denotes the state space and μ a system parameters, then the set of points $x(t)$, as a solution of (2.41) for all $t \in T$, and initial condition x_0, is called a *trajectory* or *orbit*. A picture showing the qualitatively different trajectories of the state space X, is called the *phase portrait*. The latter is drawn concerning the system's fixed points or equilibrium x_i^* where $F(x_i^*,\mu) = 0$ for all $t \in T$.

****Definition 2.15**[1]* ***(Invariant set)*** *A set $\Lambda \subset X$ that holds $x(t) \in \Lambda$, for an initial condition $x_0 \in \Lambda$,* and all $t \in T$ of a *dynamical system (2.41), is called an* ***invariant set****.*

****Definition 2.16**[1]* ***(Attractor)*** *If the invariant set $\Lambda \subset X$ is closed (contains its own boundary), it is called an* ***attractor*** *if*

i) for any sufficiently small neighbourhood $U \subset X$ of Λ, there exists a neighbourhood V of Λ, such that $x(t) \in U$ for all $x_0 \in V$ and $0 < t \in T$, and

ii) for all $x_0 \in U$, $x(t) \to \Lambda$ as $t \to \infty$.

For an attractor in Definition 2.16 of the dynamical system, it is of qualitative importance to define the domain of the initial condition that they attract.

****Definition 2.17**[1]* ***(Basin of attraction)*** *A* ***basin of attraction*** *of an attractor Λ is the maximal set U or domain for which $x_0 \in U$ implies $x(t) \to \Lambda$ as $t \to \infty$.*

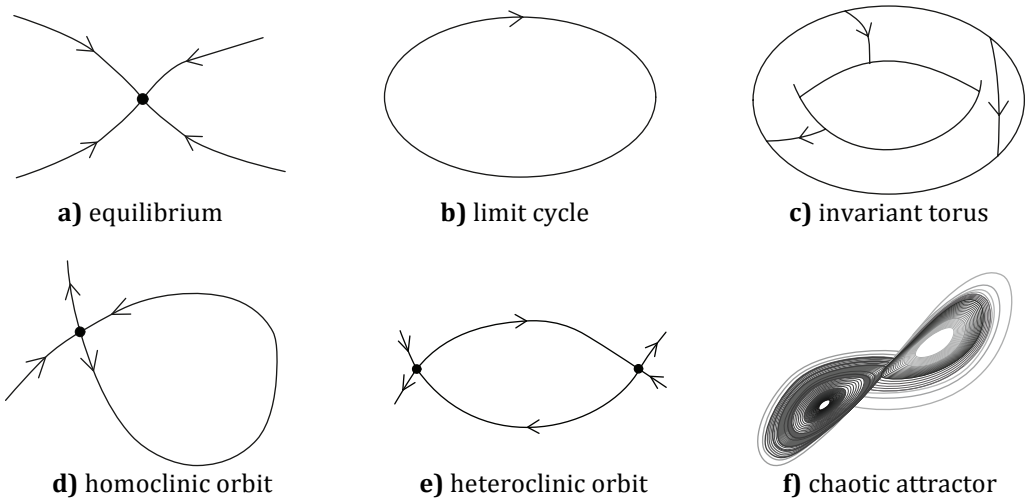

a) equilibrium **b)** limit cycle **c)** invariant torus

d) homoclinic orbit **e)** heteroclinic orbit **f)** chaotic attractor

Fig. 2.8 The phase portraits of different invariant sets [1]

These qualitative characteristics of the dynamical system must be taken into consideration before selecting the proper modelling for the final usage in the simulation and control of dynamical systems. In particular, a more complex definition of these terms is met in the examples of HS. In simpler systems, the equilibrium is just a point instead of the invariant set, but complex systems develop

different invariant sets. As typical for the control system technology the equilibrium or the invariant set is the main goal. Our control solutions will be emphasized with an ability to lead, in a controllable way, the flow of a dynamical system towards the willing equilibrium while simultaneously avoiding an unwilling attractor.
One of the examples of a more complex invariant set is a limit cycle. The periodic orbit, which is isolated and determined by an initial condition x_0, and a period T, that a flow $\Phi(x_0,T) = x_0$, for a minimal $T > 0$, is called a **limit cycle**. That means that in the neighbourhood of a closed periodic curve in the phase space, no other such curve exists. While the limit cycle is inherently a nonlinear phenomenon, in the linear systems we also find periodic orbits [81], but those are not isolated. Topologically, the limit cycle is circular. Their topological shape differentiates other complex invariant sets. Figure 2.8 presents some of the examples of the complex invariant sets.

Besides the continuous systems' interpretation of the natural processes, in broad examples of different scientific realms, a discrete mapping has an inclined dominance. In HS, we see that the presence of both is unavoidable. Similarly, as for the continuous nonlinear dynamical systems, so too the mappings develop different nonlinear phenomena. The key difference among them is a system order, which is a sufficient to guarantee such a scenario.

For a dynamical system expressed by map

$$x \mapsto \mathcal{F}(x,\mu), \ \ for \ \ x \in \Omega \subset \mathbb{R}^n, \mu \in \mathbb{R}^m , \tag{2.42}$$

a time is discrete function $t = kT$, where $k \in \mathbb{Z}_0$ and $T \in \mathbb{R}$ denotes the constant period. An evolution of map $\mathcal{F}$ through the time t_k means its k^{th}iteration and can be expressed by

$$x(t_k) = \mathcal{F}(x(t_{k-1}),\mu) \tag{2.43}$$

or as the $k - fold$ composition

$$x(t_k) = \mathcal{F}_{k-1} \circ \mathcal{F}_{k-2} \circ ... \circ \mathcal{F}_0(x_0,\mu) \ \ k > 0 \ . \tag{2.44}$$

A dynamical system is smooth if a map (2.42) has its invertible map $\mathcal{F}^{(-1)}$, so that

$x(t_1) = \mathcal{F}(x(t_0),\mu)$ and $x(t_0) = \mathcal{F}^{(-1)}(x(t_1),\mu)$.
Analogically as for the continuous system, the *fixed point* of the map is defined by the expression $x^* = \mathcal{F}(x^*,\mu)$. Furthermore, the periodic orbits are posed by *periodic points* where $x^* = \mathcal{F}_k(x^*,\mu)$, referring to the periodic appearance with the frequency of $1/t_k$. Then it defines the $period - k$ *orbit.* The *cobweb diagram* replaces the phase portrait and it is defined by ordinates $x(t_k)$ *and* $x(t_{k-1})$. Also, it is drawn related to the fixed points contained in the line $x(t_k) = x(t_{k-1})$.
Both continuous or discrete dynamical systems' nonlinear phenomena are directly related to the loss of the system's stability. There is a reach stability theory of the nonlinear dynamical systems, but rather just for continuous ones. The stability discussions are less dominant for discontinuous systems or piecewise smooth.

Apart from the established *Lyapunov stability theory* or *asymptotic* and *global* stability, for discontinuous systems, the general academia is still in the process of formalizing an equally powerful toolbox.
The qualitative theory of systems' dynamics aims for an equivalence of the analysed system, in order to preserve the qualitative characteristics of the origin, if the latter is too complex to tackle. This way, we discuss the system's *structural stability*, again referring to the system's equivalence. The minimal preconditions for their equivalence are the same dimensions of the phase space. Additionally, it has to have the same number and the type of invariant sets of their phase portraits that are in the same general position in respect to each other. Mathematically, two-phase portraits are the same if there is a smooth transformation that rotates, stretches, squashes, but does not fold one phase portrait into the other. A transformation that holds an expressed statement is called *homeomorphism*. It is a continuous function of its continuous inverse defined over the entire phase space. Further on an achievement of this transformation is possible over the system's topology in differential geometry.

****Definition 2.18**[1] Let us take two dynamical systems defined by triples* $\{X,T,x(t)\}$ *and* $\{X,T,z(t)\}$ *for* $x,z \in X$*, they are* ***topologically equivalent*** *if a homeomorphism h that maps the trajectory of the first system onto the trajectory of the second one, preserving the direction of time, exists.*

In a case of two maps (2.42) $\mathcal{F}$ *and* $\mathcal{G}$, we say that they are *topologically conjugate* if there is some homeomorphism h that satisfy

$$\mathcal{F}(x) = h^{-1}(\mathcal{G}(h(x))) \quad \rightarrow \quad h(\mathcal{F}(x)) = \mathcal{G}(h(x)) \ , \tag{2.45}$$

or shortly

$$\mathcal{F} = h^{-1} \circ \mathcal{G} \circ h \quad . \tag{2.46}$$

Similarly, for two flows, $\Phi(x,t)$ and $\Psi(h(x),t)$ holds that they are *topologically conjugate* if there is some homeomorphism h that satisfy

$$\Phi(x,t) = h^{-1}(\Psi(h(x),t)). \tag{2.47}$$

It is practically complex to provide such a proof in most of the cases, and there is a relaxing method known as *smooth topological conjugate*. Thus, between two flows we look for a differentiable homomorphism h *with its inverse* or *diffeomorphism* that holds in general

$$f(x) = \left(\frac{dh(x)}{dx}\right)^{-1} f(h(x)). \tag{2.48}$$

Understanding topological equivalence brings us closer to the definition of structural stability and opens the possibility of defining more complex nonlinear phenomena.

****Definition 2.19**[1] (**Structurally stable)** A flow or map is **structurally stable** if there is an $\varepsilon > 0$ such that all first-order perturbations of maximum size ε to the vector field or map f lead to a topological equivalent phase portrait.*

From Definition 2.19 and referring to the Taylor series, we see that the structural stability of a dynamical system in the neighbourhood of an invariant set is proven throughout the topological equivalence to the linearization of the system. Varying of the system parameters is the most crucial scenario that brings our dynamical system to the structural instability. Dynamical systems (2.41) or (2.42) can show that effect only for a specific combination of the vector μ components.

****Definition 2.20**[1] **(Bifurcation)** An occurrence at the point μ_0, where a dynamical system defined by triple $\{X,T,x(t)\}$, loses its structural stability by varying parameter μ, is called **bifurcation**.*

A bifurcation is an already complex nonlinear scenario that can manifest in numerous different forms. In literature [81,82], we can find their definitions and typical forms that are regularly presented by the *bifurcation diagrams*. These diagrams show a plot of the invariant set related to the bifurcation parameter μ. Their rough grouping brings a *local* or *global* group of bifurcations. Local bifurcations are directly related to the loss of hyperbolicity (system's eigenvalues not on the imaginary axis) of the invariant set. All the rest of the bifurcations are in the group of global ones. The presence of bifurcations in the control theory can be considered as a first step to the nonlinear uncertainty that can lead a dynamical system to more complex nonlinear scenarios and chaos.
Referring to Definitions 2.16 and 2.17, if we vary the dynamical system's parameters μ (2.41), the system can enter the neighbourhood of the strange attractors.

****Definition 2.21**[1] A closed and bonded invariant set Λ is called **chaotic** if it satisfies the two additional conditions:*

i) It has a sensitive dependence on the initial conditions:

$$\exists \varepsilon > 0 : \ \forall (x_{1,0} \in \Lambda \ \wedge \ U \subset \Lambda) \ \rightarrow \ \exists (x_{2,0} \in U, t > 0) : \ \| x(t)\big|_{x_{1,0}} - x(t)\big|_{x_{2,0}} \| > \varepsilon$$

*ii) There exists a **dense trajectory** that eventually visits arbitrarily close to every point of the attractor*:

$$\exists x_{1,0} \in \Omega : \forall (x_{2,0} \in \Omega \wedge \varepsilon > 0) \ \rightarrow \| x(t)\big|_{x_{1,0}} - x_{2,0} \| < \varepsilon, \ t \in \mathbb{R}, \ \Omega \subset \Lambda.$$

It is stated that smoothness is not a sufficient precondition in an exclusion of the nonlinear phenomena. As expected, the nonlinear anomalies exist in our state space for smooth dynamical systems defined by ODEs and maps. However, the proven scenarios in several dynamical systems, thanks to the qualitative theory, are related to the complexity as the order of the dynamical system itself. We know [81] that nonlinear and smooth dynamical systems' state space might exhibit the chaotic invariant set, if having a system's order equal or higher than three. While that constraint seems positive for the continuous flows, for the maps, we can experience the strange attractor (chaotic) from the first order. Thus, the systems with the exchange of flows and maps are hypothetically more prone to these kinds of anomalies.

Now, recalling the HS, specifically the piecewise smooth dynamical system from Definition 2.14, we see that qualitative theory has to consider all regions or boundaries of the system Ω_i, as the arbitrary amount of the switching manifolds Σ_{ij}, in order to exemplify all possible scenarios. It is almost impossible to fulfil that task for the higher order systems, but the analysis of the first and second order systems give us the rough perception of at least some scenarios. New momentum in the analysis is certainly a discontinuity boundary and the qualitative changes of topology of the invariant sets in that respect.

****Definition 2.22**[1]* ***(Piecewise-topological equivalent)*** *We say that two piecewise-smooth dynamical systems (2.34), (2.35) are called* ***piecewise-topological equivalent*** *if:*

i) there is homeomorphism h that maps the orbits of the first system onto the orbits of the second one, preserving the direction of time and
$$\Phi(x,t) = h^{-1}(\tilde{\Psi}(h(x),t)).$$
ii) The homeomorphism h can be chosen so as to preserve each of the discontinuity boundaries. Such that, for each i and j holds $h(\Sigma_{ij}) = \tilde{\Sigma}_{ij}$.

Analogically as for the smooth dynamical systems, an appearance of the nonlinear phenomena is related to the structural stability, but now related to the piecewise-topological equivalence.

****Definition 2.23 **[1]* ***(Piecewise-structurally stable)*** *A piecewise-smooth system is* ***piecewise-structurally stable*** *if there is an $\varepsilon > 0$ such that first-order perturbation of the maximum size ε of the vector field or map $\mathcal{F}$, that leave the number and degree of smoothness properties of each of the boundaries Σ_{ij} unchanged, lead to the piecewise-topological equivalent phase portraits.*

Consequently, from Definition 2.23 it is revealed that preserving of the smoothness over the switching manifolds, while the topological equivalence is guaranteed, also preserves the structural stability. Thus, in the case that any of those preconditions is violated, this scenario will certainly lead to the nonlinear phenomena as such.

****Definition 2.24**[1] If for any arbitrarily chosen parameter μ_0, of the system (2.34), (2.35) occurs so that system is not the piecewise-structurally stable, this occurrence is called a* ***discontinuity-induced bifurcation****.*

In references [1, 81, 82], we can find a thoughtful analysis of the most commonly occurring bifurcations. As this matter is considered in the core motivation of this thesis, but not the main objective, we will mention it with the short description, including the main methodology that defines it.
The most distinctive discontinuity-induced bifurcations are:

- Border collision bifurcations.
  It is assigned to bifurcations that appear when the piecewise-smooth map, has a fixed point exactly laying on the switching manifold Σ.
- Boundary equilibrium bifurcations.
  Those bifurcations are generated by flows when the equilibrium lies exactly on the switching manifold.

- Grazing bifurcations of limit cycles.
  Those bifurcations appear as the consequence of the grazing effect of limit cycles and switching manifold.
- Sliding and sticking bifurcations.
  Similarly to the grazing ones, these bifurcations we relate to the effect of the sticking and sliding of limit cycles with respect to the switching manifold.
- Boundary intersection crossing collision.
  It is related to appearance when there are two different switching manifolds Σ_i *and* Σ_j *intersecting, and the limit cycle passes that intersection.*

The powerful method in the analysis of the above-mentioned systems' ill conditions is discontinuity mapping. Although, the maps are already qualified as formalism burdened by the complex nonlinearities, it is in a same time effective tool. The perfect example is a Poincar map and the idea of the stroboscopic mapping. In the examples in which we operate with the closed orbits, even on the occasions when an orbit is a solution of the complex nonlinear and multidimensional flow, we can form the plane or the surface in the way that it is transverse to that flow. All trajectories are intersecting the plane.
If we assigned that plane as Π then the Poincar map is mapping $P:\Pi\to\Pi$.

****Definition 2.25**[1]* **(Poincaré map)** *Let* Π *be a surface transverse to the flow* $\Phi(x,T)$ through it and not parallel to it, then the **Poincaré map** P *is a mapping from* Π *to itself.*

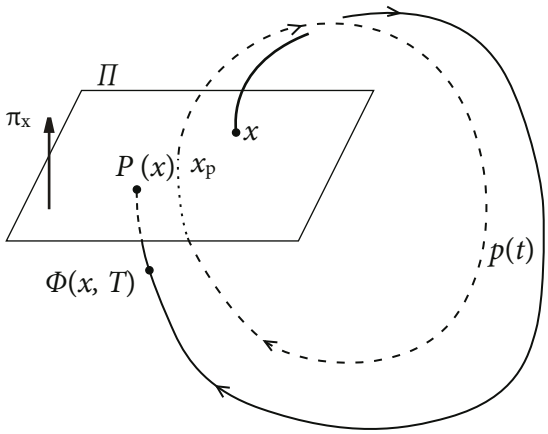

Fig. 2.9 The graphical presentation of the basic idea of Poincar mapping [1]

From Figure 2.9 it is explicitly shown that the surface Π consists of all intersecting points of the cyclic flow $\Phi(x,T)$ in the period T. If we consider that $x_k, x_{k+1}\in\Pi$ are points of trajectory $x(t)$ in time kT and $(k+1)T$ respectively, then the Poincar map is

$$x_{k+1} = P(x_k) \quad . \tag{2.49}$$

For points $x_{k+1} = x_k$ or $P(x_k) = x_k$, we have defined the closed orbit of the flow $\Phi(x,T)$.

This methodology is crucial in the qualitative theory of a dynamical system in general and certainly in HS and impact hybrid systems. In Figure 2.10 we can see some typical problems in the analysis of the piecewise-smooth systems or switching affine systems.

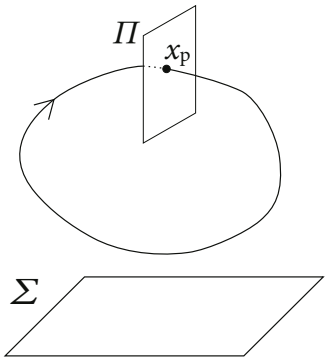

a) Analysis of orbits in a smooth region

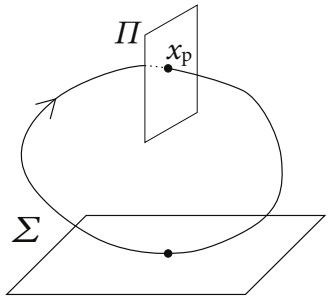

b) Example of the grazing effect of limit cycle to switching manifold

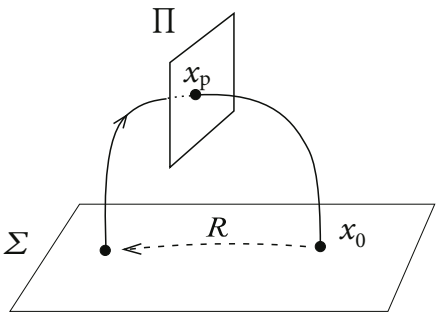

c) Example of the impact hybrid system and their orbit

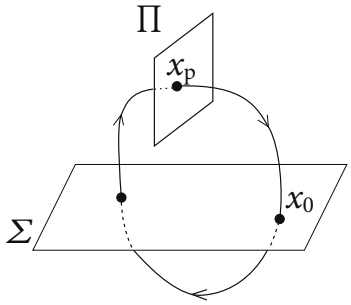

d) Piecewise-smooth system with orbit that intersects the switching manifold, but continues in other region

Fig. 2.10 Examples of periodic orbits and analysis with the Poincar mapping [1]

The comprehensive analysis of the invariant sets, the boundary regions around the switching manifold, and invariant set laying on the switching manifold itself is based on discontinuity mappings. That methodology, introduced by Nordmak [83], synthesizes the Poincar mapping just on the point at which a trajectory intersects with the discontinuity boundary. Afterwards, this map can be composed with a global Poincar map on the both sides of that boundary. We can find in the literature [1] different concepts of discontinuity maps gathered according to specific case studies. Accordingly, those maps are given terminology, i.e.

- The transverse discontinuity mappings in cases in which we have composition of two different flows on both sides of the discontinuity boundary.

- The Poincar -section discontinuity mapping that is defined close to the grazing point; it contains the grazing set and transversally intersects the discontinuity boundary.
- The zero-time discontinuity mapping is defined around the grazing point, as the composition with the maps reconstructs the smooth region orbit completely (zero-time is a convention in which the grazing point has no elapsed time).

2.3 An example of SAS, a DC-DC Boost Converter

Solely by studying the HS, and in order to pursue an example of SAS, the Pulsed Energy Converters (PEC) are emerging as a comprehensive choice. The control of PEC provides a substantial complexity that additionally contributes to the rightness of our choice. A broad presence of PEC in modern technology occupies an interest of different scientific realms. This thesis will illuminate PEC from the side of the heuristic control methodology. Certainly, the core contribution will be in the modelling of PEC despite the fact that all aforementioned formalisms have already exemplified it. We present the survey throughout the history of the modelling of PEC, but bearing in mind the mathematical and physical bases, and from that aspect highlighting just the most distinctive ones.
Almost all electronic equipment contains a power supply and then includes a PEC. Those have been dominated in the past since the first developed semiconductors. Their main role is interfacing energy sources with the consumers by controlling the power flow. While at the end of the 1980s and beginning of 1990s, most of the modelling was motivated by the engineering of electronic circuits, today's modelling is rather inspired by the increasing of the efficiency, reliability, robustness, and the minimization of the physical extents and electromagnetic interferences (EMI). The latter we connect with the coarser controls influenced either by the simplified solution or inability to pursue the advanced control algorithms. In our agenda of objectives, the control algorithm has to include EMI.
Therefore, if we divide the modelling of PEC in the levels of different interest, regarding the grade of accuracy, then we can pose three of them.

First, there is a level of modelling rendered by focusing the components' physics [84-88].

The second, dedicated more to the level of converter, it focuses the main converters' applications. That is certainly an energy transfer based on the predefined input and output parameters [3,93,94]. The converter level will also be the main interest of this thesis and accordingly referenced in the subsequent sections.

Third is a system level that puts into the focus a final objective of the system in general [89-92].
The boosting of technology in the last decade, especially the level of integration of semiconductors and their ideal forms, is diminishing the importance of components' level modelling. Moreover, the system level, mostly developed as a composition of models, requires the highest level of accuracy of the converters' model. Thus, the second or converters' level of modelling is also the most crucial one in the development of different systems.

To decompose the complexity of the broad PEC modelling field, in the following we concentrate on a DC-DC energy conversion. The fundamental members of DC-DC converters are the buck, the boost and the buck-boost DC-DC converter. Their simplified equivalence in the AC energy transfer is the transformer. Analogically, in the case of the step-down transformer, we speak about the buck DC-DC converter, and in the case of the step-up transformer it is a DC-DC boost converter. The DC-DC conversion that combines those two analogies in the AC energy transfer we call the buck-boost DC-DC conversion. Combinations of the inductance, the capacity and two semiconductors (transistor and diode) form the electronic circuits capable of transferring a DC voltage input to a DC voltage output of a different level. As shown in Figure 2.11, the two-port system differentiated in the block of semiconductors and low pass filter, represents a DC-DC converters physical topology.

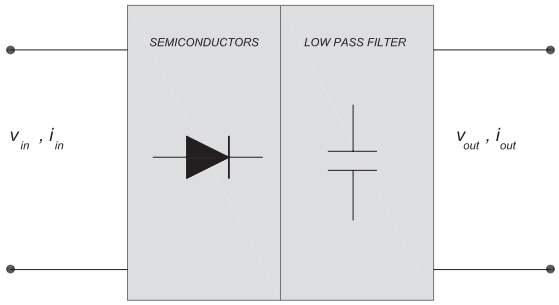

Fig. 2.11 Two-port physical topology of a DC conversion

To transfer a DC energy from the input source to the output consumer and at the same time to maintain the predefined output voltage v_o, the transistor has to be driven by the pulse width modulation (PWM), concerning the switching period T_S. In Figure 2.12 there are three different examples of the electronic circuits showing the basic principles of DC-DC conversions.

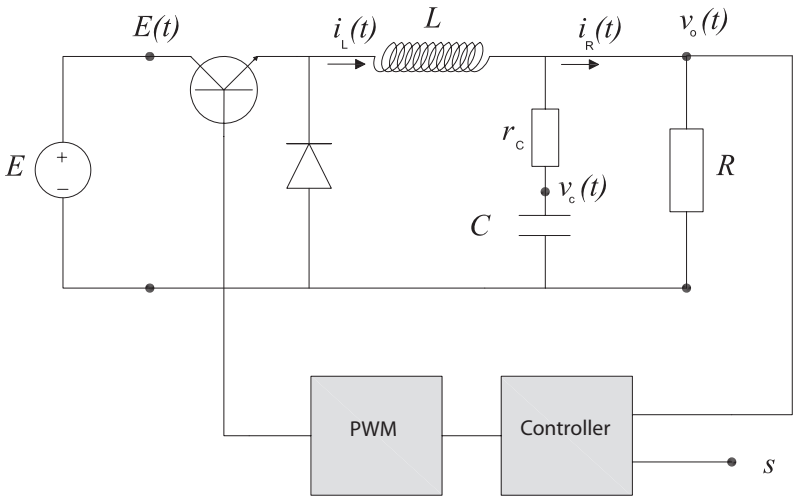

a) DC-DC buck converter circuit diagram

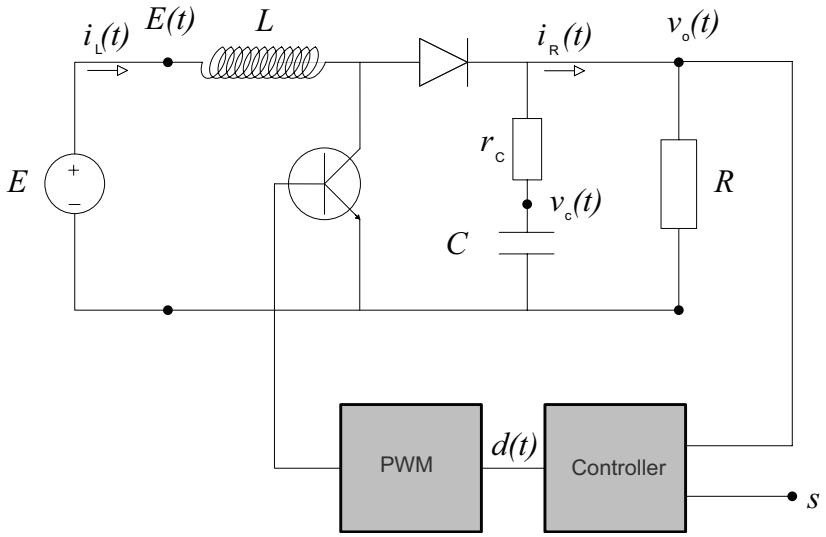

b) DC-DC boost converter circuit diagram

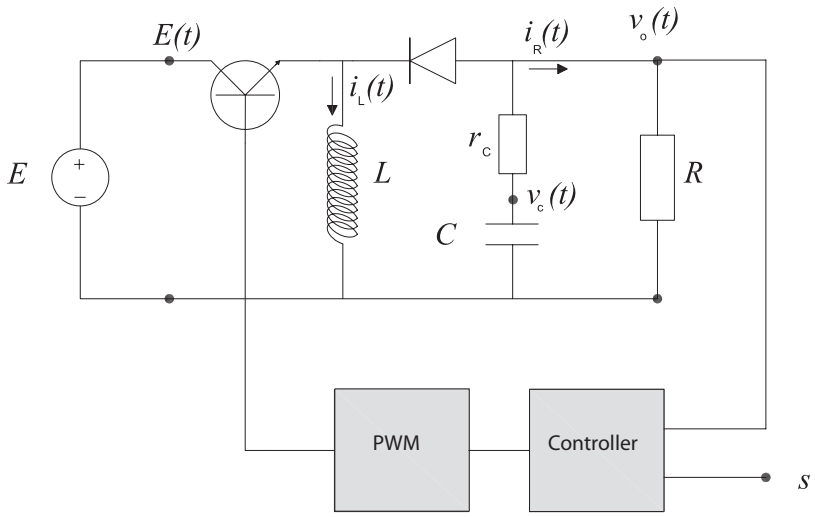

c) DC-DC buck-boost converter circuit diagram

Fig. 2.12 The basic principles of a DC-DC conversion

The PWM driving pulse will have its width in the range $[0,T_s]$, and be applied in the sequential manner. That will cause the sequential switching of the transistor and, in combination with a natural diode's switching, it forms a different circuit topology in one switching period. For each circuit topology, one can establish a system of ordinary differential equations (ODE), mostly as a second order system of variables i_L and v_c. Even certain circuit topology, neglecting the nonlinearities, can be expressed simply as a linear system; DC-DC converters are SAS systems that imply the existence of nonlinearities. The main sources of the nonlinearities are the intrinsic properties of semiconductor devices, the inductor nonlinearity and nonlinearity associated with the control circuit. Aforementioned in Subsection 2.2.2, the SAS ability to induce the nonlinear phenomena is automatically applied to DC-DC converters. Mathematical modelling of DC-DC converters, already considered at the level of the converter is closely defining the control solution. Our interest in the thesis will not be a selection of a well-known and widely used average switched

methodology, followed by the exemplification of the powerful control algorithms. Conversely, it will consist of the optimal modelling driven by the final task relying on the realistic implementation, yet bearing in mind the complexity of the basic components' level modelling. Supporting the same principles, in the selection of a proper SAS example, the DC-DC boost or buck-boost converter bring even more troublesome expressions in comparison with a DC-DC buck converter. Those have an additional real zero on the right half plane, which normally has significant influence on their dynamic behaviours and stability. Differently, the buck DC-DC converter has just a pair of poles. This observation is gathered by conventional and linear analysis based on the average switched modelling method [95]. In the subsequent studies, we have selected the DC-DC Boost converter as an example of a Hybrid Dynamical System grouped in SAS. To present the principles of modelling of a DC-DC boost converter, and explain the main contribution of this thesis different modelling, we are posing the short survey of a DC-DC boost converter modelling.

2.3.1 Small-signal model and Large-signal model of a DC-DC boost converter

Already at the end of 1980s, in the work of Middlebrook and Ćuk [23,24], we can find the valuable modelling contribution at the level of the converter modelling. The main and appealing task at that time was to transfer the physical knowledge, from the component level modelling, to the strong basis for the further control of the output voltage. A two-port system from the Figure 2.11 is extended to the three-port system, including the PWM (Figure 2.12) as the main control signal in achieving the main objective. In their exploration, as the main objective was modelling by the equivalent circuits, we find the physical insights into the qualitative behaviour that is an essential prerequisite to proper use of the more abstract, analytic and computational methods. With posing of the equivalent circuits or canonical models [23], they have delineated two main qualitative aspects in the modelling of DC-DC converters.

First, we have to distinguish the signal processing from the power processing. The term "power processing" considers the electrical energy conversion from one voltage, current and frequency to another, and preferably achieving 100% efficiency. While the signal processing is concerned with performing operations upon the input information, in the contrast, the power processing concern is with performing operations upon the power input, according to the functions specified by the information input. Thus, the interchanged power and information inputs in the power processing, is a characteristic of DC-DC converters. A development of integrated circuits and information technology has a tendency in concealing the main property of conversion and unintentionally suggests the misleading modelling guidance.

Second, the canonical circuit equivalents are constructed to find a linear equivalent that represents the properties of terminal small-signal AC variations, in which the nonlinearities are relegated to the variation of the element values with the large-signal DC operating point. DC-DC converters convert the electrical signals that are constructed as a sum of their DC and AC components, where the AC component is considered as the ripple over the main DC value. The varying of converters' parameters necessarily leads to the changing of the operating point and indicates the nonlinear characteristic of DC-DC converters. A transistor is a nonlinear device, and the model of the transistor for an active region is a function of the operating point. Furthermore, with the canonical circuit representation, in which the ideal transformer is the central element of the voltage

conversion, we see that its conversion ratio as a function of the duty cycle is also a function of other circuit parameters, i.e. a switching frequency, an inductivity and the load resistance.
The idea of canonical equivalents of the electric circuits theory, involving the analogue elements presented in the work of Middlebrook and Ćuk also shows us that DC-DC converters, in their modelling, should be considered integrating the measured feedback. Their canonical models allude to a closed loop regulation principle. At the same time, it considers the linear control theory. That is the reason that some of the model names indicate the type of closed loop solution. Basically, at that time, we can distinguish so called "voltage" and "current programmed" models and the mode of operation. Their critical observations of the term "current control mode" is supported in this thesis too. From the control strategy, the current control mode is the name given to the solution that has a main voltage control loop, but supported with an integrated current control loop. Therefore, in principle it is just a cascade control solution pointing out the importance and the impact of the inductance current to the stability of the power conversion.
In conclusion, the description of converter small-signal models by means of canonical equivalent circuits is a circuit-oriented approach. It is aimed at equivalent-circuit results having elements that retain direct physical interpretation. As the consequence of the formally upgraded equivalent circuit idea [96], and the generalization of the analysing method by which the DC and small-signal transfer function can be obtained directly without the use of an equivalent circuit, that research is brought to the state-space averaging. The approach is constructing the averaged switched model of a DC-DC converter.
Based on the abovementioned theories, we can group a DC-DC converter model in the models of small signal values. In those, the nonlinearity is neglected in the switching transitions and the semiconductors are assumed as ideal switches. Or, it is grouped in the large signal models in which the switching transistor is modelled as the controlled current source and a diode as the controlled voltage source [58].
An averaged switch model is a small signal model, sourced from the linear state space representation

$$\begin{aligned} \dot{\mathbf{x}} &= \mathbf{A}\mathbf{x}(\mathbf{t}) + \mathbf{B}\mathbf{u}(\mathbf{t}) \\ \mathbf{y} &= \mathbf{C}\mathbf{x}(\mathbf{t}) + \mathbf{D}\mathbf{u}(\mathbf{t}) \end{aligned}, \tag{2.50}$$

of every particular mode of a DC-DC converter's operation. The modes of converter's operations are a different circuit topology induced by one control cycle of the converter. During one control cycle, the electronic circuit changes the topology because of the conduction statuses of the semiconductors. Referring the current trajectory during the control cycle and the energy transfer, we differentiate the continuous conduction mode (CCM) and the discontinuous conduction mode (DCM). In CCM, the electronic circuit is driven to maintain the continuous current flow through the coil, and opposite for DCM. Those modes should not be mistaken with the modes of a DC-DC converter's operation, considering its hybrid nature. As per that fact, the number of the circuit operation modes is different for CCM and DCM. Thus, CCM contains two circuit modes of operation and DCM three. Table 2.2 presents typical circuit modes of operation for a DC-DC boost converter in DCM.

Mode	Transistor	Diode	Interval
1	conducting	no conducting	t_{k1}
2	no conducting	conducting	t_{k2}
3	no conducting	no conducting	t_{k3}

Table 2.2 Modes of operation for DCM Boost DC-DC converter

ODEs (2.50) in the state space, for a DC-DC boost converter shown in Figure 2.12b, are based on Kirchhoff's laws for an electronic circuit topology change throughout the modes of operation, Table 2.2. The equations in CCM are the following:

Mode 1:

$$\begin{aligned} \dot{v}_C &= \frac{-1}{C(R+r_c)} v_C \\ \dot{i}_L &= \frac{1}{L} E \\ v_o &\approx v_C \end{aligned} \tag{2.51}$$

Mode 2:

$$\begin{aligned} \dot{v}_C &= \frac{-1}{C(R+r_c)} v_C + \frac{R}{C(R+r_c)} i_L \\ \dot{i}_L &= \frac{-R}{L(R+r_c)} v_C - \frac{Rr_c}{L(R+r_c)} i_L + \frac{1}{L} E \\ v_o &\approx v_C \end{aligned} \quad . \tag{2.52}$$

The characteristic matrices of a state space representation (2.50), in which we assumed the constant circuit elements and the piecewise linearity of the system for particular periods t_{k1} and t_{k2} are:

$$\boldsymbol{A}_1 = \frac{1}{C(R+r_c)} \begin{bmatrix} -1 & 0 \\ 0 & 0 \end{bmatrix} \;,\; \boldsymbol{B}_1 = \boldsymbol{B}_2 = \begin{bmatrix} 0 \\ \frac{1}{L} \end{bmatrix}$$

$$\boldsymbol{A}_2 = \frac{1}{C(R+r_c)} \begin{bmatrix} -1 & R \\ \frac{-CR}{L} & \frac{-CRr_C}{L} \end{bmatrix} \;. \tag{2.53}$$

To develop the averaged model, we have to implement a function $d(t) = k \cdot d_u(t) \in [0,1]$, which denotes the duty cycle over the transistor ($d_u(t)$ is a scaled value to adopt the physical construction). The function is a relative time of the control period T_S equal to the time period t_{k1}. It also presents our control signal. The averaging in the state

space is done for a complete period $T_S = t_{k1} + t_{k2}$, and thus assuming that the third mode does not exist $t_{k3} = 0$, or is negligible

$$\begin{aligned} \dot{x}(t) &= [dA_1 + (1-d)A_2)]x(t) + [dB_1 + (1-d)B_2)]u(t) \\ y(t) &= [dC_1 + (1-d)C_2)]x(t) + [dD_1 + (1-d)D_2)]u(t) \end{aligned}. \tag{2.54}$$

The equations (2.54) evolve into the equivalent circuit state space model of a DC-DC boost converter for CCM. Now, the new equivalent state space averaged model

$$\begin{aligned} \dot{x}(t) &= \overline{A}x(t) + \overline{B}u(t) \\ y(t) &= \overline{C}x(t) + \overline{D}u(t) \end{aligned}, \tag{2.55}$$

is expressed by the following matrices:

$$\overline{A} = \frac{(1-d)}{C(R+r_c)} \begin{bmatrix} \frac{1}{(1-d)} & R \\ \frac{-CR}{L} & \frac{-CRr_C}{L} \end{bmatrix}. \tag{2.56}$$

$$\overline{B} = \begin{vmatrix} 0 \\ \frac{1}{L} \end{vmatrix} \qquad \overline{C} = \begin{vmatrix} 1 \\ 0 \end{vmatrix}$$

Without neglecting the elements' physical characteristics and the converter's hybrid nature, the problem is purely nonlinear. For the sake of complexity reduction, and based on the assumption that the modelling will only be done near the operating point, these system characteristics are neglected. We can now consider the equivalent and continuous system, but still nonlinear. The state space variables are naturally the AC signals, having its AC ripple added to a DC signal part. Thus, one could derive the linearization around the equilibrium point. That operation upon the average model is the well-known perturbation theory, considering an infinitesimal change of the state and control variables. The new substitute variables are

$$\begin{aligned} x(t) &= \overline{X} + \Delta x(t) \\ y(t) &= \overline{Y} + \Delta y(t) \\ u(t) &= \overline{U} + \Delta u(t) \end{aligned}, \tag{2.57}$$

where Δ denotes a small-signal value or a ripple.
In the linearization process, we also add the small signal value over the steady duty cycle $d(t) = \mathcal{D} + \Delta d(t)$. Thus, the state space equations (2.55), (2.56) will evolve in the small signal state space equations:

$$\begin{aligned} \Delta\dot{x}(t) &= \overline{A}\Delta x(t) + \overline{B}\Delta u(t) + \overline{B}_d \Delta d(t) \\ \Delta y(t) &= \overline{C}\Delta x(t) + \overline{D}\Delta u(t) + \overline{D}_d \Delta d(t) \end{aligned} \tag{2.58}$$

The equations (2.58) are rendered by putting the substitution variables (2.57) into the (2.55), and neglecting the products of the AC quantities $\Delta d(t)\Delta v_C$ and $\Delta d(t)\Delta i_L$. Also,

the quantities related to the products of DC values are considered to be initial conditions of the operating point and accordingly subtracted.
However, to calculate the steady state DC values, we use equations $\dot{x}(t) = 0$ or

$$\begin{aligned} 0 &= \overline{A}\overline{X} + \overline{B}\overline{U} \\ \overline{Y} &= \overline{C}\overline{X} + \overline{D}\overline{U} \\ \overline{X} &= -\overline{A}^{-1}\overline{B}\overline{U}\,. \end{aligned} \tag{2.59}$$

The capital letters are DC values of the operating point.

For our example of a DC-DC boost converter, the state space model in a certain operating point will be the following:

$$\Delta\dot{x}(t) = \frac{(1-\mathcal{D})}{C(R+r_c)}\begin{bmatrix} \frac{1}{(1-\mathcal{D})} & R \\ \frac{-CR}{L} & \frac{-CRr_C}{L} \end{bmatrix}\Delta x(t) + \begin{vmatrix} 0 \\ \frac{1}{L} \end{vmatrix}\Delta E(t) + \begin{bmatrix} \frac{-I_L R}{C(R+r_C)} \\ \frac{-(V_C + I_L r_C)R}{L(R+r_C)} \end{bmatrix}\Delta d(t)\ . \tag{2.60}$$

Now, we could also proceed to form the transfer functions in the s-space for an averaged model,

$$G_1(s) = \frac{v_o(s)}{d(s)} \tag{2.61}$$

$$G_2(s) = \frac{v_o(s)}{E(s)}\ , \tag{2.62}$$

by taking in considerations that it is for a linear and non-homogenous invariant system

$$G(s) = C[sI - A]^{-1}B. \tag{2.63}$$

The same approach can be applied to the other two types of DC-DC converters.
An example of typical transfer function computing results for a DC-DC boost averaged model is given by [59](see details in [59]):

$$G_1(s) = \frac{K_1(1 - T_b s)}{T_n^2 s^2 + 2T_n\varsigma s + 1} \tag{2.64}$$

$$G_2(s) = \frac{K_2}{T_n^2 s^2 + 2T_n\varsigma s + 1} \tag{2.65}$$

Coefficients in the transfer functions are calculated for a particular set of elements that are chosen, regarding their estimated series resistance (ESR). Therefore, the number of elements in the circuit diagram can vary. For example, the circuit diagrams in Figure 2.12a, b, and c are just some of the possible constructions related to the involvement of the ESRs.

Most of the engineering solutions in the field are based on the above formalism even though it is gathered on a strict and hard restriction around the operating point as shown

by (2.58) and (2.59). Nevertheless, the use of this formalism relies on the same idea as the equivalent canonical circuit expressed in [23]. In seeking a compact solution, to construct the equivalent state space model, but by a coarse approximation, it is certainly modelling the converter for a complete switching period.
Following the experience in the exploitation of DC-DC converters, scientifically in analysis of the stability in control of DC-DC converters, there was a continuation of the work of Erikson, Ćuk, and Middlebrook [24] in the direction of large-signal models. A model that can sustain large parameter perturbations and remain stable is devised. In those perturbations, the nonlinear terms become significant and, on some occasions, harm the system stability. DC-DC converters are open loop stable and closing the feedback loop causes an appealing stability problem. The large-signal models are nonlinear, but again rather based on the similar assumptions, and the linearity of the duty cycle function related to the state variables [24], called a "linear ripple approximation". Other approaches are strictly connected to the linear feedback control solution by the so-called "current programmed mode" [97] and again involving the averaging approach. At the later stages, the large signal models are improving the earlier assumptions made in the "current programmed mode" and tackling the nonlinearity by dividing the state space expression into slow and fast variation components [97]. Those solutions are again firmly connected to the linear control theory and limited to the simulation abilities at that time. Thus, most of those large-signal models are just used in the simulation to underline the instability regions and established the stable linear control parameters.

2.3.2 Hybrid automaton of a DC-DC boost converter

More powerful computing abilities, as a base for the construction of more accurate modelling principles, referring to the development of a digital technology, contribute to the definition of hybrid dynamical model formalisms in all their varieties. Although, the HS modelling existed in the 1990s, it was barely used in the theory of electrical circuits. Thus, the modelling of DC-DC converters, observed from the theory of HS, comes later at the end of 1990s and the beginning of this century. We can connect it with the significant contribution of Bemporad and Morari [26]. In Section 2.1 we have introduced HS formalisms that are applicable for a SAS where the DC-DC converters certainly belongs. Today, the grade of applicability of those particular formalisms in the control technology remain unknown. The theory of *Hybrid Automata* as the fundamental form of HS defined by Definition 2.1 gives us the global framework.
A DC-DC converter is a process in which the continuous and discrete states shown in Figure 2.1 are tangled together into the dynamical system. The *hybrid automaton* of a DC-DC boost converter taken in our thesis as a core example is posed in Figure 2.13.

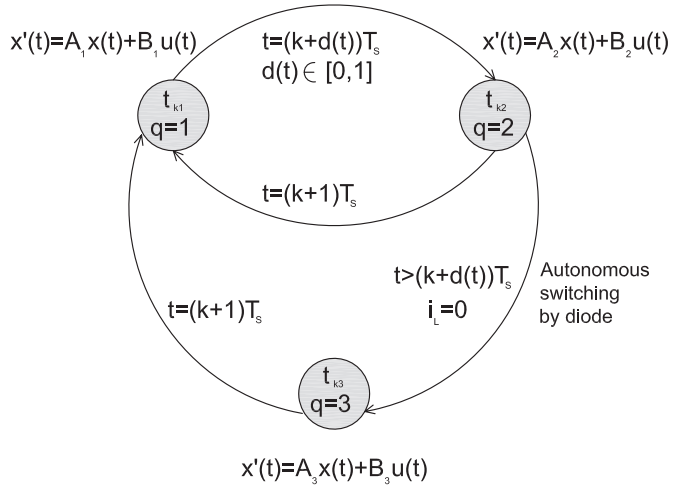

Fig. 2.13 Hybrid automaton of a DC-DC boost converter

As shown, our process contains three different discrete states; q_1, q_2 and q_3. For each discrete state, which corresponds to the mode of operation, its electrical circuit topology has an associated state space model. If we recall the equations (2.53) for CCM of a DC-DC boost converter and add the third mode state space equations for a state space vector $x(t) = [v_C(t), i_L(t)]^T$

$$\boldsymbol{A}_3 = \frac{1}{C(R + r_c)} \begin{bmatrix} -1 & 0 \\ 0 & 0 \end{bmatrix}, \quad \boldsymbol{B}_3 = \begin{bmatrix} 0 \\ 0 \end{bmatrix}, \tag{2.66}$$

we receive the model in DCM and gather the complete definition of continuous states of the *hybrid automaton* from Figure 2.13.

Further development of hybrid automaton has to continue in the direction of tackling the problem of guard and reset map. The state space equations of (2.53) and (2.66) are rendered by taking into the consideration that input into the electrical circuit is the source voltage E. If we exclude one of the modes of operation and observe it separately, it is physically meaningless. The electrical circuit will run into the saturation and physical constraints of the employed elements. Our process has a meaning if it works in CCM or DCM that includes a set of modes $\{q_1, q_2\}$ or $\{q_1, q_2, q_3\}$. The guard $\mathcal{G}(t, d(t))$ and reset $\mathcal{R}(t, d(t))$ maps from Definition 2.1 are functions of the time and the duty cycle $d(t)$. Referring to that fact, the hybrid automata bring substantial complexity in order to elevate the accuracy of modelling. This drawback is limiting model applicability in employing the established control methodologies.

In the latest work of Tabuada [63], we can find the theoretical bases of forming an approximate bisimilar symbolic model of a DC-DC boost converter and its analysis. Even as theoretically advanced approach, it is based on the hard restriction on taking the DC-DC converter as an example of SAS. It takes an abstract switch into the consideration, which must replace the diode and transistor at the same time (Figure 2.12b) and provide the *logical tautology* (see Definition 3.1, Chapter III) in the switching of two different electrical circuits. The basic theory of HS and *Hybrid Automata* is certainly a profound way to form a simulation model of a DC-DC converter and, together with the computing abilities of today's technology, formulate the accurate counterpart to the physical process. Our interest in this

thesis is a definition of the modelling that allows the applicable model-based control solution that is the genuine part of the converter itself. One of the modelling formalisms, following that direction, can be found in MLD modelling explained in Section 2.1.4.

2.3.3 MLD model of a DC-DC boost converter

In the last decade, Model Predictive Control (MPC) has taken a lead in the control techniques, mostly by the development of more powerful computing abilities. Observed from that aspect, it is expected that also a development of control in the power electronics will follow the same trend. Thus, the DC-DC converter modelling influenced by the control solution requires for a more compact and global solution, referring to the robustness. The latter excludes an observation around the operating point and promoting the global modelling. That makes the problem more compelling for a DC-DC boost converter and considering the modelling that includes both, the CCM and DCM of the converter. Added to the mentioned trend, development of the discrete controllers completely displaced the analog ones and established the solution mostly in the discrete time state space.
The MLD modelling presented in the Subsections 2.1.3 and 2.1.4, in DC-DC converters emerges in the work of Geyer [98-100]. This work addresses the main dogmas in the new era of the control of DC-DC converters. First, it is still unrealistic in industrial practice [100] to implement variable switching frequency. Second, as mentioned above the basic theory of Hybrid Automata [100] still does not suggest a physically applicable solution by satisfying the safety properties and given performance criteria [63]. Third, it is still a common practice in the state of the art solution to employ the simplified models for the description of the dynamic behaviour of DC-DC converters.
However, in the work [100], we can find the MLD solution of a DC-DC buck converter that has a simpler state space representation than a DC-DC boost converter. Additionally, it does not have a non-minimum phase dynamic in the CCM operation. Here, the nonlinearity of a DC-DC conversion is grasped and the problem of duty cycle prediction underlined. While in the continuous state space representation and the analog controls the mathematical problem of the closed loop transfer function is a transcendental, in the discrete controls, we have a restrictive formalism that makes the problem solvable. During the one scan time, the control variable has a fixed value and cannot influence differently than predicted at the predeceasing time scan, but one could predict a step-ahead evolution of states causally linked during the successor time scan. The same idea is found in the mentioned work [3,17,100] where the MLD form emphasizes the ν-resolution approach.
Closely, the suggested solution is quantizing the genuine hybrid time execution of the automaton in Figure 2.13, in the part related to the continuous evolution of Definition 2.8. However, the evolution from the discrete state q_1 to q_2 happens, derived by the new shorter discrete time quantifiers. Herein, the results show that the modelling error decreases by incrementing the ν-resolution, which can be understood as the shortening of the prediction horizons, equidistantly placed in the range $[\tau_i, \tau_i^{'}] = T_S$.
To drive the MLD model of a DC-DC buck converter, the authors of this approach lift the original state space for additional discrete variables. The subperiods

$n \in \{0,1,\ldots,\nu-1\}$ of the switching period T_S are equal to the new discrete time base $\tau_S = T_S/\nu$, where $\nu \geq 1$ and $\nu \in \mathbb{N}$. The new hybrid model was presented by

$$\xi(n) = \begin{cases} \Phi\xi(n) + \Psi & if \quad \sigma_n \wedge \sigma_{n+1} \quad (Mode\,1) \\ \Phi\xi(n) & if \quad \overline{\sigma}_n \quad (Mode\,2) \\ \Phi\xi(n) + \Psi(\nu d(k) - n) & if \quad \sigma_n \wedge \overline{\sigma}_{n+1} \quad (Mode\,3) \end{cases} . \tag{2.67}$$

In equation (2.67), the hybrid model discrete states or modes $\{q_1, q_2, q_3\}$ are defined by three different discrete time τ_S state space equations, selected by the logic variables σ_n and σ_{n+1}, where Φ and Ψ are the state space matrixes. The vector $\xi(n) = [i_L(n) \quad v_C(n)]^T$ defines the state variables. The state space expression is derived for the buck DC-DC converter related to the on/off status of the transistor on Figure 2.12b, by the similar procedure as shown in (2.51) and (2.52) of the DC-DC boost converter. In contrast to that, the equations (2.67) show three modes of operation. This additional mode is provided in order to minimize the error in the averaging of the state space for the unpredictable time of switching. While the transistor is conducting, the mode of operation is 1. The transistor's off state defines the Mode 2, and the Mode 3 is subperiod that contains the event of an opening of the transistor. We see that the control variable $d(k)$ remains a scalar variable related to the switching period T_S, and the new hybrid model in equation (2.67) has been just a sort of the nested state space that is not physically based. It is a possible programming solution in the hybrid modelling tool HYSDEL. The general hybrid model is automatically generated by HYSDEL in the form of an equation (2.18). As the explained approach afterwards appeared in [3], which considered the established methodology in solving a DC-DC boost converter, the level of applicability of this modelling remains unknown, referring to the dimensions of matrixes in (2.18) and the problem of the guard and the reset mapping in the DCM of a DC-DC boost converter.

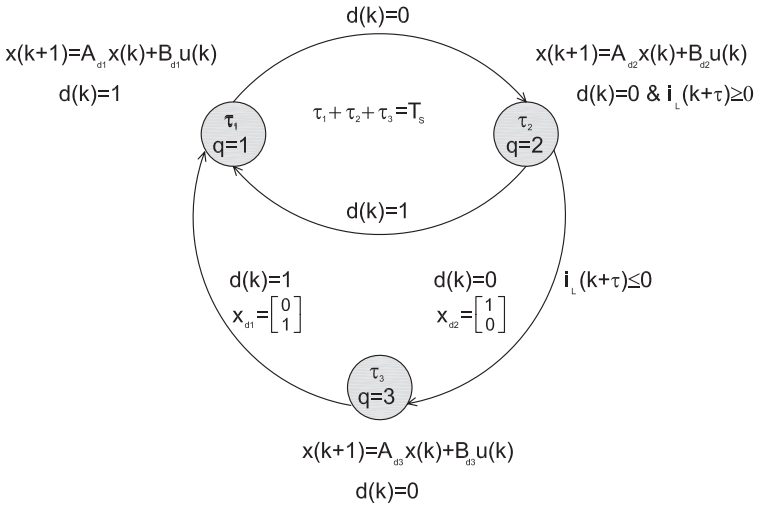

Fig. 2.14 DHA of a DC-DC boost converter

The newer research [2,3,101] and references there in reply on the above highlighted ambiguity in the control of more complex DC-DC boost converter. In Figure 2.14, we see a new hybrid automaton of a DC-DC boost converter, but now in a discrete form based on the formalism of DHA given in Subsection 2.1.3 and Figure 2.3.
The discrete counterpart of the continuous dynamics is driven based on the matrixes in (2.53), (2.66) and equations

$$A_{d_i} = e^{A_i T_S} \quad , \quad B_{d_i} = \int_0^{T_s} e^{A_i \tau} d\tau \cdot B_i E \qquad . \tag{2.68}$$

To define the discrete states of each particular mode of operation $\{q_1, q_2, q_3\}$ [101], one has to involve three logic variables $\delta(k)$, $\delta_{f1}(k)$ and $\delta_{f2}(k)$. The 3rd mode of operation is not caused by the manipulated variable directly, and discrete states, but it is the natural switching of the continuous evolution defined by

$$i_L(k+N) \le 0 \quad \leftrightarrow \quad \delta(k) = 1 \qquad . \tag{2.69}$$

As shown, we have to predict the inductance current evolution in the mode 2 and the natural switching time that will be coded by logic variable $\delta(k)$. This is because the continuous evolution in period t_{k2} is not defined by the control variable $d(k)$ only. The recursive prediction of the i_L is obtained by

$$i_L(k+N) = [0 \;\; 1](A_{d_2}{}^N x(k) + \sum_{i=0}^{N-1} A_{d_2}{}^i B_{d_2}) \qquad . \tag{2.70}$$

One has to calculate the predecessor steps in order to provide resetting of the inductor current at the time (2.69).
The resetting is done in-between modes 2 and 3 by equation:

$$x(k+1) = \begin{bmatrix} 1 & 0 \\ 0 & 0 \end{bmatrix} (A_{d_3} x(k) + B_{d_3}) = A_{d_4} x(k) + B_{d_4} \qquad . \tag{2.71}$$

In Figure 2.14, a DHA consists of a discrete state vector
$x_d(k) = [x_{d_1}(k) \;\; x_{d_2}(k)]^T$, which obtains three discrete states, i.e. $[0 \;\; 1]^T$, $[1 \;\; 0]^T$, $[0 \;\; 0]^T$, corresponding to the modes of operation. Discrete states' evolutions are substituted by the logic variables $\delta_{f_1}(k)$, $\delta_{f_2}(k)$ and yield

$$x_d(k+1) = \delta_f(k) = [\delta_{f_1}(k) \;\; \delta_{f_2}(k)]^T \qquad . \tag{2.72}$$

Now, the following logic defines a discrete state transition:

$$
\begin{aligned}
&x_{d_1}=0 \wedge x_{d_2}=0 \wedge d=0 \rightarrow \delta_{f_1}=0 \wedge \delta_{f_2}=0 \rightarrow x_d(k+1)=[0\ \ 0]^T \\
&x_{d_1}=0 \wedge x_{d_2}=0 \wedge d=1 \rightarrow [0\ \ 1]^T \\
&x_{d_1}=0 \wedge x_{d_2}=1 \wedge d=1 \rightarrow [0\ \ 1]^T \\
&x_{d_1}=0 \wedge x_{d_2}=1 \wedge d=0 \rightarrow [0\ \ 0]^T \\
&x_{d_1}=0 \wedge x_{d_2}=1 \wedge d=0 \wedge \delta_1=0 \rightarrow [0\ \ 0]^T \\
&x_{d_1}=1 \wedge x_{d_2}=0 \wedge \delta_1=0 \rightarrow [0\ \ 1]^T \\
&x_{d_1}=1 \wedge x_{d_2}=0 \wedge d=0 \rightarrow [1\ \ 1]^T
\end{aligned}
\quad . \qquad (2.73)
$$

As in the MLD model, the reset prediction of the inductor current is done based on the predecessor discrete state and the existing one, there is a need to define an extra discrete state $x_{d_3}(k) = x_{d_1}(k-1)$, and yield the new logic variable

$$
\delta_{23}=1 \leftrightarrow x_{d_1}(k)=0 \wedge x_{d_2}(k)=0 \wedge x_{d_3}(k)=1 \quad . \qquad (2.74)
$$

The logic variable δ_{23} denotes the reset state while the transition is active from mode 2 to mode 3.

The final MLD state space expression for the DC-DC boost converter is given by:

$$
\begin{aligned}
&x(k+1)=(A_{d_1}x(k)+B_{d_1})x_{d_2}(k)+(A_{d_2}x(k)+B_{d_2})x_{d_1}(k)+ \\
&+(A_{d_3}x(k)+B_{d_3})(1-x_{d_2}(k)-x_{d_1}(k)-\delta_{23}(k))+(A_{d_4}x(k)+B_{d_4})\delta_{23}(k)
\end{aligned}
\quad . \qquad (2.75)
$$

Further, if we substitute the auxiliary variables

$$
\begin{aligned}
&z_{11}(k)=(A_{d_2}-A_{d_3})x(k)x_{d_1}(k) \\
&z_{22}(k)=(A_{d_1}-A_{d_3})x(k)x_{d_2}(k) \\
&z_{33}(k)=(A_{d_4}-A_{d_3})x(k)\delta_{23}(k)
\end{aligned}
\quad , \qquad (2.76)
$$

then the equation (2.75) progresses in a more compact form as suggested in the expression (2.18)

$$
\begin{aligned}
&x(k+1)=A_{d_3}x(k)+B_{d_3}+(B_{d_2}-B_{d_3})x_{d_1}(k)+ \\
&+(B_{d_1}-B_{d_3})x_{d_2}(k)+(B_{d_4}-B_{d_3})\delta_{23}(k)+z_{11}(k)+z_{22}(k)+z_{33}(k)
\end{aligned}
\quad . \qquad (2.77)
$$

To protect the system from chattering in mode 2 and simultaneously exchanged the discrete transitions to modes 1 and 3, there is still a necessity to enrich the logic from (2.73) by following logical expression

$$
x_{d_1}(k)=1 \wedge x_{d_2}(k)=0 \rightarrow i_L(k+1)>0 \vee d(k)=0 \quad . \qquad (2.78)
$$

Let us recall the expression (2.18) again. We see that to complete the MLD expression proposal one should transfer the logic (2.69), (2.73), (2.74) and (2.78)

into mixed integer expressions. This must be done by following the propositional calculus in Table 2.1 in order to derive the matrixes $\{\boldsymbol{E}_1,\ldots,\boldsymbol{E}_5\}$.

2.3.4 A DC-DC boost converter model based on complementarity formalism

In the aforementioned formalisms of Section 2.3, where we can find the correlations, the following formalism is done differently regarding the complementarity characteristic of a DC-DC boost converter's states. The theory presented in Subsection 2.1.5 will be used to form the ODE (2.21). For the sake of the complexity reduction, the modelling will be based on the ideal switches as the source version of the applied formalism. This modelling principle is a member of the first level modelling of converters, or aforementioned group in Section 2.3 as a physical modelling. The concerns for a switching mechanism, consisting of semiconductors, are unquestionably the reason. Although emphasizing the switching electrical network for a specific location (2.21-2.23), as the combination of all possible switching states, this modelling can also be considered as the comprehensive representation of the converter's level modelling.
Further, a DC-DC boost converter presented in the LC form (2.24) could be called a switched cone complementarity system, as it satisfies the equations (2.25) and (2.26)[2]. Hence, from Figure 2.12b and by using the Kirchhoff's laws, the following equations (2.79) are derived. The equations contain the complementarity variables, voltages and currents through the ideal semiconductors.

$$\begin{aligned}
\dot{v}_C &= \frac{-1}{CR}v_C + \frac{1}{C}i_L + \frac{R+r_c}{CR}i_{Tr} \\
\dot{i}_L &= \frac{-1}{L}v_C - \frac{1}{L}v_D + \frac{r_c}{L}i_{Tr} + \frac{1}{L}E \\
v_o &\approx v_C
\end{aligned} \tag{2.79}$$

Following the complementarity formalism in rendering the equations (2.79), our complementarity variables should agree with the expression

$$\begin{aligned}
&0 \le \boldsymbol{y}(t) \perp \boldsymbol{u}(t) \ge 0 \\
&\boldsymbol{u}(t) = [v_D \;\; i_{Tr}]^T \; v_D - \textit{voltage over the diode} \;\; i_{Tr} - \textit{current through the transistor} \\
&\boldsymbol{y}(t) = [v_{Tr} \;\; i_D]^T \; v_{Tr} - \textit{voltage over the transistor} \;\; i_D - \textit{current through the diode}
\end{aligned} \tag{2.80}$$

From the equations (2.79) and (2.80) it is possible to form the state space expressions

$$\begin{aligned}
\dot{\boldsymbol{x}}(t) &= \boldsymbol{A}\boldsymbol{x}(t) + \boldsymbol{B}\boldsymbol{u}(t) + \boldsymbol{E}v(t) \\
\boldsymbol{y}(t) &= \boldsymbol{C}\boldsymbol{x}(t) + \boldsymbol{D}\boldsymbol{u}(t) + \boldsymbol{F}v(t)
\end{aligned} \quad , \tag{2.81}$$

where the matrixes are

$$\boldsymbol{A} = \frac{1}{C(R+r_c)}\begin{bmatrix} -1 & R \\ \frac{-CR}{L} & \frac{-CRr_C}{L} \end{bmatrix}, \; \boldsymbol{B} = \begin{bmatrix} -\frac{1}{C(R+r_C)} & 0 \\ 0 & \frac{1}{L} \end{bmatrix}, \; \boldsymbol{C} = \begin{bmatrix} \frac{R}{1+r_C} & \frac{Rr_C}{1+r_C} \\ 0 & 1 \end{bmatrix},$$

$$\boldsymbol{D}=\begin{bmatrix}1 & \frac{-Rr_C}{1+r_C}\\ 0 & -1\end{bmatrix},\ \boldsymbol{E}=\begin{bmatrix}0\\ -\frac{1}{L}\end{bmatrix},\ \boldsymbol{F}=\begin{bmatrix}0\\ 0\end{bmatrix} \quad . \qquad (2.82)$$

The state vector is $\boldsymbol{x}(t)=[v_C \ \ i_L]^T$ and $v(t)=E(t)$ denotes the input source. The output vector $\boldsymbol{y}(t)$ has also been defined by Kirchhoff's laws. It is now obvious that this approach implements the electronic elements, a diode and transistor, by their complementary parameters. Those are pairs $\{v_D, i_D\}$ and $\{v_{Tr}, i_{Tr}\}$, respectively. Differently than in the basic approach, this formalism can be formed in the state space expression (2.81); this is reminiscent of one of the other type of the HS formalisms. The equivalence of the different HS formalisms is introduced in the literature [25] and Chapter III.
Originally, from the first authors [12,102] that applied this theory, discussed in Section 2.1.5, equations were assuming the ideal electrical switches. In the newer releases [13] and in order to elevate the modelling accuracy, those elements are defined more physically accurately. The equations (2.79), (2.81) and (2.82) are valid for all modes of a DC-DC boost converter operation while the external control of the switches guides it through, meaning that a DCM is also tackled by the formalism. That is naturally archived by the positivity of the complementarity variables (2.80).
For the example, it is relatively easy to show that the above equations are blocking the negative values of inductor current and defines a converter operation in DCM. In the similar way, and by selecting the position of electrical switches, we can prove the consistency for the other HS modes [102].

2.3.5 A DC-DC boost converter model in DCM, the qualitative examinations

One of the analytic examinations of a DC-DC boost converter in DCM was given in [7,8]. The work has rendered a new sight in the modelling of a DC-DC boost converter. It is issued at the emerging time of the mathematical qualitative theory and the hybrid systems' modelling theories. The results of the mentioned article, together with the anomalies of the hybrid systems' modelling theories could be acknowledged as the basic inspiration for this thesis. In the simulation and the experimental tests performed in this thesis, we use the same DC-DC boost converter example with all its physical values. To receive the same results as from [7], and to continue the examination of the problem from the aspects of the state of the art academic work in this field, we have simulated and examined this example more comprehensively from the side of the theory in Subsection 2.2.2. The modelling objectives in most of the different modelling formalisms in general are taking the switching period T_S of the pulse width modulation as the genuine part of the conversion and further control. It is certainly influenced by the final goal, which is the physical implementation of derived controllers that are based on those modelling approaches.

During the period T_S and by knowing that $t_{k_1}+t_{k_2}+t_{k_3}=t_{k+1}-t_k=T_S$, we can stack the consecutive solutions for each time interval t_{k_i} and form the iterative map for the complete period. In other words, we construct the overall solution by considering the explicit linear system solution in the piecewise smooth time interval as

$$x(t) = \Phi_1(t - t_k)x(t_k) + \int_{t_k}^{t} \Phi(t - \tau)B_1 E d\tau \tag{2.83}$$

and generally through different time periods [7]

$$\Phi(t_{k_1} + t_{k_2} + t_{k_3}) = \Phi(t_{k_1})\Phi(t_{k_2})\Phi(t_{k_3}) \quad . \tag{2.84}$$

In sequel, it yields

$$\begin{aligned} x(t_{k+1}) = {} & \Phi_3(t_{k_3})\Phi_2(t_{k_2})\Phi_1(t_{k_1})\left(x(t_k) + \int_{t_k}^{t_k + t_{k_1}} \Phi_1(t_k - \tau)B_1 E d\tau \right) + \\ & + \Phi_3(t_{k_3})\Phi_2(t_{k_2})\left(\int_{t_k + t_{k_1}}^{t_k + t_{k_1} + t_{k_2}} \Phi_2(t_k + t_{k\,1} - \tau)B_2 E d\tau \right) + \\ & + \Phi_3(t_{k\,3})\left(\int_{t_k + t_{k_1} + t_{k_2}}^{t_{k+1}} \Phi_3(t_k + t_{k_1} + t_{k_2} - \tau)B_3 E d\tau \right) \end{aligned} \quad . \tag{2.85}$$

Our final and the general expression will evolve in

$$x(t_{k+1}) = f(x(t_k), d_k) \ , \tag{2.86}$$

for a duty cycle $d_k = \frac{t_{k_1}}{T_S}$ as a control signal of the closed loop control.

To derive the transition matrixes for each mode of operation, we will employ Taylor's power series

$$\Phi_i(t) = 1 + \sum_{n=1}^{\infty} \frac{1}{n!} A_i^{\,n} t^n \ \ for\ i = 1,2,3 \ , \tag{2.87}$$

and also taking into account that the selection of C and R elements in Figure 2.12b will be on the way that the time constant $\tau = RC >> T_S$.

In DCM of a DC-DC boost converter, it is indicative that sequentially in every period at the start time of the interval t_{k_3}, the inductor current drops to 0 ($i_L(t) = 0$). This means, for a time $t \in [t_k, t_{k+1}]$, the system can be presented as an iterative map, Definition 2.25. It will be a first order map, as it is constructed right in the moment $i_L(t) = 0$. That is why the further expressions with x will be scalar and denote just a voltage over the capacitor v_C.

The inductor current during the time t_{k_1} is linearly rising by the rate $\frac{E}{L}$ to its maximum value $i_{\max}$, and afterwards decreasing by the rate $\frac{x - E}{L}$ for a time t_{k_2}

Thus, our interval t_{k_2} can be expressed with a duty cycle d_k

$$\frac{t_{k_2}}{t_{k_1}} = \frac{E}{x - E} \quad t_{k_2} = d_k \frac{E}{x - E} \quad . \tag{2.88}$$

Now, we have a sufficient number of equations (2.85), (2.87), and (2.88) to form a Poincar map (see Section 2.2.2)

$$x_{k+1} = \alpha^{1} x_k + \frac{\beta^{1} d_k^{\,2} E^2}{x_k - E}$$

$$\alpha^{1} = 1 - \frac{T_s}{C(R + r_C)} + \frac{T_s^2}{2C^2(R + r_C)^2} \qquad \beta^{1} = \frac{RT_s^2}{2LC(R + r_C)}. \tag{2.89}$$

More details relating to the overall transition matrix can be found in [7].

Referring to the conclusions in the mentioned article and complexity reasons explained in Subsection 2.2.2, in the sequel the converter's control law will be simpler

$$\Delta d = -K\Delta x. \tag{2.90}$$

That equation (2.90) is deducted from a desired value $\mathcal{D}$ (see also Subsection 2.3.1), bearing in mind that the capital letters mean the steady state values, and form the final control function h(.):

$$d_k = \mathcal{D} - K(x_k - s)$$

$$h(d_k) = \begin{cases} 0 & d_k < 0 \\ 1 & d_k > 1 \\ d_k & 0 \le d_k \le 1 \end{cases}. \tag{2.91}$$

The Poincar map of the closed loop control is

$$x_{k+1} = \alpha^{1} x_k + \frac{\beta^{1} h^2(d_k) E^2}{x_k - E} \quad , \tag{2.92}$$

while the $h(d_k)$ inherits a saturating nonlinearity of the PWM [7].

As mentioned, the simulation will be done on the Simulink platform [29] with the selection of the elements in the Figure 2.12b, as in the article [7]. Table 2.3 presents those values. The electric circuit, including its elements, is designed to allow a DCM of the converter by the realistic switching period T_S.

Elements	Values
T_S	$333.33\ \mu s$
E	$16\ V$
s	$25\ V$
P	$50\ W$
L	$208\ \ \mu H$
C	$222\ \ \mu F$
R	$12.5\ \ \Omega$
r_C	$0.012\ \Omega$

Table 2.3 Elements selection related to the system in Figure 2.12b

The desired value $\mathcal{D}$, for a desired operating point, is calculated from (2.92) once the $x_{k+1} = x_k$, thus

$$\mathcal{D} = \sqrt{\frac{(1-\alpha)(s-E)s}{\beta E^2}}. \tag{2.93}$$

Pursuing the selection of an operating point based on figures from Table 2.3, we will define the Poincar map with its real coefficients

$$x_{k+1} = 0.8872 x_k + \frac{307.2(0.2874 - K(x_k - 25))^2}{x_k - 16} \quad . \tag{2.94}$$

The above-defined Poincar map will be qualitatively examined based on the theory presented in Subsection 2.2.2 and in [2,81].
The discrete equation (2.94) will be tested by the iterative change of K, with a Grapher 2.1 software, Macintosh [103]. This way, by 20000 iterations, we are varying the parameter K (recall (2.42-2.44) in general and the parameter μ) in the range from 0.06 to 0.27. It is important to note that the applied K to an approximate Poincar map (2.94) is incremented by the irregular steps, built on the simple function

$$K_{k+1} = \frac{K_k + k}{100000} \text{ for } K_0 = 0.06 \text{ and } x_0 = 25 \ . \tag{2.95}$$

The captured result is an orbit diagram presented in Figure 2.15.

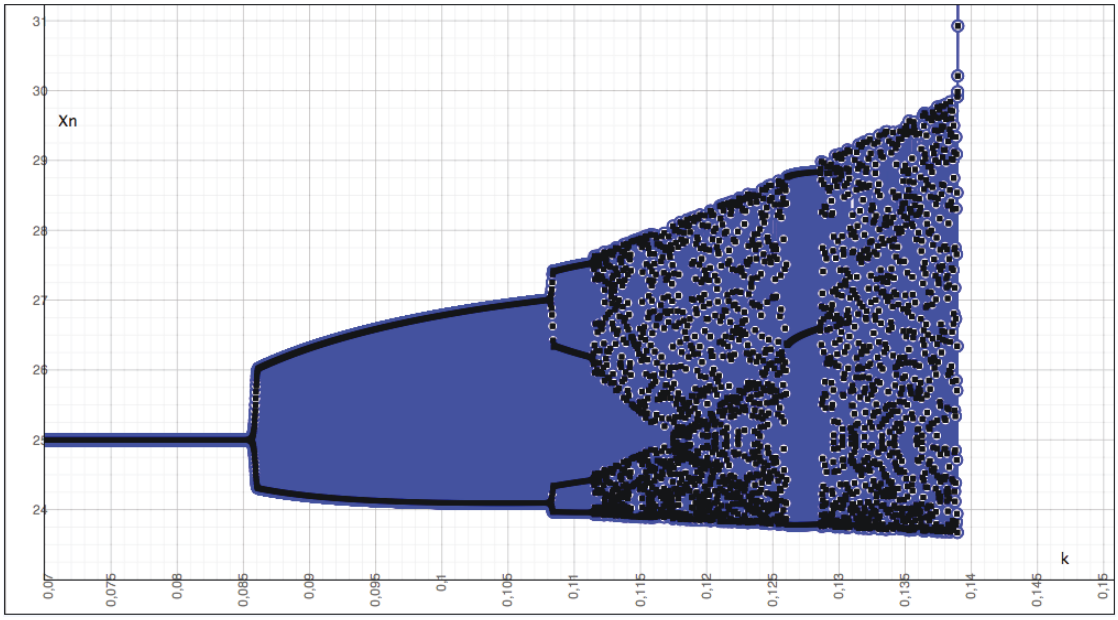

Fig. 2.15 Orbit diagram of the one-dimensional map (2.94)

With the selection of the reference $s = 25V$, our correction parameter K is limited with the stability criteria for a certain range defined by the stable multiplier $|\lambda^1| < 1$. The multiplier is defined with the first derivative of the Poincar map at the equilibrium point x^*

$$f'(x^*) = \lambda^1 \quad . \tag{2.96}$$

A first derivative is

$$f'(x_k) = \alpha^1 - \frac{2(\mathcal{D} - k\cdot(x_k - s))\beta^1 E^2}{x_k - E} k - \frac{(\mathcal{D} - k\cdot(x_k - s))^2 \beta^1 E^2}{(x_k - E)^2} \quad , \tag{2.97}$$

and to define the certain stability range, we have to simplify the equation (2.97) by knowing that at the equilibrium point the $x_k = X$. Thus, the multiplier evolves in

$$\lambda^1 = \alpha^1 - \frac{2\mathcal{D}\beta^1 E^2}{x^* - E} k - \frac{\mathcal{D}^2 \beta^1 E^2}{(x^* - E)^2} \quad . \tag{2.98}$$

If we implement the real values selected in the example, it yields

$$-1 < 0.5739 - 19.62K < 1 \tag{2.99}$$

a stability criteria for the selected reference value $s = 25V$.

The closed loop control system with the elements' values defined in Table 2.3 is stable around the reference point $s = 25V$, if our control parameter is in the range

$$0.02171 < K < 0.0802. \tag{2.100}$$

Once we have changed the parameter to violate the range (2.100), a DC-DC boost converter experiences the bifurcation or chaos.
The expected points of a bifurcation are the marginal cases when $|\lambda^1| = 1$, that is in our example once $K = 0.0802$.

If we compare the analytically driven results with one presented as an orbit diagram (simulation result) in Figure 2.15, then we can recognize just the negligible discrepancies explainable by the rounding errors in the simulation.
The map (2.94) that is analytically examined, as well as the simulation, gives two fixed points for $s = 25V$. Therefore, for any K there exists an extra fixed point.
As from equation (2.94), those are real results for an each particular K.

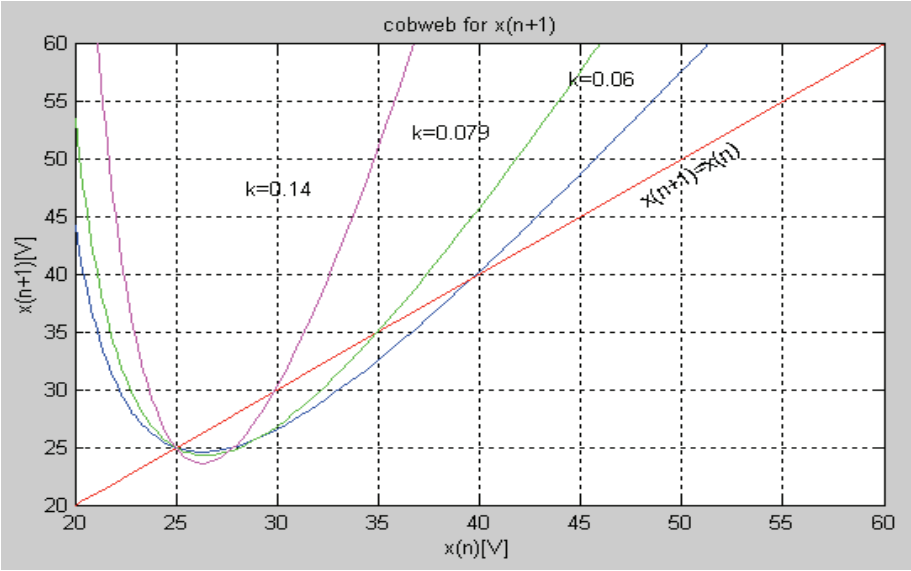

Fig. 2.16 The cobweb for a first-iterate Poincar map (2.94) and for a different K

Figure 2.16 is presenting a cobweb diagram [81] for three different parameters K. While K laying in-between the stable margins of (2.100), both fixed points are stable. At the moment we reach margin, $x^* = 25V$ becomes unstable.
That fact reminds us of a definition of transcritical bifurcation, and from that point we enter the area of the periodic windows that are in this case period-2 cycle. With the above analysis, we could only assume that it was so. As according to definitions [81], the first iteration of the unimodal map cannot develop the period-2 cycle. It develops in the second iteration and only if there are two real fixed points p and q, where $f(p) = q$ and $f(q) = p$, for $f(f(p)) = p$ and $f(f(q)) = q$. The second iteration must be derived and denoted as $f(f(p)) = f^{(2)}(p)$.
Thus, in our example it yields

$$f^{(2)}(x_k) = \alpha^1\left(\alpha^1 x_k + \frac{\beta^1(\mathcal{D} - k\cdot(x_k - s))^2E^2}{x_k - E}\right) + \frac{\beta^1(\mathcal{D} - K(\alpha^1 x_k + \frac{\beta^1(\mathcal{D} - K(x_k - s))^2E^2}{x_k - E} - s))^2E^2}{\alpha^1 x_k + \frac{\beta^1(\mathcal{D} - K(x_k - s))^2E^2}{x_k - E} - E}. \quad (2.101)$$

Equation (2.101) is a quartic polynomial equation. That gives four fixed points as solutions, once equalized with the equation for x_k by using the same constants as in

(2.94). If solutions are complex, the period-2 cycle is impossible, but opposite for solutions in the set of real numbers.

For the selection of the parameter K, which stays inside of the stable range, and equation (2.101) that is equalized with x_k, it gives two real and two complex solutions. But out of that range the all four solutions are real. Furthermore, as expected, two solutions are same as those in the first iteration done for the same K. If we set the:

$K = 0.09,$
$\alpha^1 = 0.8872,$
$\mathcal{D} = 0.2874,$
$E = 16,\ and$
$s = 25$

then for $f^{(2)}(x_k) = x_k$ the results are

$x^*_1 = 25.00 \qquad x^*_2 = 33.30 \qquad x^*_3 = 24.20 \qquad x^*_4 = 26.32$.

The aforementioned conditions for the birth of the period-2 cycle are fulfilled in the points x^*_3 and x^*_4.

As shown, a bifurcation happened by the generation of two extra fixed points will be characterized as a flip bifurcation, and those are mostly connected to the period-doubling effects. Figure 2.17 is a cobweb diagram for a second-iterate map, which clearly presents the birth of two additional fixed points at the chosen reference point.

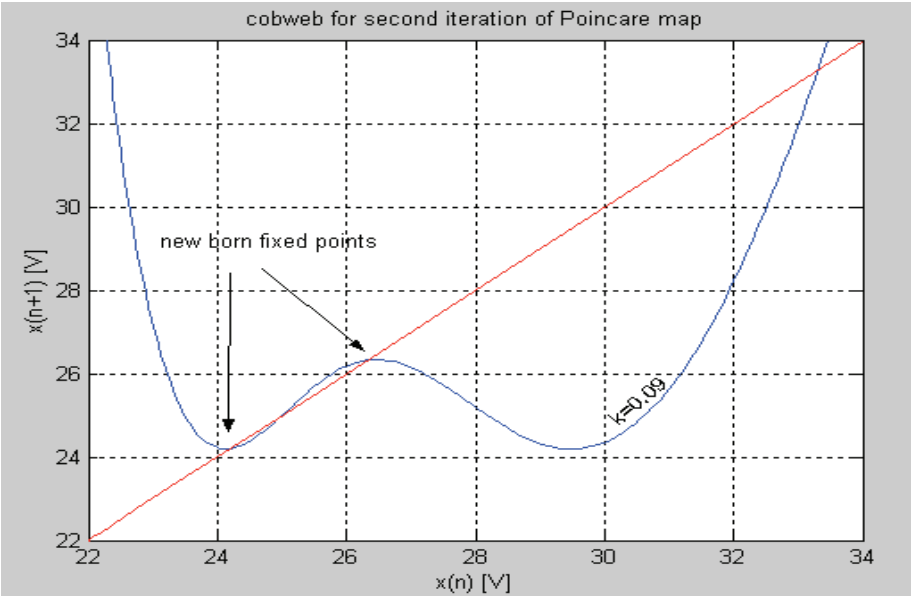

Fig. 2.17 Cobweb for second-iterate of Poincar map for k=0.09

The stable fixed points of the second iterate map will be possible to analyse in the same manner as done in (2.96), (2.97) and (2.98), except that now the function is $f^{(2)}(x_k)$.
The multiplier of the second iteration map is a large equation, and we are not going to present it, but the stability of the new born fixed points can be computed by following

$$\lambda^1 = \frac{d}{dx}(f(f(x))_{x=p} = f'(f(p))f'(p) = f'(q)f'(p) \ . \tag{2.102}$$

The above given multiplier is a stability criterion of a period-2 cycle.
For the $K = 0.09$ and

$$\begin{aligned} f'(24.20) &= -1.4282 \\ f'(26.32) &= -0.8910 \end{aligned}, \tag{2.103}$$

the multiplier λ^1 rises over the margin 1, and the period-2 limit cycle is unstable.
Higher period cycles are related to the higher order iterations, but the analytical approach produces complicated equations and mostly depends on the graphical and numerical arguments.
The orbit diagram in Figure 2.15 roughly reveals regions of the parameter K, where the doubling periods could be expected.
In the sequel, the examination of the effects in the selected example, provoked by the parameter K selection, we will test on the developed hybrid simulation model of a DC-DC boost converter driven in DCM, Figure 2.18. It is built with the control algorithm as defined in (2.90) and (2.91).

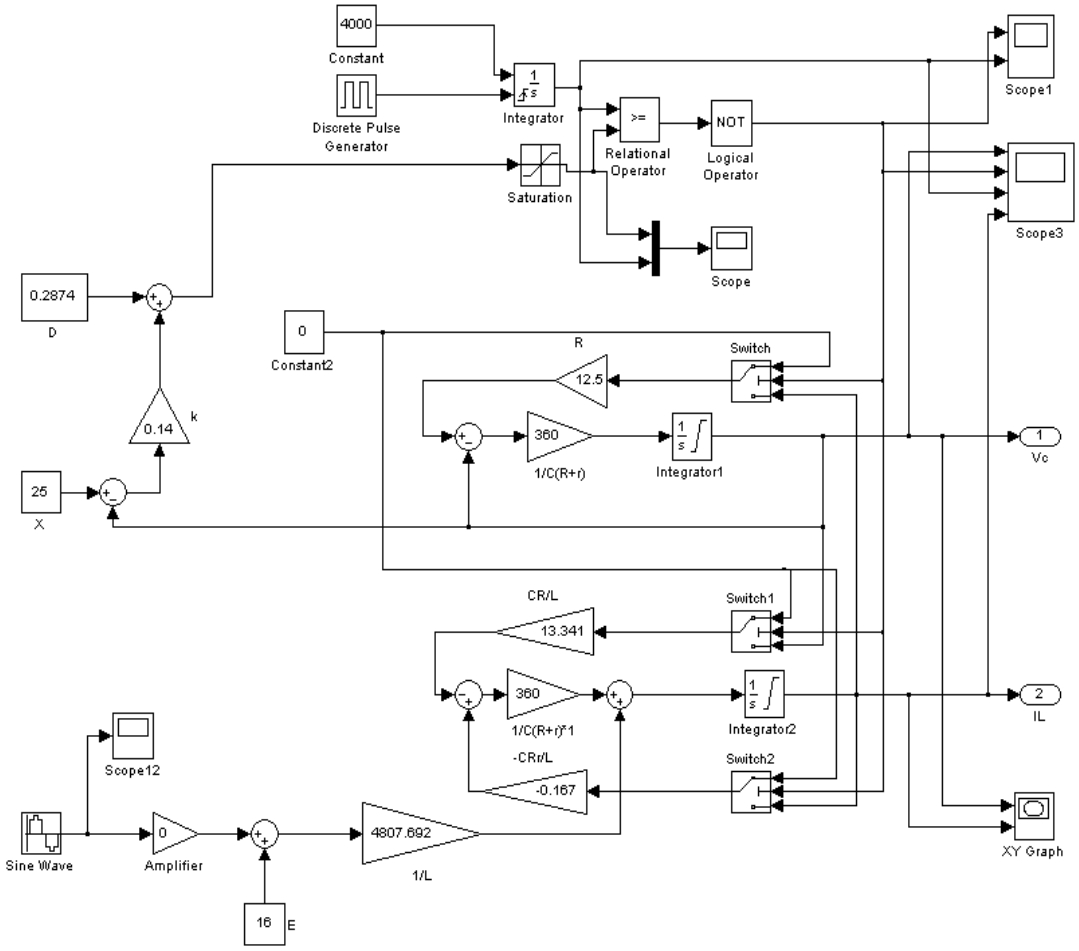

Fig. 2.18 The simulation model of a DC-DC boost converter shown in Figure 2.12b

With the selection of different K parameters, carefully chosen and based on the *Simulink* numerical simulation, we prove the existence of the expected phenomena called the intermittency route to chaos.

First, the parameter selection is done on the proven stable range. For $K = 0.06$, we see a smooth operation and the stable output voltage v_c in Figure 2.19. Then, we have crossed the marginal case, and changed the parameter to hit an analytically examined range of the period-2 cycle and bifurcations. Now, $K = 0.1$ and Figure 2.20 present the result. It can be seen that the completely discontinuous mode is no longer guaranteed, as our state variable i_L did not fall completely to 0. We have reached the edge of a partly continuous mode. The effect is worse as we go higher up with the parameter. Equally, for the parameter selection $K = 0.11$ we enter the period-4 cycle in Figure 2.21, and for $K = 0.1275$ the period-8 cycle in Figure 2.22. In the mentioned windows of the parameter selections, we have experienced a birth of an extra fixed point and the typical flip bifurcations. Those windows are intermittently interrupted by a chaotically assigned nonlinear dynamical system behaviour. The selection $K = 0.135$ in Figure 2.23 is a typical result.

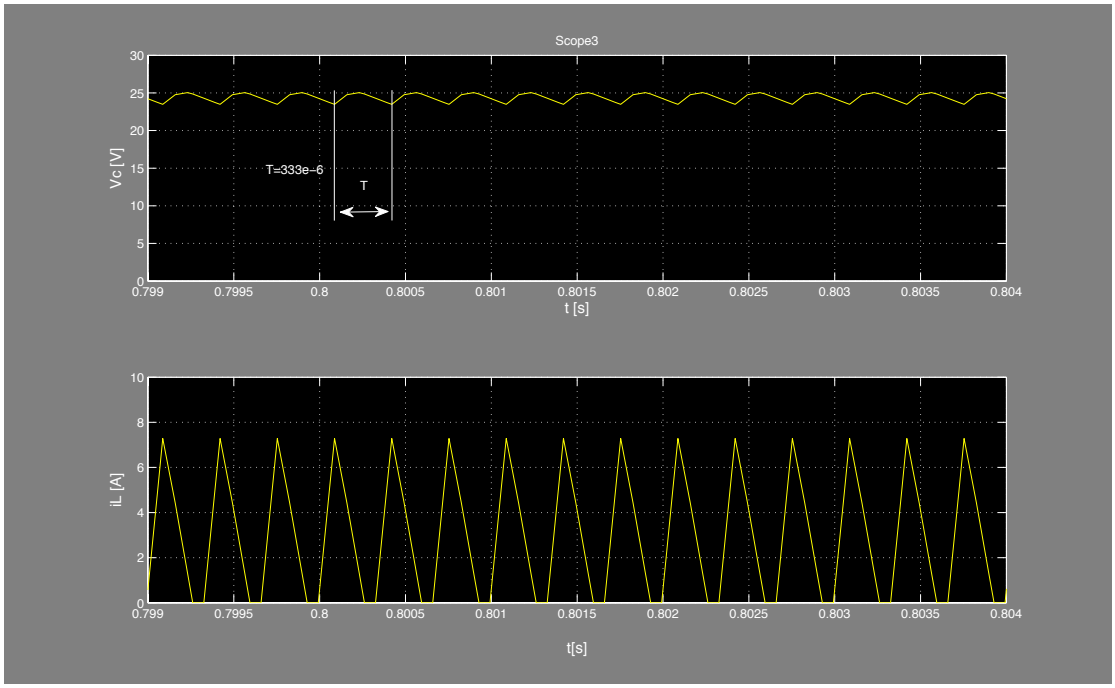

Fig. 2.19 The results of a model simulation (Figure 2.18) for K=0.06

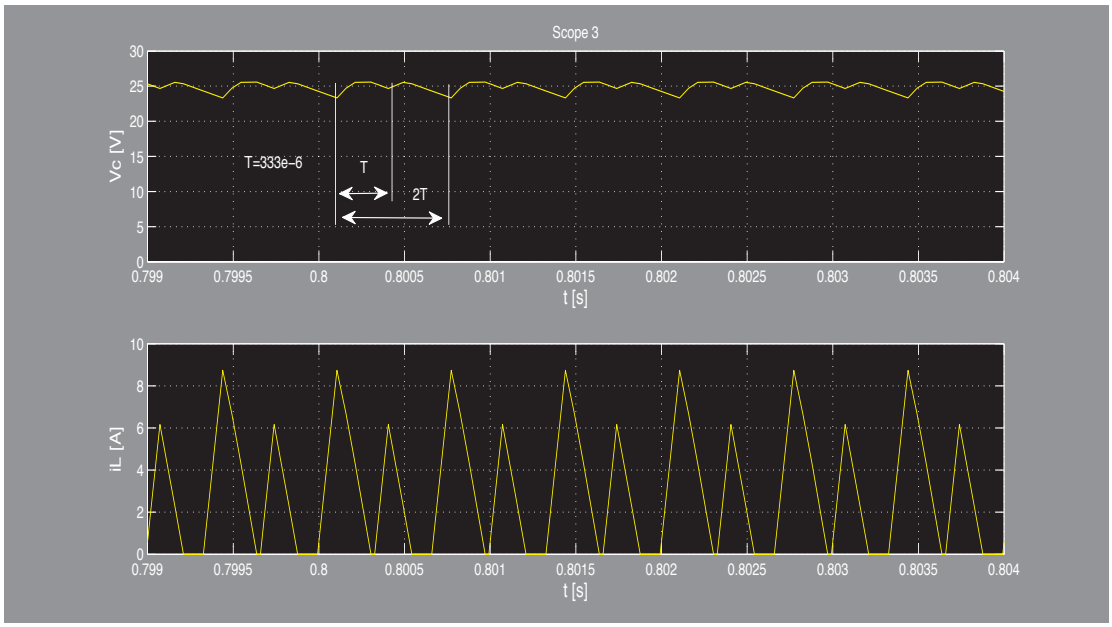

Fig. 2.20 The results of a model simulation (Figure 2.18) for K=0.1 and period-2 cycle

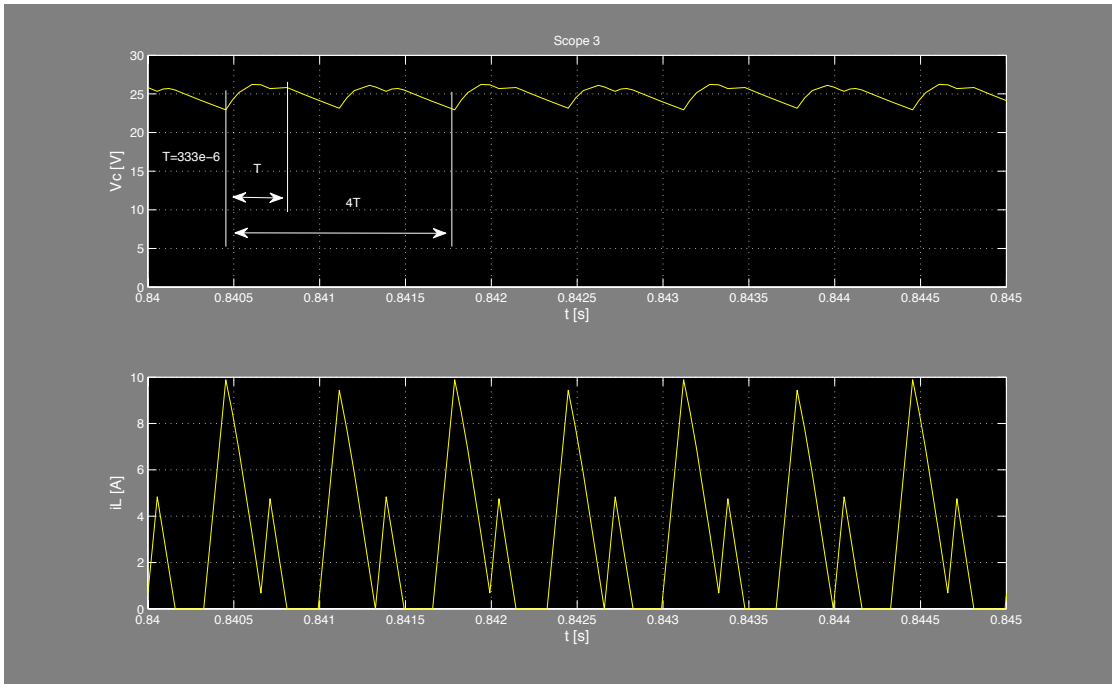

Fig. 2.21 The results of a model simulation (Figure 2.18) for K=0.11 and period-4 cycle

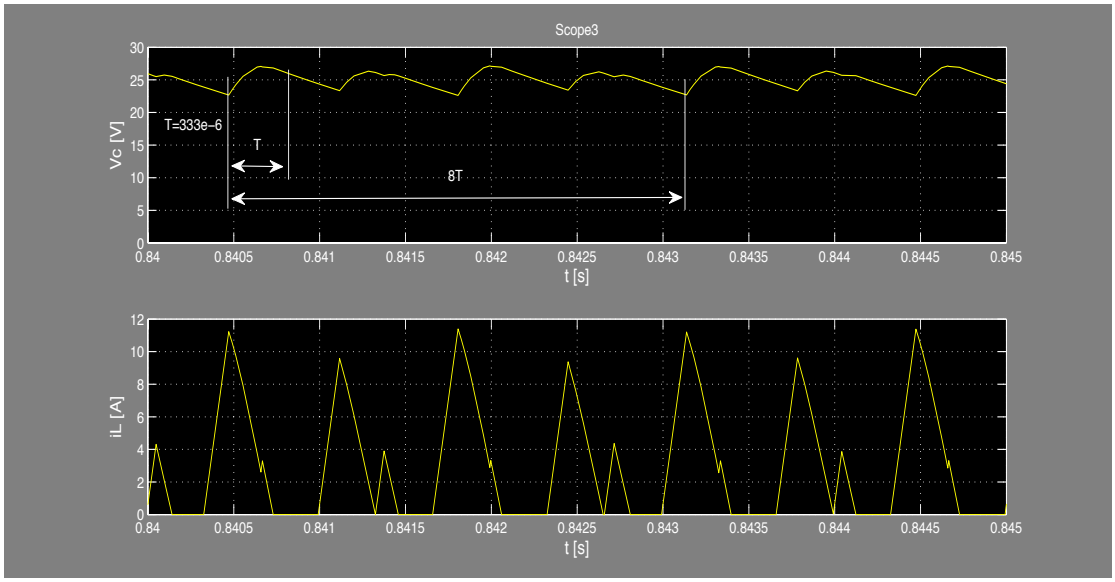

Fig. 2.22 The results of a model simulation (Figure 2.18) for K=0.1275 and period-8 cycle

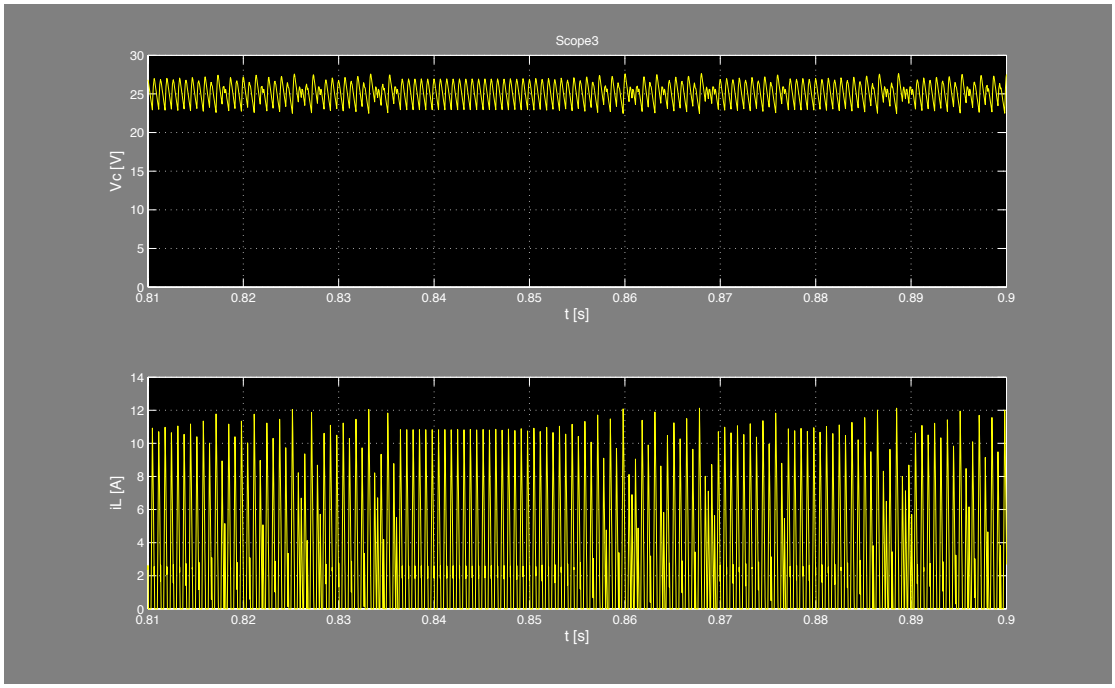

Fig. 2.23 The results of a model simulation (Figure 2.18) for K=0.135 and chaos

Our simulation model will be further tested for an input voltage change, previously assumed as constant. For a slight change of an input and selection of $K = 0.06$, the system is still stable with a clearly recognized transition period and higher the output amplitude deviation. If we consider the realistic applications, we could expect a certain change of the load and source at the same time. That would make the presented converter's control (2.91) unstable and require more sophisticated solutions [56]. The expressed statement leads to the further development of a superior control algorithm starting in Chapter III.

Chapter III

Identification of SAS, approaches to smoothing discontinuity

A comprehensive view over the controls in a nonlinear dynamical system brings about the unavoidable conclusion that a successful tackling of complexity has to be made by involving a multidisciplinary methodology. Namely, including the essential knowledge of the physical system, mathematical modelling and, finally, advanced and intelligent control algorithms have to evolve in a stable and optimal control solution. Without a doubt, HSs are appealing and modern examples. Therefore, the subsequent work integrates several areas into the control theory in order to fulfil the main goal of controlling the nonlinear dynamical system, focusing on the nonlinear phenomena exclusion.

Generally, even the most theoretical developments in the field of HSs assume a known model of the process at hand [45], and we are already questioning a well-developed model with the simple applicability test. Figure 3.0 presents the modelling paradigm in HS and its equivalence [2,25]. We additionally assign the new modelling approaches with a dashed line, except for the complex hybrid models built from the multiple basic models. An arrow is used to denote a logical inclusion; a number is the mathematical propositions of the equivalence presented in [25]; and a star is the conditioned inclusion. The diagram has to position the novel fundaments of the subsequent study in a broad view. In contrast to typical and basic model representatives in HS, i.e. PieceWise Affine (PWA) models, Linear Complementarity (LC) models, Extended Linear Complementarity models (ELC), Mixed Logical Dynamical (MLD) and Max-Min-Plus_Scaling (MMPS), the Identification Based (IDB) modelling represents a new group of models rendered by different identification approaches and algorithms.

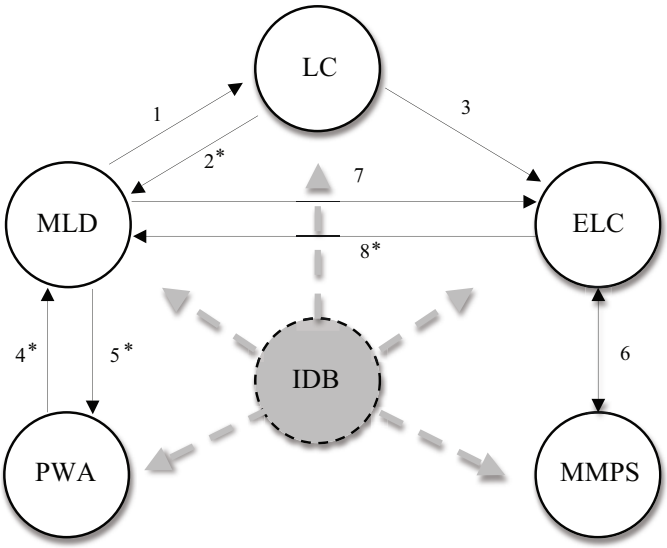

Fig. 3.0 Established types of hybrid models

Most referenced literature [2,25](and references therein) from the field very rarely mentions fuzzy approaches and fuzzy control in HS. Instead, it presents the fuzzy system merely as an example of a HS. Generally, and in contrast to subsequent work, the identification is exclusively used in examples where the process originally has the absence of a known analytical model. Those methods are usually grouped into four groups for the identification of the switched affine autoregressive exogenous (SARX) or the piecewise autoregressive exogenous (PWARX) models [2,45]: the algebraic procedure [46], the clustering-based procedure [47], the Bayesian procedure [48] and the bounded-error procedure [49]. The problems characteristically related to the specific procedure are also correlated with respect to the model order, the number of regions, the number of logical variables and the dimensions of the regression vectors. Similar problems are the objectives of a whole field of Fuzzy Identification, which includes the identification of HS [50-53]. Modern approaches combine the structure of the HS together with the features associated with the fuzzy modelling, using it in identification and control [54], or comprehensively in the identification of complex systems.

This field of systems is extremely wide and very much differs in terms of the methodology influenced by the selected process or physical system. Therefore, based on emerging technology, it is defining a new, broader discipline that is popularly called cyber-physical systems.

We will concentrate our research and studies in the direction of SAS, distinguishing it either from the switching affine systems (referring to autonomously switched) or the PWA systems.

3.1. Identification

System identification is a process that builds the mathematical model of a system, based on the observed data. For the mathematical models, analytically obtained by the difference or differential equations, we rely on the “laws of nature” that have their roots in earlier and empirical human work; the identification is directly based on the experimentation. From the recorded input and output data, the identification performs a data analysis in order to infer a model. In real-life systems, the analytical approach is rather cumbersome and the mathematical modelling is coarse to devise all physical insights. It seems that there is an impenetrable, but transparent screen between our world of the mathematical description and the real world [104]. We can just partly tackle some aspects of the physical system, but we can never establish any exact connection between them. Therefore, our acceptances of the models should be guided by their “usefulness” rather than pure “truth”. Nevertheless, to evaluate and devise the identification methods, we shall rely on the more pragmatic and mathematically defined approach. Otherwise, it is impossible to reinforce the observer’s point of view and evaluate the gathered models.

Based on those thoughts, there is a fine line dividing the analytical approach from the identification, and especially considering current computing abilities. It is certainly a motivation of this thesis to elevate the accuracy of the model, but bearing in mind a final objective, that is an applicable and cost-effective control solution in SAS.

Generally, the main course in the identification is not to estimate something that is already known, but to utilize the prior knowledge and physical insights into the modelling structure. The physical knowledge about the system that has to be identified is "color-coded" by the typical identification terminology. Related to the physical knowledge about the system, one can group the identification, i.e. the *white-box*, the *grey-box* or the *black-box* modelling. Respectively, it is a gradation of the prior knowledge from the complete physical insights to no physical insights being used. In the literature [30], we could also find the subgroups of the largest grey-box modelling that are called a "physical or a semiphysical modelling". The main difference is associated with the level of involvement of the prior knowledge. Thus, the semiphysical approach suggests a usage of the physical knowledge just in the certain nonlinear combinations of measured data, while the physical approach is already suggesting a state-space model of a given order and structure.
In the example of this work, applicable to the broader range of SAS, we suggest the combination of both subgroups, evolving in the grey-box identified model. A survey given in Section 2.1 poses the modern analytical formalisms that have a twofold impact on the control methodologies.

First, the hybrid system formalisms elevate the model accuracy, and give better selectivity in forming the proper control algorithm.

Second, which is a drawback of the accuracy, it also elevates the complexity and brings new side effects encapsulated into the restrictions of the particular formalisms.
For the example, the MLD approach to the DC-DC boost converter (Subsection 2.3.5) gives a complete analytical solution in the sense of the simulation properties, but it is certainly not cost effective in comparison with the physical merits of the problem. The authors of the method [26] proclaim that the DHA formalism is solving a problem of the Zeno Effect. On the other side, it can be achieved just with the pure synchronization, and by taking an assumption that the sampling time is the infinitesimal and the continuous system inactive during a discrete state transition, Subsection 2.3.3. In other words, the continuous system has to be transformed into the discrete system. We can find that the following authors [3,17,98,99] use the same formalism in solving the DC-DC converters, but they program the nested models to predict a natural switching that happens during the original system time sample. That is the way we upgrade the original MLD modelling, but also practice the ability of the Zeno Effect. It is obvious when we observe it from the side of the general discrete model based on the overall time sample T_S. Otherwise, if we assume only the CCM, the MLD model of a DC-DC boost converter is reduced back to the averaged switched model (2.54), yet with more accurate prediction of the switching event inside of the discrete time sample T_S. The latter is possible if the online processing abilities allow the amount of the extra workload due to the lifted state space matrices.

The main physical problem of PEC is in the nonlinearity induced by the construction of the electrical components and the fact that the system has only a physical sense if it works in the closed loop control. While it works in the closed loop control, the nonlinearity happens related to the duty cycle too (Subsections 2.2.2. & 2.3.5).
If we take, for the example, the complementarity formalism, which is closer to the physical modelling, it also collides with the strict restrictions of ideal switch involvements. The analytical upgrade by the physically accurate switching

expressions leads to the inapplicability or lack of cost effectiveness [13]. It is not clear what is the most suitable control methodology that could follow this type of modelling formalism. The sliding mode control is one of the performed control methodologies [12], but again, it is applicable if the switching time is infinitesimally small and the system has known the state variables' physical margins [105].
In contrast to those formalisms, we have also presented a distinctive analytical formalism (Subsection 2.3.5), based on the mathematical qualitative theory. Although, it is rendered for a DCM of a DC-DC boost converter, it reports all sorts of nonlinearity effects, apart from the fact that just a trivial control algorithm was examined (2.90).
All mentioned experiences support our idea of forming a new modelling formalism based on the *grey-box identification*. As we see, the example of this work asks for a nonlinear system modelling where the nonlinear structures will be tackled as the concatenation of a mapping from the observed data to regression vector, and a nonlinear mapping from the regressor space to the output space [30].

Let us take the observed data from a discrete dynamical system as the sets of input and output measured samples in the equidistant time spans:

$$\begin{aligned} \boldsymbol{u}\big|_k &= [u(1)\ u(2)\ \ldots u(k)] \\ \boldsymbol{y}\big|_k &= [y(1)\ y(2)\ \ldots y(k)] \end{aligned} \quad . \tag{3.1}$$

Our task in the identification is to look for a relationship between the past observations $[\boldsymbol{u}\big|_{k-1}, \boldsymbol{y}\big|_{k-1}]$ and future outputs $\boldsymbol{y}(k)$, which can be expressed as

$$\boldsymbol{y}(k) = g(\boldsymbol{u}(k-1), \boldsymbol{y}(k-1)) + e(k) \ . \tag{3.2}$$

From the above definition of the identification, it is expected that the identification is not an exact expression of the physical system. Thus, (3.2) takes into the consideration that the function of previously observed data $g(\boldsymbol{u}(k-1), \boldsymbol{y}(k-1))$ is an approximation of the future output associated to an error function $e(k)$. The antecedent observed data has to be linked by the arbitrary number of functions that will be parameterized by a finite-dimensional parameter vector θ, and thus the approximation is more accurate

$$g(\boldsymbol{u}(k-1), \boldsymbol{y}(k-1), \boldsymbol{\theta}) \quad . \tag{3.3}$$

To devise the most accurate approximation, we select the cost function

$$\min_{\boldsymbol{\theta}} \sum_{k=1}^{n} \left\| \boldsymbol{y}(k) - g(\boldsymbol{u}(k-1), \boldsymbol{y}(k-1), \boldsymbol{\theta}) \right\|^2 \quad . \tag{3.4}$$

The convex programming has to be done based on the sampled data (3.1) for $k = 1,2,\ldots,n$ samples, at the time kT_S. As the (3.3) expression is too general, it is more convenient to express it by the concatenation of two distinctive mappings. Therefore, the complex (3.3) will be decomposed into

$$g(\boldsymbol{u}(k-1),\boldsymbol{y}(k-1),\boldsymbol{\theta}) = g(\boldsymbol{\varphi}(k),\boldsymbol{\theta}) = g(\boldsymbol{\varphi}(\boldsymbol{u}(k-1),\boldsymbol{y}(k-1)),\boldsymbol{\theta}). \quad (3.5)$$

The vector $\boldsymbol{\varphi}(k)$ is called the *regression vector* and, in a more general form, it can be a function of an extra argument $\boldsymbol{\varphi}(k,\eta)$. All diversities of different identification principles and methodologies are based on the aforementioned equations (3.1)-(3.5). It can be objectively surveyed by two crucial points of view. First, it has to be observed from the corner of the proper selection of a regression vector or vectors. Second, there has to be a model structure in the mapping from the regressor space to the system's output. That point of view was emphasized by the plausible work in [30], where the objective sight is given to the different directions in identification methodologies at the end of the 1990s. Herein, we are mentioning the most distinctive approaches.

There is still a tendency to name different identification principles driven by the selection of the regression vector, which is a known and established approach in the linear systems' theory [106]. As our interest is to identify a nonlinear model, the final identification structure will have added just a nonlinear prefix. So, we distinct between the following types of models related to the selection of the regression vector components:

- Usage of only antecedent inputs $u(k-i)$, for $i=1,\ldots,k-1$, as regressors is characterized by Nonlinear Finite Impulse Response (NFIR) models.
- Usage of combinations of antecedents, $u(k-i)$ and $y(k-i)$, is grouped to a Nonlinear Autoregressive eXogenous (NARX) models.
- Usage of combinations of antecedents, $u(k-i)$ and $\hat{y}_u(k-i)$ that denote simulated outputs from the $u(k-i)$, is grouped to a Nonlinear Output Error (NOE) models.
- Usage of combinations of antecedents, $u(k-i)$, $y(k-i)$ and $\varepsilon(k-i|\theta)$ that denotes a prediction error $\varepsilon(k-i|\theta) = y(k-i) - \hat{y}(k-i|\theta)$, is grouped to a Nonlinear Autoregressive Moving Average eXogenous (NARMAX) models.
- Usage of combinations of antecedents, $u(k-i)$, $\hat{y}(k-i|\theta)$, $\varepsilon(k-i|\theta)$ and $\varepsilon_u(k-i|\theta)$ that denotes a simulation error $\varepsilon_u(k-i) = y(k-i) - \hat{y}_u(k-i)$, is grouped to a Nonlinear Box-Jenkins (NBJ) models.
- The group is based on the selection of nonlinear state space models that are characterized by the involvement of the virtual outputs from a complex networked model structure. It is certainly reserved for heuristic approaches, i.e. neural network and fuzzy modelling.

A different model structure, $g(\boldsymbol{\varphi}(\boldsymbol{u}(k-1),\boldsymbol{y}(k-1),\iota),\boldsymbol{\theta})$ (ι-regression vector parameters in general), means the function expansion, defines modern nonlinear identification approaches. If we select the regressor vector as $\boldsymbol{\varphi}(k)\in\mathbb{R}^l$, then the characteristic function expansion

$$g(\boldsymbol{\varphi},\boldsymbol{\theta}) = \sum_i \alpha_i g_i(\boldsymbol{\varphi}) \quad , \quad (3.6)$$

is the model structure based on *basis functions* g_i. The selection of (3.6) and the regressors unify most identification methodologies. In the sequel, the basis functions

$$g_i(\varphi) = \kappa(\varphi, \beta_i, \gamma_i) = \kappa(\beta_i(\varphi - \gamma_i)) \tag{3.7}$$

generically denoted by $\kappa(.)$, will be a main discourse in the definition of the methodology. New parameters β_i and γ_i, which respectively denote directional property and position or translation, are parameters that have to define a different nature of basis function. Simple examples of $\kappa(.)$ are the *unit step*, the *interval indicator*, the *sigmoid* function, the *Fourier series,* etc. The latter is a typical example of a *Global basis function*, where β_i are the frequencies and γ_i the phases. Former functions are representative of *Local basis functions*. Both groups of functions are a subgroup of the broader group of single-variable functions.
In contrast to the *single-variable* functions, there is a group of methodologies using the multivariable basis functions:

- *Tensor products*, which are constructed by the product of single basis functions, e.g. $g_1(\varphi_1) \cdot g_2(\varphi_2) \cdot \ldots \cdot g_d(\varphi_d)$.
- *Radial construction,* which is formed by the typical expression

$$g_i(\varphi) = \kappa(\left\|\varphi - \gamma_i\right\|_{\beta_i}) \quad , \tag{3.8}$$

  and the function argument is a typical norm in the regression vector space, e.g. quadratic as $\varphi^T \beta_i \varphi$ for $\beta_i > 0$ and $\gamma_i = 0$.
- *Ridge construction*, which is given by the expression

$$g_i(\varphi) = \kappa(\beta_i^T \varphi + \gamma_i) \quad , \tag{3.9}$$

  where $\varphi(k), \beta_i \in \mathbb{R}^l$ and $\gamma_i \in \mathbb{R}$. Characteristically the basis functions are constant in some directions as $\beta_i^T \varphi = const$.

More complex identification methods are differing in their *networked* construction. Those constructions we can mostly recognize in the heuristic approaches. Some of the methodologies are differentiated by *Multilayer* networks [107,108] or *Recurrent* networks, characteristically for *neural-networks* [109,110].
Throughout the literature, we see that the broad identification realm can be more objectively considered by applying the above-mentioned extents in the identification theory. Consequently, some well-established methodologies give a good example where the names of the basis functions become the names of the identification methodologies. The *wavelets identification* can be considered a typical one. Furthermore, some other well-known basis functions are to be mentioned, e.g. the *Kernel estimators* as typical bell-shaped functions, or *B-splines*, *Hinging Hyperplanes* that are respectively the piecewise polynomials or *hinge* functions [111]. The latter is also representative of the basis functions in the neural network identification. Similarly, the combinations of the *ridge basis* functions and the *sigmoid mother basis function,* altogether constructs the multilayer network called the *sigmoid neural network*. Another representative of the heuristic identification approach is a fuzzy identification that can be seen as identification with the particular choice of the basis functions constructed from the fuzzy set membership functions.

Common to all identification methods is to achieve a minimal error of the approximation to the real process by different minimization methods applied in (3.4). Accordingly, the result of that routine is a definition of the model parameters $\boldsymbol{\theta} = \{\alpha_i, \beta_i, \gamma_i\}$. The minimization is performed on function

$$\min_{\boldsymbol{\theta}} V(\boldsymbol{\theta}, Z_e^N) = \frac{1}{N} \sum_{k=1}^{N} \left\| \boldsymbol{y}(k) - g(\boldsymbol{\varphi}(k), \boldsymbol{\theta}) \right\|^2 \tag{3.10}$$

by regarding a given finite set of the measured pairs

$$Z_e^N = \{(\boldsymbol{y}(k), \boldsymbol{\varphi}(k)) : k = 1, \ldots, N\} \quad . \tag{3.11}$$

The accuracy of our identification is proportional to the selected number of pairs N. In equations (3.4) and (3.10), we have selected a quadratic norm as one of the most used cost functions. The most efficient search routines are based on the iterative local search in the "downhill" direction from the current point. Generally, the iterative process of parameter definition is assigned by

$$\hat{\theta}^{(n+1)} = \hat{\theta}^{(n)} - {}_{st}\mu_n R_n^{-1} \nabla \hat{f}_n \tag{3.12}$$

where ${}_{st}\mu_n$ denotes the step size, R_n a matrix of search direction modifiers and $\nabla \hat{f}_n$ the estimated gradient V' of the equation (3.10). There are different and established methods of search directions that have known and distinctive names:

- *Gradient method*
  $R_n = I \qquad I - identity\ matrix$
- *Gauss-Newton method*
  $R_n = H_n = V_n''(\theta)$
- *Levenberg-Marquardt method*
  $R_n = H_n + \partial I \quad \partial - real\ number\ that\ assigns\ the\ step\ size$
- *Conjugate gradient method*
  It is reformulated Gauss-Newton direction by difference approximation of $V_n''(\theta)$.

It is still a boosted growth of the academic solution, suggesting different minimization approaches that are strictly related to the different model structure. Certainly, there is no automated tool that can define the most efficient methodology for our identification problem, referring to the aforementioned identification merits. Similarly, all finial minimization algorithms can easily "be stuck" into the local minima and result in an ill-conditioned model. The prior physical knowledge is the key solution of those problems, but in absences of that path, one should use a random search, random restarts, simulated annealing and genetic algorithms [30].

3.2 Fuzzy identification as the universal approximation

The complexity of our objectives in the modelling of SAS directs in the selection of the applicable identification framework. In Chapter II, we introduced different

analytical approaches that are framed by strict formalisms and restrictions. We can generally conclude that HS modelling has distinctive constraints that have once been applied to some of the SAS. The example in this thesis, a DC-DC boost converter, should not be taken so often in HS modelling theories as a trivial representative of the method's applicability. The natural processes are too complex to be framed by some assumptions, e.g.:

1. Synchronization of the sampling with the continuous dynamical system evolution
2. Assumption that switching is ideal
3. Definition of the maximum and the minimum constraint of the system state variables for the physical systems
4. Assumption that in physical systems we deal with the finite set of the initial conditions and the ability to define a reachable set of HS in real time
5. Definition of the reset mapping and guards is at least similarly complex as modelling itself on an infinite set of discrete states and initial conditions, etc.

With awareness of mentioned assumptions that are strictly related to the selected analytical formalism in Section 2.1, the identification conducted in order to identify the physical system, rather than applying the imperfect analytic formalism, emerges as an advanced solution. In this thesis, we question the pragmatic approach of the analytic modelling in the cases in which the transcendental mathematical problems exist on the border of indeterminism. The intention to model a DC-DC boost converter in the only physically proper way, that is a model of the closed loop system, led us to the problem that antecedents has to be defined by knowledge about descendants. We see that employment of DHA and MLD modelling gives the solution by taking into the consideration that a discrete step of sampling is infinitesimally small in comparison with the natural frequency of the system. In the example of this thesis, it is not the case. The natural frequency of the PWM in driving the DC-DC boost converter disapproves it. Attempting to supersede and overcome that problem by the prediction, based on the elevating of the sampling frequency (Subsection 2.1.4), brings unnecessary complexity in comparison with the accuracy (Subsection 2.3.5).
From the side of the controls, our objectives in the modelling of SAS are not different, but integrating all known about the way to raise the applicability and accuracy for the natural examples. The identification will be comprehensively guided to tackle all physical problems, and to produce a model that can be further used in the well-established control methodologies. The main objective in the following identification methodologies has to generally reconcile the model's complexity with accuracy, thus:

1. The model produced shall not elevate a simple state space averaging model rank, but rather minimally preserve it.
2. The physical constraints in the subsequent modelling approaches will be put in the function of reducing the real-time complexity and not the opposite.
3. The level of accuracy will be predictive throughout the whole universes of discourses of the state variables, previously defined and based on the physical constraints.

4. The model has to be global and give an ability to develop a robust control solution.

This way has to evolve the method's usefulness, and precede an exemplification of the formalism that is frequently the final result.
To succeed, we will select a heuristic methodology in the identification. The Fuzzy Identification is certainly a heuristic approach built on the principles of the human reasoning based logic, commonly called Fuzzy Logic (FL). The FL becomes a popular logic methodology in different disciplines of science. It has a growing use in cybernetics, and software programming, but also in the medicine and social science that makes it the "new logic" of science. In the work of Licata [112], from a philosophical point of view about the FL, the theory demystifies a dominant success in current science. On a general basis, he explains the usefulness in the treatment of the natural phenomena and quantities by many-valued logic.
It is explained that the number of truth-values and the possibility to vary the number of truth-values assign different degrees of complexity in a logical sense. Thus, we can differ three logical complexities:

- True/false logic
- True/false logic enriched by a fix number of truth values (simple polyvalence)
- True/false logic enriched by a variable number of truth-values (complex polyvalence).

The latter is a multiple system containing the subsystems with different numbers of truth-values. FL belongs to the complex polyvalence. The variable truth values are placed between the classical logic extremes of 0 as a false and 1 as a truth. Modern science proves that many of the dogmas related to the above classifications are unrealistic and unfounded. The most common is between the probabilistic theory and FL. Based on the experience in the applied cases, it would be wrong to reduce the FL onto the probabilistic theory. Nevertheless, it is wrong to use the FL to express and devise probability problems. In conclusion, the probabilistic theory is rather used to formalize "uncertainty" and the FL to treat "vagueness". Those two terms could be formulated in the technical sense. An uncertainty could be understood as an incompleteness of information while the vagueness regards an indefinite relationship between words and objects. It would be unfair to group the former into the "subjective knowledge" methodology, but this work or thesis is selecting FL as the basis for the well-defined identification methodology, employed to improve our objective knowledge of the system.

3.2.1 Fuzzy Logic Modelling in General

Already from the several formalisms of HSs, and from the history of modelling the HSs, the switching of continuous natural processes necessarily brings complexity. As we have seen from the qualitative theory, the nonlinear phenomena are strictly connected to the *grade of smoothness* on the switching border (Subsection 2.2.2). Even if the analytic approach exists, we have to magnify the fundamental assumptions in applying of those approaches. In turn, we recognize that the most of HS formalisms assumed that the switching as a no-time event. It pragmatically constrains the performance of the modelling methodology and makes it applicable

for relatively "slow" dynamical systems. Generally, for the nonlinear dynamical systems, a decomposition strategy leads to the PWL systems, and systems' linearization around the operating point. Therefore, the assumption that the nonlinear system behaves linearly around the operating point, consequently put an extra constraint on the modelling accuracy and stability margins of the future control system, based on that modelling principle. Lastly, the robust modelling considers that the process is prone to the operating point deviation, but in most of the cases assumes that the constructive process elements and their parameters are not functions of the operating point. That assumption is elevating our analytic modelling uncertainty and strongly interferes with the prediction of the modelling accuracy.
In the example of our work we use a modern and heuristic identification approach in formalizing a model that has to devise a predictive modelling accuracy. The abovementioned assumptions will be neutralized by the identification and modelled in the static FL model of known accuracy margins for wider and defined operating point fluctuations. Our methodology in the identification of SAS will use FL to encode the natural system's vagueness, from the human perspective.
Instead of being limited by the bivalent logic, in our approach the mathematical logic *rules of inference* [70] will evolve from the traditional propositional logic *rules*

$$\begin{array}{ll} \textit{modus ponens} & \dfrac{A,\ A \rightarrow B}{B} \\ \textit{modus tollens} & \dfrac{A \rightarrow B,\ \overline{B}}{\overline{A}} \end{array} , \tag{3.13}$$

where A and B denote the *formulas* of the propositional logic, and $\overline{A}$ and $\overline{B}$ their negations. The logic rules (3.13) of the propositional logic are considering the *tautology* of formulas.

****Definition 3.1**[70] (**Tautology**) A formula A of propositional logic is tautology if* $f(A) = T$ *for every truth assignment f.*

In Definition 3.1 the truth assignment is always true (*T*) or otherwise false. Simply, the tautology can be expressed by the logical '*or*' connective as $A \vee \overline{A}$. This approach is a complete certainty and is not appropriate to encode uncertainty. By underlining the heuristic principle in the FL, we emphasize the idea that the human reasoning could approximate the unlimited uncertainty and contribute to the objectivity in the modelling of the natural processes. We belief that following this way, the physical extents of the process should stay proportional to the finial model complexity and preserve a designed and predicted accuracy for the natural processes. As a consequence, and conclusion of the above discussion, if there is no ambiguity present in the decision-making, then the FL approach is unnecessary and we should rely on the tautology. However, if there is a doubt in isolating of our model from the unexpected and non-defined influences, then there is ambiguity present in the decision-making.
This type of the many valued logics and so-based inference rule has been emerging in the work of Zadeh [114,115] and is called the *compositional rule of inference.* Preserving the causality in the decision-making, also characteristic for human

reasoning, the rules (3.13) in FL become the generalized inference where the antecedents contain a conditional proposition with the fuzzy concepts:

$$\textit{generalized modus ponens}\quad \frac{\begin{array}{l}\textit{antencendent}\,1:\ \textit{If}\quad u\ \textit{is}\ \mathcal{A}\quad \textit{then}\quad y\ \textit{is}\ \mathcal{B}\\ \textit{antencendent}\,2:\ u\ \textit{is}\ \mathcal{A}'\end{array}}{\textit{consequence}:\ y\ \textit{is}\ \mathcal{B}'}$$

$$\textit{generalized modus tollens}\quad \frac{\begin{array}{l}\textit{antencendent}\,1:\ \textit{If}\quad u\ \textit{is}\ \mathcal{A}\quad \textit{then}\quad y\ \textit{is}\ \mathcal{B}\\ \textit{antencendent}\,2:\ y\ \textit{is}\ \mathcal{B}'\end{array}}{\textit{consequence}:\ u\ \textit{is}\ \mathcal{A}'} \qquad (3.14)$$

Differently than in (3.13), $\mathcal{A}, \mathcal{A}'$, $\mathcal{B}$ and $\mathcal{B}'$ are fuzzy concepts represented by the fuzzy sets in the universes of discourse $\mathbb{U}, \mathbb{U}$, $\mathbb{Y}$ and $\mathbb{Y}$ respectively. In (3.14) u and y denote the names of objects. There are different fuzzy reasoning concepts in the generalized rules (3.14). The comprehensive discussion on different types of fuzzy reasoning can be found in [114].

Generally, FL based modelling consists of four principal elements:

- Fuzzification interface, Fuzzifier
- Fuzzy inference engine
- Fuzzy rule base, including linguistic variables and connectives
- Defuzzification interface, Defuzzifier.

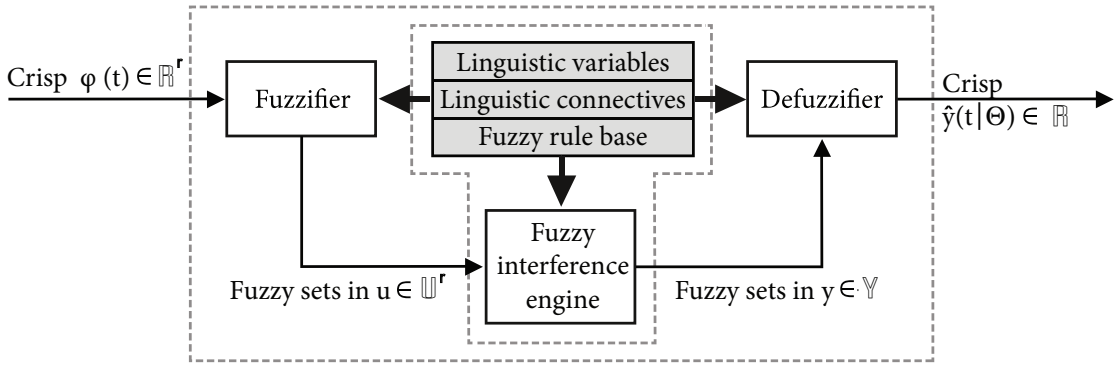

Fig. 3.1 MISO structure of a FL based model

3.2.1.1 Fuzzification

Figure 3.1 presents the MISO structure of the general FL-based model; we can see all fuzzy constructive elements in the processing flow, from the crisp input regression vector $\boldsymbol{\varphi}(t)$ to the crisp output $\hat{y}(t,\boldsymbol{\theta})$. Thin arrows represent the computation and thick ones the information flow.
Our regressors in the regression vector will be given the linguistic names presented by vector $\boldsymbol{u}$ from the fuzzy set, subsequently forming the "Fuzzy rule base", Figure

3.1. Differently than a pure membership, the fuzzy set members have a weight of their membership on the span from completely "being a member" to not being a member in a range [1,0].

****Definition 3.2**[115]* (***Fuzzy set***) *If* u *is an element in the universe of discourse* $\mathbb{U}$, *then a fuzzy set* $\boldsymbol{A}$ *in* $\mathbb{U}$ *is the set of ordered pairs*

$$\boldsymbol{A} = \{(u, \mu_A(u)) : u \in \mathbb{U}\}, \tag{3.15}$$

where $\mu_A(u)$ *is a membership function carrying an element from* $\mathbb{U}$ into *membership value between* [0,1], *also called a degree of membership.*

The process of associating the regressors to the linguistic names $\boldsymbol{u}$, and mapping to the fuzzy set as stated in Definition 3.2, is called the fuzzification (Figure 3.1). The mapping is derived by employing the membership functions that can be arbitrarily defined by the designer of a model. Even the membership function (MF) is generally any function associating the value in closed set [0,1], their selection is driven by the final modelling objectives and has the influential impact on the model accuracy and the final control stability. As this part of the fuzzy logic is related to the vagueness, here we find heuristic fuzziness, certainly based on the experience or intuition. By the experience, we consider a previously applied pragmatic mathematical knowledge and the probabilistic theory. Consequently, the certain grouping of the MFs is established, and that will be inherited from [115] and the references therein. The important characteristics of the MFs are their convexity and shape, which are then set into three distinctive groups:

- Network-classic MF
  This group has to be given special attention because of its smoothness that will be used in this work to achieve a smooth transformation from analytically recognized HS to a more natural continuous. The sigmoidal and Gaussian functions are members of this class

$$MFsig(u,\beta,\gamma) \quad \rightarrow \quad \mu_A = \frac{1}{1+e^{-\beta(u-\gamma)}}$$

$$MFgauss(u,\beta,\gamma) \quad \rightarrow \quad \mu_A = e^{-\frac{1}{2}\left(\frac{u-\gamma}{\beta}\right)^2}$$

  The smoothness of those functions certainly contributes to the popularity in the fuzzy modelling and their group name is associated with more complex and networked identification structures.

  - Zadeh-formed MF
    The name is given referring to the Zadeh, who is recognized as the author originally suggesting this formulation of MFs. Yield, the group of MFs that consists of $Z-$, $S-$, and $\Pi-$ *functions*:

$$MFz(u,\gamma_1,\gamma_2) \quad \rightarrow \quad \mu_A = \begin{cases} 1 & u \le \gamma_1 \\ 1-2\left(\dfrac{u-\gamma_1}{\gamma_2-\gamma_1}\right)^2 & \gamma_1 < u \le \dfrac{\gamma_1+\gamma_2}{2} \\ 2\left(\dfrac{u-\gamma_2}{\gamma_2-\gamma_1}\right)^2 & \dfrac{\gamma_1+\gamma_2}{2} < u \le \gamma_2 \\ 0 & u > \gamma_2 \end{cases}$$

$$MFs(u,\gamma_1,\gamma_2) \quad \rightarrow \quad \mu_A = 1 - MFz(u,\gamma_1,\gamma_2) \quad .$$

$$MF\pi(u,\gamma_1,\gamma_2,\gamma_3,\gamma_4) \quad \rightarrow \quad \mu_A = \begin{cases} MFs(u,\gamma_1,\gamma_2) & u \le \gamma_2 \\ 1 & \gamma_2 < u \le \gamma_3 \\ MFz(u,\gamma_3,\gamma_4) & u > \gamma_3 \end{cases}$$

- Piecewise linear MF
  Considering the name of the group, these functions are constructed from the piecewise lines forming the open left, the open right, the triangular and the trapezoidal functions of parameters $(\gamma_1 \le \gamma_2 \le \gamma_3 \le \gamma_4)$:

$$MFol(u,\gamma_1,\gamma_2) \quad \rightarrow \quad \mu_A = \max\left(\min\left(\frac{\gamma_2-u}{\gamma_2-\gamma_1},1\right),0\right)$$

$$MFor(u,\gamma_1,\gamma_2) \quad \rightarrow \quad \mu_A = \max\left(\min\left(\frac{u-\gamma_1}{\gamma_2-\gamma_1},1\right),0\right)$$

.

$$MFtri(u,\gamma_1,\gamma_2,\gamma_3) \quad \rightarrow \quad \mu_A = \max\left(\min\left(\frac{u-\gamma_1}{\gamma_2-\gamma_1},\frac{\gamma_3-u}{\gamma_3-\gamma_2}\right),0\right)$$

$$MFtrap(u,\gamma_1,\gamma_2,\gamma_3,\gamma_4) \quad \rightarrow \quad \mu_A = \max\left(\min\left(\frac{u-\gamma_1}{\gamma_2-\gamma_1},1,\frac{\gamma_4-u}{\gamma_4-\gamma_3}\right),0\right)$$

If we recall the general identification theory (Section 3.1), we see the close relation of MFs to the basis functions with their distinctive parameters β_i and γ_i. While the first group of MFs is more convenient for identification and modelling, the last two are certainly representative of the wider and classical group of *Fuzzy Control* MFs.
The fuzzification system becomes easily massive with the involvement of the multiple regressors and the adequate multiple *Fuzzy Sets*. Accordingly, the expression (3.15) evolves in

$$\boldsymbol{A}_i^{\,j} = \{(u_i, \mu_{\boldsymbol{A}_i^{\,j}}(u_i)) : u_i \in \mathbb{U}_i\} \quad . \qquad (3.16)$$

In the expression (3.16), the new indices $i = 1,...,r$ correspond to the span of regressors in the regression vector $\varphi(t)$. Every linguistic variable u_i associated with the degree of membership $\mu_{A_i j}(u_i)$, in the fuzzy set $\boldsymbol{A}_i{}^j$, could have a different number of the fuzzy sets $j = 1,...,l$ in the universes of discourse $\mathbb{U}_i$. All universes of discourses for every particular fuzzy input are subsets of a general input universe of discourse $\mathbb{U}_1,...,\mathbb{U}_r \subset \mathbb{U}$. Because of different physical values and a different scaling, the number of fuzzy sets l can differ related to the particular linguistic variable, and it is a function $l(i)$. Similarly, as the regressor is given a linguistic name, the fuzzy sets are given adjectives.
For the example, if we 'code' the antecedent of a measured current $i_L(t)$ by the variable 'INDUCTOR CURRENT-1' then the fuzzy sets could be assigned by adjectives in the universe $\mathbb{U}_1$

$$\left\{\boldsymbol{A}_1{}^1 = 'LOW', \boldsymbol{A}_1{}^2 = 'MODERATE', \boldsymbol{A}_1{}^3 = 'HIGH'\right\} \subset \mathbb{U}_1.$$

In the above example, we defined $l(1) = 3$.
Therefore, in (3.16) the fuzzification is simplified by an assumption that we have the maximum certainty that the measured variable takes only one exact value u_i. That way, the linguistic variables are not the fuzzy projection of inputs, as is generally the case, but they are defined by the fuzzy sets

$$\mu_{A_i} = \begin{cases} 1 & \varphi_i = u_i \\ 0 & otherwise \end{cases}, \tag{3.17}$$

and the process of fuzzification is called *singleton fuzzification*. Bearing in mind to present the core fuzzy logic projection and its clarity, in the following we continue with that assumption.

3.2.1.2 Fuzzy Inference and Fuzzy Rule Base

Once the fuzzification is completed, the next step in fuzzy computation is the *Fuzzy Inference*. Now, we can recall the expressions (3.14) and take a simplification of the *generalized modus ponens* to the *modus ponens* by an equalizing $\mathcal{A}' = \mathcal{A}$, $\mathcal{B}' = \mathcal{B}$. This type of fuzzy inference we can find in most of the FL examples, thus

IF *premise* **THEN** *consequence* . (3.18)

From a simple inference (3.18) the fuzzy inference engine is building the *rule base* considering the previous fuzzification:

$$
\begin{array}{ll}
\mathcal{R}_{1,1,\ldots,1} & \textbf{IF } (u_1 \textit{ is } A_1^{1}) \textbf{ and } (u_2 \textit{ is } A_2^{1}) \textbf{ and } \ldots \textbf{and } (u_r \textit{ is } A_r^{1}) \textbf{ THEN } (y \textit{ is } B_{1,1\ldots,1}) \\
\mathcal{R}_{1,1,\ldots,2} & \textbf{IF } (u_1 \textit{ is } A_1^{1}) \textbf{ and } (u_2 \textit{ is } A_2^{1}) \textbf{ and } \ldots \textbf{and } (u_r \textit{ is } A_r^{2}) \textbf{ THEN } (y \textit{ is } B_{1,1,\ldots,2}) \\
\vdots & \vdots \\
\mathcal{R}_{1,2,\ldots,l_r} & \textbf{IF } (u_1 \textit{ is } A_1^{1}) \textbf{ and } (u_2 \textit{ is } A_2^{2}) \textbf{ and } \ldots \textbf{and } (u_r \textit{ is } A_r^{l_r}) \textbf{ THEN } (y \textit{ is } B_{1,2,\ldots,l_r}) \\
\vdots & \vdots \\
\mathcal{R}_{\eta,1\ldots,1} & \textbf{IF } (u_{_1} \textit{ is } A_1^{\eta}) \textbf{ and } (u_2 \textit{ is } A_2^{1}) \textbf{ and } \ldots \textbf{and } (u_r \textit{ is } A_r^{1}) \textbf{ THEN } (y \textit{ is } B_{\eta,1\ldots,l}) \\
\mathcal{R}_{\eta,1\ldots,2} & \textbf{IF } (u_{_1} \textit{ is } A_1^{\eta}) \textbf{ and } (u_2 \textit{ is } A_2^{1}) \textbf{ and } \ldots \textbf{and } (u_r \textit{ is } A_r^{2}) \textbf{ THEN } (y \textit{ is } B_{\eta,1,\ldots,2}) \\
\vdots & \vdots \\
\mathcal{R}_{l_1,l_2,\ldots,l_r} & \textbf{IF } (u_{_1} \textit{ is } A_1^{l_1}) \textbf{ and } (u_2 \textit{ is } A_2^{l_2}) \textbf{ and } \ldots \textbf{and } (u_r \textit{ is } A_r^{l_r}) \textbf{ THEN } (y \textit{ is } B_{l_1,l_2,\ldots,l_r})
\end{array}
\qquad (3.19)
$$

As is transparent from the rule base (3.19), our premise is built from all possible combinations of the statements related to the number of regressors or the linguistic names and their associated numbers of MFs $l_1 = l(1), l_2 = l(2),\ldots,l_r$. Also, we see that every premise is associated with the crisp output y. As we have presented the MISO structure, the output is a member of the output universe of discourse $\mathbb{Y}$, and each regressor implies a different fuzzy subset in that universe. A degree of membership of output crisp value, throughout the fuzzification, as equally as inputs, is defined by the MF that yields $\mu_{B_i} \in [0,1]$, for the fuzzy linguistic output adjectives $B_1, B_2, \ldots, B_r$. Conclusively, the *fuzzy rule* in the MISO structure is a mapping defined by the MFs from the input universe of discourse to the output universe of discourse

$$\mu_{\boldsymbol{A}_i \to B_i}(\boldsymbol{u}, y, \cdot) = \mu_{A_1} \times \mu_{A_2} \times \ldots \times \mu_{A_r} \to B_{1,\ldots,r}(u_1, u_2, \ldots u_r, y;) \qquad (3.20)$$

in the space $\mathbb{U}_1 \times \mathbb{U}_2 \times \ldots \times \mathbb{U}_r \times \mathbb{Y}$.

Complexity of so constructed inference is rapidly becoming a huge computing problem. The number of rules in the rule base can be easily calculated by

$$\mathbb{R} = \prod_{i=1}^{r} l_i \quad . \qquad (3.21)$$

It exponentially increases with each additional input in the case of MISO structure and by the fact that every input has an equal number of MFs. The problem becomes worse in MIMO structures, where we can expect $\mathbb{R} \cdot \dim(\boldsymbol{y})$ number of the rules in the rule base, or in the case wherein (3.16) or (3.19) inputs are not the singleton fuzzified, $\boldsymbol{u \neq \varphi(t)}$. The latter is usually used to express the uncertainty in the measuring process. If our fuzzification is not the singleton, the projection of fuzzy inputs to fuzzy outputs (3.20) yields a more involved expression

$$\mu_{B_{1,\ldots,r}}(y, \cdot) = \underset{\boldsymbol{u} \in \mathbb{U}^r}{proj}(\mu_{\hat{\boldsymbol{A}}}(\boldsymbol{u}) \; AND \; \mu_{\boldsymbol{A}_i \to B_i}(\boldsymbol{u}, y, \cdot)) = \underset{\boldsymbol{u} \in \mathbb{U}^r}{sup}(\mu_{\hat{\boldsymbol{A}}}(\boldsymbol{u}) * \mu_{\boldsymbol{A}_i \to B_i}(\boldsymbol{u}, y, \cdot)) \quad . \qquad (3.22)$$

The expression (3.22) is known as a *sup-star composition.* It yields the final output as the projection of measured and fuzzified inputs, associated with their fuzzy set in one degree of membership $\mu_{\hat{\boldsymbol{A}}}(\boldsymbol{u}) = \mu_{\hat{A}_1}(u_1) * \mu_{\hat{A}_2}(u_2) * \ldots * \mu_{\hat{A}_r}(u_r)$, to output degree of membership $\mu_{B1,\ldots,r}(y;)$.

Apart from using the singleton fuzzification, the physical knowledge of the system to be identified could significantly decrease the total number of rules, and in some points also diminish the unnecessary logic that each has every premise term. The simplification goes in the direction of finding a special MF that is unity over the entire universe of discourse. Instead of straightening the FL complexity, we decompose the physical problem and use FL only where the physical vagueness is present.
In the presented rule base (3.19), we have selected just one example of the *fuzzy connectives or* the *conjunctions* **and,** but in general there is a wide range of possibilities. For a better clarity, we will express the most dominant fuzzy logic connectives and operators over the fuzzy sets $\boldsymbol{A}_i^{\,j}$ for $i=1,2,..,r$ and $j=1,2,..,l(i)$ in the inference engine:

- Fuzzy Complement
  Complement of a *Fuzzy Set* $\boldsymbol{A}_i^{\,1}$ with a membership function $\mu_{\boldsymbol{A}_i 1}(u_i)$ has a membership function $(1-\mu_{\boldsymbol{A}_i 1}(u_i))$
- Fuzzy Intersection (AND)
  The intersection of fuzzy sets $\boldsymbol{A}_i^{\,1}$ and $\boldsymbol{A}_i^{\,2}$, defined on the universe of discourse $\mathbb{U}_1$, is a fuzzy set denoted by $\boldsymbol{A}_i^{\,1} \cap \boldsymbol{A}_i^{\,2}$, with a membership function:
  1. *Minimum*: $\mu_{\boldsymbol{A}_i 1 \cap \boldsymbol{A}_i 2} = \min\left\{\mu_{\boldsymbol{A}_i 1}(u_i), \mu_{\boldsymbol{A}_i 2}(u_i) : u_i \in \mathbb{U}_i\right\}$
  2. *Algebraic Product*: $\mu_{\boldsymbol{A}_i 1 \cap \boldsymbol{A}_i 2} = \left\{\mu_{\boldsymbol{A}_i 1}(u_i) \cdot \mu_{\boldsymbol{A}_i 2}(u_i) : u_i \in \mathbb{U}_i\right\}$
- Fuzzy Union (OR)
  1. *Maximum*: $\mu_{\boldsymbol{A}_i 1 \cup \boldsymbol{A}_i 2} = \max\left\{\mu_{\boldsymbol{A}_i 1}(u_i), \mu_{\boldsymbol{A}_i 2}(u_i) : u_i \in \mathbb{U}_i\right\}$
  2. *Algebraic Sum*:
     $\mu_{A_i 1 \cup A_i 2} = \left\{\mu_{\boldsymbol{A}_i 1}(u_i) + \mu_{\boldsymbol{A}_i 2}(u_i) - \mu_{\boldsymbol{A}_i 1}(u_i) \cdot \mu_{\boldsymbol{A}_i 2}(u_i) : u_i \in \mathbb{U}_i\right\}$
     also called the "triangular co-norm" and given by symbol $\oplus$. *The symbol is also generally used for the fuzzy union.*
- Fuzzy Cartesian Product
  That generally represents the **and** operator in (3.19), and quantifies the operations between many fuzzy sets of the universe of discourse $\mathbb{U}_1,\ldots,\mathbb{U}_r \subset \mathbb{U}$. The result is a fuzzy set being defined by fuzzy function
  $\mu_{\boldsymbol{A}_1 \times \boldsymbol{A}_2 \times \ldots \times \boldsymbol{A}_r}(u_1,u_2,\ldots,u_r) = \mu_{\boldsymbol{A}_i}(u_1) \times \mu_{\boldsymbol{A}_2}(u_2) \times \ldots \times \mu_{\boldsymbol{A}_r}(u_r)$ *for* $\boldsymbol{A}_1 = \bigcup_{j=1}^{l_1} \boldsymbol{A}_1^{\,j}$.

3.2.1.3 Defuzzification

Knowing the above FL inside the fuzzy engine can easily demonstrate all diversities in the *Fuzzy Logic Identifiers.* In looking for a final crisp output value $\hat{y}(t,\boldsymbol{\theta}) \in \mathbb{R}$, as the result of the projection of fuzzy sets from the input universes of discourses to the output universe of discourse, in MISO structure (3.20), (3.22), we have to devise a

type of aggregation of the generated fuzzy sets into the unique form. This process is called *defuzzification*.

There are different types of defuzzification techniques looking from the side of the inferred fuzzy sets by two different general inference approaches. First, we build the inference engine on the way to compute the "*implied fuzzy set*" of each particular rule *n*

$$\mu_{\hat{B}_n}(y;\cdot) = \mu_{\hat{\mathbf{A}}_n}(\boldsymbol{u}) * \mu_{B_n}(y;\cdot). \tag{3.23}$$

Second, the inference engine computes the overall '*implied fuzzy set*' for all rules and aggregates it into the overall output degree of membership

$$\mu_{\hat{\boldsymbol{B}}}(y;\cdot) = \mu_{\hat{\boldsymbol{B}}_1}(y;\cdot) \oplus \mu_{\hat{\boldsymbol{B}}_2}(y;\cdot) \oplus \ldots \oplus \mu_{\hat{\boldsymbol{B}}_R}(y;\cdot). \tag{3.24}$$

Defuzzification referring the *rule implied fuzzy set* could be characterized as the *Centre of Gravity* (COG) or the *Centre-average*.

****Definition 3.3** [36] If the crisp output* $\hat{y}(t,\boldsymbol{\theta}) \in \mathbb{R}$ *is computed by equation*

$$\hat{y}(t,\boldsymbol{\theta}) = \frac{\sum_{n=1}^{\mathbb{R}} c_n \int_{\mathbb{Y}} \mu_{\hat{\boldsymbol{B}}_n}(y;\cdot)dy}{\sum_{n=1}^{\mathbb{R}} \int_{\mathbb{Y}} \mu_{\hat{\boldsymbol{B}}_n}(y;\cdot)dy}, \tag{3.25}$$

where $\mathbb{R}$ *denotes a number of rules in the rule base,* c_n *is the centre of area of the membership function of* B_n*, associated with the implied fuzzy set* $\hat{\boldsymbol{B}}_n$ *for the n^th^ rule, and* $\int_{\mathbb{Y}} \mu_{\hat{\boldsymbol{B}}_n}(y;\cdot)dy$ *denotes the area under* $\mu_{\hat{\boldsymbol{B}}_n}(y;\cdot)$*, then this computation is called the Centre of Gravity Defuzzification.*

****Definition 3.4** [36] If the crisp output* $\hat{y}(t,\boldsymbol{\theta}) \in \mathbb{R}$ *is computed by equation*

$$\hat{y}(t,\boldsymbol{\theta}) = \frac{\sum_{n=1}^{\mathbb{R}} c_n \sup_y\{\mu_{\hat{\boldsymbol{B}}_n}(y;\cdot)\}}{\sum_{n=1}^{\mathbb{R}} \sup_y\{\mu_{\hat{\boldsymbol{B}}_n}(y;\cdot)\}}, \tag{3.26}$$

where R *denotes the number of rules in the rule base,* c_n *is the centre of area of the membership function of* B_n *associated with the implied fuzzy set* $\hat{\boldsymbol{B}}_n$ *for the n^th^ rule and* $\sup_y\{\mu_{\hat{\boldsymbol{B}}_n}(y;\cdot)\}$ *denotes the 'supremum' meaning the highest value* $\{\mu_{\hat{\boldsymbol{B}}_n}(y;\cdot)\}$*, then this computation is called the Centre-average Defuzzification.*

We see that in both types of defuzzifications, special attention has to be given to the construction of the fuzzy systems to avoid 0 in the denominators of (3.25) and (3.26). Thus, $\sum_{n=1}^{\mathbb{R}} \int_{\mathbb{Y}} \mu_{\hat{B}_n}(y;\cdot)dy \neq 0$ or $\sum_{n=1}^{\mathbb{R}} \sup_y\{\mu_{\hat{B}_n}(y;\cdot)\} \neq 0$.

Other than the abovementioned, once the defuzzification is rendered by using the overall implied fuzzy set, the following technique of defuzzifications is known:

- *Max criterion*

This way the $\hat{y}(t,\boldsymbol{\theta})\in\mathbb{R}$ is computed as $\hat{y}(t,\boldsymbol{\theta})\in\{\arg\sup_{\mathbb{Y}}\{\mu_{\hat{\boldsymbol{B}}}(y,\cdot)\}\}$, where it takes the maximum certainty value $\mu_{\hat{\boldsymbol{B}}_n}(y,\cdot)$ *for* $n = 1,\ldots,\mathbb{R}$ from (3.24).

- *Mean of Maximum*
  It can be considered as the upgrade of the *Max criterion* and computed as
  $$\hat{y}(t,\boldsymbol{\theta}) = \frac{\int_{\mathbb{Y}} y\cdot\ \mu_{\hat{\boldsymbol{B}}_*}(y,\cdot)dy}{\int_{\mathbb{Y}}\mu_{\hat{\boldsymbol{B}}_*}(y,\cdot)dy}.$$
  To derive this defuzzification, it is necessary to form a new output membership function $\hat{\boldsymbol{B}}_*$ that has a degree of membership defined by
  $$\mu_{\hat{\boldsymbol{B}}_*}(y,\cdot) = \begin{cases} 1 & \mu_{\hat{\boldsymbol{B}}}(y,\cdot) = \hat{c}_{max} \\ 0 & otherwise \end{cases}.$$
  Now the $\hat{c}_{max}$is a supremum of the membership function $\hat{\boldsymbol{B}}$ over the universe of discourse $\mathbb{Y}$. It is anticipated that in equation (3.24) we have more than one supremum, and it should be devised a mean value.

- *Centre of area*
  Analogically to the latter defuzzification technique, from a side of the *overall implied fuzzy set,* the centre of area is computed as
  $$\hat{y}(t,\boldsymbol{\theta}) = \frac{\int_{\mathbb{Y}} y\cdot\ \mu_{\hat{\boldsymbol{B}}}(y,\cdot)dy}{\int_{\mathbb{Y}}\mu_{\hat{\boldsymbol{B}}}(y,\cdot)dy},$$
  where $\mu_{\hat{\boldsymbol{B}}}(y,\cdot)$ is the degree of membership from (3.24).

Except that the defuzzification methods computed from an aspect of the overall output fuzzy set suffer the same complexity (the denominator ill condition) as those defined by (3.25) and (3.26), its complexity is elevated by the construction of the inference engine that provide the overall fuzzy set $\hat{\boldsymbol{B}}$ from (3.24). That makes these defuzzifications rarely used in practice. Certainly, the COG and Centre-average methods are the most dominant.

As mentioned, the complexity of a FL can exponentially develop by the selection of rules in the rule base (3.19), but equally influenced with the selection of the FL conjunctions, fuzzification of inputs and outputs and finally with the defuzzification. Significantly, over the past twenty years, some of the FL structures have been given the broad attention from the engineering and the academic societies. For the example, the Mandami [116] and Takagi-Sugeno (T-S) [21] FL structures, observed from the identification point of view the model structures, are typical representatives. There is a twofold reason for their popularity that brought those two methods to the level of the basic FL perception of the wider community. The given attention led to the integration into the MATLAB platform [29] as a standardized fuzzy logic control framework. First, they are a simple heuristic reasoning strategy that is easy to grasp in *modus ponens* implications. Second, the mathematical expression (arithmetic) of the crisp output values is compact and simple to compute by the microprocessors.
Further on, the simplification of the FL used here is based on three different levels:

- Singleton fuzzifications of inputs and outputs,
- Algebraic product in the fuzzy premise,
- Centre-average defuzzification.

The mathematical expression of the crisp outputs then evolves in

$$\hat{y}(t,\boldsymbol{\theta}) = \frac{\sum_{n=1}^{\mathbb{R}} c_n \cdot \mu_{\hat{A}_n}(\boldsymbol{\varphi}(t))}{\sum_{n=1}^{\mathbb{R}} \mu_{\hat{A}_n}(\boldsymbol{\varphi}(t))} \quad . \tag{3.27}$$

Trivially to prove, equation (3.27) does represent a simplified Mandami and T-S reasoning. The difference in the latter involves a mathematical function instead of c_n, which in the former denotes the pure centre maximum real value of the output. The singleton output fuzzification and the algebraic product of the n^{th} rule premise simplifies the equation (3.23) to $\mu_{\hat{B}_n}(y;) = c_n \cdot \mu_{\hat{A}_n}(\boldsymbol{u})$. Additionally, the singleton input fuzzification yields $\mu_{\hat{B}_n}(y;) = c_n \cdot \mu_{\hat{A}_n}(\boldsymbol{\varphi}(t))$.

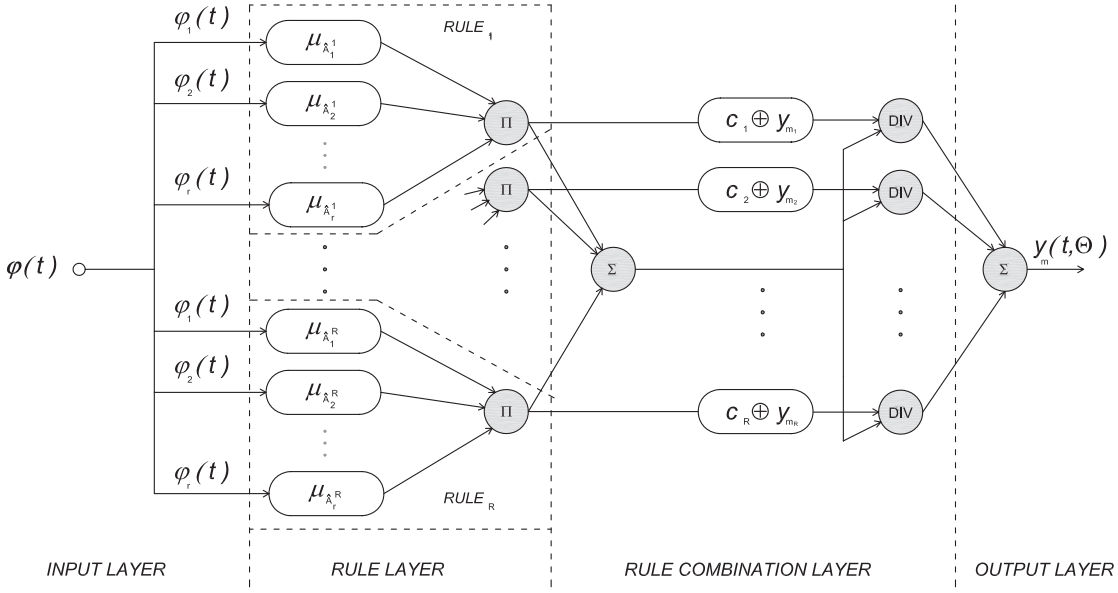

Fig. 3.2 Fuzzy model structure (3.27) suitable for identification purposes

We see that the output singleton fuzzification of MISO systems gives only the centre and one consequence of the output fuzzy MF, which is in the sequel scaled and assigned as c_n. Differently, in the T-S fuzzy model structure, the output presents the mathematical model that is a unique consequence of the n^{th} rule premise. If we now recall a defuzzification (3.26), the supremum of the set of degrees of the membership for each specific rule, in singleton output fuzzification, is just $\mu_{\hat{A}_n}(\boldsymbol{u})$ the *degree of fulfilment* of c_n. In Figure 3.2, we pose the identification model structure of (3.27), considering the above simplifications. Centre singletons are expressed in a sense of different local models y_{m_n} *for* $n = 1,..,\mathbb{R}$.

Using the FL for the identification purposes projects a different light on fuzzy logic in general. Particular attention has to be given to the selection of MFs. The identification suitable MFs are those from the Network-classic group or the bell-shaped functions. Those functions are from one side, preserving the system's smoothness, but also guarding the computation process from the ill conditions in (3.25) and (3.26). The former is not a problem when the FL is used in the *Fuzzy Logic Controllers (FLC)*. The strength of the FL approximation is exemplified on the FLC, starting with the simple examples and later progressing to the more complicated one. For example, in the work of Buckley [117,118], it is proven for a modified T-S modelling strategy, in which the consequent functions are also the polynomials and not only the linear functions, including the matching of the input value with the rule as an upgrade to the centre-average defuzzification. Later, in the work of Castro [34], it was proved that FLCs are capable to approximate any real continuous functions on a compact set to arbitrary accuracy. The class of the fuzzy identifier or in that case the FLC structure was defined by:

1. Gaussian membership functions
2. Product as the fuzzy conjunction
3. Product as the fuzzy implication
4. Centre of area defuzzification.

Further, in the same work, the proofs continued on the wider classes, including:

1. Trapezoidal and Triangular MFs among the others
2. Fuzzy conjunction modelled by and arbitrary T-norm
3. Fuzzy implications only need to satisfy a weak property (R-implications and T-norms satisfy it)
4. Defuzzification methods only need to satisfy weak conditions ((3.25) and (3.26))

3.3 Fuzzy identification of SAS, the redefined approaches

Referring to the statements in the introduction of this chapter, we base the new methodology in the fuzzy identification of SAS on two distinctively constructed approaches. Both are rendered from a control point of view. First, looking from the side of the system robustness, it is a way to identify a system global space of the stable points or equilibriums. Second, that is a more comprehensive methodology that has to include the dynamics of the system in the global sense. The latter we will call the quantitative/qualitative property of the natural system to control, while the former is the quantitative system property. As the modern control of the nonlinear dynamical systems is widening the objectives, we found it crucial to redefine a standard and pragmatic approaches in the modelling of SAS.

3.3.1 Fuzzy static model of a DC-DC boost converter

Previously emphasized distinctive problems of the analytical approaches in the modelling of a DC-DC boost converter, as an example of SAS, will be considered and a more objective modelling approach that will overcome the uncertainties by FL will

be built. If we recall the *reachability set* (*Definition 2.10*) in HS, then we can recognize the similarity with the idea of constructing the space of feasible and realistic steady states of the modelled systems. In this thesis, with the example of SAS, the control technique is a genuine part of the system, and it cannot be simply decomposed. The continuous modes of the HS cannot exist by themselves, but rather they should coexist in combination with others in the perfectly defined and fixed time base. The control pulse that is driving the transistor has its natural time constraint $d_u = (1-d)k \; for \; d \in [0,1]$ (duty cycle), where $0 \leq k < 1$. The duty cycle $d_u \in [0,1)$ is scaled to suite the physical sense of the range that guaranties the system's functionality. In Subsection 2.3.1, the meaning is explained: it controls the voltage conversion in the electrical energy transfer from the source to the consumer. The top duty cycle border 1 should not be maintained, as it causes a destruction of the inductance and the semiconductors. If the mentioned borders are not violated, the specific electronic circuit topology will be exchanged together with the associated HS continuous modes. That sequence of modes is recurrent by the time base T_S. So too, the duty cycle is a scalar that defines the transistor's "on state" in a time $d_u T_S$.

In order to achieve a more objective modelling, and more accurate in physical cases, our modelling complexity will be decomposed by a physical knowledge of the system. Differently than in the analytic approaches earlier, we will look for a quantitative system property in the normed space of the system states that will give us the energy information at a glance, instead of deriving it from the dynamical system's model. It seems to be a logical way for the complexity decomposition from two points of view. First, the selected system is a representative of PEC, so the energy-directed discussion is not unexpected. Second, and looking from a side of the law of the conservation of energy, it provides the transformation of a HS to the nonlinear dynamical and smooth system. If we observe from a side of the fixed time period the energy is a continuous function of time. In the case of the DC-DC boost converter it will be a switching period T_S. The process of measuring of the states and system parameters will transfer the process to the normed space. In the simulations, it will be rendered by the numerical integration methods, and in the realistic environment by the measuring devices. The emphasizing an idea of modelling the HS by defining the system's continuous counterpart does not necessarily lead to the inaccurate modelling [2] and the coarse approach, but conversely defines a strong base for a complexity reduction and stable control methodology. The accuracy of model constructed in this manner has to be at least equal to one exemplified in the more accurate analytic approaches, Section 2.3.

The main physical meaning of the selected example is to transfer the energy from the source to the consumer and at the same time maintaining the voltage ratio between them (Figure 2.11). The system's equilibrium is achieved once the energy demand from the consumer is delivered preserving the output DC voltage and the constant duty cycle. Generally, the construction of the electrical circuit is built (Figure 2.12) to provide the certain energy storage, which has to compensate for a short time load demand deviation. It is fulfilled by the implementation of the output capacitor. At one operating point, if there is no change in the system parameters, after the arbitrary time of transition, while the duty cycle is constant, the process has achieved equilibrium. This means that the steady duty cycle will provide a certain and steady voltage output of the consumer and the steady periodic energy flow in-between the input and output ports of a DC-DC converter, Figure 2.11.

Measurements of an input port voltage and current, and the output port voltage and current will prove an energy balance if we neglect the energy losses. Even in the physical cases in which the losses are present, in the identification methodology, it will be measured and recognized as the port energy imbalance. Driven by the final control technique point of view, our task is to identify the mapping of the duty cycle to the previously mentioned measured energy balance or imbalance.
From our smoothing operations, the measured inputs and outputs are now more in harmony with the final goal of controlling a DC output signal, which is not a pure DC signal, but it is a combination of a DC signal and the AC ripple (Subsection 2.3.1). The integration of measured signals in the T_S period will give a proper signal contribution to the periodic energy balance and our DC output signal assumption. In practice, the measured signals will be RMS values and the control algorithm will control the output voltage RMS value. It is straightforward to see that, generally in this example, we have two possible feedback control approaches. One, which is a control of the output voltage trajectory, or the other more simplified, that controls the output normed value. The latter and the one taken in our work is more according to the fundamental assumption that the task is to control an output DC signal. These statements are leading to the mathematical transformation of the original and the analytic state space model to the new Lebesgue 2 normed state space. In such a transformed state space, we are deriving the new space of a DC-DC boost converter equilibriums.

A new pseudo-norm $\|.\|$ on the vector space $(V,\|.\|)$

$$\|z\|_{L^p} = \frac{1}{t}\left(\int |z|^p dt\right)^{\frac{1}{p}} \quad , \quad z \in \mathbb{L}^p \tag{3.28}$$

will be derived from the simulation process of the hybrid mathematical model and a numerical integration based on the explicit Runge-Kutta (4,5) method and developed in the "ode45(Dormand-Prince)" MATLAB [29] for $p = 2$.
We have to recall equations (2.53), (2.66) and Table 2.2 to devise the mathematical expression

$$\dot{\boldsymbol{z}}(t) = \begin{cases} \boldsymbol{A}_1 \boldsymbol{z}(t) + \boldsymbol{B}_1 E(t) & kT_S \le t \le kT_S + t_{1,k} \\ \boldsymbol{A}_2 \boldsymbol{z}(t) + \boldsymbol{B}_2 E(t) & kT_S + t_{1,k} < t \le kT_S + t_{1,k} + t_{2,k} \\ \boldsymbol{A}_3 \boldsymbol{z}(t) + \boldsymbol{B}_3 E(t) & kT_S + t_{1,k} + t_{2,k} < t < (k+1)T_S \end{cases}$$
$$k = 0,1 \ldots \infty \quad , \tag{3.29}$$

as the complete mathematical model of the hybrid automaton from Figure 2.13. Hence, the continuous equations (3.29) for the state variables $\boldsymbol{z}(t) = [v_C(t)\ i_L(t)]$ provide the basic blocks in the SIMULINK [29] that will be connected with the discrete events. The final hybrid simulation model is equivalent to the one presented in Figure 2.3, but with the major difference that it will not be executed in the real-time span. This has to give us sufficient information about the processing complexity if that is to be our final model for the predictive control solution, as it is presented in Subsections 2.1.4 and 2.3.3. Subsequently, in the offline regime, we have sufficient time to execute the simulation with the as short as possible basic time of execution (1e-06s) and integration, which gives the highest grade of accuracy of the switching

events. Accordingly, that is our closest estimate of the real events in the DC-DC boost converter.

The space transformation filters out the high-frequency nonlinearities or the high-scaled oscillations. In the continuation, a pseudo norm space $(V,\|.\|)$ will be further transformed to the pseudo-Banach subspace of an augmented dimension.

The simulation process Q of the hybrid system (3.29) will expand the origin three-dimensional space including time to the six-dimensional space $Q:\mathbb{R}^3 \to \mathbb{R}^6$. In the Figure 3.3 we present the simulation model constructed to allow the space transformation of the original simulation model from the Figure 2.18. That is possible by knowing that our physical system is state measurable. The extra measured process parameters are E as the input voltage source to the converter, the output current i_R, the control variable to process $d_u = (1-d)0.66 = t_{k1}/T_s \; for \; d \in [0,1]$ scaled to suite to the Pulse Width Modulator (PWM). The measurement of the i_R and together with the controlled voltage value will reconstruct the converter's load in a physical environment. Less demanding is a measurement of the load in simulations, as shown in Figure 3.3.

From the simulations, we know that the process is open-loop stable. Even when transformed, the system still preserves its nonlinear dynamical characteristics. With the intention to predict the stable control parameter d_u, our work will concentrate on an examination of the stable steady state of a DC-DC boost converter.

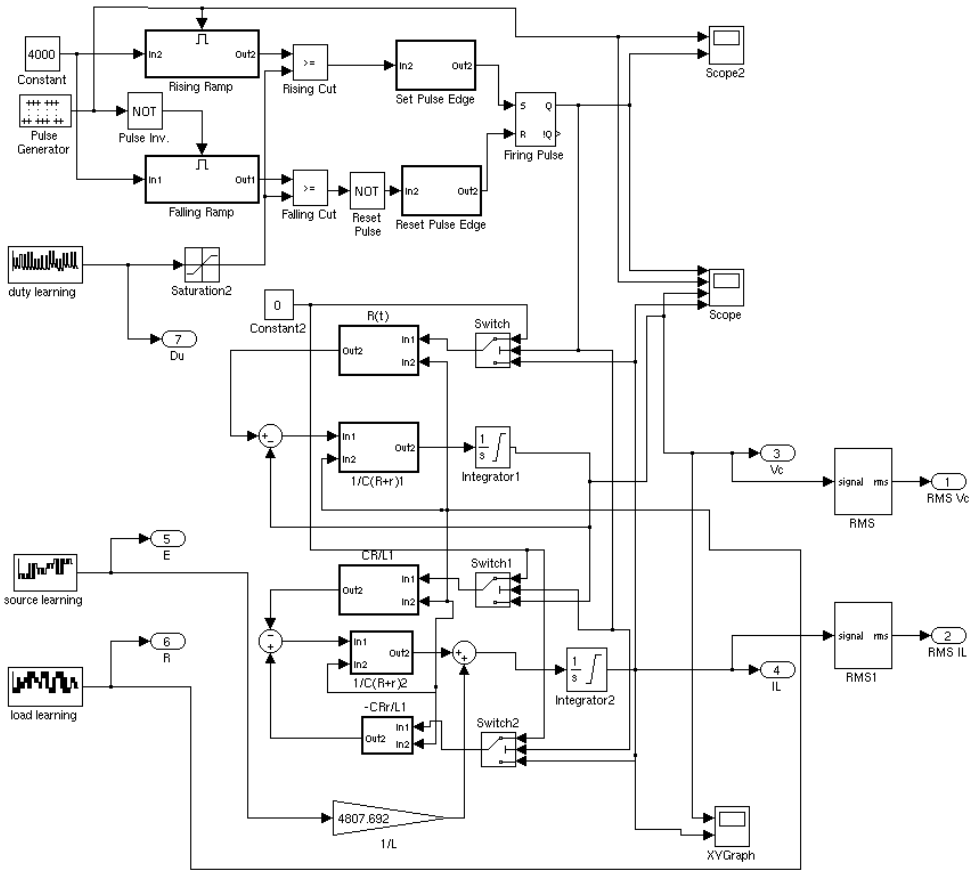

Fig. 3.3 The hybrid simulation model constructed to allow the state space transformation and accordingly the identification

A mapping Q derived the trajectories over the six-dimensional pseudo-Banach space and opens the ability for an orthogonal slicing of the new vector space $(V^6,\|.\|)$ to the tangent vector space $(V_1{}^6,\|.\|)\subset(V^6,\|.\|)$. Geometrically, $(V^6,\|.\|)$ is a smooth manifold M_1, which consists of the targeted six-dimensional tangent space $T_{\hat{x}0}M_1$. The steady and stable state of the converter is assigned as $\hat{x}_0\in M_1$. The vector of transformation $\tau=\left\{\left.\frac{\partial}{\partial t}\right|_{\hat{x}0},\left.\frac{\partial}{\partial \bar{i}_L}\right|_{\hat{x}0},\left.\frac{\partial}{\partial \bar{v}_C}\right|_{\hat{x}0},\left.\frac{\partial}{\partial E}\right|_{\hat{x}0},\left.\frac{\partial}{\partial R}\right|_{\hat{x}0},\left.\frac{\partial}{\partial d_u}\right|_{\hat{x}0}\right\}$ is a natural base of $T_{\hat{x}0}M_1$, and $T_{\hat{x}_0}M_1=\tau\circ M_1|_{\hat{x}_0}$ ($\circ$-composition). Throughout the tangent space $T_{\hat{x}0}M_1$ we pull an affine surface orthogonally on the first coordinate of $T_{\hat{x}0}M_1$ kernel. The thus-obtained surface S consists of the system steady states. The trajectories driven from the simulation process Q intersect the surface S at particular points $\hat{x}_{0,i}$ for $i=1,\ldots,n$, and n is the number of the final and time-filtered test samples. Because n is a limited number $n<\infty$, our surface S is not dense and it applies for an interpolation. Our transformed original space is now based on affine functions, and by the employment of the identification method; we construct the modelled surface with its minimal error to the representatives $\hat{x}_{0,i}$ of the physical surface.
The main task of the following work is the mathematical definition of a mapping $\psi(V_1{}^6):\mathbb{R}^{5-1}\rightarrow\mathbb{R}^{2-1}$and the construction of the explicit fuzzy model of the control signal d_u, which guarantees a true and predicted system steady state as a consequence of the vector of a measured and $\|.\|_2$values $\bar{x}=\left[\bar{v}_C\ \bar{i}_L\ \bar{i}_R\ E\right]^T$.

The objectively accepted results of the mapping identification could be reached only with the thoughtful selection of the measured process data. This task, by examination of the quantitative system dynamical behaviour, has to exclude always-possible preliminary conclusions that mostly lead to severe model/process errors. In order to support that approach, in this paper we involve the process excitation only with a random pattern. The vector of the process changes $\boldsymbol{\xi}(kT_\infty)=\left[E(kT_\infty)\ R(kT_\infty)\right]$ originated by the MATLAB white noise and random function together with the excitation duty cycle form the overall input vector $\boldsymbol{u}(kT_\infty)=\left[d_u(kT_\infty)\,|\,\boldsymbol{\xi}(kT_\infty)\right]$. Figure 3.4 expresses the simulation principle in which the discrete time kT_∞ is selected to preserve the steady-state measurement, afterwards resulting in the database and forming the identification training data set.

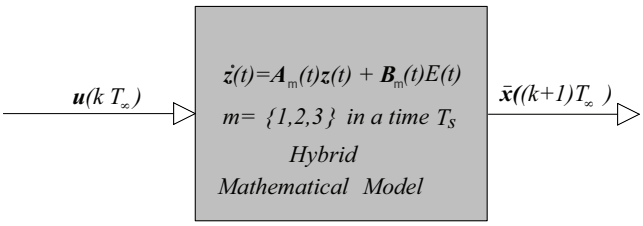

Fig. 3.4 Mathematical model simulation principle of construction the system-scanned database

Based on the heuristic assumption that there exists a deterministic and unique mapping in the pseudo Banach space $(V^6, \|.\|)$ we form the fuzzy identified model $\mathbf{F}(V_1^6): \mathbb{R}^{5-1} \rightarrow \mathbb{R}^{2-1}$ in which the steady state holds the expression for the duty cycle

$$d_u = \mathbf{F}(\hat{\mathbf{x}}) \quad . \tag{3.30}$$

The input vector to the fuzzy mapping will be $\hat{\boldsymbol{x}} = \left[\bar{v}_o \; \bar{i}_L \; E \; R\right]^T$, partly simplified from an $\bar{x}$ with the assumption that $v_c \approx v_o$ and the implementation of $R = \frac{\bar{v}_o}{\bar{i}_R}$, $\bar{i}_R > 0$. Generally, mapping is a function of the input vector $\hat{\boldsymbol{x}} = \boldsymbol{x}$ (in the following assigned as $\boldsymbol{x}$ for reasons of simplicity) defined by its parameters and hence

$$d_u = y = f(\boldsymbol{x} \mid \boldsymbol{\theta}). \tag{3.31}$$

In equation (3.31) the $\boldsymbol{\theta} = \{\boldsymbol{a}, \boldsymbol{c}\}$ denotes the set of fuzzy model parameters, and in our example

$$\boldsymbol{a} = \begin{bmatrix} a_{1,1} & a_{1,2} & a_{1,3} & a_{1,4} & a_{1,5} \\ a_{2,1} & a_{2,2} & a_{2,3} & a_{2,4} & a_{2,5} \\ \vdots & \vdots & \vdots & \vdots & \vdots \\ a_{b,1} & a_{b,2} & a_{b,3} & a_{b,4} & a_{b,5} \end{bmatrix} \quad . \tag{3.32}$$

$$\boldsymbol{c} = \begin{bmatrix} \boldsymbol{c}_1 & \boldsymbol{c}_2 & \cdots & \boldsymbol{c}_b \end{bmatrix}$$

The constant b is a number of rules in the fuzzy rule base.
For all systems [36] if there is a function

$$g: \; \tilde{X} \rightarrow \tilde{Y}$$

that $\tilde{X} \subset \mathbb{R}^l, \tilde{Y} \subset \mathbb{R}$ then with the process of identification we approximate the mapping g in the way that

$$g(\boldsymbol{x}) = f(\boldsymbol{x}|\boldsymbol{\theta}) + e(\boldsymbol{x}) \quad . \tag{3.33}$$

The approximation $f(\boldsymbol{x}|\boldsymbol{\theta})$ of a physical system was derived from examinations of the training data set

$$\boldsymbol{G} = \{(\boldsymbol{x}^1, d_u{}^1), \ldots, (\boldsymbol{x}^M, d_u{}^M)\} \subset \tilde{X} \times \tilde{Y}$$

constructed by M data pairs of the steady-state representatives, from a complete data set gained in the simulation Q and corresponding to (3.30).

In this study, the selected C-means clustering method will iteratively minimize the distance

$$J = \sum_{i=1}^{M}\sum_{j=1}^{b}(\mu_{ij})^{p}\left\|\boldsymbol{x}_i - \boldsymbol{c}_j\right\|^2 \tag{3.34}$$

from a bonding data representative centre vector $\boldsymbol{c_1},\boldsymbol{c_2}\ldots,\boldsymbol{c_b}$ in vector space $(V_1^{\,6},\|.\|)\subset(V^6,\|.\|)$, of our predefined universes of discourses. The process of clustering will be performed on M data pairs of $\boldsymbol{G}$.

The parameter p is the so-called "fuzziness factor" [36], which determines the factor of overlap in-between clusters and μ the grade of membership.
Accordingly in this study the selected fuzzy model is the Takagi-Sugeno MISO model, which consists of the rule base, presented with an equation

if H^j **then** $g_j(\boldsymbol{x})$

where H^j denotes the fuzzy set

$$\boldsymbol{H}^j = \{(\boldsymbol{x},\mu_{\boldsymbol{H}^j}(\boldsymbol{x})) : \boldsymbol{x}\in\tilde{\boldsymbol{X}}_1\times\ldots\times\tilde{\boldsymbol{X}}_n\}$$

and

$$g_j(\boldsymbol{x}) = a_{j,0} + a_{j,1}x_1 + \ldots + a_{j,4}x_4$$

for $j = 1,2,..b$.
The complete fuzzy function is given by

$$f(\boldsymbol{x}|\boldsymbol{\theta}) = \frac{\sum_{j=1}^{b}(a_{j,0} + a_{j,1}x_1 + \ldots + a_{j,4}x_4)\mu_{H^j}(\boldsymbol{x})}{\sum_{j=1}^{b}\mu_{H^j}(\boldsymbol{x})}\,. \tag{3.35}$$

As the clustering method does not tune the complete fuzzy parameters $\boldsymbol{\theta}$ but only $\boldsymbol{c}$, consequence function parameters $\boldsymbol{a}$ will be defined by the least-squares method

$$\boldsymbol{a}_j = (\boldsymbol{X}^T\boldsymbol{W}_j^{\boldsymbol{2}}\boldsymbol{X})^{-1}\boldsymbol{X}^T\boldsymbol{W}_j^{\boldsymbol{2}}\boldsymbol{Y}$$
$$\boldsymbol{X} = \begin{bmatrix} 1 & \cdots & 1 \\ \boldsymbol{x}_1 & \cdots & \boldsymbol{x}_M \end{bmatrix}^T \quad \boldsymbol{Y} = \left[d_{u,1},\cdots,d_{u,M}\right]^T \tag{3.36}$$
$$\boldsymbol{W^2}_j = (diag(\left[\mu_{1j},\cdots,\mu_{Mj}\right]))^2$$

and again, in order to minimize the cost function

$$J_j = \sum_{i=1}^{M}(\mu_{ij})^2\left(d_{u,i} - \left[1,\boldsymbol{x}_i^{\,T}\right]\boldsymbol{a}_j\right)^2 \tag{3.37}$$
$$j = 1,2,\ldots,b$$

Accordingly, all the identification processes can be briefly presented in the following algorithm steps:

1. *Simulation of the physical system (hybrid simulation model) excited with* $\boldsymbol{u} = [d_u \;\; \xi]$
2. *Forming of* M *data pairs of the training data set* $\boldsymbol{G}$
3. *Definition of* μ_{ij} *the new grades of membership* ($p = 2$) *by the C-means clustering*

$$\mu_{ij} = \left[\sum_{m=1}^{b} \frac{\left| \boldsymbol{x}_i - \boldsymbol{c}_j \right|^2}{\left| \boldsymbol{x}_i - \boldsymbol{c}_m \right|^2} \right]^{-1} \qquad i = 1,\ldots,M \tag{3.38}$$

$$j = 1,\ldots,b \quad \boldsymbol{c} = \left[\boldsymbol{c}_1, \boldsymbol{c}_2, \ldots, \boldsymbol{c}_b \right] \quad \textit{initialy selected}$$

4. *Definition of* $\boldsymbol{c}_j$ *the new centres by the C-means clustering*

$$\boldsymbol{c}_j = \frac{\sum_{i=1}^{M} \boldsymbol{x}_i \mu_{ij}{}^2}{\sum_{i=1}^{M} \mu_{ij}{}^2} \tag{3.39}$$

$$j = 1,\ldots,b$$

5. *Definition of* $\boldsymbol{a}_j$ *the consequence parameters by the weighted least-squares method*
6. *Defuzzification (3.35) by implementation of the grade function*

$$\mu_{H\,j}(\boldsymbol{x}) = \left[\sum_{m=1}^{b} \frac{\left| \boldsymbol{x} - \boldsymbol{c}_j \right|^2}{\left| \boldsymbol{x} - \boldsymbol{c}_m \right|^2} \right]^{-1}$$

$$j = 1,\ldots,b \quad \boldsymbol{c} = \left[\boldsymbol{c}_1, \boldsymbol{c}_2, \ldots, \boldsymbol{c}_b \right] \quad c - \textit{means tuned}$$

In our simulation example Figure 3.3, the constructed fuzzy model is the mapping, which transfers a converter's parameters from the input universes of discourse

$$\bar{v}_o = x_1 \in \tilde{\boldsymbol{X}}_1 = \left[0V, 700V \right]$$
$$\bar{i}_L = x_2 \in \tilde{\boldsymbol{X}}_2 = \left[0A, 1030A \right]$$
$$E = x_3 \in \tilde{\boldsymbol{X}}_3 = \left[10V, 16V \right] \qquad .$$
$$R = \frac{\bar{v}_o}{\bar{i}_R} = x_4 \in \tilde{\boldsymbol{X}}_4 = \left[10\Omega, 32\Omega \right]$$

to the output universe of discourse or simply a duty cycle

$$d_u = y \in \tilde{\boldsymbol{Y}} = \left[1{,}5\% \,, 98{,}5\% \right] = \left[0.65 \,, 0.01 \right].$$

The fuzzy rule base consists of $b = 33$ rules, and the fuzzy parameters $\boldsymbol{\theta} = \{\boldsymbol{a}, \boldsymbol{c}\}$ were reconstructed and based on the knowledge gained by $M = 635$ pairs of $\boldsymbol{G}$.

It can be now presented geometrically as an invariant foliation in the tangent subspace $T_{x0} M_1$. For an understandable graphical presentation, it is drawn in three-dimensional space formed by the original and appreciated dependence of a duty

cycle d_u from the coil current i_L and the output voltage v_o, while the remaining dimensions are fixed in the $\boldsymbol{x}_0$ points of their constrained universes. Figure 3.5 expresses the sliding effect in the three-dimensional space of the original nonlinear dynamical system in its equilibriums, influenced by a source voltage change. In a similar way, Figure 3.6 shows the sliding effect with a load change.

3.3.2 Fuzzy static model of a DC-DC boost converter evaluation

In order to evaluate the fuzzy modelling and achieved results, the evaluation test will be done in such a way that the physical system or the hybrid simulation model in Figure 2.18 will be excited with a ramping duty cycle, from 0% to 100%, varying as discrete input in the time nT_∞, while the source voltage and the load resistance are fixed. The received data, as the testing data set, will now be the input data to the explicit fuzzy model. The resulting outputs from the explicit model testing (3.35) will then be back-compared with the original excitation duty cycle of the physical model.
Approximation error from the explained test

$$e_n = d_{fuzzy,n} - d_n \tag{3.40}$$

for n^{th} the data equilibrium set is further evaluated by comparison with the analytical results from [7] and the results based on the average switched method.

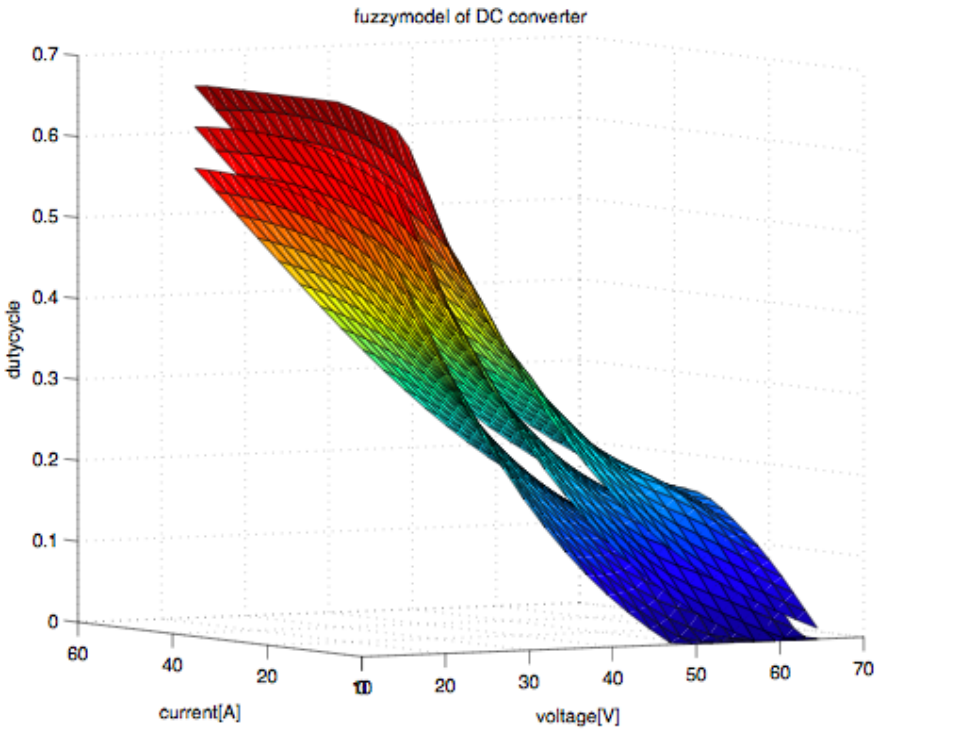

Fig. 3.5 Explicit Fuzzy Model invariant foliation for step changes of E=10, 13, 16 V (source voltage) and R=12.5 Ω

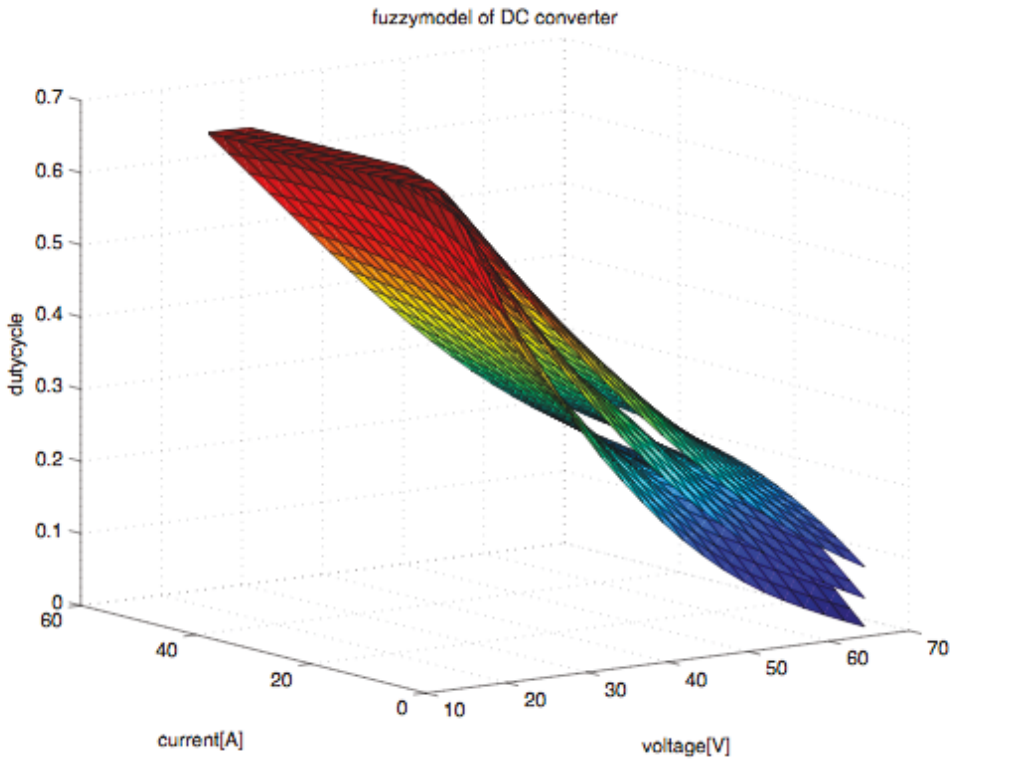

Fig. 3.6 Explicit Fuzzy Model invariant foliation for step changes of load R=12.5, 20, 30 Ω and E=16 V

Figure 3.7 is a graphical presentation of the fuzzy model testing results, compared with the real excitation duty cycle. The graph is drawn for one combination of the fixed load and the source voltage, which means that a similar test can be done for a different combination of the fixed process parameters.
For the same data in Figure 3.7, a comparison of the results has been made to the analytically calculated duty cycles on two different ways. One calculation is based on small signal values and the averaged model in Subsection 2.3.1, and the other is based on the stroboscopic Poincar map analytically derived in Subsection 2.3.5. Figure 3.8 shows all the evaluations together. We see that the stroboscopic Poincar map approximation

$$v_o(k+1) = \alpha^1 v_o(k) + \frac{\beta^1 d(k)^2 E^2}{v_o(k) - E} \qquad \alpha^1 = 1 - \frac{T_s}{C(R+r_C)} + \frac{T_s^2}{2C^2(R+r_C)^2}$$
$$\beta^1 = \frac{RT_s^2}{2LC(R+r_C)} \tag{3.41}$$
$$d_{Poin} = \sqrt{\frac{(1-\alpha^1)(s-E)s}{\beta^1 E^2}}$$

or the averaged system method approximation, developed for the DC-DC boost converter in this investigation

$$d_{lin} = \frac{(E - s)(R + r_c)}{sR} \tag{3.42}$$

are providing globally less accurate results in the steady-state duty-cycle prediction than the one resulting from the fuzzy model (3.30), (3.35). If we calculate the arithmetically averaged error in all three cases:

$$\bar{e}_{Poin} = 0.3592 \quad or \quad 53.61\%$$
$$\bar{e}_{lin} = 0.0149 \quad or \quad 2.22\%$$
$$\bar{e}_{fuzzy} = 0.0079 \quad or \quad 1.17\%.$$

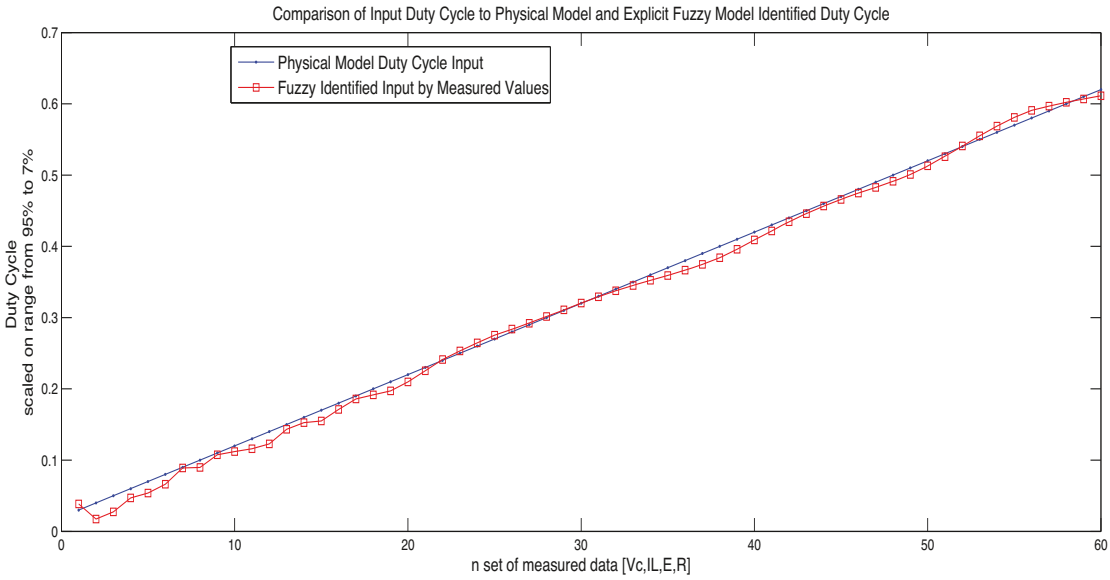

Fig. 3.7 Comparison of ramping duty cycle to Physical Model and reconstructed duty cycle by Explicit Fuzzy Model, while constant E=16V and R=12.5 Ω

Figure 3.8 explains a very inaccurate Poincar stroboscopic map approximation of the steady-state duty cycle for a complete range of duty cycles. However, if we transfer a comparison in the limited range of interest **[***16,50***]** the VDC of the reference voltage, or only the DCM converter's operation, then the results are more comparable. A stroboscopic map (2.92), (2.94) is derived for the converter DCM and it is expected to be non-applicable for a complete range of DC-DC converter operations. The methods driven in this work that are the same as the averaged model approximation are the global methods and comparable for a quantitative examination of the physical system. Thus, if we limit the range of interest to that mentioned, the following results are found:

$$\bar{e}_{Poin} = 0.0132 \quad or \quad 1.97\%$$
$$\bar{e}_{lin} = 0.0199 \quad or \quad 2.97\%$$
$$\bar{e}_{fuzzy} = 0.0065 \quad or \quad 0.97\%.$$

Now, the results of all the methods are comparable and still the fuzzy model is the best approximation of the steady-state duty cycle, and it will be used in a duty-cycle prediction of the control algorithm for the infinity time horizon.

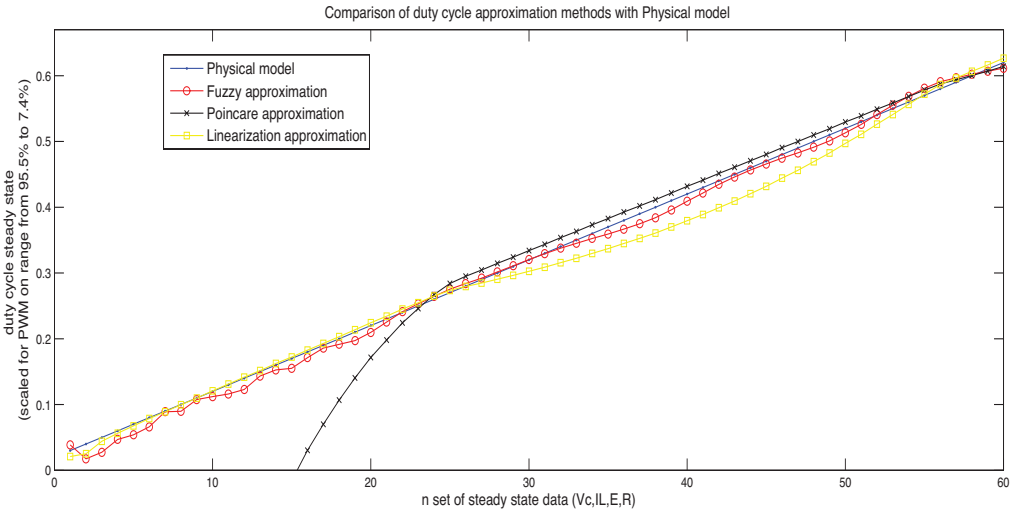

Fig. 3.8 Comparison of three methods of approximation with a physical model steady-state duty cycle while *constant E=16V and R=12.5* Ω

3.3.3 Fuzzy dynamic model of a DC-DC boost converter

Knowing the encouraging results from the previous subsection in the identification of the quantitative system's properties (the global space of the converters steady states), we will continue with the identification of quantitative and qualitative converter characteristics. It can be formulated as the identification of the dynamical converter's model in the global system's extents.

Most of the natural processes belong to the group of nonlinear dynamical systems. In order to design the proper control algorithms, a global knowledge of the system behaviour is of crucial importance. Differently than above, the following work is contained in the same reconstructed space, but it concentrates on the transition system's properties between the earlier reconstructed steady states.

DC-DC converters are a good example for which the nonlinear dynamical system inspires with complexity in the forming of global system knowledge or modelling. The following work presents the global process modelling known as NARX (Nonlinear AutoRegressive with eXogenous inputs). Generally, the nonlinear system

$$\begin{aligned} \boldsymbol{x}(k+1) &= f(\boldsymbol{x_k}, u_k) \\ y(k) &= g(\boldsymbol{x_k}, u_k) \end{aligned} \tag{3.43}$$

is a complex mapping over the vector of transformed states $\boldsymbol{x} \in \mathbb{R}^2$ and the input $u = d_u \in \mathbb{R}$ into the output $y \in \mathbb{R}$, which will be identified as a T-S fuzzy model

$$y_m(k+1) = \mathbf{F}(\boldsymbol{\varphi}_k) \quad . \tag{3.44}$$

The Takagi-Sugeno fuzzy model as a global model approximates the nonlinear model (3.44) as a mapping $\mathbf{F}$ of the unknown regression vector $\boldsymbol{\varphi}_k$ in a time kT_s to the step-ahead predicted output $y_m(k+1)$. All this is possible by assuming that f, g are mapping over smooth functions consisting of a vector of states $\boldsymbol{x} \in \mathbb{R}^2$ in a space $\mathbb{R}^l$.

Concerning our DC-DC converter as a process, the state variables are now RMS-transformed continuous functions (transformed space, Subsection 3.3.1) $\boldsymbol{x} \in \mathbb{L}^2 \subset \mathbb{R}^l$. The identification of (3.43) is a continuation of the research [30,31,32] based on a heuristic approach by implementing the fuzzy identification as a Universal Approximation [34,35]. Equation (3.44) is reconstructed throughout the two grades of the identification process and hence

$$y_m(k+1) = \boldsymbol{\beta}(\boldsymbol{\varphi}_2(k))\boldsymbol{\theta}_1\boldsymbol{\varphi}_1(k)^T. \tag{3.45}$$

Referring to all possible nonlinearities presented in Subsection 2.2.2, our example is analytically descriptive with the arbitrary high grade of accuracy (2.53), (2.66), (3.29) in its piecewise continuous and linear modes of operation. This physical knowledge of the specific example will group the identification process in the grey box identification [30]. This knowledge helps us in the selection of the regression vectors and those typically consist of measured values in a time $t \leq kT_S$.

By experimentally comparing several selections for regression vectors and minimizing the model/system error thus proposed, the vectors

$$\begin{aligned} \boldsymbol{\varphi}_1(k) &= [v_o(k) \;\; v_o(k-1) \;\; i_L(k) \;\; d_u(k) \;\; 1] \\ \boldsymbol{\varphi}_2(k) &= [E(k) \;\; v_o(k)/i_R(k) \quad i_L(k)] \quad for\ i_R(k) > 0 \end{aligned} \tag{3.46}$$

where the indices 1&2 correspond to different grades of identification. The $\boldsymbol{\theta}_1$ (3.45) denotes the parameter matrix of the first-grade identification resulting in a set of p linear models, evolved from the number of rules in the fuzzy rule base and equal to the number of OPs,

$$\boldsymbol{\theta}_1 = \begin{bmatrix} a_{1,1} & a_{1,2} & a_{1,3} & a_{1,4} & a_{1,5} \\ a_{2,1} & a_{2,2} & a_{2,3} & a_{2,4} & a_{2,5} \\ \vdots & \vdots & \vdots & \vdots & \vdots \\ a_{p,1} & a_{p,2} & a_{p,3} & a_{p,4} & a_{p,5} \end{bmatrix} = \begin{bmatrix} {}_1\boldsymbol{\theta}_{1,1} \\ {}_1\boldsymbol{\theta}_{2,1} \\ \vdots \\ {}_1\boldsymbol{\theta}_{p,1} \end{bmatrix} \tag{3.47}$$

and ${}_1\boldsymbol{\theta}_{11}$, for example, is the vector of the model coefficients of the first operating range identified ARX linear model. In spite of the ability to use an averaged mathematical model [3,58,59] in certain operating points of the DC-DC converter (Subsection 2.3.1), which would be derived by the perturbation method at that point, we propose a linear quadratic problem and a least-squares identification method around the selected point. This approach gives a predicted and better variance of the model error, especially by observing from applicability aspects on physical models.

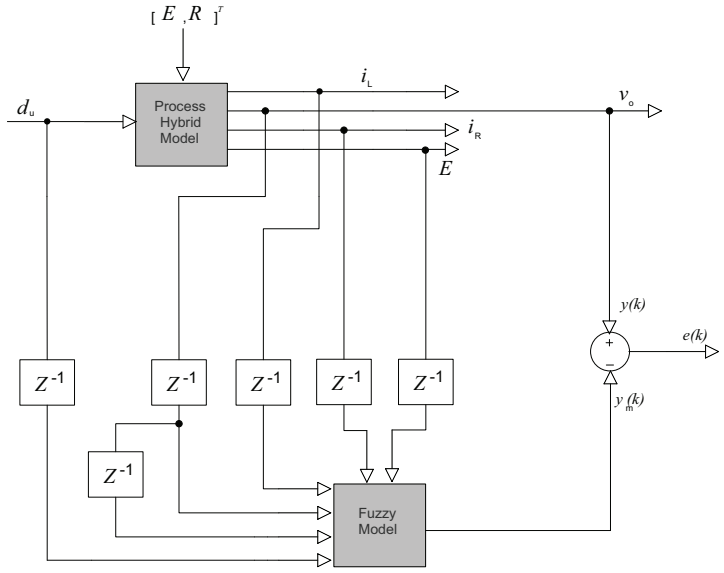

Fig. 3.9 Fuzzy Identification Model for DC-DC boost converter

Thus, linear models around the operating points will be identified by the least-squares method

$$ {}_1\boldsymbol{\theta}_{n,1} = (\Psi_n^T \Psi_n)^{-1} \Psi_n^T \mathrm{Y}_n \tag{3.48} $$

where $\Psi_n \in \mathbb{R}^{SX5}$ is a matrix of measured S training samples of the regression vector $\boldsymbol{\varphi}_1$ components for the operating point n and $\mathrm{Y}_n \in \mathbb{R}^S$ is for MISO processes the vector of the step-ahead responses. To gain the training data set (3.48) for a particular operating point (OP) the physical model is primarily tested in order to experimentally define the steady-state $d_{u,n}$ for the nth OP $(n \in [1,2,...,p])$. This gives us the centre duty cycle, which is expanded in the excitation function $d_{u,n}(t)$ for the nth OP region that has to be identified.

The vector of coefficients ${}_1\boldsymbol{\theta}_{n,1}$ are afterwards further tuned in the 2nd grade of identification and together with $\boldsymbol{\varphi}_1(k)$ express

$$ x_{T-S,n}(k+1) = {}_1\boldsymbol{\theta}_{n,1} \boldsymbol{\varphi}_1(k)^T \tag{3.49} $$

the n^{th} Takagi –Sugeno Fuzzy Model consequence function.

The second grade of the identification performed on the identification model in Figure 3.9 builds the nonlinear model structure NARX and mapping (3.44), which is also called the generalized output error model [31].

The fuzzy rules $\boldsymbol{\mathcal{R}}^i$ *for* $i = 1...p$ form the rule base of the identification model in Figure 3.9 and constructed for DC-DC boost converter in example of this work are the following

$$ \begin{aligned} &\boldsymbol{\mathcal{R}}^i : IF \quad E(k) \; is \; \boldsymbol{\mathcal{A}}_{1,j_1} \; AND \quad v_o(k)/i_R(k) \; is \; \boldsymbol{\mathcal{A}}_{2,j_2} \; AND \quad i_L(k) \; is \; \boldsymbol{\mathcal{A}}_{3,j_3} \\ &THEN \quad y_m(k+1) = a_{i,1} v_o(k) + a_{i,2} v_o(k-1) + a_{i,3} i_L(k) + a_{i,4} d(k) + a_{i,5} \\ &for \; i = 1,...,p \quad and \; unique \; set \; [j_1, j_2, j_3]^i \; if \; j_1, j_2, j_3 \in \{1,2,3\} \end{aligned} \tag{3.50} $$

where $\{\mathcal{A}_{1,1},\mathcal{A}_{1,2},\mathcal{A}_{1,3}\}\subset\mathcal{A}_1$ are the membership functions of the input universe of the discourse for the source input $E(k)$ and, similarly, $\mathcal{A}_2$ and $\mathcal{A}_3$ are universes of discourse for the load and the coil current, respectively, Figure 3.10-3.12.
The process of fuzzification is carried out based on Gaussian membership functions followed by the product to represent the conjunction in the premise and ending with the typical centre-average defuzzification. As a product of selected fuzzy construction the vector of normalized degrees of fulfilment in fuzzy mapping (3.45) is presented by

$$\boldsymbol{\beta}(\boldsymbol{\varphi}_2(k))=\frac{\left[\boldsymbol{\mu}_{\mathcal{A}_1}(\varphi_{2,1}(k))\otimes\boldsymbol{\mu}_{\mathcal{A}_2}(\varphi_{2,2}(k))\cdots\otimes\boldsymbol{\mu}_{\mathcal{A}_i}(\varphi_{2,i}(k))\right]}{\left\|\boldsymbol{\mu}_{\mathcal{A}_1}(\varphi_{2,1}(k))\otimes\boldsymbol{\mu}_{\mathcal{A}_2}(\varphi_{2,2}(k))\cdots\otimes\boldsymbol{\mu}_{\mathcal{A}_i}(\varphi_{2,i}(k))\right\|_1} \tag{3.51}$$

The vector $\boldsymbol{\beta}(k)\in\mathbb{R}^p$ has a length equal to the number of rules in the rule base of the fuzzy model and the symbol $\otimes$ is the Kronecker product. Furthermore, $\boldsymbol{\mu}_{\mathcal{A}_n}$ denotes in general the matrix of the degree of fulfilment. In our case, that is one row vector with a length equal to the number of membership functions for a particular fuzzy input variable. Those input variables consist of the supplementary regression vector $\boldsymbol{\varphi}_2$.
Closely, the 1st grade of identification sets the ${}_1\boldsymbol{\theta}_{n,1}$ (3.48) model parameters that will be initial parameters for the second grade of identification or fuzzy modelling. Except matrix $\boldsymbol{\theta}_1$ that consisted of ${}_1\boldsymbol{\theta}_{n,1}$ and gained by the least squares method, the T-S fuzzy model additionally consists of the membership function parameters, the centres and the standard deviation of the Gaussian functions. Altogether, we construct the $\boldsymbol{\theta}_2$ as a set of fuzzy model parameters and in our example thus

$$\begin{gathered}\boldsymbol{\theta}_2=\{\boldsymbol{\theta}_1,\boldsymbol{c},\boldsymbol{\sigma}\}\\ \boldsymbol{c}=\begin{bmatrix}c_{1,1}&c_{1,2}&c_{1,3}\\c_{2,1}&c_{2,2}&c_{2,3}\\c_{3,1}&c_{3,2}&c_{3,3}\end{bmatrix}\quad\boldsymbol{\sigma}=\begin{bmatrix}\sigma_{1,1}&\sigma_{1,2}&\sigma_{1,3}\\\sigma_{2,1}&\sigma_{2,2}&\sigma_{2,3}\\\sigma_{3,1}&\sigma_{3,2}&\sigma_{3,3}\end{bmatrix}\\ \boldsymbol{c},\boldsymbol{\sigma}\in\mathbb{R}^{ixj}\end{gathered} \tag{3.52}$$

where $\boldsymbol{c}$ and $\boldsymbol{\sigma}$ denote the matrixes of the membership function parameters, i is the size of the regression vector $\boldsymbol{\varphi}_2$, j is the maximum number of membership functions per fuzzy input and
$p=\dim(\boldsymbol{\mu}_{\mathcal{A}_1})\dim(\boldsymbol{\mu}_{\mathcal{A}_2})\dim(\boldsymbol{\mu}_{\mathcal{A}_3})=27$ equals the number of rules in the fuzzy rule base. Hence, in equation (3.51) $\boldsymbol{\beta}$ or the vector of the normalized degrees of fulfilment [30] can be expressed as $\boldsymbol{\beta}=f(\boldsymbol{\varphi}_2,\boldsymbol{c},\boldsymbol{\sigma})$, by knowing that the degrees of fulfilment $\boldsymbol{\mu}_{\mathcal{A}}$ are vectors of the functions and for a first linguistic variable hence

$$\boldsymbol{\mu}_{\mathcal{A}_1}=[\,e^{-\frac{1}{2}\left(\frac{\varphi 2,1-c1,1}{\sigma 1,1}\right)^2}\quad e^{-\frac{1}{2}\left(\frac{\varphi 2,1-c1,2}{\sigma 1,2}\right)^2}\quad e^{-\frac{1}{2}\left(\frac{\varphi 2,1-c1,3}{\sigma 1,3}\right)^2}\,].$$

The vector $\boldsymbol{\beta}$ as it is a vector of normalized values (3.51); thus, the $\sum_{i=1}^{p}\beta_{1,i}=1$ by taking into consideration that the Gaussian functions are fuzzy membership functions.

To optimize the selected T-S fuzzy model or to precisely define the parameters in the second grade of identification, the gradient tuning method was applied. By minimizing the cost function

$$J = \sum_{i=1}^{M} \frac{1}{2} (y_m(\boldsymbol{\varphi}_2, \boldsymbol{\varphi}_1 \mid \boldsymbol{\theta}_2)^i - y^i)^2 \tag{3.53}$$

over the training set of data $\{(\boldsymbol{\varphi}_2, \boldsymbol{\varphi}_1)^M, y^M\} \in \boldsymbol{\Gamma}$ the overall parameters of the fuzzy model $\boldsymbol{\theta}_2$ will be tuned [36]. The simulation process resulting in the definition of the training data set $\boldsymbol{\Gamma}$ can be performed after the selection of the excitation input functions of the duty cycle $d_{u,b}(t)$, the source voltage $E_b(t)$ and the resistance $R_b(t)$. First, the b =1 set of simulation input functions is used for the training of the final construction of the fuzzy model and other sets, mostly for the evaluation process.

3.3.4 Fuzzy dynamic model of a DC-DC boost converter, evaluation of the modelling based on simulation

The parameters defined in the first grade of identification $\boldsymbol{\theta}_1$ are not expected to differ to a large extent by performing the $\min_{\boldsymbol{\theta}_2}(J)$ convex optimization in the second grade of identification. To a much larger extent we expect differing of heuristically chosen initial values of $\boldsymbol{c}$ and $\boldsymbol{\sigma}$. Accordingly, and in order to accomplish the final fuzzy model by faster convergence, the step sizes related to the membership function parameters $(\boldsymbol{c}, \boldsymbol{\sigma})$ are bigger. Figures 3.10-3.12 present the tuned membership functions of the fuzzy model for the chosen example of a DC-DC boost converter.
In a nonlinear dynamical system identification, the minimum of the convex programming is just a rough approximation in some of the operating points. Our approach with two grades of identification, first least squares and second the gradient method of identification, gives special attention to the selection of the identification sets of the data in both grades. The validation test results can be seen in Figure 3.13-3.15.

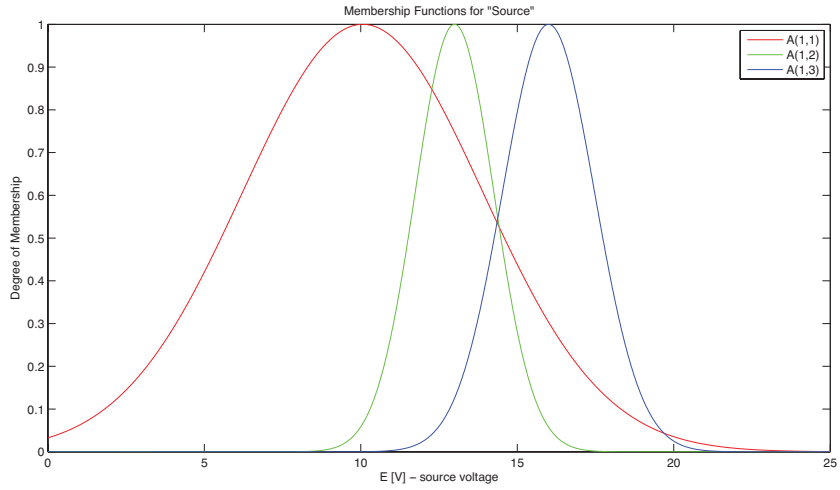

Fig. 3.10 Membership functions for linguistic variable "Source"

The final equation of the fixed FNARX model gained by the offline identification for the process of the DC-DC converter in this work is

$$\begin{aligned} y_m(k+1) &= a_{m1_k} v_o(k) + a_{m2_k} v_o(k-1) + a_{m3_k} i_L(k) \\ &\quad + a_{m4_k} d_u(k) + a_{m5_k} \\ y_m(k) &= y(k) - e(k) \quad e(k) - identification\ error \end{aligned} \tag{3.54}$$

where $\boldsymbol{a}_m(k) = [a_{m1}(k)\ a_{m2}(k)\ a_{m3}(k)\ a_{m4}(k)\ a_{m5}(k)]$ denotes the vector of the model time-dependent coefficients. Those are defined in each step of the control $\boldsymbol{a}_m(k) = \boldsymbol{\beta}(\boldsymbol{\varphi}_2(k))\boldsymbol{\theta}_1$ that takes care of the model adaptive tracking of the process' dynamical changes.

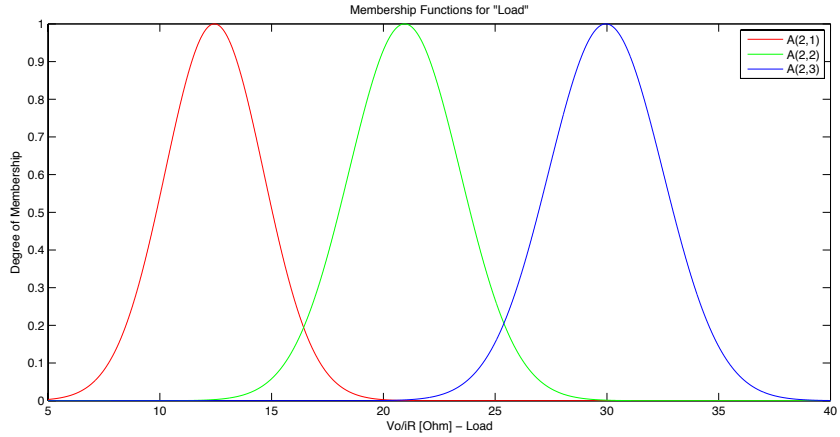

Fig. 3.11 Membership functions for linguistic variable "Load"

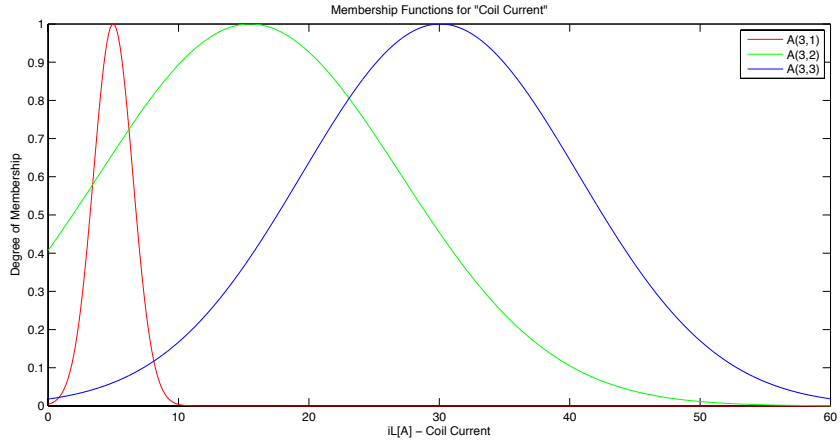

Fig. 3.12 Membership functions for linguistic variable "Coil Current"

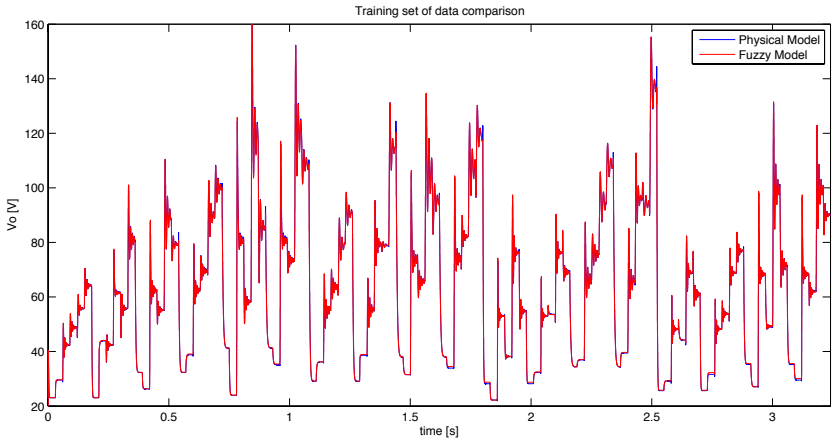

Fig. 3.13 Results of comparison simulation combining v_O and y_m for the training set of data $\boldsymbol{\Gamma}$

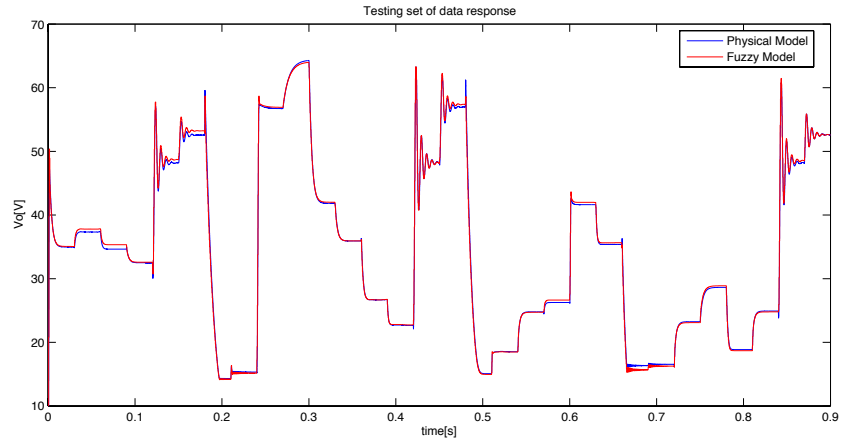

Fig. 3.14 Comparison simulation results combining v_O and y_m for the testing set of data. The input variable to the process and disturbances are selected to test the complete ranges of the fuzzy universes of discourses and for a 'load' even higher to simulate possible natural occasions.

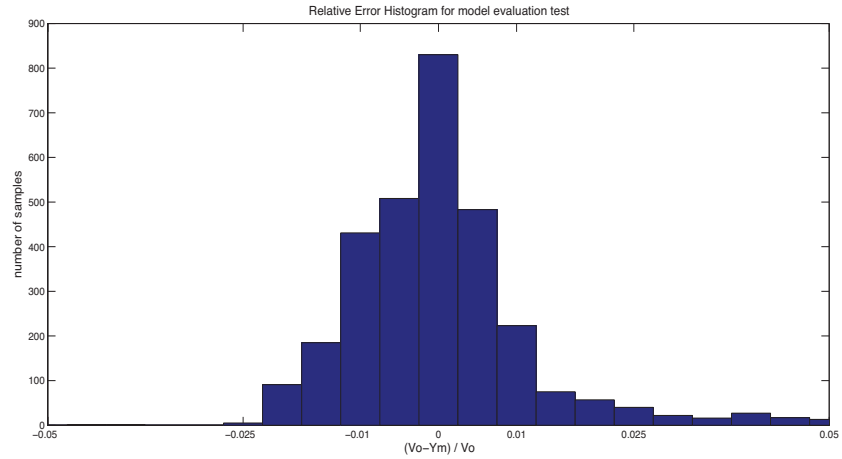

Fig. 3.15 Histogram of relative error $e(k)/y(k)$ (Fig. 3.9)

3.3.5 Fuzzy dynamic model of the experimental DC-DC boost converter, evaluation

Thus, fruitful results rendered by this examination of the simulation model led us in an experimental evolution of the identification-developed methods on the physical system, Figure 3.16. The selection of the electrical components in Table 3.1 (T_s =333 μs) is conducted to achieve a meaningful comparison with the simulation results.

The new and experimental identification training data set $\{(\varphi_2,\varphi_1)^M, y^M\} \in \mathbf{\Gamma}$ is constructed by using the same microcontroller and its storage place (Figure 3.16) in an open-loop regime. A process of convex programming in the minimization of the cost function $\min_{\theta_2}(J)$ is programmed and executed on a standard laptop. As expected, the identification results are less accurate than those based on an examination of the simulation model in Figure 3.17. Figure 3.18 presents the comparison of the measured testing data set and the "*1 step ahead prediction"* based on the experimentally identified fuzzy model. As the new methodology is seeking for a robust solution, so the process of identification is more appealing in the sense of test-bench preparation. The major part of the identification process of such a robust system is in the construction of the variable sources capable of sustaining substantial surges in the current and instabilities caused by that. This problem is certainly influencing the final model accuracy, but also fortifying the methodology and its applicability in realistic systems.

Element	Code or value
Inductor L	211 μH
Capacitor C	222 μF
Transistor	FDB2532
Diode	RURP3020
Current Shunt Monitor	INA193
True RMS IC	AD637
Microcontroller	TMS320F28069

Table 3.1 Constructive elements of the examined and controlled DC-DC boost converter Figure 3.16.

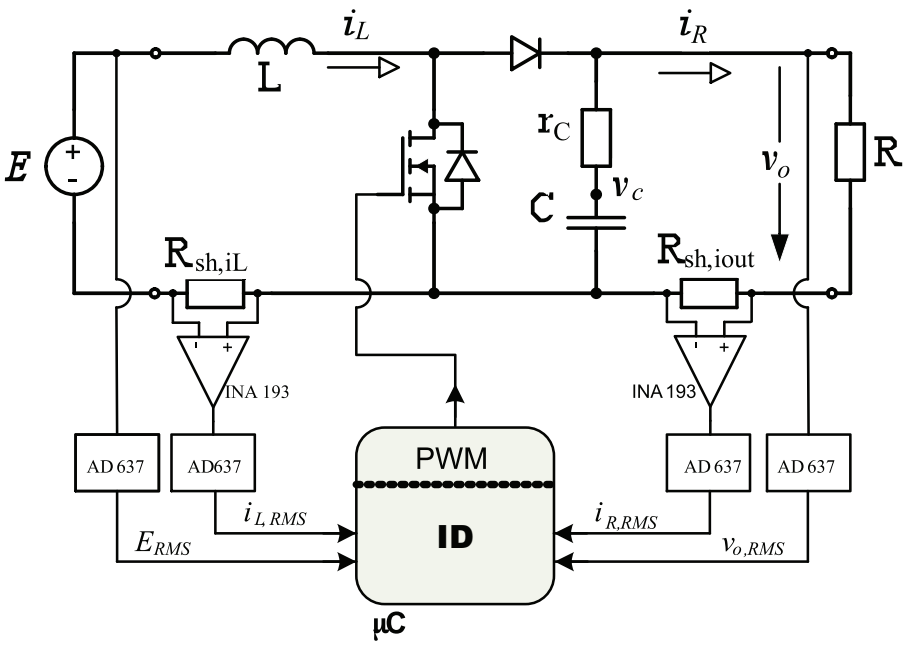

Fig. 3.16 Experimental process for performing of the new identification method

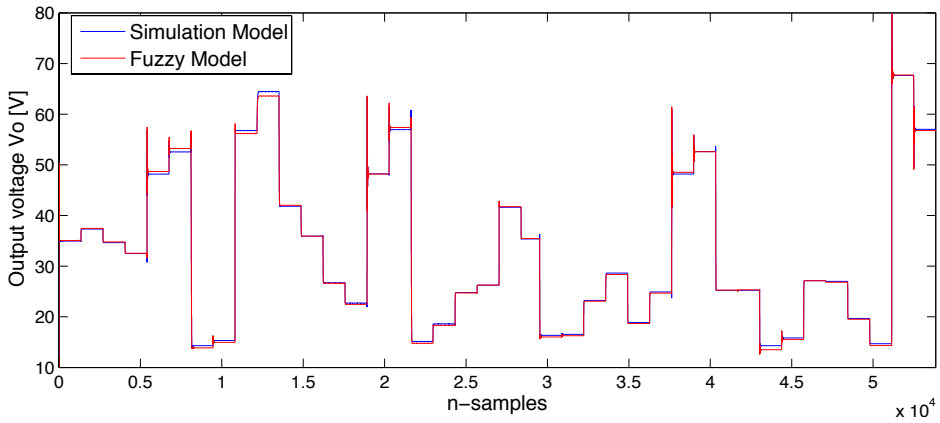

Fig. 3.17 Results of comparison simulation combining v_o and y_m (the identified simulation model) for the 53843 testing samples;
$SSE = 5.93 \cdot 10^3$ & $MSE = 0.1101$

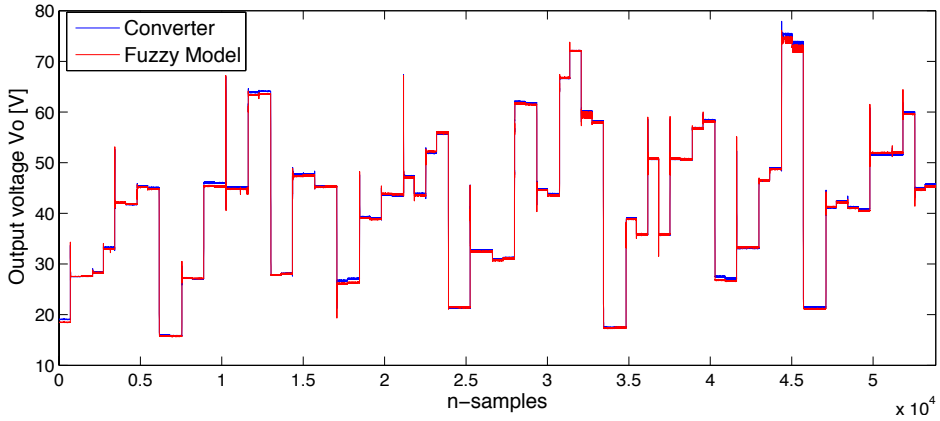

Fig. 3.18 Results of a comparison of the experimental prediction y_m (the identified converter) and v_o as the process output on the 53843 testing samples for the real physical system Figure 3.16 $SSE = 8.53 \cdot 10^3$ & $MSE = 0.1584$

3.3.6 Evaluation of the new dynamic modelling vs. the established methods

Except for the model evaluation carried out with a typical identification framework, it is not less important to point out the main innovation featured in the new method vs. the already well-established methods.

The presented "troublesome" identification is primarily bringing more precise modelling in processes with lower processing capabilities, where the sampling time is equal to the switching period T_S, and conciliating the control efficiency with its complexity. Most of the present methods are originally based on averaging (Subsection 2.3.1) and building the models on the typical involvement of an integer variable $\delta_i(k) \in \{0,1\}$ (Subsection 2.3.3) by assuming that the two-circuit topologies exchange happened instantaneously $t \equiv 0$, but in reality $t \leq \varepsilon$ for $\varepsilon > 0$. The topologies in that time are physically correlated, which brings necessary complexity in analytical examinations. For a discussion on this topic the reader is referred to [12,13,27] and Subsections 2.1.5 and 2.3.4.

Presenting the system via typical linear or bilinear state-space presentation is just a continuation of the well-known averaging method [37]. Accordingly, to make a meaningful comparison, three differently built models, i.e. the hybrid simulation model (3.29), the identified fuzzy nonlinear dynamical model (3.54) (in this work), and the analytically linearized averaged-switched model of the DC-DC boost converter (Subsection 2.3.1) are simulated and excited by the sinusoidal function around the OP. Based on the MATLAB [29] ID toolbox, the model responses' data gave the expected results. The drift effect related to the gain and the phase margin of the averaged-switched model is obvious on the sinusoidal excitation in the duty cycle range of $d_{u,OP}$ ±0.004, while the fuzzy identified model tracks the original hybrid simulation model with estimated preciseness, as shown in Figure 3.19. Furthermore, this comparison is carried out in CCM OP, where the standard analytical approaches [37] based on one integer variable (integer programming) have comparable precision. The superiority is more obvious in DCM, where the identified model still preserves the same accuracy, again with the assumption that

other methods are also based on the fixed switching period equal to the sampling time.

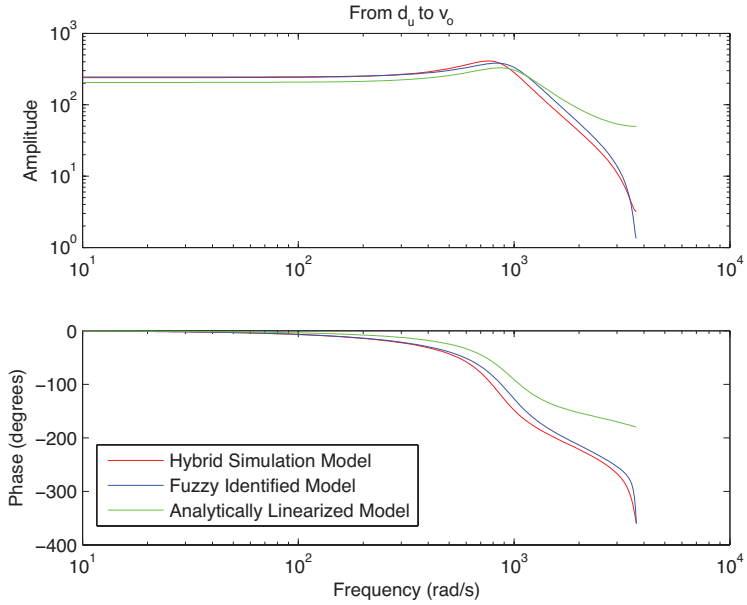

Fig. 3.19 Comparison of second-order identified linear models in narrow regions around the OP, identification vs. analytical averaging

Chapter IV

Control of SAS based on Fuzzy Modelling

All previous chapters are discussed in accordance with the final objective, an intelligent and the state-of-the-art controlling methodology capable to cope with the SAS as the nonlinear dynamical system. Herewith, in this study underlined the complexity of SAS is decomposed and emphasized to pursue the comprehensive solution, but yet wider applicability for the systems with the lowest processing capabilities. Certainly, the Model Predictive Control (MPC) brings the structurally standardize and comprehensive control, but in the majority of applications it is too complex and a cost-insensitive solution. Generally, it is rather appropriate for a larger, slower, and the multivariable systems. Subsequently, and with the mentioned decomposition, we are rendering the different approach in combination with the Fuzzy Logic, which has to fulfil all objectives of this thesis. It is designed and based on the heuristic approach, integrating the standard and widely known MPC as the methodology and not the unique control technique.

4.1 Model Predictive Control

During the 1970s, the first control methodologies revealing the milestones of modern Model Predictive Control (MPC) can be recognized. Significantly supported by developments in technology, including the environmental and profitable interests, it is recognized as a supervisory control methodology [19]. Pioneering in the *Predictive Control,* we can witness this control technology trend in the work of Richalet [119, 120] and Cutler and Ramaker [121]. Later, it is found in different references [122-126], all contributing to the same and the main stream of the model-based control systems, designed and reported for multivariable and robust systems. The comparative study expressed in [127], as a long horizon predictive control method, generally focuses the main method's objectives. Those are recognized in the system robustness, the solutions for unmodelled dynamics in the systems with parameter variations, the process noise and varying dead time. Additionally, the authors have made efforts in supporting the unified approach in distinguishing it from the well-known linear quadratic control [128]. The same work gives directions in applying the method to the nonlinear systems. Discussions about the method's prediction horizon, indicating the receding horizon principle as the method's core tool, appear in [129] and devises the constrained receding horizon predictive control. Therein is the optimization of the quadratic function over a costing horizon taken in order to achieve a final and the stabilized linear process. Furthermore, it suggests the finite–horizon methodology.
The basic principle of the methodology can be found in deriving the mathematical model of the process, formed to predict the future progress of the system states. Consequently, the typical representatives of the MPC methods are named regarding the constructed model. Thus, the generalized predictive control (GPC) emphasizes the polynomial-based models [130,131] and connects it naturally to the quadratic

performance index. Similarly, we can mention the Dynamic Matrix Control (DMC) [121], or also the Predictive Function Control (PFC) in the work of Richalet in [132]. During the history of these methods, it was not only the model that was assigning a specific method's name, but the chosen performance indexes also had the same role. In our work, we will concentrate more on the advancing of the MPC, the way to support the opinion that the MPC is not a single control technique, but rather a complex methodology [19]. This statement is a product of the long-term academic contribution towards the forming of the systematic and structural methodology, which copes with the most modern control objectives, but also preserves the basic principles of the control technique. Originally, as a Linear Systems Methodology, the method was also developed for the nonlinear systems, and continues to improve in that direction. Our contribution will be given to the control of Hybrid Dynamical Systems, in general, but focusing on the SAS. The popularity of the method must be seen throughout the main characteristics:

1. Mathematical model definition of the dynamical system
2. Prediction of the system's state progress regarding a defined model
3. Preceding horizon principle
4. Optimization of the control signal in accordance with the predefined performance index
5. Implementation of the trajectory that will be followed to achieve the final and stable, controlled value, mostly called the reference model
6. Simplified tuning and integrated natural feed-forward characteristic
7. A structurally designed handling of the system constraints in general.

Most of the recognized authors [18,19] will agree that the abovementioned characteristics of the MPC methods are sufficient in resolving the non-minimum phase systems, the systems with large time-delay and finally the unstable systems. Further on, it is an applicable methodology for advanced systems, as it allows a large number of constraints, which also includes the economic or financial aspects of the modelled system. As mentioned, the methodology is also applicable to the nonlinear systems. In the work of Tor A. Johansen [133] we can find the valuable survey on Nonlinear Model Predictive Control (NMPC) that is associated with the nonlinear modelling, the nonlinear moving horizon estimation and the nonlinear programming in order to achieve a complex optimum. Naturally, the MPC has drawbacks, despite its popularity in academia. Those are excessively more obvious in NMPC. The main drawbacks are:

1. Complexity and importance of the modelling of dynamical systems that requires a good physical insight into the problem
2. Complexity of the optimization algorithms, their variable and unpredictable time of execution
3. Even very successful in handling the unstable systems, widely applicable, the method has a complex theoretical analysis of stability and robustness.

The indicated drawbacks are the main aspects of criticism and emerging opinion that the MPC is an adequate methodology for the slow processes. Our objective of this work is to prove the opposite by rational decomposition of some pragmatic trends in the modelling and optimization of the control of dynamical systems. MPC

that is also applicable for the controls of the HS will be our realm of interest, but performed with the SAS. A great contribution following the equivalent direction can be found in the work of Bemporad and Morari, starting with [26]. The approach bridges the wide gap in-between the theoretical and practical application of the MPC methodology. Their work is later progressing towards the Explicit Model Predictive Control (EMPC), with the main idea of putting into focus a simplification of the online processing burden. Bearing in mind the method's systematic and structural solution for the linear systems, our approach will use that feature, but in the combination with the decomposition of the nonlinear dynamical modelling complexity and the reduction of the crucial method's processing time consumption. The latter is recognized in the optimization algorithms and the rank of the dynamical system. The survey of EMPC methods can be found in [6] and in the references therein. The method's new trend in achieving and developing the computer-based algorithms to overcome the main problem of complexity in the MPC is explicitly presented in their work, which is certainly related to the optimization algorithms traditionally executed online. The main distinction from the established methodologies is the intention to transfer the main processing burden to the offline regime. Therefore, the linear and quadratic programming of the multiple constraints on the state variables and input variables will now receive a new form in Mulitiparametric Linear Programming (MLP) or Multiparametric Quadratic programming (MQP). It is crucial that the offline numerical algorithms, in looking for a local minimum, are not endangering the software certification problem. Conversely, the explicit relation of system's IO promotes the pricewise linearity and smoothness in occasions where the nonlinear model is obtained. In these cases, the solution of the optimized control signal series is called the suboptimal solution.
Following the similar trend in EMPC, we have to note:

1. Optimization algorithms employed only offline
2. Model of dynamical system has to be explicit through the prediction horizon
3. Decomposition of the nonlinear dynamical system into the set of the local piecewise smooth systems.

Our new control methods are simply correlating with the above stated. In the previous chapters, it is shown that a good physical insight to the model should be in favour of reducing the method's complexity and not the opposite. Thus, we cannot completely agree that one of the drawbacks recognized in the literature [18,19] is the necessity of a good physical insight into the system. Oppositely, and in this thesis underlined, it should be a basic precondition in the rendering of a stable and intelligent control solution. Instead of considering the MPC as the overall applicable control technique encapsulated into the comprehensive package, we find and underline it as the methodology that proclaims the analytic and systematic approach to the complex systems. That is why its final form, defined as the control algorithm, should be the physical case-oriented product. This statement is emphasized in the previous chapters. Additionally, it is important to include a decomposition of the nonlinear control problem and the appliance of the MPC, of this thesis, that together reduce the online overall complexity and support the method's wider applicability to the faster processes.
In the example of this work, the modelling of a dynamical system in the alternative way might reduce the complexity, not only in the offline optimization, but also in the amount of the state variables, strictly related to the rank of the system. Another innovation is shown in the reduction of the number of characteristic pricewise

regions, which should not be considered the hybrid system modes (3.29), but more in the robust sense of the system's overall solution.

4.1.1 Two degrees of freedom methodology, the way to control law

Although the physical system has been identified and the global model derived, implementation into the final control algorithm will not follow the regular MPC framework. As already mentioned in the introduction, the main lead will be final control simplicity. In order to utilize a well-established PID control, which is sufficiently applicable in the narrow range around the predefined operating point, and at a same time by having known the global process pattern, we form a robust control structure presented by the block diagram of Figure 4.1. In Chapter III, the derived *Fuzzy Explicit Model* (FEM) will be enriched by integration block and expressed in the common transfer function

$$G_{FEM}(z) = F(\hat{\boldsymbol{x}}(k))\frac{T_S}{T_a(z-1)}.$$

Inputs assigned by $N_1(z), N_2(z)$ denote the noise signal supplemented to the manipulated variable and measured output respectively. The $\chi = \left[v_o, i_L, i_R, E\right]$ is a vector of measured process variables integrated into the control concept and providing the fuzzy model's tracking lead.

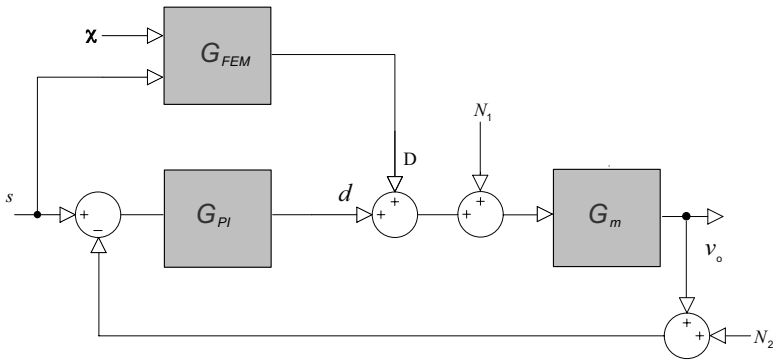

Fig. 4.1 Implementation of the Fuzzy Explicit Model in the typical two degrees of freedom control structure

By forming all the SISO possible closed loop transfer functions from the control structure on Figure 4.1, assuming that other inputs are 0 and $d\chi/dt = 0$, one can easily examine the existence of only two independent transfer functions. Hence, it defines our control structure as the Two Degrees of Freedom control [44].
This control methodology complies with our main goal of partitioning the standard MPC method and allowing independent adjustment of the system's response, linked up to the process constraints and steady state stability. Following the above methodology, the controller consists of the steady-state fuzzy-model in the feed-forward line and the optimized PI controller in the main controller's line.
The control law is formed from the two non-correlated (in a phase of designing) control signals

$$d_u(t) = \frac{1}{T_a}\int d_{FEM}(kT_S)dt + d_{PI}(t) \tag{4.1}$$

where

$$d_{FEM}(k) = \mathbf{F}(\hat{x}(k)) = \mathbf{F}(s(k), \hat{I}_L, E(k), \frac{\bar{v}_o(k)}{\bar{i}_R(k)}) \tag{4.2}$$

is the predictive part of the control algorithm based on the *Explicit Fuzzy Model* derived from the offline identification process in Chapter III (Subsection 3.3.1), and $d_{PI} = G_{PI}(s - v_o)$ is the output from the analog PI controller.
Conceptually similar to the *Explicit Model Predictive Controls* [6] in the sense of the offline identified model-based control, but advanced in minimization of the online computation complexity, this method opens up the ability to conciliate a better controller's performance with avoidance of the complex *Multiparametric Programming*. This method does not solve the standard predictive control problem, and it is not based on the receding horizon principle and thus, in correlation with standardized MPC methods, points out:

- *The prediction horizon is infinite, it goes for an open-loop stable system and the prediction is related to the system's steady state.*
- *The reference trajectory is implemented by an extra integration on the output of the explicit model. The time of integration is a tuning parameter and affects the controller's aggressiveness in the transient time.*
- *The internal model is the Fuzzy Explicit Model of the steady-state duty cycle and not the Fuzzy Dynamical Model, and accordingly it does not suffer a typical feedback problem.*
- *The steady-state error is compensated with a standard analog PI control tuned in the highest process gain regime and it is not treated by the predictive control itself.*
- *The feed-forward characteristic of the standard MPC method is explicitly fulfilled by the controller's configuration.*

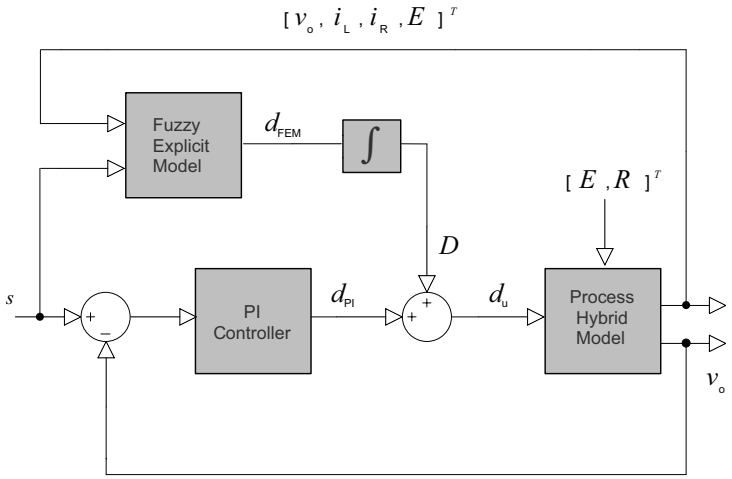

Fig. 4.2 Simulation model for the TDOF Control method based on Global and Explicit Fuzzy Model of the converter's steady-state duty cycle

For the simulation purpose of this work, shown in Figure 4.2, and without loss of generality, the optimized PI controller will be constructed based purely on the MATLAB tools for the SISO controllers [29]. The original boost DC-DC converter or process in this investigation is shown in Figure 2.12b and will be linearized by the well-known perturbation method around the operating point (Subsection 2.3.1), and accordingly as an "Averaged-Switch Model" [43] introduced in the control optimization of the PI controller.
The construction and tuning of the PI controller is done in the two standard steps of the "sisotool" MATLAB toolbox:

1. Construction of the PI controller by the auto-tuning method based on the singular frequency and minimizing the ITAE (Integral Time Absolute Error) performance
2. Optimization-based tuning by the Gradient Descent Algorithm for a Medium Scale.

The transfer function of the analog controller in its equivalent discrete form for a sample time $t_{sample} = 10^{-6}\ s$ is

$$G_{PI}(z) = 5.648 \cdot 10^{-4}\left(\frac{z - 1.000354}{z - 1}\right) \quad . \tag{4.3}$$

The offline optimization is done around the operating point

$$s = 50\,V, \quad E = 10\,V, \quad R = 12.5\,\Omega \tag{4.4}$$

which is selected closer to the top border of the process gain and the coil current range in order to achieve a stable operation even with a large difference in the process parameters.
Optimization is performed on the "averaged-switch model" linearized around the operating point and in its discrete form

$$G_m(z) = \frac{-0.090237z + 0.0904}{z^2 - 2z + 0.9996} \quad . \tag{4.5}$$

From equation (4.2), it is clear that the input in the fuzzy model is a vector of the measured values, except the one related to the predicted coil current in the steady state $\hat{I}_L$.
The steady-state coil current is calculated by involving the conserved energy law and the assumption that the load in the secondary circuit of the DC-DC converter will be changed only in a time that is incomparably wider than the scan time or $\Delta t >> T_S$. Also, the current efficiency factor has been taken as an average for a specific converter's operating range, already predefined with universes of discourses.

4.1.1.1 Simulation of the control algorithm

The simulation of the control algorithm involves a continuous disturbance, which in its final meaning has to result in the performance comparison of the TDOF method and the classic optimized PI control. The objectives in this control technique are primarily the robustness and minimization of the transient time. Thus, the process step parameter changes are commenced in combination, or all together for a wider operating range of the DC-DC converter. By altering the reference point s, the converter will be guided from the current discontinuous mode of operation to the continuous mode, where the highest process gain is expected at the top border of the coil current universe of discourse. The process parameters in the simulation are

$$T_S = 333.33\,\mu s,\ L = 208\,\mu H,\ C = 222\,\mu F\,.$$

The aggressiveness of the model control is tuned and results in

$$T_a = 0.004$$

by taking care of the current i_L constraint and the duty cycle d_u first derivation constraint.
Figure 4.3a shows the controlled process output responses for a certain controller on the step changes of the source voltage E, the load resistance R and the voltage set-point *s*. The optimized PI controller is tested in the two control structures: first, as pure PI control with the feed-forward line disconnected; second, as a PI control integrated into the complete TDOF control structure. In the same test, Figure 4.3b shows the controllers' manipulated variables. Furthermore, Figure 4.3c shows the manipulated variable of TDOF controller presented by its two constructive parts. That explicitly presents the main features of the TDOF control methodology.
The disturbance of the process parameters is synchronized with the set point change or separately to simulate a possibly realistic DC-DC converter's operating regime.
Generally, in this work, the developed TDOF controller features stable and robust operation. We see that the two-dynamic approach, also affirmed by the decomposition of the general controller parameters, fulfilled expectations and

presents the remarkable results relative to the complexity of the design and the online processing time. The stability of the control method relies on the stability of the PI controller and that is not a chain related to the delays in the transient time, which is now only related to the physical constraints. The only drawback is a naturally present model/process error and its effect on the steady-state error, manifesting as an overshoot, but now less harmful than the perspective cause of the nonlinearities in the standard MPC methods.
The offline optimized PI controller is comparable in the process higher gain range where the optimization was done. The constraints handling of the input signal in the PI optimized controller can be achieved as well as with MPC controllers by the selection of the highest gain operating point. In the TDOF controller, this feature is already integrated into the steady-state fuzzy model; therefore, a proper tuning of the PI parameters preserves it.

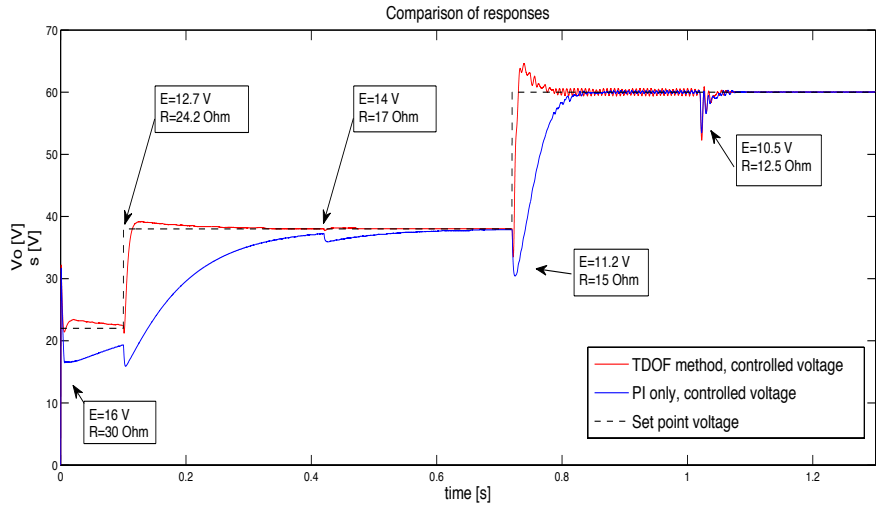

a) Controlled variable v_o compared in between optimized PI and TDOF controller including FEM

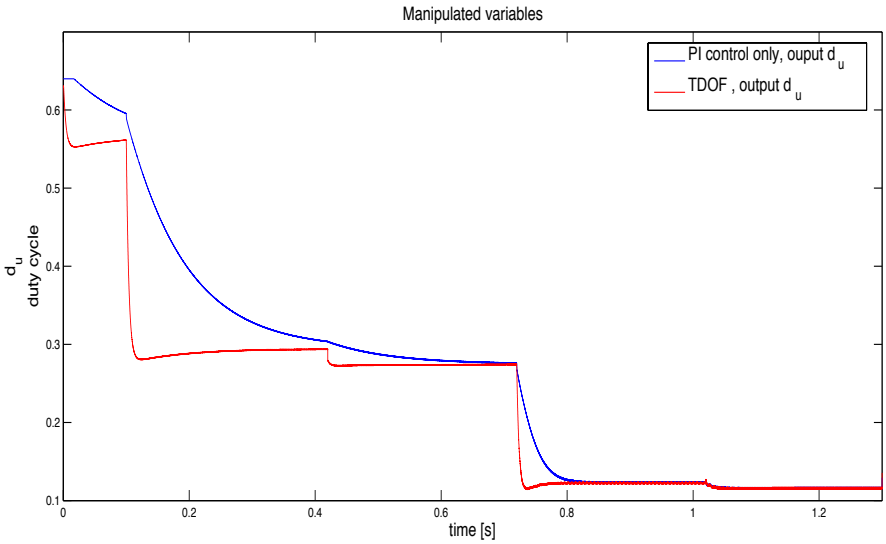

b) Manipulated variable d_u compared in between optimized PI and TDOF controller

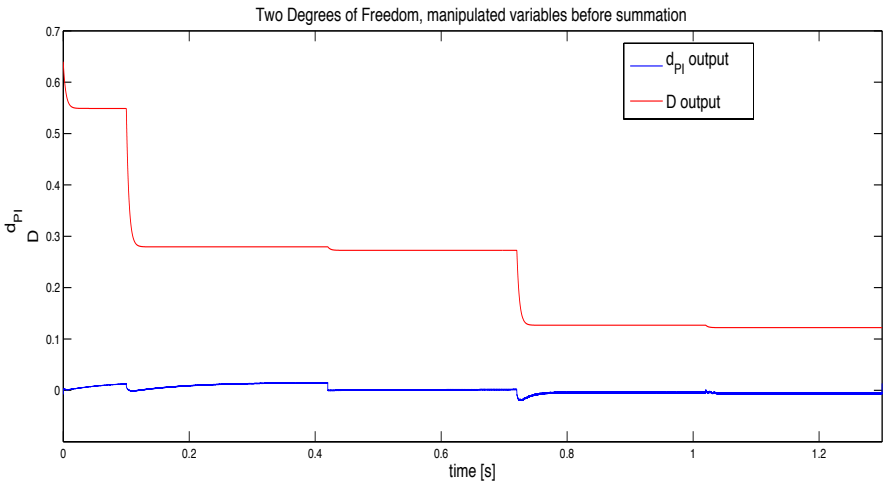

c) Manipulated variables of TDOF controller before the summation point in the control loop

Fig. 4.3 Simulation results: a, b and c.

4.1.1.2 Conclusion about the TDOF control

The above-presented control method is new in SAS, and in general could be considered as the model-based method. It involves the TDOF principle applied to an open-loop stable hybrid system that is state measurable. Instead of focusing on the transient process characteristics, the method points out the global process knowledge of the steady state. As shown, this knowledge is integrated into the explicit fuzzy model gained by the identification process from Chapter III, Subsection 3.3.1. Each processor's scan time, and controller predicts the steady-state duty cycle and by concerning the physical constraints adopts with the fastest transient time to the process parameters' change. The misfortune in the model/process approximation error is compensated by the small signal PI optimized controller, developed with the standard toolbox. The stability of the control system is related only to the stability of the feedback-related and standard PI controller by taking into consideration that the process parameters' change period is incomparable longer than the controller's scanning time.
Further examinations will be conducted at the direction of a qualitative/quantitative MPC solution.

4.1.2 Paradigm in the modelling of a DC-DC Boost Converter, synthesis to general control of SAS

Inspired by the qualitative problems of HSs in general and their established modelling principles, presented in Chapter II, the alternative modelling way should contribute to the better applicability of MPC, generally relying on the pragmatic and deterministic modelling principles. Our intention is to emphasize the importance of the physical knowledge of the particular process and the active reformulation of modelling principles from a side of the control applicability and physical knowledge. The modelling paradigm of a DC-DC boost converter, synthesized in the alternative

MPC approach, will be again highlighted briefly, followed by an application to the real process of SAS.

For the principal part of the electronic circuit in Figure 2.12b, apart from the pulse-width modulator (PWM) and the controller with its set point *s*, by using Kirchhoff's voltage and current laws, we can form the ordinary differential equations (ODEs) $\dot{z}(t) = f(z(t)) + g(z(t))u(t)$. By selecting the state vector $z(t) = \left[v_C(t)\ \ i_L(t)\right]^T$ and the input as an independent voltage source $E(t)$, the mathematical model can be driven with the assumption that semiconductors are ideal switches and that the inductivity has no equivalent series resistance (ESR) [7]

$$\dot{\boldsymbol{z}}(t) = \boldsymbol{A}_i \boldsymbol{z}(t) + \boldsymbol{B}_i E(t) \qquad i \in [1,2,3]\ \ i - circuit\ topology \qquad .$$
$$\boldsymbol{A}_1 = \frac{1}{C(R+r_c)}\begin{bmatrix} -1 & 0 \\ 0 & 0 \end{bmatrix}, \boldsymbol{B}_1 = \boldsymbol{B}_2 = \begin{bmatrix} 0 \\ \frac{1}{L} \end{bmatrix} \boldsymbol{B}_3 = \begin{bmatrix} 0 \\ 0 \end{bmatrix} \tag{4.7}$$
$$\boldsymbol{A}_2 = \frac{1}{C(R+r_c)}\begin{bmatrix} -1 & R \\ \frac{-CR}{L} & \frac{-CRr_C}{L} \end{bmatrix},\ \boldsymbol{A}_3 = \frac{1}{C(R+r_c)}\begin{bmatrix} -1 & 0 \\ 0 & 0 \end{bmatrix}.$$

The mathematical modelling of switched-mode electrical circuits faces problems of discontinuity and all the related side effects or nonlinearities [1].
Even if a simple switching algorithm is selected, the analytical definition of the duty cycle becomes a transcendental mathematical problem and it can only be solved by numerical methods. The reader is referred to the extensive literature [1,7-10], and references therein, that define the aforementioned problems.
Based on the authors' opinions and knowledge about this particular physical system, further well-established analytical modelling mostly develops in two different directions: first, already found in the earlier work of Middlebrook, Ćuk, and Erikson [23,24], modelling by *small signal models* or *large signal models,* more from the side of elementary circuit theory (Subsection 2.3.1); and second, also the one comprising the previously mentioned, but more analytically structured in the modern theory of modelling hybrid systems (Subsection 2.3.3). The latter is conceptually connected to the system's piecewise linearity (PWL), with the implementation of logical variables, constraints, or inequalities as the product of the natural form of the system. A distinctive presentation on the equivalence of classes of hybrid dynamical models is available in [25]. The methods that can be recognized as the most efficient and the general parameters that decide it are still unknown.
Therefore, if we agree that the aforementioned assumptions (4.7) are negligible, we can proceed with the subsequent steps of modelling into the *hybrid system* model (3.29)
Now, we simply recognize a *hybrid automaton,* Figure 2.13, with three discrete states defining different continuous dynamics. In the hybrid system modelling, those discrete states are connected to the mode of the system's operation. From equation (3.29) we find that the modes are defined by the converter's switching period T_S and the sub-intervals $t_{1,k} + t_{2,k} + t_{3,k} = T_S$. The converter is driven by the PWM and the duty cycle $d = t_{1,k} T_S^{-1}$. Thus, our system is representative of the Switched Affine Systems (SAS). From the aforementioned, with a known T_S, a definition of the sub-intervals relies on the duty cycle, which is defined as a function of the state variables $z(t)$. The

problem that has to be handled by the hybrid system's formalisms is the prediction of the time sub-intervals. That is critical in the prediction of $t_{3,k}$ naturally controlled by the diode's (Figure 2.12b) disconnection, which is a distinctive mode of the converter's functioning called DCM. The time of the transistor's on-state is $t_{1,k}$. In the following sequence $t_{2,k}$ is the time of the transistor's off-state, dependent on the natural diode's commutation that lasts $t_{3,k}$ before the next cycle T_S appears (Table 2.2). Nevertheless, from the aspects of the control techniques the input signal to our model has to be the duty cycle, and in (3.29) the PWL continuous systems are based on the source voltage as an input (Subsection 2.3.1). The well-established hybrid system formalisms take a DC-DC boost converter as an illustrative example [2], but it is far from that from our point of view (Subsections 2.2.1 & 2.2.2).

Our final goal is to render the modern and intelligent control methodology for a nonlinear dynamical system. Analysing the process and selecting its qualitative/quantitative properties based on the physical system's knowledge will achieve the main control objective once the mentioned knowledge is properly integrated to the control algorithm. More comprehensive and advanced control methodologies are based on a mathematical model of the process evolving to the model control solution. The compact and well-developed methodology is a MPC [18,19]. Our work is conducted in that direction. It is why the modelling discussion starting in Chapter II and evolved in Chapter III is of crucial importance.

The first concern emerging in the analysis of the modelling formalism (3.29) is that in our example of SAS the physical process is a combination of modes. The mode by itself has no physical background if it is not related to other modes that are in harmony with the physical meaning. If there is no exchange of hybrid modes, the electronic circuit does not function. To fulfil that, a controlled variable is a *periodic orbit* (Subsection 2.2.2), and it must be observed from the point of view of its periodicity.

Second, the nonlinearity of the system is not only its hybrid structure, but it is by assumption (4.7) also excluded from the nonlinear circuit elements together with the anomalies caused by the energy dissipation. Our process is PEC and the main physical meaning is the energy transfer.

Third, a modelling problem is a multidisciplinary task and from the control aspects it should be driven by the final goal, the controllability and the stability of the process [20], which includes an exclusion of the nonlinear phenomena (Subsection 2.2.2).

Yield, a decomposition of the nonlinear system problem to the PWL (3.29) is plausible, but it has to be done carefully in order to avoid any unnecessary complexity and increase the accuracy in realistic applications.

As a conclusion about the objectives, we are focused on a system with a fixed switching period T_S equal to the sampling time, where $t_{1,k}, t_{2,k}, t_{3,k} < T_S$ are the times related to a different circuit topology. From the side of the nonlinear dynamical system examinations, a general expression must evolve in the yet-unknown $\dot{z}(t) = f(z(t), d(t)) + g(z(t), d(t))d(t)$, for the duty cycle $d = t_{1,k} T_S^{-1}$ as a control signal for closed-loop control and scalar input signal in the process. The duty cycle and PWM is the genuine part of our process and must be modelled accordingly.

By the involvement of identification (Subsection 3.3.3) in the robust modelling of switched mode converters and the avoidance of strict assumptions, we propose refinements to the general modelling approach

$$\begin{aligned}
&\hat{\boldsymbol{z}}(k+1) = \begin{cases} \hat{\boldsymbol{A}}_1\hat{\boldsymbol{z}}(k) + \hat{\boldsymbol{B}}_1 u(k) & if\ \delta_1(k)=1 \\ \vdots & \\ \hat{\boldsymbol{A}}_{n_i}\hat{\boldsymbol{z}}(k) + \hat{\boldsymbol{B}}_{n_i} u(k) & if\ \delta_{n_i}(k)=1 \end{cases} \\
&\delta_i(k) \in \{0,1\} \quad \forall i = 1,...,n_i \\
&\bigoplus_{i=1}^{n_i} [\delta_i(k)=1] \quad n_i - number\ of\ integer\ variables \\
&\hat{\wp}_i \cap \hat{\wp}_j = \varnothing, \quad \forall i \neq j \quad \hat{\wp}_i - i^{th}\ polytop, \\
&[\delta_i(k)=1] \leftrightarrow \left[\begin{bmatrix}\hat{\boldsymbol{z}} \\ u\end{bmatrix} \in \hat{\wp}_i\right] \quad \bigcup_{i=1}^{n_i} \hat{\wp}_i = \hat{\wp}
\end{aligned} \tag{4.8}$$

which then evolves into general approximations of the nonlinear dynamical system using the equation

$$\hat{\boldsymbol{z}}(k+1) = \sum_{i=1}^{n_i} \left[\hat{\boldsymbol{A}}_i \boldsymbol{z}(k) + \hat{\boldsymbol{B}}_i u(k)\right] \delta_i(k). \tag{4.9}$$

The reader is referred to [26] and the references therein.

The modelling approach (4.8), (4.9) is generally derived from (4.7) and (3.29) and finalized by the MLD modelling (Subsection 2.3.3). To derive the final MLD expression for the DC-DC boost converter in Figure 2.12b, a naturally hybrid system (3.29) or *hybrid automaton* will be approximated by a *discrete hybrid automaton,* Figure 2.14. The new formalism has to be seen as a final discrete-time model, as shown in (4.8) and (4.9) in the general sense. As shown in Subsection 2.3.3 and in literature [2,3,5,6,17], the MLD modelling is explained by the HYSDEL framework. The recognition of the integer variables $\delta_i(k) \in \{0,1\}$, and accordingly the appropriate model for $i = 0,..n_i$, is based on the time that has to be shorter than the discrete time step, $kT_s < t < (k+1)T_s$. In the online processor's operation, this methodology assumes that the definition of $\delta_i(k)$ and the calculation of the $\hat{A}_i$, $\hat{B}_i$ matrices (4.9) (see (2.68-2.78)), that are the approximation of the system's operation in the contemporary linear region $\hat{\wp}_i \subset \hat{\wp}$, are possible during the time $t < T_s$. From the point of view of a fixed switching period T_S equal to the sampling time, the state-space matrices $\hat{A}_i$, $\hat{B}_i$ in (4.9) do not correspond to (4.7). That is not only because the matrices A_i, B_i (4.7) are of the continuous space, it is also that $\hat{A}_i$, $\hat{B}_i$ in (4.9) are assumed to be discrete time $t = kT_s$ sate-space matrices. Further on, those must be accordingly predicted for the system's evolution through the time $kT_s < t < (k+1)T_s$ based on the predecessor control variable $u(k) = d(k)$. For a DC-DC boost converter, it is a result of *propositional logic* equations built on the multiple logic variables that are defined from the A/D and D/A variables' transformations during each time step kT_s, (2.73-2.74) & (2.78). The general approach discussed elevates the original state-space model (4.7) by the involvement of the new discrete state variables, thus $\dim(\hat{z}) > \dim(z)$. Hence, it necessarily affects the complexity of

the state-space model and accordingly limits the applicability. Besides the underlined online complexity, the MLD model is valid for an assumption made in (4.7) added to ESR assumptions as a constructive part of the electronic circuit. Therefore, the modelling uncertainty that is characteristic for the example of this work is not completely grasped for natural processes.

This thesis is carried out differently to find accurate modelling, which also preserves the robust and general knowledge of the system. Furthermore, it results in a mathematical form that is subsequently applicable for the well-developed MPC. The method is based on a state measurable system, including the source and output current, and transfers the main burden of nonlinear dynamical system examination strictly to the offline problem with all its complexity. Hence, it can be simply considered as one of the EMPC methods [6].

The mathematical framework will not be exact and focused on the problem of *differential inclusion* and *complementarity formalism* [12,13,27], but rather on solutions in the pseudo-norm vector space (Subsection 3.3.1).

Theoretically, the idea is strongly supported in [28, Chapter 3], and elementarily connected to the approximate continuity and smoothing operation of the disjoint sets in the Lebesgue space.

If we now reconsider the averaging idea in Subsection 2.3.1 to derive the local model, but numerically emphasizing the mathematical expression of the electronic circuit equivalent for the time $t \geq T_s$, we are smoothing the disjoint model structure in $t < T_s$. This smoothing operation, with the assumed measuring ability of $E(t)$, $i_L(t)$, $v_o(t)$, and $i_R(t)$, will, unlike the known analytical averaging process, find an approximation on a wider range of system parameter variation around the operating points (OPs). At the same time, the derived local model is a part of a new pseudo-norm space $\wp$, and containing the discrete equivalents of approximately continuous functions $f_i(\boldsymbol{x_m(k)}) \subset \wp_i \subset \wp$. The edges of previous polytopes (4.8) are softened by fuzzy logic in Subsection 3.3.3 and new-formed regions smoothly passing from one to another, tracking the system parameters' fluctuations.

Equation (4.8) now obtains a form different from any of the aforementioned (Section 2.3) analytically driven approaches

$$\begin{aligned} &\boldsymbol{x_m}(k+1) = \sum_{i=1}^{p} [\boldsymbol{A}_{m_i} \boldsymbol{x}_m(k) + \boldsymbol{B}_{m_i} u(k) + \boldsymbol{R}_{m_i} w(k)] \beta_i(\boldsymbol{\varphi}_2(k)) \\ &\beta_i(\boldsymbol{\varphi}_2(k)) \in [0,1] \qquad \sum_{i=1}^{p} \beta_i(\boldsymbol{\varphi}_2(k)) = 1 \quad i = 1,\ldots,p \end{aligned} \tag{4.10}$$

where the matrices $\boldsymbol{A}_{m_i}$, $\boldsymbol{B}_{m_i}$ are the new numerically identified state-space matrices, $\boldsymbol{R}_{m_i}$ is the residual matrix and $\beta_i(\boldsymbol{\varphi}_2(k))$ (3.51) are the normalized degrees of fulfilment. The state-space matrices are explained in detail in the following section. Even though the p (3.47) is not an equivalent to the n_i (4.8), as it is about completely different linear regions, $p < n_i$ and reduces the online processing work load. In the equation (4.10) we can recognize the main difference with respect to a typical MLD approach based on (3.29) that is conceived in the normalized degree of fulfilment and new matrices. The former is a function of a regression vector $\boldsymbol{\varphi}_2(k)$, particularly common for an identification process and consisting of measured system variables in a time $t \leq kT_S$. In other words, the bivalent logic encoding of the uncertainties in

(3.29) and (4.8) (Section 3.2) is evolved by the polyvalent *fuzzy logic,* more convenient for a complexity of realistic examples. Apart from that, the matrices $\boldsymbol{A}_{m_i}$, $\boldsymbol{B}_{m_i}$ and $\boldsymbol{R}_{m_i}$ are rendered by the identification process, performed without the subjective assumptions and simplification of an electronic circuit. The new vector of state variables $\boldsymbol{x}_m(k)$ is not augmented (2.77), but maintains a dimension of 2 as in (4.7).

However, the theory of *discrete hybrid automata* and in general the analytical modelling (4.8) of the physical system from Figure 2.12b was conducted using MATLAB [29] continuous/discrete functions in a hybrid simulation model in Figure 2.3 and 3.3. Considering the processing power of a PC, and the advanced MATLAB tool with the possibility of *embedded functions*, the constructed model will provide an acceptably accurate approximation of the physical model and the basis for the development of the subsequent methodology.
At this point, we have seen in Chapter III that further examinations were based on the numerical methods in the simulation and control design of the predictive control algorithm, and in contrast to most of the known developed methods, they do not consist of PWL expressions (4.7) (see Section 2.3). By knowing that the major objective of the control in the example of this thesis is control of the output voltage, which is assumed to be a DC signal, the physical approach including the aforementioned leads us to the selection of the root-mean-square (RMS) measured values. That was the reason that in Section 3.3 the new state variables cause a mathematical transformation of the original state-space (4.7) to the pseudo-norm vector space. It is feasible and based on the assumption that a new state vector $\bar{z} = \left[\bar{v}_o\ ,\ \bar{i}_L\right] \in \mathbb{L}^2$ (Lebesgue), as a product of the numerical integration methods with an approximate solution in the system discontinuity. The transformation was made using MATLAB embedded functions applied to the simulation model, Figure 3.3. Accordingly, for a final experiment, we present a realistic counterpart of the numerical integration in the rendering of the Lebesgue 2 normed space. Figure 3.16 presents an integrated circuit (IC) AD637 that is built to provide continuous states of the transformed hybrid system state-space. Its role is to reduce the online processing workload, and to inherit the continuous system like the accuracy of the integration in the rendering of the RMS values. The RMS measurement of the original state-space variables and the measurement of $E(t)$ and $i_R(t)$ is carried out in the time period T_S, excited by PWM scaled duty cycle d_u.

4.2 Applied MPC methods' overview

The fuzzy identification of the DC-DC boost converter derived FIRM (Finite Impulse Response Model) is generally in the form (3.54) or also typically called input/output model [19], where the indices *k* denote a time-variable linear model.
By assuming a full-state measurement system, a novel approach in the research of the DC-DC boost converter is the fact that the current of a primary circuit $i_L(k)$ will be obtained by a further mathematical modelling assumed to be a part of the measured disturbance matrix $\boldsymbol{R}_{m_k}$ (4.10). The $\boldsymbol{R}_{m_k}$ also consists of the *residual component* a_{m5_k} of our identified model (3.54). The following control algorithms

based on a fuzzy internal model are derived for only one natural state variable that is simultaneously the output and controlled variable.
The MPC problem will be solved online in one scan of the processor time *k* for the model

$$\begin{aligned}\mathbf{x}_m(k+1) &= \boldsymbol{A}_{m_k}\mathbf{x}_m(k) + \boldsymbol{B}_{m_k}d_u(k) + \boldsymbol{R}_{m_k}\boldsymbol{w}(k)\\ y_m(k) &= \boldsymbol{C}_{m_k}\mathbf{x}_m(k) + \boldsymbol{D}_{m_k}y_m(k)\end{aligned} \tag{4.11}$$

, which will be an approximated linear model in the state-space form $y_{\boldsymbol{m}} = \boldsymbol{C}_{m_k}\boldsymbol{x}_m$. The state-space matrices at time $t = kT_s$ are

$$\begin{aligned}\boldsymbol{A}_{m_k} &= \begin{bmatrix} a_{m1_k} & a_{m2_k} \\ 1 & 0 \end{bmatrix} \quad \boldsymbol{B}_{m_k} = \begin{bmatrix} a_{m4_k} \\ 0 \end{bmatrix}\\ \boldsymbol{R}_{m_k} &= \begin{bmatrix} a_{m3_k} i_L(k) + a_{m5_k} \\ 0 \end{bmatrix} \qquad .\\ \boldsymbol{C}_{m_k} &= \begin{bmatrix} 1 & 0 \end{bmatrix} \qquad \boldsymbol{D}_{m_k} = 0\end{aligned} \tag{4.12}$$

and $v_o(k), d_u(k), \boldsymbol{w}(k) = \mathbb{1}$ denotes output voltage, duty cycle and unit step disturbance of a DC-DC converter, respectively.

This will be a basic representation of the internal model in the following *Finite Horizon* Fuzzy MPC (FMPC) algorithms applied in the simulation and experiment.

As the introduction of this chapter mentioned, the MPC methods are traditionally considered for the processes with slow dynamics. Their limitation can be recognized in the computing complexity, which is a multilayer problem. Despite being aware of this limitation, our work was driven by the final goal: implementing a MPC into the processes with faster dynamics. In the last 20 years, the MPC methodology has been developed to become the most dominant in process technology. It was given great attention by academia. That developing process has constructed a control framework as a result of long-term research in the field of control techniques. Therefore, it is a respective control solution for a broad number of different processes. Unfortunately, it is too pragmatic to expect that one control toolbox can grasp all possible natural processes and automatically devise the most efficient way of controlling them. We refer the reader to [6] and the references therein, where the authors present a survey of EMPC. That work certainly gives the diversities of the MPC complexity, in general.
Shown in Chapter III and continued here, the physical system's extents and constraints do not necessarily lead to the complexity of the applied control technique. In our work, we found the MPC method to be more a methodology than a single technique [19]. We have to underline its compact and standardized framework in looking for a stable control technique in the robust sense. The main drawback of the method is its complexity. As discussed in [6], the EMPC emerges as the solution to that problem. It suggests a transferring of the online processor's work to the offline regime. Our methodology is correlated to that idea. The

optimization algorithms or solvers are the biggest processing time consumer. Because of that fact we performed a different recognition of the problem for an example of this work. Our online processing related to the MPC method is reduced to the *unconstrained standard predictive control problem* [18,19]. It is driven to the complete exclusion of the optimization algorithms and it can be considered as the sub-optimal control. The MPC online optimization is derived by the basic linear algebra problem $\partial J(k)/\partial u(k) = 0$, in which $J(k)$ denotes the performance index and $u(k)$ an input variable. A DC-DC boost converter's input variable $u(k) = d_u(k)$ is constrained with the interval $[0, \max(d_u(k)) < 1)$. This critical constraint should not be a problem of the control algorithm, but rather a problem of the physical process, and it is tackled by the process itself. Although an unrealistic combination of the process parameters can lead to a violation of that constraint, the fuzzy identified model (3.54), (4.10-4.11), will even in that case saturate the control variable to the assigned margins. Furthermore, the state variables' constraints are grasped by the suppression factors λ of the MPC performance index $J(k)$, to decelerate a quick controller's response. In the case of the high peaks of the state variables, which are the characteristic events of the PEC, our controller will be disturbed proportionally to the energy level of the particular transient, Figure 3.16. This is obvious by recalling the external RMS measured values (AD637). The unexpected peaks are products of the process parameters' change and it is sufficiently treated by the method's *reference model* interpolation. The complex LMI is considered unnecessary, if the previous modelling work has achieved the most accurate linear approximation of the system at the specific operating point. In the absence of any processing time 'luxury', that assumption performs acceptably. The time of the processing is not only burdened by the optimization as a cumbersome solution, but also by the rank of the process model. Our suggested modelling solution preserves the original rank of the system, characteristically for the traditional state-space averaging. The global model identification strategy discussed, and based on the objective physical constraints renders the explicit control solution in the sense of the EMPC main goal. In contrast, the physical constraints are not simply assumed as being fixed. The online T-S fuzzy logic will select the consequence linear function that is a product of a measurement at the time kT_S, and treat a realistic violation of the assumed constraints. Using a case-oriented implementation of the MPC, we reduce the processing complexity, but do not endanger the objectivity and the accuracy. Reducing the problem of the nonlinear dynamical system to the PWL constrains the MPC on the short horizon prediction and control solution. So, a physical limitation should work in the sense of the MPC reduction complexity in combination with the aforementioned.

4.2.1 Fuzzy Dynamic Matrix Control

The first and the most basic MPC is the one strictly based on the Dynamic Matrix [18,32,38]. As our system is proven to be open-loop stable, the DMC can be performed over the *Finite Impulse Response Model* (FIRM) (3.54) by transformation in the *Finite Step Response Model* (FSRM), which is one of the main characteristics of the DMC algorithm. The control law must minimize the performance index.

The transformation of FIRM by the use of successive substitution progresses in

$$\boldsymbol{K}_{m_k}(i) = \boldsymbol{C}_{m_k}(\boldsymbol{A}_{m_k}{}^{i} - \boldsymbol{I})(\boldsymbol{A}_{m_k} - \boldsymbol{I})^{-1} \qquad i \in \left[N_m, N_u\right]$$

$$\begin{aligned} y_m(k+N_u) &= \boldsymbol{C}_{m_k}\boldsymbol{A}_{m_k}{}^{N_u}\boldsymbol{x}_m(k) + \\ &+ \boldsymbol{K}_{m_k}(N_u)\{\boldsymbol{R}_{m_k} + \boldsymbol{B}_{m_k}[u(k-1) + \sum_{i=1}^{N_u}\Delta u(k+N_u-i)]\} \end{aligned} \tag{4.13}$$

$$y_{mp}(k+N_u) = \boldsymbol{C}_{m_k}\boldsymbol{A}_{m_k}{}^{N_u}\boldsymbol{x}_m(k) + \boldsymbol{K}_{m_k}(N_u)[\boldsymbol{R}_{m_k} + \boldsymbol{B}_{m_k}u(k-1)] \tag{4.14}$$

$$y_{mf}(k+N_u) = \sum_{i=1}^{N_u}\boldsymbol{K}_{m_k}(N_u)\boldsymbol{B}_{m_k}\Delta u(k+N_u-i) \tag{4.15}$$

thus, explicitly presents the predicted model output in the maximum prediction interval N_u.

Equation (4.13) in accordance with DMC gives the FSRM consisting of two responses: one related to model free y_{mp} (4.14) and the other to the forced y_{mf} (4.15) response.

The strategy of MPC is receding-horizon control. That approach considers each step prediction of the complete sequence of the control signal in the assigned horizon, necessary to be applied to the process in order to follow the previously defined reference trajectory. Only the first predicted control signal will also be applied to the process. The reference trajectory $r(k+i) = s(k) - a_r{}^{i}[s(k) - y(k)]$ selected in our paper is a first-order model interpolated in-between the last measured output signal and the set point including the control aggressiveness parameter a_r. The control law must minimize the following performance index

$$J(k) = \sum_{i=1}^{N_u} q_i(y_m(k+i\,|\,k) - r(k+i\,|\,k))^2 + \sum_{i=0}^{N_u-1}\lambda_{i+1}(k)\Delta u(k+i\,|\,k)^2. \tag{4.16}$$

or in matrix equation

$$J(k) = \left\|\boldsymbol{G}(k)\Delta\boldsymbol{U}(k) - \boldsymbol{W}(k)\right\|^2_{\boldsymbol{Q}} + \left\|\Delta\boldsymbol{U}(k)\right\|^2_{\boldsymbol{R}(k)} \quad . \tag{4.17}$$

In equation (4.17) $\boldsymbol{G}$ denotes the dynamic matrix, $\boldsymbol{W}(k)$ vector of errors over the predicted horizon in-between the reference trajectory and free model response $\boldsymbol{y}_{mp}(k+i)$ in i coincidence points, and $\Delta\boldsymbol{U}(k)$ vector of control variable steps through the complete horizon N_u. $\boldsymbol{Q}$ and $\boldsymbol{R}(k)$ are the state and control weighting matrixes, respectively. Realization of the optimal control law leads further in the calculation of the performance index gradient $\nabla J(\Delta u,k)_{\Delta u}$ and in the final control-law equation

$$\Delta u(k) = \boldsymbol{\Lambda}(\boldsymbol{G}^T\boldsymbol{Q}\boldsymbol{G} + \boldsymbol{R})^{-1}\boldsymbol{G}^T\boldsymbol{Q}\boldsymbol{W} \ . \tag{4.18}$$

The dynamic matrix $\boldsymbol{G}$ derived for the process example in this work is

$$\boldsymbol{G} = \begin{bmatrix} \boldsymbol{C}_{m_k}\boldsymbol{B}_{m_k} & 0 & 0 & \cdots & 0 \\ \tilde{K}(2) & \boldsymbol{C}_{m_k}\boldsymbol{B}_{m_k} & 0 & 0 & \vdots \\ \tilde{K}(3) & \tilde{K}(2) & \boldsymbol{C}_{m_k}\boldsymbol{B}_{m_k} & \ddots & \\ \vdots & \ddots & \ddots & \ddots & \\ & & & & 0 \\ & & & \boldsymbol{C}_{m_k}\boldsymbol{B}_{m_k} & 0 \\ \tilde{K}(N_u) & \cdots & \tilde{K}(3) & \tilde{K}(2) & \boldsymbol{C}_{m_k}\boldsymbol{B}_{m_k} \end{bmatrix} \tag{4.19}$$

$$\tilde{K}(j) = \sum_{i=N_m}^{j} \boldsymbol{K}_{m_k}(i)\boldsymbol{B}_{m_k} \quad j \in \left[N_m, N_u\right]$$

The matrix $\boldsymbol{\Lambda}$ in general presents a selection of only the first in the sequence of control variables. Our example from the control aspects studies the SISO case and $\boldsymbol{\Lambda}$ will be a vector with the scalar 1 only in the first column and all others 0.

The DC-DC boost converter is a constrained process and represents the sub-optimal solution with a lack of complex quadratic programming (4.18). In this way, we achieve the expected and stable results of control with a smaller calculation. The only drawback is the involvement of the time-variable matrix $\boldsymbol{R}(k)$ in (4.16), or (4.17) consisting of the control variable suppression factor $\lambda(k)$.

4.2.2 Fuzzy Generalized Predictive Control

To be able to compare the achieved results with other MPC methods, we are going to use the Generalized Predictive Control (GPC) as the most standardized with respect of workability in the wide range of processes, even those that are open loop instable or non-minimum phase systems [136]. Our GPC algorithm will be expanded with the output filter presented in very early works of Clarke [137] and in nowadays publications [19]. As the example in this thesis is a highly nonlinear, but stable

system, and at the same time we are achieving robustness, the output auxiliary function is added in a sense to more strongly penalize the overshoots for the large variety of the set-point.
Similarly, as done in DMC, our solution will be based on FSRM, or the increment input-output model form, but now with a more generalized approach in the state-space. Including the proofs, it is very well presented in [19].
The model will firstly be transferred from (4.11) and (4.12) into the FSRM (4.20), by the new state-space matrixes that are developed from the substitution of the state-space variables, where d_i denotes disturbance, e_i noise and Δx_m one step difference of the previously posed state variables (4.11) (for details see [19]).

$$\begin{aligned}\mathbf{x}_i(k+1) &= \boldsymbol{A}_{i_k}\mathbf{x}_i(k) + \boldsymbol{B}_{i_k}\Delta\mathbf{u}(k) + \boldsymbol{K}_{i_k}\mathrm{e}_i(k) + \boldsymbol{L}_{i_k}\mathrm{d}_i(k)\\ \mathbf{y}_m(k) &= \boldsymbol{C}_{i_k}\mathbf{x}_i(k) + \boldsymbol{D}_H\mathrm{e}_i(k) + \boldsymbol{D}_F\mathrm{d}_i(k)\end{aligned} \tag{4.20}$$

We see that the disturbance is just differently modelled from (4.11), where $\mathbf{x}_i$ denotes a new state vector consisting of the increments Δx_m, by expression in bi-linear form

$$R_{m_k}\boldsymbol{w}(k) = \boldsymbol{K}_{i_k}\mathrm{e}_i(k) + \boldsymbol{L}_{i_k}\mathrm{d}_i(k) \tag{4.21}$$

in order to preserve the general approach. The matrices $\boldsymbol{A}_{i_k}, \boldsymbol{B}_{i_k}, \boldsymbol{K}_{i_k}, \boldsymbol{L}_{i_k}, \boldsymbol{C}_{i_k}, \boldsymbol{D}_H$ and $\boldsymbol{D}_F$ are of the suitable dimensions. In the sequel, the matrix $\boldsymbol{D}_F = 0$ for the GPC method as the output will be filtered.
As previously mentioned by the filter, the increment input-output model (4.20) will be expanded in a cascade form by the 2nd order system ($P(z) = 1 + p_1 z^{-1} + p_2 z^{-2}$) as $\boldsymbol{y}(k) = P(x_p(k), y_p(k))\boldsymbol{y}_m(k)$
, and for a state space matrixes of $P(x_p(k), y_p(k))$;

$$\boldsymbol{A}_p = \begin{bmatrix}0 & 1\\ 0 & 0\end{bmatrix} \quad \boldsymbol{B}_p = \begin{bmatrix}p_1\\ p_2\end{bmatrix} \quad \boldsymbol{C}_p = \begin{bmatrix}1 & 0\end{bmatrix} \quad \boldsymbol{D}_p = [1] \quad , \tag{4.22}$$

also called the weighting filter [137]. The standard predictive control problem that has to be derived for the GPC, will be applied to a new transformed model (4.20) [19]. The solution evolves in the lifted state-space model (4.23), which will be used bearing in mind a standardize expression for the involvement of the various performance indexes.
Any known type of the performance index can be applied to the standard expression in the state-space

$$\begin{aligned}\boldsymbol{x}(k+1) &= \boldsymbol{A}\boldsymbol{x}(k) + \boldsymbol{B}_1\mathrm{e}(k) + \boldsymbol{B}_2\psi(k) + \boldsymbol{B}_3\nu(k)\\ \boldsymbol{y}(k) &= \boldsymbol{C}_1\boldsymbol{x}(k) + \boldsymbol{D}_{11}\mathrm{e}(k) + \boldsymbol{D}_{22}\psi(k) + \boldsymbol{D}_{23}\nu(k)\\ \boldsymbol{x}_J(k) &= \boldsymbol{C}_2\boldsymbol{x}(k) + \boldsymbol{D}_{21}\mathrm{e}(k) + \boldsymbol{D}_{22}\psi(k) + \boldsymbol{D}_{23}\nu(k)\end{aligned} \tag{4.23}$$

where the new state-space variables $\boldsymbol{x}(k)$ denote the state vector, $\mathrm{e}(k)$ the noise signal, $\psi(k)$ the known external signals (the reference point or disturbance) and $\nu(k)$ the standardize input signal in the model. The latter could be either the input to FIRM $u(k)$ or the increment input to FSRM. In our case, it is $\Delta\boldsymbol{u}(k)$(4.20). Thus, the

new equation $\boldsymbol{x}_J(k)$ in the lifted state-space (4.24) already consists of the selected performance index. All the state-space matrixes $\boldsymbol{A}$, $\boldsymbol{B}_i$, $\boldsymbol{C}_i$ and $\boldsymbol{D}_i$ are of the appropriate dimensions.
We have selected the standardized GPC performance index

$$\boldsymbol{J}(k) = \sum_{j=1}^{N_u} \tilde{\boldsymbol{x}}_J{}^T(k+j\,|\,k)\boldsymbol{\Gamma}(j)\,\tilde{\boldsymbol{x}}_J(k+j\,|\,k) \quad . \tag{4.24}$$

The matrix $\boldsymbol{\Gamma}(j)$ is a diagonal selection matrix and, more generally, a part of the general selection matrix

$$\boldsymbol{E}(j) = \begin{bmatrix} \boldsymbol{\Gamma}_1(j) & 0 \\ 0 & \boldsymbol{I} \end{bmatrix} \quad \boldsymbol{\Gamma}_1(j) = \begin{cases} 0 & \forall \quad 0 \le j < N_m - 1 \\ 1 & \forall \quad N_m - 1 \le j < N_u - 1 \end{cases} \tag{4.25}$$

,

where N_m and N_u denote the minimum cost horizon and the prediction horizon respectively.
The expressions with the diacritical marks on top of variables are related to the prediction horizon. The y_p is a predicted output of the overall expended original model and $\boldsymbol{x}_J$ is the new vector in the state-space considering the control performance

$$\boldsymbol{x}_J(k) = \begin{bmatrix} \boldsymbol{x}_{J1}(k) \\ \boldsymbol{x}_{J2}(k) \end{bmatrix} = \begin{bmatrix} \boldsymbol{y}_p(k+1) - r(k+1) \\ \lambda \Delta u(k) \end{bmatrix} \quad . \tag{4.26}$$

The variable $r(k+1)$ denotes a reference trajectory point in the one-step-ahead predicted time.
For a standard predictive control problem, the state-space (4.23) is by successive method developed for a complete control horizon, and in our example to
$\tilde{\boldsymbol{x}}_J(k) = \tilde{\boldsymbol{C}}_2\boldsymbol{x}(k) + \tilde{\boldsymbol{D}}_{21}\mathrm{e}(k) + \tilde{\boldsymbol{D}}_{22}\psi(k) + \tilde{\boldsymbol{D}}_{23}\upsilon(k)$

$$\tilde{C}_2 = \begin{bmatrix} C_2 \\ C_2A \\ C_2A^2 \\ \vdots \\ C_2A^{N_u-1} \end{bmatrix} \quad \tilde{D}_{22} = \begin{bmatrix} D_{22} & 0 & \cdots & 0 & 0 \\ C_2B_2 & D_{22} & \ddots & \vdots & \vdots \\ C_2AB_2 & C_2B_2 & \ddots & 0 & 0 \\ \vdots & & \ddots & D_{22} & 0 \\ C_2A^{N_u-2}B_2 & & \cdots & C_2B_2 & D_{22} \end{bmatrix} \quad . \tag{4.27}$$

$$\tilde{D}_{21} = \begin{bmatrix} D_{21} \\ C_2B_1 \\ C_2AB_1 \\ \vdots \\ C_2A^{N_u-2}B_1 \end{bmatrix} \quad \tilde{D}_{23} = \begin{bmatrix} D_{23} & 0 & \cdots & 0 & 0 \\ C_2B_3 & D_{23} & \ddots & \vdots & \vdots \\ C_2AB_3 & C_2B_3 & \ddots & 0 & 0 \\ \vdots & & \ddots & D_{23} & 0 \\ C_2A^{N_u-2}B_3 & & \cdots & C_2B_3 & D_{23} \end{bmatrix}$$

With the thus-expanded state space model, we continue with the construction of the suboptimal control algorithm, and minimizing the performance index (4.24), (4.26). Thus, the control law that is expressed as follows

$$\upsilon(k) = \Delta \boldsymbol{u}(k) = -\boldsymbol{F}\boldsymbol{x}(k \mid k) + \boldsymbol{D}_e \mathrm{e}(k \mid k) + \boldsymbol{D}_w \psi(k \mid k)$$

$$\begin{aligned} F &= E(\tilde{D}_{23}{}^T \overline{\Gamma} \tilde{D}_{23})^{-1} \tilde{D}_{23}{}^T \overline{\Gamma} \tilde{C}_2 \\ D_e &= -E(\tilde{D}_{23}{}^T \overline{\Gamma} \tilde{D}_{23})^{-1} \tilde{D}_{23}{}^T \overline{\Gamma} \tilde{D}_{21} \\ D_w &= -E(\tilde{D}_{23}{}^T \overline{\Gamma} \tilde{D}_{23})^{-1} \tilde{D}_{23}{}^T \overline{\Gamma} \tilde{D}_{22} \\ E &= [I \ 0 \ \ldots \ 0] \\ \overline{\Gamma} &= diag\left[\Gamma(0), \Gamma(1), \ldots, \Gamma(N_u - 1)\right] \end{aligned} \quad . \qquad (4.28)$$

It is derived by assuming that the standard predictive control is a feasible problem or, generally, [19]:

1. The equality process constraints are a feasible problem
2. The matrix $(\tilde{D}_{23}{}^T \overline{\Gamma} \tilde{D}_{23})$ has a full row rank
3. The (A, B_3) (4.23) matrixes are stabilizable.

In the example of this thesis, the process is open-loop stable, and constraints will be treated by the suboptimal control manner.

4.2.3 Fuzzy Predictive Functional Control

The Predictive Functional Control (PFC) method originally developed by Richalet [39,40], and further in [41], has been chosen precisely because of its main distinction, when compared with the already explained DMC and GPC methods. Thus, the reduction of the algorithm calculation workload and the simultaneous achievements in the fast response processes make this method very suitable for the objectives given in the example of this work. The control law must minimize the performance index

$$J(\hat{\boldsymbol{u}}, k) = \sum_{j=1}^{n_H} \left(y_R(k + H_j \mid k) - y_m(k + H_j \mid k) \right)^2 + \sum_{j=1}^{n_H} \lambda_j{}^2(k) \hat{\boldsymbol{u}}(k + j - 1 \mid k)^T \hat{\boldsymbol{u}}(k + j - 1 \mid k). \qquad (4.29)$$

The nonlinear model that is going to be used in the construction of the control law is already expressed by (4.13) and by its forced (4.15) and free (4.14) response. The source equation in this type of MPC is

$$\begin{aligned} &\Delta p = y_R(k + N_u \mid k) - y(k) = \\ &= \Delta m = y_m(k + N_u \mid k) - y_m(k) \end{aligned} \quad , \qquad (4.30)$$

this means one process objective increment will be equalized with one increment of the predicted internal model output [31,33].

The second characteristic, which is very different from the previous MPC algorithm, is that the maximum predicted horizon and control horizon together with the coincident point are mostly equal $N_u = H$.
In our example and because the third main characteristic that the input signal is constructed of simple basis functions (step, ramp, parabola, etc.),

$$\hat{u}(k+i\,|\,k) = u_0(k) + u_1(k)i + u_2(k)i^2 + \ldots + u_n(k)i^n \tag{4.31}$$

the second characteristic has to be softened to a minimum of the coincidence points, which corresponds to a number of basis functions in order to agree with the problem feasibility.
We are choosing the most common reference trajectory in PFC and for the prediction horizon N_u

$$y_R(k+N_u) = a_r^{N_u} y_R(k) + (1 - a_r^{N_u}) s(k)\,, \tag{4.32}$$

where a_r denotes the main parameter of the control aggressiveness in the PFC and $s(k)$ is the set-point function.
Therefore, as the selections of the basis functions are tightly connected to the process characteristics the following equation will be the input variable to the PFC

$$\Delta\hat{u}(k+i\,|\,k) = u_0(k) + u_2(k)i^2 \qquad . \tag{4.33}$$

Now the set of prediction equations in the PFC algorithm and according to (4.13), (4.14), (4.15) & (4.33) result in

$$\begin{bmatrix} y_R(k+H_1) \\ y_R(k+H_2) \end{bmatrix} = \begin{bmatrix} y_{mp}(k+H_1) \\ y_{mp}(k+H_2) \end{bmatrix} + \begin{bmatrix} \tilde{K}(H_1) & \tilde{K}(H_1)\sum_{i=1}^{H_1} i^2 \\ \tilde{K}(H_2) & \tilde{K}(H_2)\sum_{i=1}^{H_2} i^2 \end{bmatrix} \cdot \begin{bmatrix} u_0 \\ u_2 \end{bmatrix} \qquad . \tag{4.34}$$

or

$$\boldsymbol{\Omega} = \boldsymbol{\Xi} + \boldsymbol{V}\hat{\mathbf{u}}$$

By minimizing the performance index

$$J(\hat{\boldsymbol{u}},k) = \sum_{j=1}^{n_H}\left(y_R(k+H_j\,|\,k) - y_m(k+H_j\,|\,k)\right)^2 + \\ + \sum_{j=1}^{n_H} \lambda_j{}^2(k)\hat{\boldsymbol{u}}(k+j-1\,|\,k)^T\,\hat{\boldsymbol{u}}(k+j-1\,|\,k) \tag{4.35}$$

suboptimal control, thus

$$\Delta u(k) = \boldsymbol{\Lambda}(\boldsymbol{V}^T\boldsymbol{V} + \lambda^2\boldsymbol{I})^{-1}\boldsymbol{V}^T(\boldsymbol{\Omega} - \boldsymbol{\Xi}) \qquad . \tag{4.36}$$

In equation (4.35), n_H denotes the number of coincidence points and λ the control-variable suppression factor.

The next applied input signal from (4.36) is only $u_0(k)$.

Suppression factor λ

All selected finite-horizon MPC methods and their *objective functions* or *performance indexes* consist of the suppression factor λ applied to the manipulated variable. Furthermore, it is time dependent and updated for each scan time by the controller's algorithm.
The update or $\lambda(k)$ is derived from the simple proportional dependence of the predicted process gain in the time $(k+1)T_s$ and hence

$$\lambda(k) = a_{SUPP} \cdot \frac{y_m(k+1)}{u(k)} \quad . \tag{4.37}$$

The involvement of the suppression factor in the MPC methods is mostly used to achieve smoother control [38,40].

4.3 Simulation and experimental results of applied methods to the DC-DC boost converter

In a manner similar to that in Subsection 4.1.1, and related to the newly developed control that was applied to the simulation model in Figure 4.2, FMPC methods gathered in Subsections 4.2.1-4.2.3 will be applied to the simulation model in Figure 4.4. The identified fuzzy model (3.54) is assigned as the FNARX model in Figure 4.4. Its transformation into the state space model (4.7) is used as the internal model of the particular FMPC method and assigned as the MPC Controller block in Figure 4.4. Thus, the developed control methodology will be applied to the simulation model of a DC-DC boost converter (Process Hybrid Model), and tested with the same testing pattern as done in Figure 4.3. That is to be able to render the meaningful comparison. In the sequel, the result of the simulation process for the FPFC, FGPC, FDMC, the optimized PI and the TDOF method is presented in Figures 4.5-4.9 respectively. Exceptionally and to contribute to an easier comparison, the Figure 4.3 is split into Figures 4.8 and 4.9.

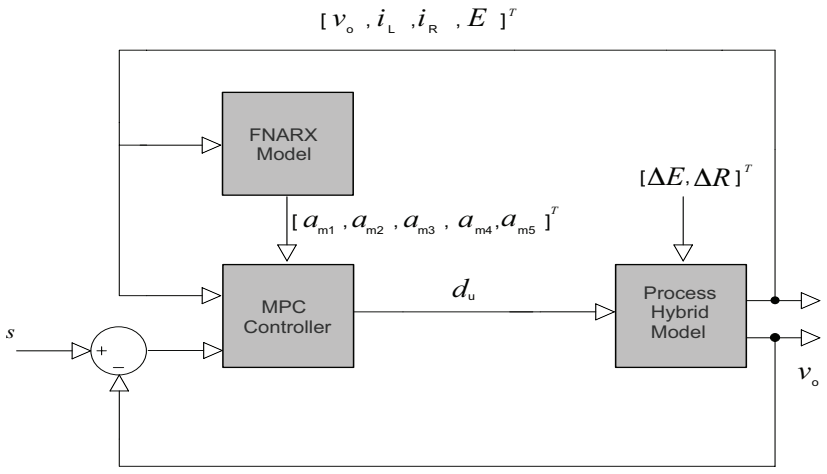

Fig. 4.4 Simulation model for FMPC-applied methods

From the results, we can see the similarities related to the aggressiveness in transitions and the accuracy in the steady state of the applied FMPC methods. The best performance is experienced with the FPFC in Figure 4.5, and other methods can be compared to that reference. Closer to the performance of the FPFC, we found the FDMC. The FGPC has been found to be just a bit coarser in the steady state, but in some occasions faster in the response. As expected, the optimized PI controller is slower in transitions, especially for the operating point where the optimizations are not performed. That is for the time periods while the lower system gains have been experienced.

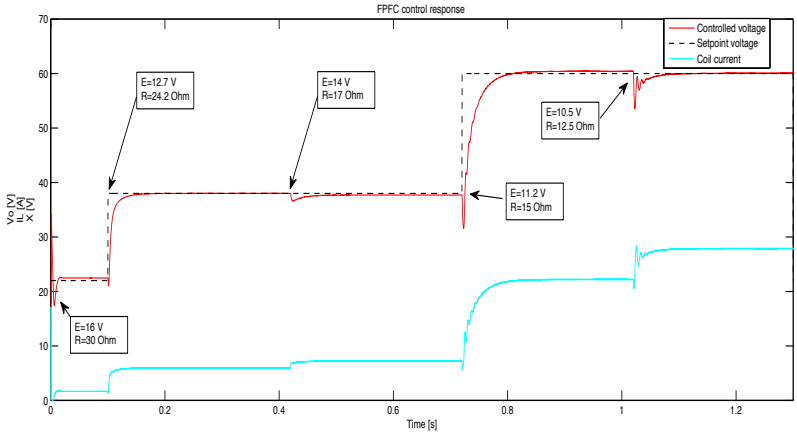

a) Controlled variable by the FPFC controller v_o and coil current i_L

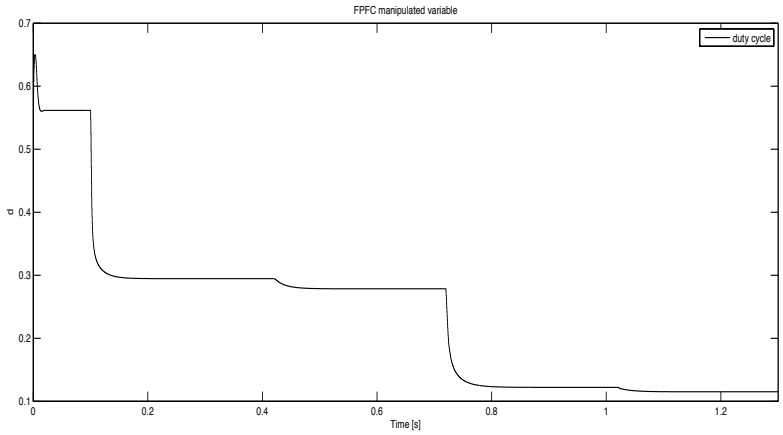

b) Manipulated variable from the FPFC controller (duty cycle)
$d_u = [0.01, 0.66]$ *range* $98.5 \div 1.5\%$

Fig. 4.5 Simulation results: a and b.

Differently than the aforementioned, the TDOF methodology performs as the fastest in transitions, but while in transitions the control algorithm cannot attenuate the gradient of change and, in some occasions, violates the reference point. This scenario is initiated by the error of the identified steady state, which is filtered out by the preceding horizon strategy in other FMPCs. On the other side, the TDOF algorithm will certainly demand significantly less the processor time of execution.

From that point of view, the optimized PI controller will use the shortest time of execution, but it is not the robust solution and, in some occasions, cannot reach the reference value before another is selected, Figure 4.8.

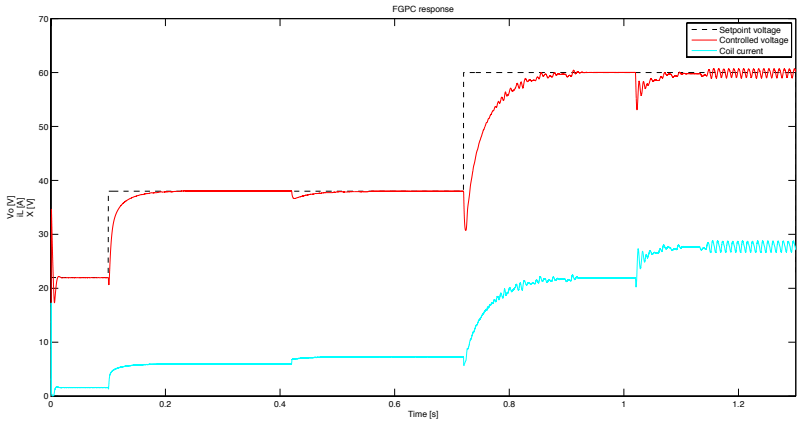

a) Controlled variable by the FGPC controller v_o and coil current i_L

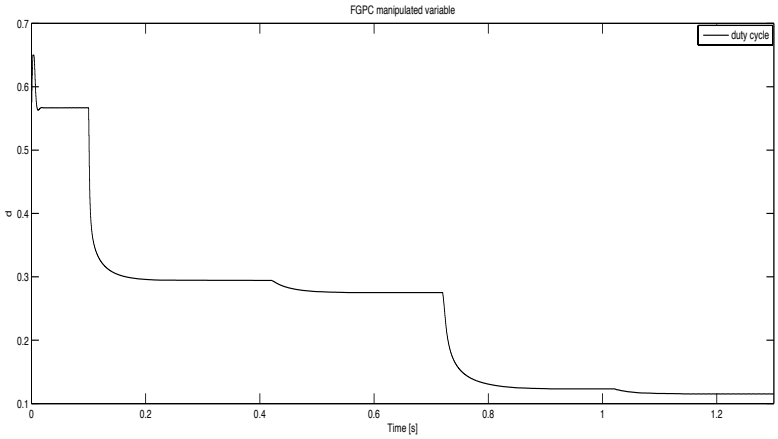

b) Manipulated variable from the FGPC controller (duty cycle)

$$d_u = [0.01, 0.66] \quad range \quad 98.5 \div 1.5\%$$

Fig. 4.6 Simulation results: a and b.

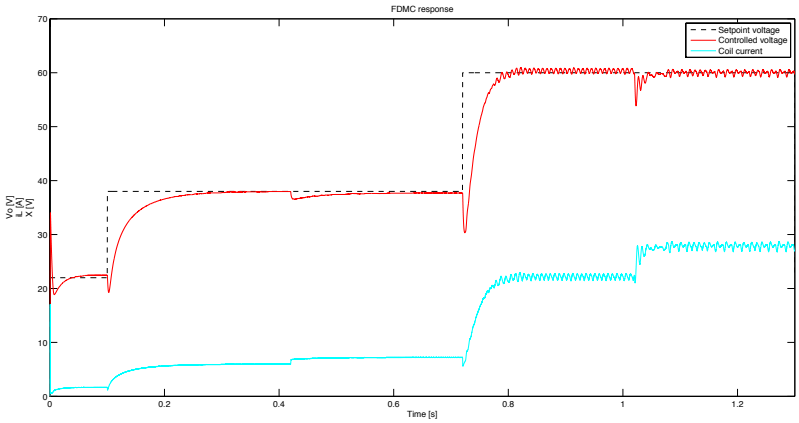

a) Controlled variable by the FDMC controller v_o and coil current i_L

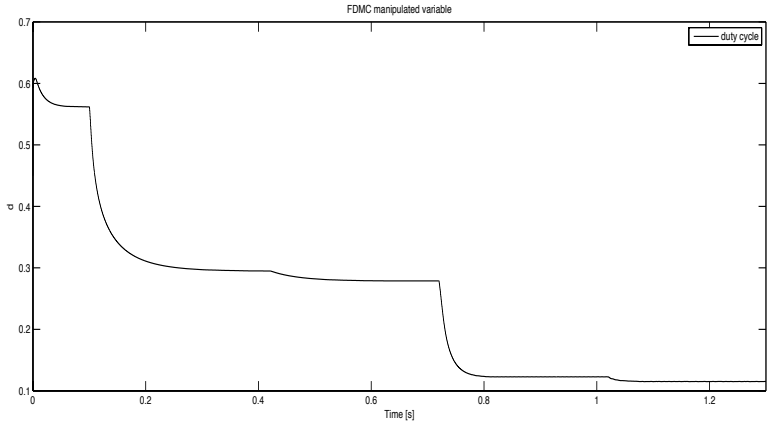

b) Manipulated variable from the FDMC controller (duty cycle)

$d_u = [0.01, 0.66]$ *range* $98.5 \div 1.5\%$

Fig. 4.7 Simulation results: a and b

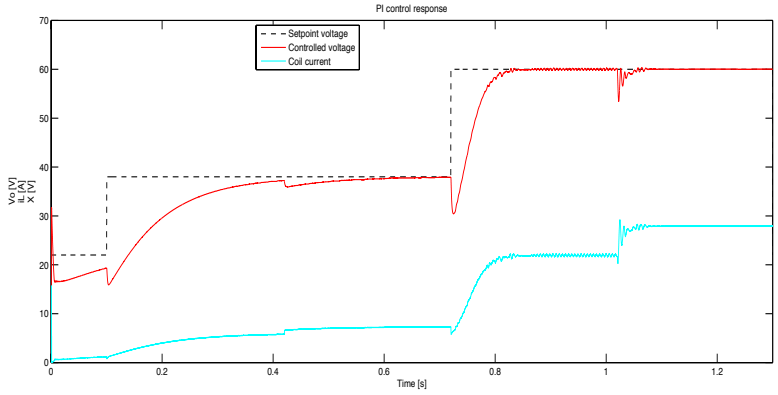

a) Controlled variable by the Optimized PI controller v_o and coil current i_L

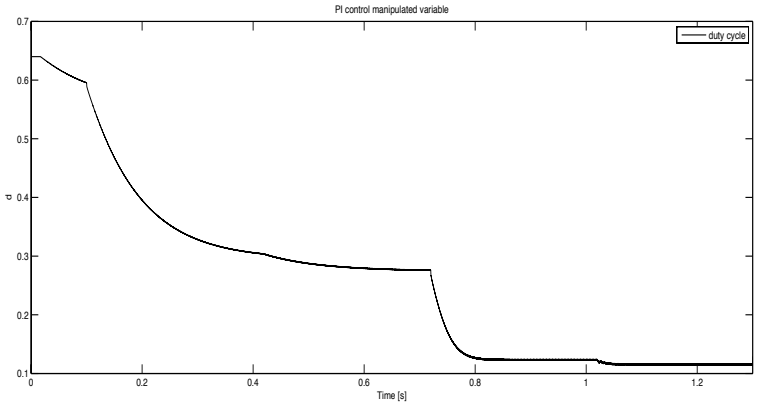

b) Manipulated variable from the Optimized PI controller (duty cycle)

$d_u = [0.01, 0.66]$ *range* $98.5 \div 1.5\%$

Fig. 4.8 Simulation results: a and b.

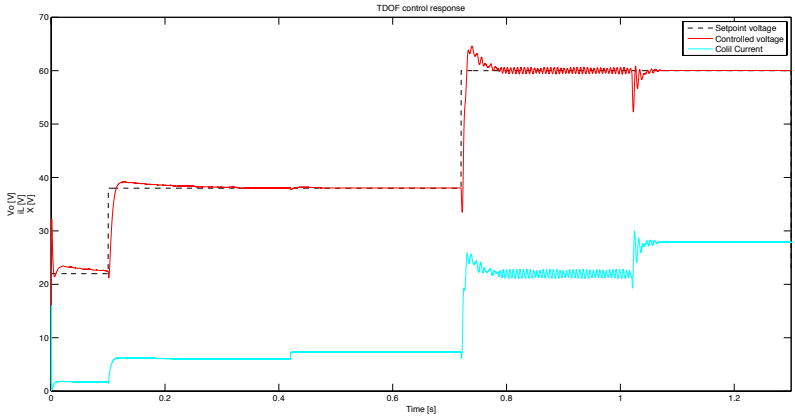

a) Controlled variable by the TDOF controller v_O and coil current i_L

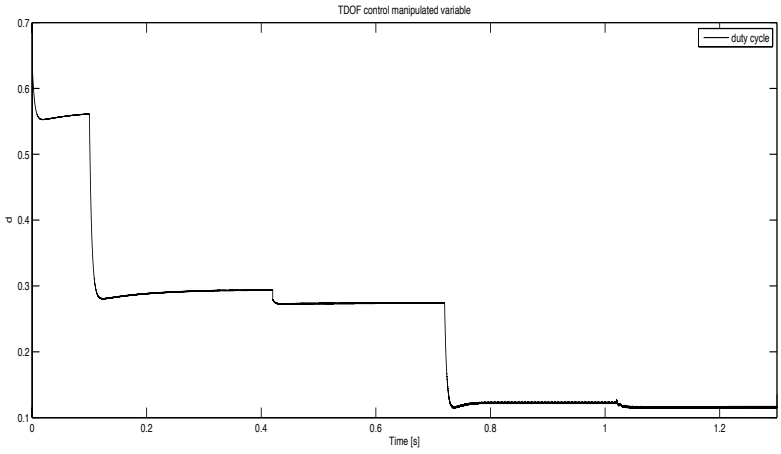

b) Manipulated variable from the TDOF controller (duty cycle)

$d_u = [0.01, 0.66]$ *range* $98.5 \div 1.5\%$

Fig. 4.9 Simulation results: a and b.

Figure 4.10 presents all methods together and additionally simplifies the comparison.

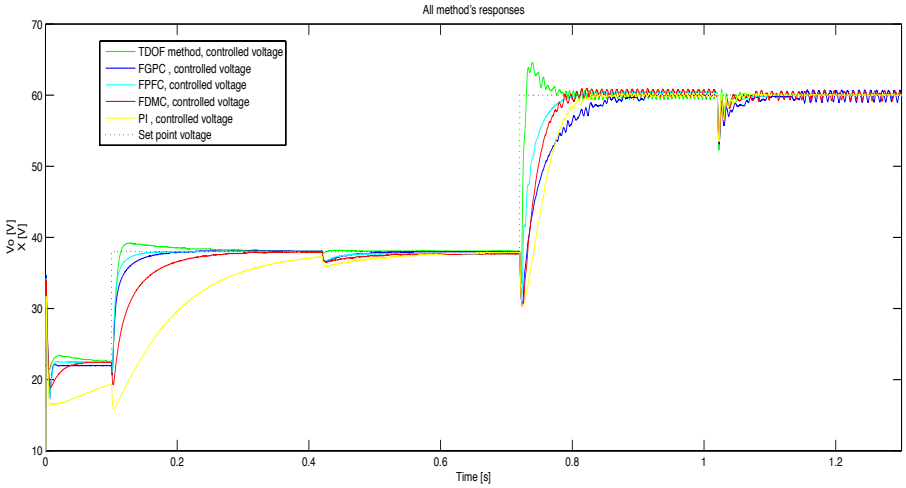

a) Controlled variable v_o compared for all methods

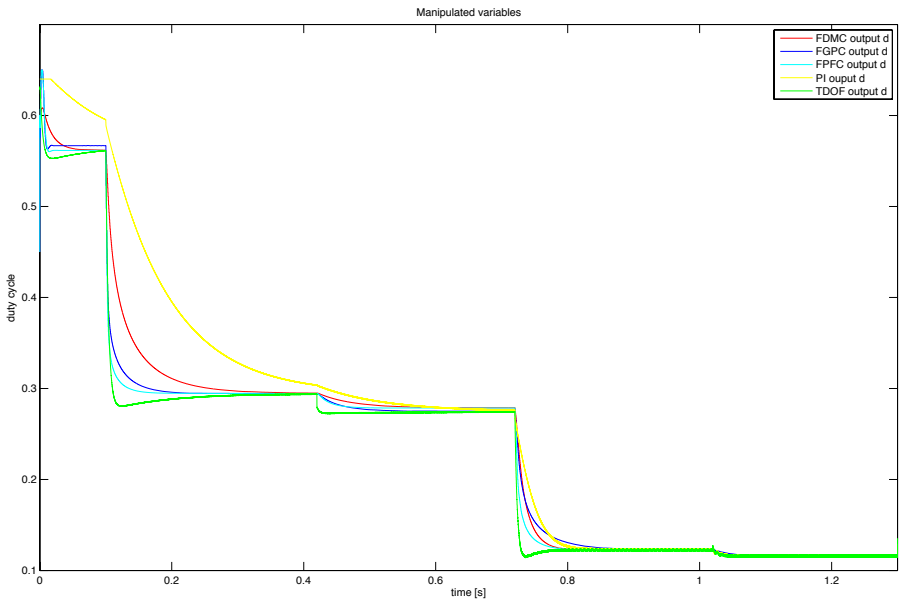

b) Manipulated variable d_u compared for all methods

Fig. 4.10 Simulation results: a and b.

4.3.1 Fuzzy Dynamic Matrix Control parameters:

The FDMC method is minimizing the (4.17) objective function and asks for the tuning of $\boldsymbol{Q}$ and $\boldsymbol{R}$ quadratic, diagonal and positive matrixes that are now:

$$\boldsymbol{Q} = \begin{bmatrix} 0.0001 & 0 & 0 \\ 0 & \ddots & 0 \\ 0 & 0 & 0.0001 \end{bmatrix} \qquad \boldsymbol{R}(k) = \begin{bmatrix} \lambda(k) & 0 & 0 \\ 0 & \ddots & 0 \\ 0 & 0 & \lambda(k) \end{bmatrix}.$$

$\boldsymbol{Q}, \boldsymbol{R}(k) \in \mathbb{R}^{12x12}$

$\lambda(k) \in [50,1500]$

The control horizon is equal to the prediction horizon $N_c = N_u = 12$ and with the reference trajectory coefficient $a_r = 0.1$. To achieve a meaningful comparison to the other methods the control horizon is selected in all MPC methods equally.

4.3.2 Fuzzy Generalized Predictive Control parameters:

The objective function (4.24), (4.26) minimized by this control method requests a tuning of suppression factor $\lambda(k) \in [100,2500]$.

The selected transfer function of weighting output filter in accordance with GPC method is

$P(z) = 1 - 1.6z^{-1} + 0.6z^{-2}$.

The control horizon and the reference trajectory coefficients are $N_c = N_u = 12$ and $a_r = 0.996$ respectively.

4.3.3 Fuzzy Predictive Functional Control parameters:

The *step* and *parabola* selected basis functions are the most suitable in accordance with the process response on step changes of manipulated variable. These functions request two coincident points n_H =2, H_1 and H_2 to be able to construct a feasible MPC problem, and hence, H_1 = 1 and H_2 = 12.

Referring the objective function (4.30), and the equation (4.33), the reference trajectory y_R coefficient is a_r = 0.01 and the suppression factor $\lambda(k) \in [40,400]$.

4.3.4 PI offline optimized parameters:

The PI controller parameters are inherited from the Subsection 4.1.1.

Discrete equivalents are achieved based on a theoretical sample time to be as close as possible to the continuous form (t_{sample} = 10^{-6} *s*)

$G_{PI}(z) = 5.648 \cdot 10^{-4}(z - 1.000354)(z - 1)^{-1}.$

The offline optimization is carried out around the operating point *s*=50V, *E*=10V, *R*=12.5Ω, for

$G_m(z) = (-0.090237z + 0.0904)(z^2 - 2z + 0.9996)^{-1}$.

4.3.5 Experimental results

Therefore, the fruitful results rendered by the simulations led us in an experimental evolution of the identification and control-developed methods on the physical system Figure 3.16. The selection of the electrical components Table 3.1 (T_S =333 μs) is conducted with a sense to achieve a meaningful comparison with the expertise in the previous Chapter II, Subsection 2.3.5, which was also experimentally examined in [7], and generally with the previous simulation results (Section 4.3). Already, the simulation was showing an incomparably better result than one rendered by the simple control algorithm in Subsection 2.3.5. It is proving the statement and objective that the nonlinear phenomena could be reduced or filtered out by the more intelligent control algorithm. The identification and the predictive control are tools that are integrated into the controller's physical knowledge and used to avoid the isolated attractors if they are not willing stable states. Even the nonlinear phenomena are present, those are attenuated and driven to the stable states in-between the fractal system's structure.

As stated, because of the promising simulation results and a positive experience with developed Fuzzy Model Predictive Controls, and one of the major objectives of this thesis that is a reduction of complexity, only FPFC will be experimentally presented. FDMC and FPFC were showing similar results in the simulation of control, but the FDMC is more tedious in terms of calculations. The implementation of FDMC, because of the method's construction, limits its applicability on more powerful microcontrollers. A less successful FGPC at the time of simulation equally suffers that problem. The main limitation is strictly connected with the prediction and the control horizon $N_c = N_u = 12$, which builds up complexity in the calculation of the inverse matrix and matrices' multiplications. Differently than the underlined FMPC main complexity issue in this work, apart from those resolved by the identification approach, the TDOF methodology certainly diminishes the tedious matrix calculation, but on the other side has a weak control over the transition states. That is why the FPFC takes a lead over the other performed methods.

It can be said that the main processing time of this method would be the accessibility to the offline-learnt knowledge, but this experimental example occupies just 1.6% of the sampling time calculated for the worse-case scenario, if the processor for each data word uses the accessing time to the internal memory (which is Paged Flash access time). For the processor used, that would be 5.5 μs. Furthermore, the complete system's learnt knowledge is compressed into 153 data words in the processor's internal memory of 4G words. Even though the tedious work of the identification is conducted offline, which is related to the static part (3.44), the comprehensive and the accurate model of the contemporary process operating point must be selected online, as it is a dynamic function of regression vectors (3.45). The FNARX model parameters' vector $\boldsymbol{a}_m(k)$ in Figure 4.4 is calculated throughout the processor's *fuzzy engine* from the offline rendered global and distinctive knowledge. That significant processor's workload together with the FPFC devised optimal control signal takes approximately 180 μs of the processor's time of execution.

The PI controller, purely based on MATLAB tools for SISO controllers [29], was back-compared with the new derived FPFC, without any loss of generality and presenting the overall reference to any known, modern control solution. It was gained via the auto-tuning method, based on a singular frequency and minimization of the ITAE

(Integral Time Absolute Error), and subsequently optimized by the Gradient Descent Algorithm for a Medium-Scale performance. A meaningful comparison was derived with the process step parameter changes, for the wider operating range of the DC-DC converter. By applying the variable set point *s*, the converter will be guided from the DCM operation to a CCM, where the highest process gain is expected.
The disturbances of the process parameters are commenced, simulating the possibly realistic DC-DC converter's operating regime.
The internal model discrepancy grows with the prediction horizon, but it is strongly influenced by the construction of the fuzzy model, where the inductor current is the measured value and assumed to be constant during the prediction horizon. This is also the reason the prediction and control horizon are limited to the low value of N_c=N_u=12. The stability is improved with the selection of the objective functions and fine-tuning of the manipulated value suppression factor. This is, for example, atypical in PFC. Furthermore, the tuning of the suppression factor and the construction of its time-dependent function preserve the sub-optimal solution.
The offline optimized PI controller is comparable in the process with a higher gain range, where the optimization is carried out. Analogically, it is incomparably slow in the lower gain range. Figure 4.11 and a detailed Figure 4.12, from the oscilloscope, present the responses together to simplify the comparison. The FPFC method shows its robust advantage and for a wide range of different operating points performs similarly in its aggressiveness and steady-state stability. The main difficulty can be found in the steady-state error, which was not obvious in the simulation results in which the model/process error was negligible, but also in the online processing demands that are incomparably higher than for the PI. To a realistic extent, the error reflects in a significant steady-state offset. It is also a feature of the developed methodology to tackle this kind of problem and compensate for it. Model-based control gives us the ability to use the predecessor model/process error data in forming a simple correction to the reference model.

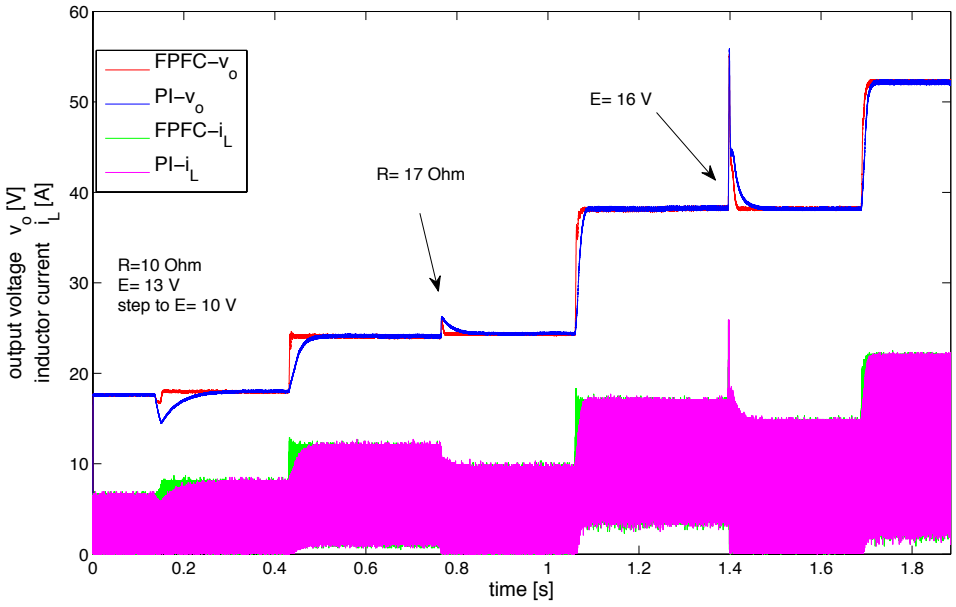

Fig. 4.11 Experimental results of PI and FPFC controllers on step changes of the process parameters and reference point

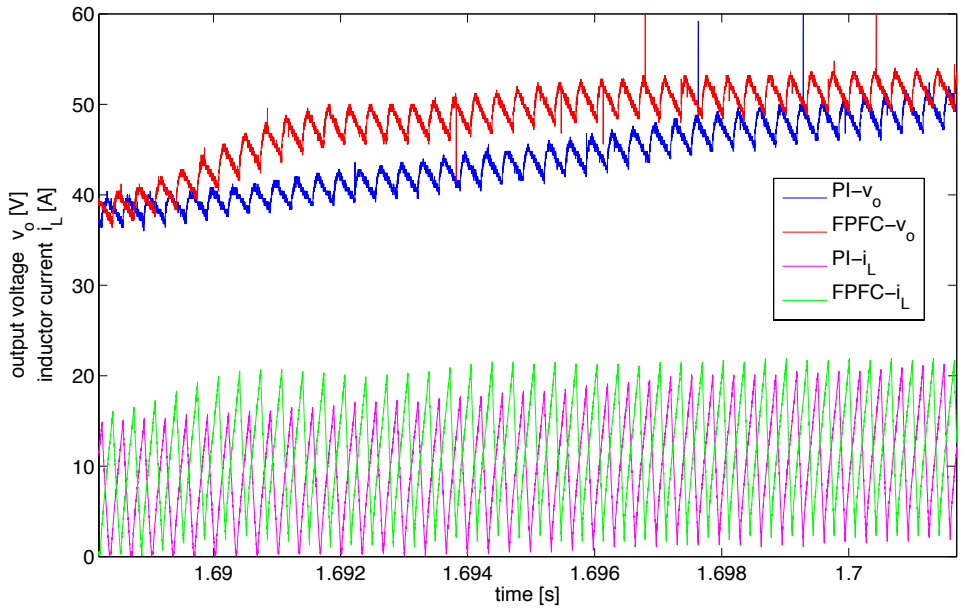

Fig 4.12 Detail from Figure 4.11, transient on the reference change

4.3.6 Conclusion about the FMPC

The EMPC certainly brings a standardized control toolbox that is applicable to PEC nonlinear dynamical systems, as a typical example of the SAS. Different modelling may minimize the main drawback in the complexity. In this thesis, we emphasized the idea that fuzzy modelling, as a universal approximation, is an applicable method. The EMPC approach together with the mentioned idea is synthesized in the FMPC methodology for the SAS. The presented complexity of the identification and the time-consuming convex programming was integrated into a global model derived from offline algorithms, Subsection 3.3.3, which allowed an expectedly shorter execution time, but still preserved the adaptive tracking of the process dynamic changes. For each time scan, the fuzzy model produced the closest approximated linear model (3.54) in a form (4.10) that is applicable to the employment of standard finite horizon MPC methods, which then performed similarly and achieved all the control objectives. In simulation and especially in the experimental results, after the employment of the physical knowledge based on the complexity reduction, we still have experienced the online complexity limitations with several FMPC methods. The FPFC method has performed the best referring the objectives given in this thesis. The selection of the performance index (4.29), including the suppression factor, was acknowledged to have high importance in guarding the stability and robustness of the constructed control algorithms. To fortify the knowledge gathered by the simulation, the complete methodology was tested on a real process of a DC-DC boost converter Figure 3.16. The meaningful comparison with the still broadly used optimized PI controller, because of its applicability and simplicity, presented in Figures 4.11 and 4.12, must support all previously defined objectives of this thesis.

Chapter V

Conlusion

The DC-DC Boost converter, as the example taken in this study, is a good representative of an SAS and gives the qualitative platform for the evolution of the new control methodologies. The main objective of this thesis unconditionally drives the new control methodology in the direction of implementing the modern and developed strategies for the systems that are physically small, but complex in their behaviour. This objective drives the research in the direction of the fundamental problem of decomposition and the learning of the most basic system's behaviour. Thus, the thesis provides a precise simulation model based on the MLD theory and performed on the Simulink/Matlab toolbox. A DHA of the DC-DC boost converter presented here is compared with the results from the previous studies [7]. We found a high grade of accuracy even in comparison with the experimental results given in the literature [7]. This certainly supports the obtained results if we refer to the main objective. Most of the known methods performed on this particular problem employ the analytical methods in forming the model-based solution [3]. In this thesis, all widely known objectives are achieved and added to the main objective of forming a solution that is conciliating the method's complexity with the applicability on the physical processes by also considering the investment feasibility.

To achieve the abovementioned, Chapter II provides the comprehensive analysis of the state-of-the-art solutions but also underlines the complexity of the task untaken. The theory presented must address problems in the control algorithms so as to provide a more advanced and optimal solution. The problems that appear in HS modelling, also including those typically inherited by the feedback control systems, are considered in the selection of the control methodology. Differently than in the established methodologies, our approach indicates that a purely analytical construction of the process model is inadequate to address all the highlighted problems. That is exclusively when there is a task to stay in the applicability limits, referring to the physical extents of the process and the feasible employability. Therefore, it is stated that the physical knowledge of the system is of crucial importance in taking of different decisions, which will finally lead to the applicable mathematical model. As the known analytical and precise modelling unconditionally carries the complexity burden, equally heavy for the processor's time of the execution as for the access to the extended memory of the future controller, the heuristically devised solution aids in overcoming that complexity. The main bearing, viewed from the aspect of the control technology, stays unchanged when considering that most of the state-of-the-art methods propagate the model control solutions. Eventually, the thesis promotes the heuristic control not as the counterpart of the existing methodologies, but an upgrade to these methodologies. It focuses the process throughout which the physical knowledge is transferred to the mathematical model. The idea is inspired by the qualitative mathematical theory in a way in which the following control solutions avoid an unnecessary and known complexity, already discovered at the time of forming the model. As shown in the simulation, the selected example consists of different nonlinear phenomena.

In this thesis, the presented new methods, in a phase of modelling, are transforming the natural HS to the continuous. Unlike for the established methodologies, this research employs the identification of the local models by numerical methods; even a well-explored averaging method for the selected process exists. As known and elaborated in this thesis, for the selected example, the standard averaging is based on the integer programming and the perturbation method around the operating point. Here, we found the main conflict in establishing the global and continuous model. It emerges from the fact that the perturbation methodology is based on the infinitesimal differentials around the operating points while the identification involves the wider space of the absolute solutions around the operating points. In more developed methodologies, i.e. the MLD or the LC solutions, authors preserve the hybrid nature and, by forming the global models, propagate the model's scattered nature.

Chapter III presents the analytical thoughts that lead to the construction of the identification processes and their evaluation. The main idea to maintain the continuity of the rendered model is achieved by the involvement of the TS fuzzy modelling. We stated that the HS, and closely the SAS, has the alternative in the powerful methodology of the mathematical modelling based on the identification. The results presented show and support this thesis. Thus, the fuzzy identified model in comparison with the analytically rendered model of HS gives an equal or higher grade of accuracy in robust modelling. Furthermore, identification methodology is certainly more accurate for the experimental cases in which the nonlinearities are not neglected, as it is an example in the analytically derived models. The identification is done offline, and that has a major benefit in minimizing of the final processing complexity of the control algorithm. The selection of the regression vectors that is based on the physical and the experimental knowledge of the system groups the presented identification methodologies in the grey box identifications. In the modelling of SAS, two different types of the identification methodologies are here constructed. First, the identification methodology that provides the fuzzy global model of the system's steady states, or differently said the static model. Second, the identification methodology provides the fuzzy global model as the approximation of the system's nonlinear dynamic model. The selection of the identification methodologies is driven by the final selection of two different controllers of the SAS system. One controller is defined as the two degrees of freedom control and other as the MPC.

Those controllers are presented in Chapter IV. The intention to reduce the online processing complexity of the controller guides the development of two different control algorithms. Both of controllers are members of the model-based control. In the case of two-degrees-of-freedom control, the problem was decomposed in a way to compensate the main drawback of the numerically optimized linear controller recognized for its robustness for a wider range of the process parameter change. While the linear controller is designed to stabilize the small deviation around the operating point, the model-based controller output is incomparably faster and brings the controller as close as possible to the stable operating point. On the other side, the model-based control part that inherits the model/process error, in the expected limits, still requires fine adjustments built with the linear controller. The first differential of the control variable, as the output of the fuzzy model, is tuned to comply with the maximum current constrain of the primary

circuit of the DC-DC converter. The aforementioned function is fulfilled by the integration time with the integrator that is added to the fuzzy-model-devised steady state. The tested simulation model was exposed to the different parameters change at the same time, and the converter reaches the stable operating point extremely quickly and approaches to the previously identified steady state on a first-order response manner. The fuzzy model response is connected as the controller's feed-forward line, which explains this behaviour.

The transition period in two-degrees-of-freedom methodology is fast, but sometimes overshoots as that depends on the positivity of the system/model error in that operating point. To synthesize the solution that considers a dynamic model based prediction, it also rectifies the overshoots. Furthermore, the MPC certainly puts more burdens on the processing time, and we have presented the way in which the EMPC idea integrated differently into the fuzzy model based MPC gives expected results. The methodology that rectifies the aforementioned is certainly the MPC. The fuzzy model predictive control in this thesis has the final goal of implementing the modern methodology that has the suboptimal control over the complete transition period and steady state of the system. Therefore, it must provide a conciliation of the MPC methods in its application for the fast response systems. This thesis with the previous theory and modelling approach achieves the final objective in FPFC, as the member of FMPC. The simulation and experimental results prove the statement.

Further research will go in the direction of implementing this methodology into the more complex SAS, but also as the continuation of implementing the qualitative mathematical theory in designing and exploring the new control methodologies.

Bibliography

[1] M. di Bernardo, C.J. Budd, A.R. Champneys, P. Kowalczyk, "Piecewise-smooth Dynamical Systems – Theory and Applications", Springer- Verlag London Limited, 2008.

[2] J. Lunze, F. Lamnabhi-Lagarrigue,"Handbook of Hybrid Systems Control; Theory, Tools, Applications", Cambridge University Press , New York 2009.

[3] S. Mari thoz, S. Alm r, Mihai Bâja, A.G. Beccuti, D. Patino, A. Wernrud, J. Buisson, H. Cormerais, T. Geyer, H. Fujioka, U.T. Jönsson, Chung-Yao Kao, M. Morari, G. Papafotiou, A. Rantzer, P. Riedinger, "Comparison of Hybrid Control Techniques for Buck and Boost DC-DC Converters", IEEE Transactions on Control Systems Technology, vol. 18, no. 5, September 2010.

[4] H. Fujioka, C.-Y. Kao, S. Alm r, U. Jönsson, "Robust tracking with H_∞ performance for PWM systems," *Automatica*, vol. 45, pp. 1808– 1818, 2009.

[5] A.G. Beccuti, G. Papafotiou, R. Frasca, M. Morari, "Explicit Hybrid Model Predictive Control of the dc-dc Boost Converter." In: IEEE, PECS 2007, pp. 2503–2509.

[6] Alessandro Alessio, Alberto Bemporad, "A Survey on Explicit Model Predictive Control in Nonlinear Model Predictive Control", LNCIS 384, pp. 345-369, Springer-Verlag, Berlin Heidelberg, 2009.

[7] C.K. Tse, "Flip Bifurcations and Chaos in Three-State Boost Switching Regulators", IEEE Transactions on Circuits and Systems-1; Fundamental Theory and Applications, vol. 41, no. 1, January 1994.

[8] Yanfeg Chen, C.K. Tse, Siu-Chung Wong, "Interaction of Fast-Scale and Slow-Scale Bifurcation in Current-Mode Controlled DC/DC Converters", International Journal of Bifurcation and Chaos, vol. 17, no. 5, pp. 1609–1622, 2007.

[9] K. Guesmi, N. Essounbouli, A. Hamzaoui, J. Zaytoon, N. Manamanni, "Shifting nonlinear phenomena in a DC-DC converter using fuzzy logic controller", Elsevier, 2007.

[10] K. Mehran, D. Giaouris, B. Zahawi, "Stability Analysis and Control of Nonlinear Phenomena in Boost Converters Using Model-Based Takagi–Sugeno Fuzzy Approach", IEEE Transactions on Circuits and Systems—I: Regular Papers, vol. 57, no. 1, January 2010.

[11] B. Lincoln, A. Rantzer, "Relaxing dynamic programming," *IEEE Trans. Autom. Control*, vol. 51, no. 5, pp. 1249–1260, Aug. 2006.

[12] M. Santos, "Chapter 2: Modelling switched power converters using the complementarity formalism", doctoral thesis. In: December 2006, Universitat Politècnica Catalunya.

[13] F. Vasca, L. Iannelli, M. Kanat Camlibel, R. Frasca, "A New Perspective for Modeling Power Electronic Converters: Complementarity Framework", In: IEEE Transactions on Power Electronics, vol. 24, no. 2, February 2009.

[14] Rong-Jong Wai, Li-Chung Shih, "Design of Voltage Tracking Control for DC-DC Boost Converter Via Total Sliding-Mode Technique", IEEE Transactions on Industrial Electronics, vol. 58, no. 6, June 2011.

[15] E. Vidal-Idiarte, C.E. Carrejo, J. Calvente, L. Martínez-Salamero, "Two-Loop Digital Sliding Mode Control of DC-DC Power Converters Based on Predictive Interpolation", IEEE Transactions on Industrial Electronics, vol. 58, no. 6, June 2011.
[16] R. Baždarić, I. Škrjanc, D. Matko, "Two Degrees of Freedom in the Control of a DC-DC Boost Converter, Fuzzy Identified Explicit Model in Feed-forward Line", Journal of Intelligent and Robotic Systems, Vol. 82, Issue 3, pp. 479-483, June 2016
[17] T. Geyer, G. Papafotiou, M. Morari, "Hybrid Model Predictive Control of the Step-Down DC-DC Converter," *IEEE Trans. Control Syst. Technol.*, vol. 16, no. 6, pp. 1112–1124, Nov. 2008.
[18] J.M. Maciejowski, "*Predictive Control",* Englewood Cliffs, NJ: Prentice- Hall, 2002.
[19] A.A. Stoorvogel, T.J.J. van den Boom, "Model Predictive Control", DISC Course Lecture Notes, January 2010.
[20] M. V. Kothare, V. Balakrishnan, M. Morari ,"Robust Constrained Model Predictive Control using Linear Matrix Inequalities", Automatica, Vol. 32, pp. 1361-1379. ,1996 , Elsevier Science
[21] T. Takagi, M. Sugeno, "Fuzzy identification of systems and its applications to modeling and control", *IEEE Trans. Syst., Man, Cybern.*, no. SMC-15, pp. 116–132, 1985.
[22] S. El Beid, S. Doubabi, "DSP-Based Implementation of Fuzzy Output Tracking Control for a Boost Converter", IEEE Transactions on Industrial Electronics: Regular Papers, vol. 61, no. 1, January 2014.
[23] R.D. Middlebrook, "Small-Signal Modeling of Pulse-Width Modulated Switched-Mode Power Converters", In: Proceedings of the IEEE, vol. 76, no. 4, April 1988.
[24] R.W. Erickson, S. Ćuk, R.D. Middlebrook, "Large-Signal Modelling and Analysis of Switching Regulators", In: IEEE, 1982 PESC Rec., pp. 240-250.
[25] W.P.M.H. Heemels, B. De Schutter, A. Bemporad, "On the equivalence of classes of hybrid dynamical models", Proceedings of the 40th IEEE Conference on Decision and Control, Orlando, Florida, pp. 364–369, Dec. 2001.
[26] A. Bemporad, M. Morari, "Control of systems integrating logic, dynamics, and constraints", Automatica, vol. 35, pp. 407-427, 1999.
[27] A.J. van der Schaft, J.M. Schumacher, "Complementarity Modeling of Hybrid Systems", In: IEEE Transactions on Automatic Control, vol. 43, no. 4, April 1998.
[28] C. Goffman, G. Pedrick," First Course in Functional Analysis", In: Prentice-Hall Inc., Englewood Cliffs, N.J., 1965.
[29] The MathWorks Inc., "MATLAB ", R2009a, 7.8.0.347, February 2009.
[30] Sjöberg, Q. Zang, L. Ljung, A. Beveniste, B. Delyon, P.-Y. Glorennec, H. Hjalmarsson, A. Juditsky, "Nonlinear Black-Box Modeling in Systems Identification: a Unified Overview", Automatica, vol. 31, no. 12, pp. 1691-1724, 1995.
[31] I. Škrjanc, D. Matko, "Predictive Functional Control Based on Fuzzy Model for Heat-Exchanger Pilot Plant", IEEE Transactions on Fuzzy Systems, vol. 8, no. 6, pp. 705-712, 2000.

[32] K. Kavšek-Biasizzo, I. Škrjanc, D. Matko, "Fuzzy Predictive Control of Highly nonlinear pH process", Elsevier Science Ltd, Computers Chem. Engng, vol. 21, Suppl., pp. S613-S618, 1997.
[33] I. Škrjanc, S. Blažič, S. Oblak, J. Richalet, "An approach to predictive control of multivariable time-delayed plant: Stability and design issues", ISA Transactions, vol. 43, pp. 585-595, 2004.
[34] J. Castro, " Fuzzy Logic Controllers are Universal Approximators", IEEE Trans. Syst., Man. Cybern., vol. 25, pp. 629-635, 1995.
[35] L.X. Wang, "Design and Analysis of Fuzzy Identifiers of Nonlinear Dynamics Systems", IEEE Trans. Automat. Contr., vol. 40, pp. 11-23, Jan. 1995.
[36] Kevin M. Passino, Stephen Yurkovich, "Fuzzy control", Addison Wesley Longman, Inc., 1998.
[37] P. Karamanakos, G. Papafotiou, S.N. Manias, "Model predictive control of the interleaved DC-DC boost converter", 15th International Conference on System Theory, Control, and Computing (ICSTCC), 2011.
[38] K.S. Holkar, L.M. Waghmare, "An Overview of Model Predictive Control", International Journal of Control and Automation, vol. 3, no. 4, December 2010.
[39] H.B. Kuntze, A. Jacubasch, J. Richalet, Ch. Arber, "On the Predictive Functional Control of an Elastic Industrial Robot", Proceedings of 25th Conference on Decision and Control, Athens, Greece, December 1986.
[40] S. Abu el Ata-Doss, P. Fiani, J. Richalet, "Handling Input and State Constraints in Predictive Functional Control", Proceedings of 30th Conference on Decision and Control, Brighton, England, December 1991.
[41] I. Škrjanc, D. Matko, "Fuzzy Predictive Functional Control in the State Space Domain", Journal of Intelligent and Robotic Systems, vol. 31, pp. 283-297, 2001.
[42] Fujioka, H., Kao, C.-Y., Alm r, S., Jönsson, U.: LQ optimal control for a class of pulse width modulated systems. In: *Automatica*, vol. 43, no. 6, pp. 1009–1020, 2007.
[43] Middlebrook, R.D., Ćuk Slobodan: A General Unified Approach to Modeling Switching-Converter Power Stages. In: IEEE, 1976 Record, pp. 18-34 (IEEE Publication 76CH1084-3 AES)
[44] Ogata K.: Modern Control Engineering-Fifth Edition. In: Prentice Hall, 2010
[45] S. Paoletti, LJ. A. Juloski, G. Ferrari-Trecate, R. Vidal.," Identification of hybrid systems: a tutorial", Eur. J. Control, 513(2-3), pp. 242-260, 2007.
[46] Y. Ma, R. Vidal," Identification of deterministic switched ARX systems via identification of algebraic varieties", In: Morari M., Thiele L., Rossi F. (eds), "Hybrid Systems: Computation and Control", vol. 3414 of Lecture Notes in Computer Science, Springer-Verlag, Berlin/Heidelberg. 2005, pp 449
[47] G. Ferrari-Trecate, M. Muselli, D. Liberati, M. Morari , "A clustering technique for the identification of piecewise affine systems", Automatica 2003; 39(2):205–217
[48] A. Juloski, S. Weiland, WPMH. Heemels ,"A Bayesian approach to identification of hybrid systems", IEEE Trans Autom Control 2005; 50(10):1520–1533
[49] E. Münz, V. Krebs, "Continuous optimization approaches to the identification of piecewise affine systems", In: Proceedings of the 16th IFAC World Congress, Prague, Czech Republic. 2005

[50] S. Nefti, M. Oussalah, U. Kaymak, "A new fuzzy set merging technique using inclusion-based fuzzy clustering,", IEEE Transactions on Fuzzy Systems, 16 (1)(2008) 145–161.
[51] S. Blažič, I. Škrjanc, S. Gerkšič, G. Dolanc, S. Strmčnik, M. Hadkiski, A. Stathaki, "Online fuzzy identification for an intelligent controller based on a simple platform", Engineering Applications of Artificial Intelligence 22 (4) (2009)628–638.
[52] G. Karer, G. Mušič, I. Škrjanc, B. Župančič, "Hybrid fuzzy model-based predictive control of temperature in a batch reactor", Computers & Chemical Engineering31 (12) (2007) 1552–1564.
[53] M.E. Gegundez, J. Aroba , J.M. Bravo, "Identification of piecewise affine systems by means of fuzzy clustering and competitive learning,", Engineering Applications of Artificial Intelligence 21 (8) (2008) 1321–1329.
[54] A. Núñez, B. De Schutter, D. Sáez, I. Škrjanc," Hybrid-fuzzy modeling and identification", Applied Soft Computing, vol. 17,pp.67-78, 2014.
[55] M. di Bernardo, C.J. Budd, A.R. Champneys P. Kowalczyk, "Picewise-smooth Dynamical Systems – Theory and Applications", Springer-Verlag London Limited 2008
[56] B.R. Andrievskii, A.L. Fradkov, "Control of Chaos: Methods and Applications. I. Methods", Automation and Remote Control, Vol.64, No. 5, 2003, pp. 673-713
[57] Y. Kolokolov , P. Ustinov , N. Essounbouli , A. Hamzaoui, "Bifurcation-free design method of pulse energy converter controllers" , Chaos, Solitons and Fractals, www.elsevier.com/locate/chaos , Elsevier, 31. March 2009.
[58] F. Misoc," A comparative study of DC-DC converters effects on the output characteristics of direct ethanol fuel cells and NiCd Batteries ", An abstract of a dissertation, Kansas State University 2007.
[59] Ž. Ban, T. Bjazić, I. Volarić, "Voltage Control of a DC/DC Boost Converter Powered by Fuel Cell Stack", FER Zagreb, MIPRO 2009.
[60] M. Grötsch, M. Mangold, A. Kienle, "Analysis of the Coupling Behavior of PEM Fuel Cells and DC-DC Converters", Energies 2009, 2, 71-96; doi:10.3390/en2010071
[61] J. Wang, Z. Duan, Ying Yang, L. Huang, "Analysis and Control of Nonlinear Systems with Stationary Sets – Time Domain and Frequency Domain Methods " , World Scientific Publishing Co. Pte. Ltd. 2009.
[62] T. A. Henzinger, "The Theory of Hybrid Automata", Proceedings of the 11th Annual IEEE Symposium on Logic in Computer Science (LICS96), pp.278-292.
[63] P. Tabuada, "Verification and Control of Hybrid Systems, A Symbolic Approach", Springer LLC 2009.
[64] B. De Schutter, W. P. M. H. Heemels, J. Lunze, C. Prieur, "Survey of modeling, analysis, and control of hybrid systems, Chapter 2 in Handbook of Hybrid System Control-Theory, Tools, Applications ", Cambridge University Press, ISBN 978-0-521-76505-3, pp. 31-55, 2009.
[65] H. K. Lang, F. H. F. Leung, "Stability Analysis of Fuzzy-Model-Based Control Systems, Linear-Matrix-Inequality Approach" , Springer-Verlag Berlin Heidelberg, 2011.
[66] Michael Stephen Branicky, " Studies in Hybrid Systems: Modeling, Analysis, and Control ", Massachusetts Institute of Technology, 26 May 1995.
[67] Xu Jun, " Control and Estimation of Piecewise Affine Systems" , Nanyang Technological University, Singapore, 2006.

[68] Fabio Danilo Torrisi, Alberto Bemporad, "HYSDEL—A Tool for Generating Computational Hybrid Models for Analysis and Synthesis Problems", IEEE Transactions on Control Systems Technology, vol. 12, no. 2, March 2004.
[69] H. Paul Williams, "Logic and Integer Programming", DOI 10. 1007/978-0-387-92280-5, Springer Science+Business Media, LLC 2009.
[70] Richard E. Hodel, "An Introduction to Mathematical Logic", ISBN-13: 978-0-486-49785-3, ISBN-10: 0-486-49785-2, Dover Publications INC., Mineola, New York, 2013.
[71] W.P.M.H. Heemels, J.M. Schumacher, S. Weiland,"Linear Complementarity Systems", SIAM Journal on Applied Mathematics, DOI: 10.1137/S0036139997325199, Volume 60, Issue 4, pp. 1234-1269, July 2006.
[72] R. W. Cottle, J. S. Pang, and R. E. Stone, " The Linear Complementarity Problem", Academic Press, Boston, MA, 1992.
[73] M.K. Çamlıbel, W. P. M. H. Heemels and J. M. Schumacher, " Well-posedness of a class of linear networks with ideal diodes" , In Proc. 14th Int. Symp. Mathematical Theory of Networks and Systems, Perpignan, France, 2000.
[74] M.K. Çamlıbel, L. Iannelli, and F. Vasca, "Passivity and Complemenatrity", Mathematical Programming, Volume 145, Issue 1, pp. 531-563, June 2014.
[75] W.P.M.H. Heemels, M.K. Çamlıbel , and J.M. Schumacher, "On the dynamic analysis of picewise-linear networks", IEE Trans. Circuits and Systems I, 49 (3), pp. 315-327, 2002.
[76] M.K. Çamlıbel, W.P.M.H. Heemels, and J.M. Schumacher, "Stability and Controlability of planar bimodal complementarity systems", In Proc. 42nd IEEE Conf. Decision and Control, Maui, USA, 2003.
[77] B. De Schutter and T.J.J. van den Boom, "Model predictive control for max-min-plus scaling systems," Proceedings of the 2001 American Control Conference, Arlington, Virginia, pp. 319–324, June 2001.
[78] John Lygeros, "Lecture Notes on Hybrid Systems", Department of Electrical and Computer Engineering University of Patras, Rio, Patras, GR-26500, Greece, February 2004.
[79] John Lygeros, Karl Henrik Johansson , Shankar Sastry and Magnus Egerstedt, "On the Existence of Executions of Hybrid Automata", In Proc. of the 38th Conf. on Decision and Control Phoenix, Arizona, USA, December 1999.
[80] John Lygeros, Karl Henrik Johansson, Slobodan N. Simić, Jun Zhang, and S. Shankar Sastry," Dynamical Properties of Hybrid Automata", IEEE Transactions on Automatic Control, Vol.48, No. 1., January 2003.
[81] Steven H. Strogatz, "Nonlinear Dynamics and Chaos; With application to Physics, Biology, Chemistry, and Engineering", Addison-Wesley Publishing Company, MA, USA, November 1994.
[82] Yu A. Kuznetsov, "Elements of Applied Bifurcation Theory, Second edition", Springer-Verlag, New York, USA, Applied Mathematical Science, Volume 112, 1998.
[83] A. B. Nordwark, "Non-periodic motion caused by grazing incidence in an impact oscillators", Journal Of Sound and Vibration, Volume 145, Issue 2, pp. 279-297, March 1991.
[84] L. Lu, A. Bryant, E. Santi, J.L Hudgins, and P.R Palmer, "Physics-based model of IGBT including MOS side two-dimensional effects", In Proc. of the 41st IEEE Industry Applications Conference, Volume 3, pp. 1457 – 146, Oct 8-12., 2006.
[85] A. Bajolet,. R. Clerc.; G. Pananakakis, D. Tsamados, E. Picollet, N. Segura, J.-C.

Giraudin, P. Delpech, L. Montes, and G. Ghibaudo, **"**Low-frequency series-resistance analytical modeling of three-dimensional metal–insulator–metal capacitors", *IEEE Transactions on Electronic Devices*, Volume 54, pp.742 – 751, April 2007.

[86] R. Hocine, M. A, Boudghene Stambouli, and A. Saidane, "A three-dimensional TLM simulation method for thermal effect in high power IGBTs", In Proc. of 18th Annual, IEEE Symposium Semiconductor Thermal Measurement and Management, pp. 99-104, March 2002

[87] B. Beydoun, H. Tranduc, F. Oms, G. Charitat, and P. Rossel, "Power MOSFET design and modeling tool for power electronics", In Proc. of the 5th European Conference on Power Electronics and Applications, Vol.2, pp. 390 – 395, September 1993.

[88] A.F Witulski, "Modeling and design of transformers and coupled inductors", In Proc. of IEEE Conference on Applied Power Electronics, pp.589 – 595, March 1993.

[89] B.H Cho and F.C. Lee, "Modeling and analysis of spacecraft power systems**",** IEEE Transactions on Power Electronics, Volume 3, Issue 1, pp.44 – 54, January 1988.

[90] J.R Lee, B.H Cho, S.J Kim, and F.C Lee, "Modeling and simulation of spacecraft power systems**",** IEEE Transactions on Aerospace and Electronic Systems, Volume 24, Issue 3, pp. 295 – 304, May 1988.

[91] Kai Zenger, Ali Altowati, and Teuvo Suntio, "Dynamic Properties of Interconnected Power Systems A System Theoretic Approach**",** In Proc. of the 1st IEEE Conference on Industrial Electronics and Applications, pp.1 – 6, May 2006.

[92] T. Suntio and D. Gadoura, "Use of unterminated two-port modeling technique in analysis of input filter interactions in telecom DPS systems**"**, In Proc. of the 4th IEEE International Telecommunications and Energy Conference, pp.560 - 565, October 2002.

[93] Daniele Corona, Jean Buisson, Bart De Schutter and Alessandro Giua," Stabilization of switched affine systems: An application to the buck-boost converter", In Proc. of the American Control Conference, New York, USA, Julay 2007.

[94] D. Corona, J. Buisson, and B. De Schutter, "A Hamiltonian approach for the optimal control of the switching signal for a DC-DC converter," In Proc. of the 17th IFAC World Congress, pp. 7654–7659, Seoul, Korea, July 2008.

[95] Janos Hamar, Zoltan Suto, and Istvan Nagy," Signal Processing by Multimedia in Nonlinear Dynamics and Power Electronics: Review", In Proc. of World Academy of Science, Engineering and Technology, Vol. 13, May 2006, ISSN 1307-6884.

[96] R. D. Middlebrook and ***S.*** Cuk, "A general unified approach to modeling switching converter power stages," in Proc. IEEE Power Electronics Specialists Conf., pp. 18-34, 1976**.**

[97] Francisco Guinjoan, Javier Calvente, Alberto Poveda, and Luis Martínez, "Large-Signal Modeling and Simulation of Switching DC–DC Converters", IEEE , Transactions on Power Electronics, Vol. 12, No.3, May 1997.

[98] Tobias Geyer, Georgios Papafotiou, and Manfred Morari," On the Optimal Control of Switch-Mode DC-DC Converters", Chapter in Hybrid Systems: Computation and Control, pp. 342-356, 7th International Workshop,

Philadelphia, PA, USA, March 2004.
[99] Tobias Geyer, Georgios Papafotiou and Manfred Morari," Model Predictive Control in Power Electronics: A Hybrid Systems Approach", In Proc. of the 44th IEEE Conference on Decision and Control, and the European Control Conference 2005, Seville, Spain, December 2005.
[100] Tobias Geyer," Low Complexity Model Predictive Control in Power Electronics and Power Systems", PhD Thesis ETH No. 15953, Swiss Federal Institute of Technology, 2005
[101] Mohammad Hejri, and Hossein Mokhtari, " Hybrid Modeling and Control of a DC-DC Boost Converter via Extended Mixed Logical Dynamical Systems (EMLDs)", In Proc, of the 5th Power Electronics, Drive Systems and Technologies Conference (PEDSTC 2014), pp. 373-378, , Tehran, Iran, February 2014.
[102] M.K. Çamlıbel, L. Iannelli, and F. Vasca, "Modelling switching power converters as complementarity systems", In Proc. of the 43rd IEEE Conference, Decision and Control, pp.2328-2333, Paradise Islands, Bahamas, 2004.
[103] Apple Inc., "Grapher", Software Version 2.1(43), 2005-2009.
[104] Lennart Ljung, " System Identification: Theory for the User", PTR Prentice Hall, Englewood Cliffs, New Jersey, USA, 1987.
[105] V.I. Utkin," Sliding Mode Control: Mathematical Tools, Design and Applications", Department of Electrical Engineering, 205 Dreese Laboratory, The Ohio State University, 2015 Neil Avenue, Columbus, OH 43210, USA
[106] L. Ljung and T. Söderström, "Theory and Practice of Recursive Identification", MIT press, Cambridge, MA, 1983.
[107] G. Cybenko, "Approximation by superposition of a sigmoidal function", Mathematics of Control, Signals and Systems, Vol.2, Issue 4, pp. 303-314. , December 1989.
[108] A. Barron, "Universal approximation bounds for superpositions of a sigmoidal function", IEEE, Transaction on Information Theory, Vol. 39, Issue 3, pp.930-945, May 1993.
[109] M. Matthews, "On the uniform approximation of nonlinear discrete-time fading-memory systems using neural network models" PhD thesis, ETH, Zurich. ,1992.
[110] 0. Nerrand, P. Roussel-Ragot, L. Personnaz and G. Drefys, "Neural networks and nonlinear adaptive filtering: unifying concepts and new algorithms", Neural Computation, 5, 165-19, January 1993.
[111] L. Breiman, "Hinging hyperplanes for regression, classification and function approximation", IEEE, Transactions on Information Theory, Vol. 39, pp. 999-1013, June 1993.
[112] Gaetano Licata, "Fuzzy Logic, Knowledge and Natural Language", Chapter 1, In: Fuzzy Inference System – Theory and Applications, InTech, Rijeka, Croatia, 2012.
[113] Hans-Jürgen Zimmermann, "Comparison of Fuzzy Reasoning Methods", Fuzzy Sets and Systems, Volume 8, pp. 253-283, September 1982
[114] L. A. Zadeh, "Calculus of fuzzy restrictions", In: Fuzzy sets, fuzzy logic, and fuzzy systems, pp. 210 - 237 , World Scientific Publishing Co., Inc. River Edge, NJ, USA, 1996
[115] P. Lindskog, "Fuzzy Identification from a Grey Box Modeling Point of View", In: Fuzzy Model Identification, pp. 3-50, Springer-Verlag, Berlin Heidelberg,

1997.
[116] C. C. Lee, “Fuzzy logic in control systems: fuzzy logic controller, Parts 1 & 2”, IEEE Transactions on Systems, Man, and Cybernetics, Vol. 20, No. 2, pp. 404-435, April 1990
[117] J. J. Buckley, “Universal Fuzzy Controllers,” Automatica, Vol. 28, No. 6, pp.1245-1248, November 1992.
[118] J. J. Buckley, “Sugeno Type Controllers are Universal Controllers,” Fuzzy Sets and Systems, Vol. 53, Issue 3, pp. 299-304, February 1993
[119] J. Richalet, A. Rault, J.L. Testud and J. Papon, “Algorithmic control control of industrial processes” In proceedings of the 4th IFAC Symposium on Identification and Systems Parameter Estimation, Tbilisi, 1976
[120] J. Richalet, A. Rault, J.L. Testud, and J. Papon, “ Model predictive heuristic control: Applications to industrial processes”, Automatica, 14(1): 413-428, 1978
[121] C. R. Cutler and B. L. Ramaker, “Dynamic matrix control – a computer control algorithm”, In AlChE Nat. Mtg, 1979.
[122] S.P. Boyd and C.H. Barratt, “Linear Controller Design, Limits of Performance”, Prentice Hall, Information and Systems Science Series, Englewood Cliffs, New Jersey, 1991.
[123] J. C. Doyle, B.A. Francis, and A.R. Tannenbaum, “Feedback control systems”, MacMillan Publisjhing Company, New York, USA, 1992.
[124] J.C. Doyle, K. Glover, P.P. Khargonekar and B.A. Francis, “State-space solutions to standard H_2 and H_∞ control problems”, IEEE AC, 34:pp831-847, 1989.
[125] J.M. Maciejowski,” Multivariable Feedback Conrtrol Design”, Addison-Wesley Publishers, Wokingham, UK, 1989.
[126] M.Morari and E. Zafiriou, Robust Process Control”, Prentice Hall, Englewood Cliffs, New Jersey, 1989.
[127] R. M. C. De Keyser, PH. G. A. Van De Velde and F.A.G. Dumortier, “ A comparative Study of Self-adaptive Long range Predictive Control Methods”, Automatika, Vol. 24 (Issues 2), 1988, pp. 149-163.
[128] Carlos E. Garcia, David M. Prett , and Manfred Morari, “ Model Predictive Control: Theory and Practice a Survey”, Automatica, Vol. 25, (Issues 3), 1989, pp. 335-348.
[129] D.W. Clarke and R. Scattolini, “Constrained receding-horizon predictive control”, IEE proceedings-D, Vol. 138 (Issue 4), July 1991.
[130] D.W. Clarke and C. Mohtadi, ”Properties of generalized predictive control”, Automatica, 25(6):859-875, 1989.
[131] D.W. Clarke, C. Mohtadi and P.S. Tuffs, ”Generalized predictive control - part 1. The basic algorithm”, Automatica, 23(2):137-148, 1987.
[132] J. Richalet, “Industrial applications of model based predictive control. Automatica, 29(5):1251-1274, 1993.
[133] Tor A. Johansen, “Introduction to Nonlinear Model Predictive Control and Moving Horizon Estimation”, Chapter 5, pp. 187-239, In: Selected Topics on Constrained and Nonlinear Control, by Miloslav Roubal ROSA, Dolny Kubìn , Slovakia, January 2011., ISBN: 978–80–968627–4–0
[134] C. Budd, and F. Dux, “ Chattering and related behavior in impact oscillators”, In Philosophical Transactions of the Royal Society A Mathematical, physical and Engineering Science, Vol. 347, No. 1683, pp.365–389, May 1994.
[135] A.B. Nordmark , and P.T. Piiroinen, “Simulation and stability analysis of

impacting systems with complete chattering", Journal of Computational and Nonlinear Dynamics, American Society of Mechanical Engineers (ASME), Vol. 58, No. 1, pp.85-106, 2009.

[136] K.S.Holkar, L.M.Waghmare, "An Overview of Model Predictive Control", International Journal of Control and Automation ,Vol. 3 No. 4, December 2010.

[137] D. W. Clarke, C. Mohtadi, P. S. Tuffs, " Generalized Predictive Control-Part II. Extensions and Interpretations", Automatica, Vol. 23, No. 2, pp. 149-160, 1987.

[138] R. Baždarić, D. Matko, A. Leban, D. Vončina, I. Škrjanc, "Fuzzy model predictive control of a DC-DC boost converter based on non-linear model Identification", Mathematical and Computer Modelling of Dynamical Systems, Vol. 23, Issue 2, pp.116-134, 2017.